DOCTOR OF PHILOSOPHY

# Post-translational control of Bacillus subtilis biofilm formation

Kiley, Taryn Blair

*Award date:*
2011

*Awarding institution:*
University of Dundee

DOCTOR OF PHILOSOPHY

# Post-translational control of Bacillus subtilis biofilm formation

Taryn Blair Kiley

2011

University of Dundee


University of Dundee
Division of Molecular Microbiology

# Post-translational control of *Bacillus subtilis* biofilm formation

Taryn Blair Kiley

A thesis submitted for the degree of Doctor of Philosophy

February 2011

## Declaration

I declare that I am the author of this thesis. Unless otherwise stated, all references cited have been consulted by myself. I declare that the experiments of which the thesis is a record of have been conducted by myself and that any work conducted by other researchers has been noted accordingly. I declare that the thesis has not been previously accepted for a higher degree.

Taryn Blair Kiley

(candidate)

Dr. Nicola Stanley-Wall

(supervisor)

**Acknowledgements**

I would like to thank my supervisor Nick for all of her support over the past four years. I can't begin to express how grateful I am for giving me the opportunity to study for a PhD in your lab. Thank you for everything!

I would also like to thank the BBSRC for funding me.

Thanks to all of the NSW lab members, past and present. A special thanks goes to Adam, Ewan and Victoria for keeping me smiling thought thick and thin! You guys are great!

A big thanks must go to the Molecular Microbiology Division…I'm sure I've asked everyone something over the years! Thank you to Jackie Heilbronn for keeping the whole show running!

I also want to thank my family, especially my Mom, who taught me that if I work hard and persevere I can achieve anything.

Above all, I would like to thank Matt for his endless support. You've been everything I needed and more.

## Publications

Verhamme, D. T., Kiley, T. B., and Stanley-Wall, N.R. (2007). DegU co-ordinates multicellular behaviour exhibited by *Bacillus subtilis*. Molecular Microbiology **65**(2): 554-568

Murray, E. J., Kiley, T. B., and Stanley-Wall, N.R (2009). A pivotal role for the response regulator DegU in controlling multicellular behaviour. Microbiology **155**:1-8

Kiley, T. B. and Stanley-Wall, N. R. (2010). Post-translational control of *Bacillus subtilis* biofilm formation mediated by tyrosine phosphorylation. Molecular Microbiology **78** (4): 947-963.

## Abstract

A biofilm is a complex community of cells enveloped in a self-produced polymeric matrix. Entry into a biofilm is exquisitely controlled at the level of transcription and in *Bacillus subtilis* it requires the concerted efforts of several major transcription factors including the repressor SinR and the activator DegU. I initially identified that these transcriptional regulators control biofilm formation via parallel pathways. Through investigating the regulation of biofilm formation by SinR and DegU, I discovered that biofilm formation is also regulated at the post-translational level. This was achieved by identifying three key proteins which are needed for biofilm formation. These proteins are PtkA, a bacterial tyrosine kinase; TkmA, the cognate modulator of PtkA; and PtpZ, a bacterial tyrosine phosphatase. By introducing amino acid point mutations within the catalytic domains of PtkA and PtpZ it was identified that the kinase and phosphatase activities, respectively, are essential for function. In addition, PtkA contains a conserved C-terminal tyrosine cluster that is the site of autophosphorylation. Investigation of the role of the C-terminal tyrosine cluster tentatively suggests that this domain acts to block access to the active site of PtkA, thus affecting the ability of PtkA to phosphorylate its targets. Deletion of the gene coding for TkmA demonstrated that this modulator was also required for biofilm formation. It was also demonstrated that TkmA may interact with other protein partners, at least in the absence of PtkA, raising the question of how signal specificity is maintained. Finally, a systematic mutagenesis approach was used with the aim of identifying the target(s) of PtkA and PtpZ during biofilm formation but, despite extensive efforts, it remained elusive. The findings presented in this thesis highlight the complexity of biofilm formation by *B. subtilis* by revealing an additional level of regulation in the form of protein tyrosine phosphorylation.

## General Abbreviations

| | |
|---|---|
| 5'RACE | 5 prime rapid amplification of cDNA ends |
| amp | ampicillin |
| APS | ammonium persulfate |
| ATP | adenosine-5'-triphosphate |
| BSA | bovine serum albumin |
| BY-Kinase | bacterial tyrosine kinase |
| cDNA | complementary DNA |
| cml | chloramphenicol |
| DNA | deoxyribonucleic acid |
| DTT | dithiothreitol |
| e.g. | *exempli gratia* (for example) |
| EDTA | ethylene diamine tetraacetic acid |
| EGTA | ethylene glycol tetraacetic acid |
| EMSA | electrophoretic mobility shift assay |
| EPS | exopolysaccharide |
| *et al.* | *et alii* (and others) |
| FPLC | fast protein liquid chromatography |
| gDNA | genomic DNA |
| GFP | green fluorescent protein |
| GTP | guanosine-5'-triphosphate |
| IMAC | immobilized metal ion affinity chromatography |
| IPTG | isopropyl β-D-1-thiogalactopyranoside |

| | |
|---|---|
| kan | kanamycin |
| kDa | kilo Dalton |
| LB | Luria-Bertani medium |
| MLS | macrolide-lincosamide-streptogramin |
| Ni-NTA | nickle-nitrilotriacetic acid |
| O.D. $_{600}$ | optical density measured at wavelength 600 nm |
| PAGE | polyacrylamide gel electrophoresis |
| PBS | phosphate buffered saline |
| PCR | polymerase chain reaction |
| RNA | ribonucleic acid |
| RT-PCR | reverse transcription polymerase chain reaction |
| SDS | sodium dodecyl sulfate |
| SEM | standard error of the mean |
| spc | spectinomycin |
| TAE | Tris/acetate/EDTA |
| TBE | Tris/Borate/EDTA |
| TBS | Tris buffered saline |
| TEMED | N, N, N', N'-tetramethylethylenediamine |
| U | units |
| UV | ultra violet |
| v/v | volume per volume |
| w/v | weight per volume |
| YFP | yellow fluorescent protein |

# Table of contents

# List of Figures

# List of Tables

# 1 Introduction

## *1.1 Multicellular behaviour displayed by bacteria*

Bacteria are capable of living in a wide range of different environments which can be changeable, and at times, unfavourable. Bacteria may encounter environmental stresses which include, but are not limited to, high salinity, DNA damage by exposure to UV, desiccation, and nutrient limitation. Displaying multicellular behaviour is one method that bacteria use to cope with these stresses (Shapiro 1998). Multicellularity is defined here as a type of behaviour that requires cooperation from a population of cells in order for a task to be accomplished. By utilising the multicellular potential within the population, the cells can achieve tasks which they would otherwise not be able to accomplish as individuals. Cooperation of the population depends on being able to correctly activate the appropriate behaviour, at the right time. Therefore communication between bacteria within the population is paramount.

Examples of multicellular behaviour displayed by bacteria include swarming motility, the secretion of exoproteases for acquiring nutrients, and quorum sensing which is a mechanism for detecting population size that is often coupled to triggering behaviours which rely on high cell density for success (Shapiro 1998). In addition to these examples, many different species of bacteria can form biofilms. The multicellular behaviour of biofilm formation will be discussed in more detail in section 1.1.1.

### *1.1.1 Biofilm formation*

In their natural habitats, bacteria will exist predominantly as part of a biofilm (Costerton, Lewandowski et al. 1995). A biofilm is described here as a dense

population of cells that forms either attached to a surface or at an air-liquid interface that is surrounded by a self produced exopolymeric matrix. When forming at the air-liquid interface, biofilms are referred to as pellicles. However, biofilms are far more than a dense population of homogenous cells. Within a biofilm of genetically identical bacteria, groups of cells can differentiate into specialised sub-populations whose roles include producing enzymes, extracellular proteins or polysaccharides which the population as a whole will utilise (Lopez, Vlamakis et al. 2010). Through division of labour, the population can achieve multiple 'multicellular' tasks simultaneously, thus increasing the chance of survival for the population in a changeable environment. Biofilm formation is therefore a very useful survival strategy for bacteria.

There are many practical reasons for studying biofilm formation. The study of biofilms can provide a simplified model for the investigation of how cell function is controlled in a multicellular structure. Also, biofilms have long been associated with chronic infections (Hoiby, Bjarnsholt et al. 2010). A contributing factor to the association of biofilms and chronic infection is the fact that bacteria living within a biofilm are far more resistant to antibiotics than their planktonic counter-parts, which can make the treatment of chronic infections more challenging (Hoiby, Bjarnsholt et al. 2010). Conversely, biofilms can act as a biocontrol agent, colonising the rhizosphere and preventing fungal and bacterial infections of commercially important crops such as potato (Morikawa 2006). For these, and many other, reasons biofilms are an attractive bacterial lifestyle to study.

### *1.1.2 Bacillus subtilis*

*Bacillus subtilis* is a Gram-positive bacterium commonly found in soil that has been extensively studied under laboratory conditions for many decades. Due to the extensive laboratory use of *B. subtilis* and the subsequent vast knowledge of its physiological, biochemical and genetic pathways, *B. subtilis* is considered to be a model organism for Gram-positive bacteria in the way that *Escherichia coli* is for Gram-negative bacteria. The growing use of *B. subtilis* as a tool for investigating many different processes, and its industrial relevance, prompted the sequencing of the complete genome in 1990. The genome sequence of the *B. subtilis* isolate 168 was subsequently completed in 1997 and the chromosome was found to contain approximately 4,100 genes (Kunst, Ogasawara et al. 1997). The 168 strain is a domesticated isolate of *B. subtilis* (Burkholder and Giles 1947). In this case, the term domesticated is used to describe an isolate which has lost certain characteristics that its progenitor strain possesses such as the ability to form robust biofilms or to swarm, but has improved traits such as its ease of genetic manipulation. The progenitor strain of 168 is the undomesticated *B. subtilis* isolate, NCIB3610, which is strongly believed to be a descendant of the original Marburg strain of *B. subtilis* that was first isolated from soil in Marburg, Germany (Zeigler, Pragai et al. 2008). The 168 isolate was constructed by exposing the Marburg strain to UV and X-ray mutagenesis (Burkholder and Giles 1947). The resulting 168 strain was auxotrophic for tryptophan and was subsequently found to grow well on a defined medium under laboratory conditions (Burkholder and Giles 1947). It was later identified that the 168 isolate could be readily transformed with DNA from other domesticated *B. subtilis* strains (Spizizen 1958).

The extensive use of *B. subtilis* under laboratory conditions can be attributed to several factors. In addition to its ease of genetic manipulation, *B. subtilis* is a spore forming bacterium (Sonenshein 2000) that provides a simplified system to increase our understanding of complex processes such as cell division and development. Furthermore, *B. subtilis* is a 'safe' organism that shares significant similarity with pathogenic bacteria including *Bacillus cereus*, which causes food poisoning (Drobniewski 1993); *Bacillus anthracis*, which forms spores capable of causing fatal pulmonary and gastrointestinal infections (Spencer 2003); and *Listeria monocytogenes* which can spoil dairy produce and cause listeriosis (Farber and Peterkin 1991).

As well as its basic scientific interest, *B. subtilis* is also used extensively in industrial settings. For example, the enzyme subtilisin is one of several industrially important secreted enzymes produced by *B. subtilis* (Morikawa 2006) and was an important predecessor to the enzymes found in modern biological washing powders (Gupta, Beg et al. 2002). Production of the fermented soybean foodstuff, natto, is produced by *B. subtilis natto* isolates (Nishito, Osana et al. 2010) and *B. subtilis* is also used agriculturally as a biocontrol agent (Emmert and Handelsman 1999). For these reasons it is of interest to understand the formation of biofilm formation by *B. subtilis*.

## *1.2 Biofilm formation by B. subtilis*

### *1.2.1 Structural components of the* B. subtilis *biofilm matrix*

An important component of the biofilm is the self-secreted complex exopolymeric matrix which supports cells living within the biofilm (Sutherland 2001; Flemming and Wingender 2010). Despite the significant genetic variation between different species of

biofilm-forming bacteria, bacterial biofilm matrices possess common attributes. The matrix is largely composed of water, polysaccharides, cellular proteins and some bacteria also use extracellular nucleic acids to support the formation of the biofilm matrix (Flemming and Wingender 2010).

It has been previously demonstrated that a polysaccharide component and a protein component of the biofilm matrix of *B. subtilis* are essential for biofilm formation (Branda, Gonzalez-Pastor et al. 2001; Kearns, Chu et al. 2005; Chu, Kearns et al. 2006). In the sections below I will introduce these components in more detail and I will also introduce other genes which encode proteins of unknown function which are also essential for biofilm formation by *B. subtilis*.

### *1.2.1.1 EPS is essential for biofilm formation by* B. subtilis

The extracellular polysaccharide component (EPS) is synthesised by the proteins encoded by the 15 gene *epsA-O* operon (formally known as *yveK-yvfF* operon) (Kearns, Chu et al. 2005) (Figure 1-1).

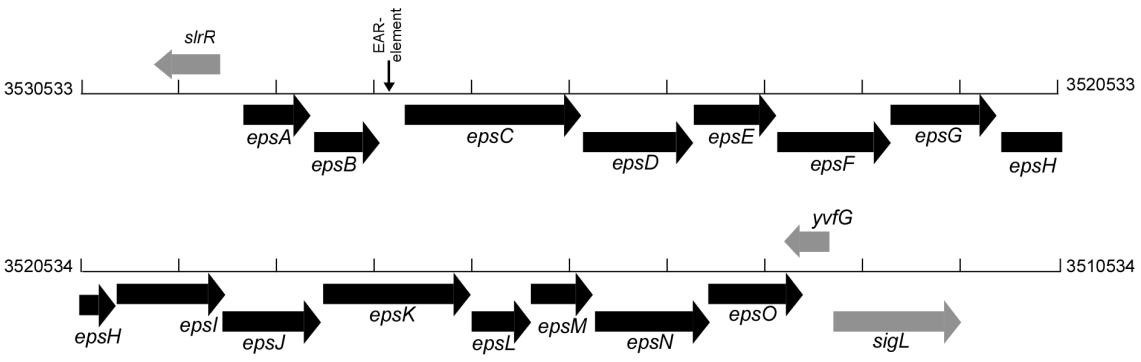


**Figure 1-1: Schematic representation of the *epsA-O* operon**
Organisation of the *epsA-O* operon on the chromosome is depicted to scale; genes flanking the *epsA-O* operon are depicted in grey; the location of the regulatory RNA element (EAR-element) (Irnov and Winkler 2010) is indicated by an arrow between *epsB* and *epsC*. The numbers represent the location on the chromosome with respect to the origin of replication.

Deletion or disruption of this operon results in a severe loss of colony complexity, which clearly demonstrates the important role of the polysaccharide component during the formation of robust biofilms (Branda, Gonzalez-Pastor et al. 2004; Kearns, Chu et al. 2005) (Figure 1-2).

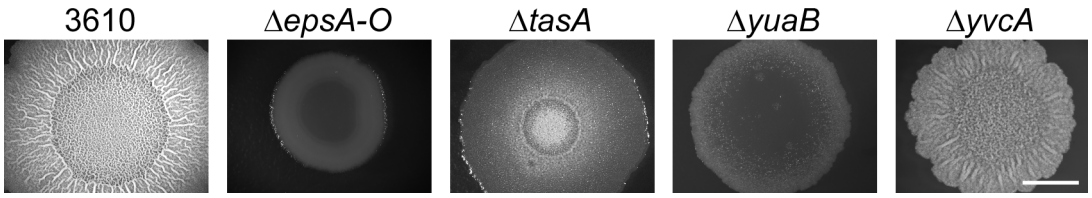


**Figure 1-2: Colony morphology of *eps*, *tasA*, *yuaB* and *yvcA* mutants**
Strains NCIB3610, Δ*epsA-O*, Δ*tasA*, Δ*yuaB* and Δ*yvcA* were grown on MSgg media for 40h at 37˚C. Scale bar represents 5 mm.

The biochemical composition of the polysaccharide synthesised by the EpsA-O machinery is currently unknown. Furthermore, the function of all of the proteins encoded by the *epsA-O* operon is not yet known. However it is known that most members of the *epsA-O* operon are essential for the correct synthesis of the EPS as successive deletion of the first 14 genes (*epsA-N*) results in the formation of fragile pellicles (Nagorska, Ostrowski et al. 2010). One protein for which more information is known is EpsE. EpsE is a dual-functional protein which acts to regulate matrix production and motility (Guttenplan, Blair et al. 2010). EpsE interacts with the *B. subtilis* flagella motor, known as FliG, and acts to uncouple the motor from the flagella, thus inhibiting motility (Blair, Turner et al. 2008; Guttenplan, Blair et al. 2010). In addition to its role during motility, EpsE is also a putative family II glycosyltransferase (Blair, Turner et al. 2008).

Consistent with biofilm formation being a highly regulated process, the transcription of the *epsA-O* operon is tightly controlled (see section 1.2.2) and full transcription of the *epsA-O* genes requires the presence of an EAR-element (eps-associated RNA) (Figure 1-1), which allows progression of RNA polymerase (Irnov and Winkler 2010). The environmental signal to which the EAR-element responds is currently unknown.

### *1.2.1.2 The TasA protein is essential for biofilm formation by* B. subtilis

In addition to the EPS found in the biofilm matrix, *B. subtilis* requires the production of a protein called TasA to form robust biofilms (Branda, Chu et al. 2006; Chu, Kearns et al. 2006) (Figure 1-2). TasA is encoded by the third gene in the *yqxM-sipW-tasA* operon (Stover and Driks 1999) (Figure 1-3).

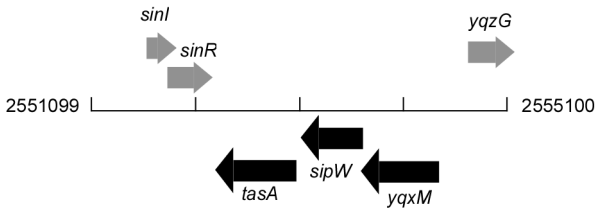


**Figure 1-3: Schematic representation of the *yqxM-sipW-tasA* operon**
Organisation of the *yqxM-sipW-tasA* operon on the chromosome is depicted to scale; genes flanking the *yqxM-sipW-tasA* operon are depicted in grey. The numbers represent the location on the chromosome with respect to the origin of replication.

TasA was first identified due to its antibacterial properties and its role as a component of the mature spore coat (Stover and Driks 1999). It was subsequently shown that TasA formed a significant component of the biofilm matrix and that mutant strains for *tasA* do not form robust biofilms (Branda, Chu et al. 2006; Chu, Kearns et al. 2006) (Figure

1-2). Recently, it has been demonstrated that TasA forms amyloid fibres which presumably give structural support to the matrix architecture (Romero, Aguilar et al. 2010). Also encoded within the *yqxM-sipW-tasA* operon is the protein YqxM, which is required for biofilm formation (Branda, Chu et al. 2006; Chu, Kearns et al. 2006). The presence of TasA in the matrix relies on expression of YqxM (Branda, Chu et al. 2006) and it was subsequently identified that YqxM acts by anchoring the TasA fibres to the cell (Kolodkin-Gal, Romero et al. 2010).

YqxM is translationally coupled to the second gene product, called SipW, which is essential for biofilm formation (Hamon, Stanley et al. 2004; Chu, Kearns et al. 2006). SipW is a signal peptidase (Tjalsma, Bolhuis et al. 1998) and is responsible for processing TasA by removing the 27 amino acid signal sequence from the N-terminal of TasA prior to export out of the cell (Stover and Driks 1999).

#### *1.2.1.3 Additional components that are required for biofilm formation*

In addition to the well-characterised EPS and TasA components of the biofilm matrix, additional proteins and a polysaccharide have been identified as important for biofilm formation and may assist in providing the biofilm with additional structural support. One component is the putative membrane anchored lipopeptide YvcA (Tjalsma, Kontinen et al. 1999). YvcA was identified as being essential for robust biofilm formation by Verhamme *et al*. (Verhamme, Kiley et al. 2007) (Figure 1-2). Strains lacking *yvcA* displayed a gross loss of colony architecture, yet its exact role during biofilm formation remains to be established. YuaB is an additional component required for biofilm formation (Kobayashi 2007; Verhamme, Murray et al. 2009) (Figure 1-2).

Again, the exact function of YuaB during biofilm formation remains to be established. Also required for biofilm formation is YoaW, a predicted secreted protein which functions to activate the latter stages of biofilm formation through an undefined method in a laboratory isolate of *B. subtilis* (Hamon, Stanley et al. 2004). The requirement of *yoaW* during biofilm development has been brought into question as other groups have shown that mutations in *yoaW* do not significantly alter colony phenotype in an undomesticated isolate of *B. subtilis* (Chu, Kearns et al. 2008). However, the use of different isolates of *B. subtilis* may explain this discrepancy. Another component which is required for biofilm formation is the polysaccharide γ-polyglutamic acid (γ-PGA). However, it must be noted that γ-PGA is not required by all isolates of *B. subtilis* (Stanley and Lazazzera 2005), including the undomesticated NCIB3610 strain that was used in this study (Branda, Chu et al. 2006).

### *1.2.2 Transcriptional regulation of biofilm formation by B. subtilis*

The formation of a biofilm is a highly regulated process. As such the level of transcription and timing of transcriptional activation of the operons required for robust biofilm formation must be tightly regulated. To achieve this, *B. subtilis* has developed a complex regulatory network to control biofilm formation which relies on the activation of two major transcriptional regulators, Spo0A and DegU. In the next sections I will discuss the mechanisms by which Spo0A and DegU regulate biofilm formation.

### *1.2.2.1 Spo0A activates biofilm formation*

Spo0A is a transcriptional activator of *B. subtilis* biofilm formation (Branda, Gonzalez-Pastor et al. 2001; Hamon and Lazazzera 2001). Originally, Spo0A was identified as essential for the development of environmentally resistant endospores (Sonenshein 2000). Later it was noted by Branda *et al*. that an undomesticated isolate of *B. subtilis* deleted for *spo0A* was unable to form spores and that this mutation also resulted in a loss of biofilm formation in comparison to the wild type strain (Branda, Gonzalez-Pastor et al. 2001). In addition, an independent investigation by Hamon *et al.* using a domesticated *B. subtilis* isolate noted that mutation of *spo0A* resulted in a dramatic reduction in biofilm depth (Hamon and Lazazzera 2001). Since these discoveries, a significant effort has been made to identify the mechanism by which Spo0A activates biofilm formation. An important step during the regulation of biofilm formation is the phosphorylation of Spo0A. In the following section I will introduce the mechanism by which Spo0A becomes phosphorylated.

#### 1.2.2.1.1 Activation of Spo0A requires phosphorylation via a phosphorelay cascade

Spo0A is activated by phosphorylation and this is mediated through a phosphorelay cascade which is initiated by the histidine kinases KinA-E and includes the sporulation initiation phosphotransferases Spo0B and Spo0F (Sonenshein 2000) (Figure 1-4). It was demonstrated by Hamon *et al*. that only KinC, KinD and KinE were required for activating biofilm formation in a domesticated isolate of *B. subtilis* (Hamon and Lazazzera 2001). The role of KinE during biofilm formation has since been disputed as a mutant strain for *kinE* did not appear to differ from the wild type undomesticated *B.*

*subtilis* strain (McLoon, Kolodkin-Gal et al. 2010). However it must be noted that these studies were conducted using different *B. subtilis* isolates and this may account for the differences observed. It is interesting to note that while the initiation of biofilm formation and sporulation are linked by a common transcriptional regulator (Spo0A), the kinases required to trigger the activation of each developmental process appear to be clearly defined (Sonenshein 2000; Hamon and Lazazzera 2001).

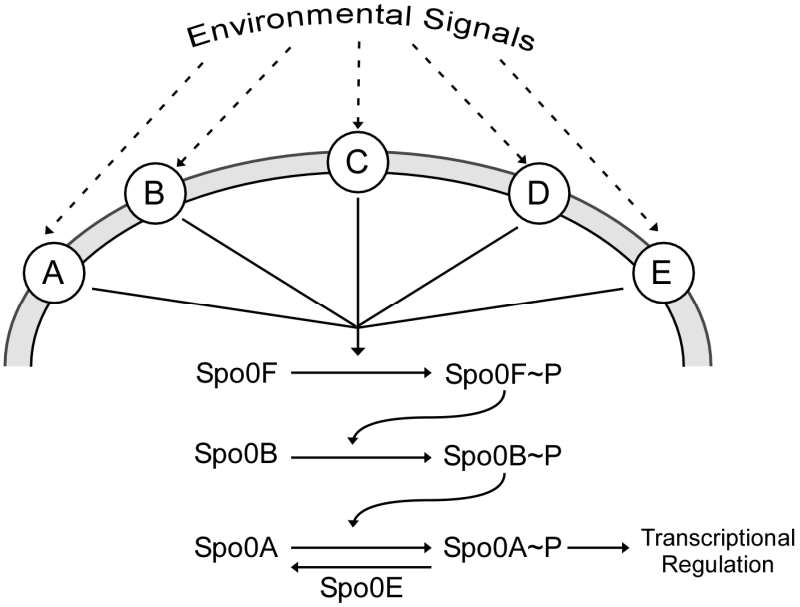


**Figure 1-4: The Spo0A phosphorelay system**
Schematic representation of the phosphorelay system culminating in the phosphorylation and activation of the transcriptional regulator Spo0A. The circles containing A, B, C, D and E denote the kinases which feed into the phosphorelay system. The grey semi-circle represents the cell membrane. Spo0E is a phosphatase which dephosphorylates Spo0A~P.

Little is known about the environmental signals that trigger the activation of the kinases; however it has been shown that KinC phosphorylates Spo0A in response to potassium leakage caused by the interaction of the cell with the extracellular lipopeptide surfactin (Lopez, Fischbach et al. 2009). Additionally KinC has been shown to respond to sub-lethal doses of the biocide $ClO_2$ (Shemesh, Kolter et al. 2010). Thus, KinC is able to sense cell stresses, such as a reduction in membrane potential, and can respond to this

by phosphorylating Spo0A and promoting biofilm formation. The role of KinD during the phosphorylation of Spo0A has also been investigated. It has been proposed that KinD acts as both a kinase and a phosphatase, maintaining Spo0A~P at a low level until a signal is sensed. On detection of the appropriate signal KinD then acts only as a kinase and subsequently increases Spo0A~P in the cell to a level sufficient to trigger sporulation (Aguilar, Vlamakis et al. 2010). It is thought that KinD changes from acting as a phosphatase to a kinase in response to the presence of extracellular matrix components (Aguilar, Vlamakis et al. 2010). In addition to the activity of the aforementioned kinases, the level of Spo0A~P is further regulated by the presence of Spo0A~P specific phosphatase called Spo0E (Figure 1-4) (Ohlsen, Grimsley et al. 1994).

#### 1.2.2.1.2 Mid-levels of Spo0A~P activate biofilm formation

Spo0A~P regulates the transcription of approximately 120 genes. Furthermore, a range of thresholds has been determined which group these genes by the intracellular level of Spo0A~P required to activate or inhibit their transcription (Molle, Fujita et al. 2003; Fujita, Gonzalez-Pastor et al. 2005). Sporulation is a last resort survival mechanism utilised by sporulation competent bacteria during prolonged periods of stress and consistent with this the level of intracellular Spo0A~P required to activate sporulation is higher than that of biofilm formation. Having a single transcriptional regulator that is able to regulate multiple behaviours provides the cell with the ability to integrate divergent processes in response to changing environmental signals.

In the following sections I shall discuss the role of Spo0A~P during biofilm formation and it should be noted that Spo0A~P activates biofilm formation via an indirect mechanism. The principal role of Spo0A~P is to activate the transcription of operons required for biofilm formation that are repressed by the transcriptional regulators AbrB and SinR. In the next sections I will detail the mechanism by which AbrB and SinR repress biofilm formation. The way in which Spo0A~P activates biofilm formation via AbrB constitutes a relatively simple genetic pathway (Figure 1-5). However, for SinR it is a more complicated system that results in the control of single cell fate within an isogenic population of cells (Figure 1-8).

#### *1.2.2.2 AbrB mediated repression of biofilm formation*

AbrB was originally identified as a transcriptional repressor of the gene *aprE*, which encodes an alkaline protease (Ferrari, Henner et al. 1988). AbrB was subsequently shown to regulate a large number of genes (Hamon, Stanley et al. 2004) and is widely regarded as a global 'transition state' regulator (Phillips and Strauch 2002). In this role AbrB inhibits several multicellular behaviours including sporulation, exoprotease production and biofilm formation in actively growing cells (Ferrari, Henner et al. 1988; Hamon and Lazazzera 2001; Hamon, Stanley et al. 2004). In the sections below I will discuss the mechanism by which AbrB is controlled and introduce the targets of AbrB which are regulated during biofilm formation.

#### 1.2.2.2.1 Transcriptional and post-translational regulation of AbrB

The level of AbrB within the cell is controlled at the transcriptional and post-translational level. Addressing transcriptional control first; the transcription of *abrB* is regulated in two ways. Firstly, *abrB* transcription is directly repressed by low levels of Spo0A~P (Perego, Spiegelman et al. 1988; Greene and Spiegelman 1996; Fujita, Gonzalez-Pastor et al. 2005) (Figure 1-5). Secondly, AbrB directly represses its own transcription (Strauch, Spiegelman et al. 1989). The post-translational regulation of AbrB involves two mechanisms. Firstly, AbrB is a rapidly degraded protein (O'Reilly and Devine 1997). Secondly, the ability of AbrB to regulate the transcription of its target genes is repressed by a small protein called AbbA (Figure 1-5) (Banse, Chastanet et al. 2008). The transcription of *abbA* is also subject to regulation by low levels of Spo0A~P, however in contrast to *abrB*, *abbA* is activated by Spo0A~P (Molle, Fujita et al. 2003; Fujita, Gonzalez-Pastor et al. 2005; Banse, Chastanet et al. 2008). Thus low levels of Spo0A~P inactivates AbrB in two ways: *i)* by direct transcriptional repression and *ii)* by transcriptional activation of a repressor of AbrB. The combined effect of increasing levels of Spo0A~P on the level of active AbrB in the cell results in the de-repression of the transcription of operons encoding products needed for biofilm formation.

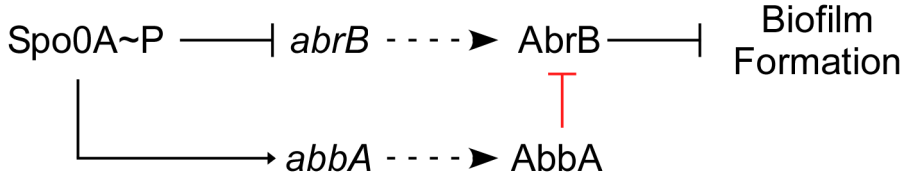


**Figure 1-5: Spo0A represses AbrB**
Schematic representation of the regulation of AbrB by Spo0A~P. Black T-bars indicate repression of genes by the transcription regulators. Red T-bars indicate repression by protein-protein interaction. Dashed arrows indicate translation.

#### 1.2.2.2.2 AbrB represses the transcription of genes required for biofilm formation

AbrB regulates the transcription of a number of genes (Hamon, Stanley et al. 2004), including genes which are required for biofilm formation. Genes known to be repressed by AbrB which contribute to biofilm formation include the *yqxM-sipW-tasA* operon, the *epsA-O* operon, the *yxaAB* operon, *yvcA, yuaB* and *yoaW*. AbrB represses the transcription of these genes as detailed below:

- AbrB directly represses the transcription of the *yqxM-sipW-tasA* operon which encodes the protein component of the biofilm matrix, TasA (Chu, Kearns et al. 2008).
- AbrB directly represses the transcription of the *epsA-O* operon which encodes the biosynthetic machinery for the production of EPS (Chu, Kearns et al. 2008) (Murray, Strauch et al. 2009).
- AbrB directly represses the transcription of the *yxaAB* operon, containing *yxaB* which is predicted to encode a exopolysaccharide synthase (Nagorska, Hinc et al. 2008). The mechanism by which the *yxaAB* operon activates biofilm formation is currently unknown.
- Deletion of *abrB* results in an increase in the transcription of a gene called *yoaW* (Hamon, Stanley et al. 2004). As mentioned in section 1.2.1.3, the requirement of YoaW during biofilm formation of undomesticated isolates remains in question. It is not yet known whether AbrB regulates the transcription of *yoaW* directly or indirectly.
- AbrB directly represses the transcription of *yvcA,* which encodes a putative lipopeptide, during exponential growth (Verhamme, Murray et al. 2009). The role of *yvcA* during biofilm formation remains to be established.

- Finally, AbrB directly represses the transcription of *yuaB* during stationary phase (Verhamme, Murray et al. 2009). The role of *yuaB* during biofilm formation remains to be established.

Taken together, it can be seen that AbrB plays a significant role in the regulation of a number of key genes that are important for biofilm formation.

#### *1.2.2.3 Spo0A determines cell fate via a bistable switch involving SinR and SlrR*

Within an isogenic population of *B. subtilis* cells differentiation occurs which leads to the formation of specialised subpopulations (Veening, Smits et al. 2008). An example of cell differentiation can be seen in mature biofilms where genetically identical cells can exist as motile cells, matrix producers or spores (Vlamakis, Aguilar et al. 2008). Additionally a subpopulation of cells secreting exoproteases can also arise (Veening, Igoshin et al. 2008). By differentiating into subpopulations, all of the cells within the community can benefit from the communal production of EPS and acquisition of nutrients by production of exoproteases without the need for each cell to produce these components for themselves. Spo0A~P acts upon a bistable switch comprised of the regulators SinR and SlrR, switching cells from one specialised subpopulation to another in response to environmental signals.

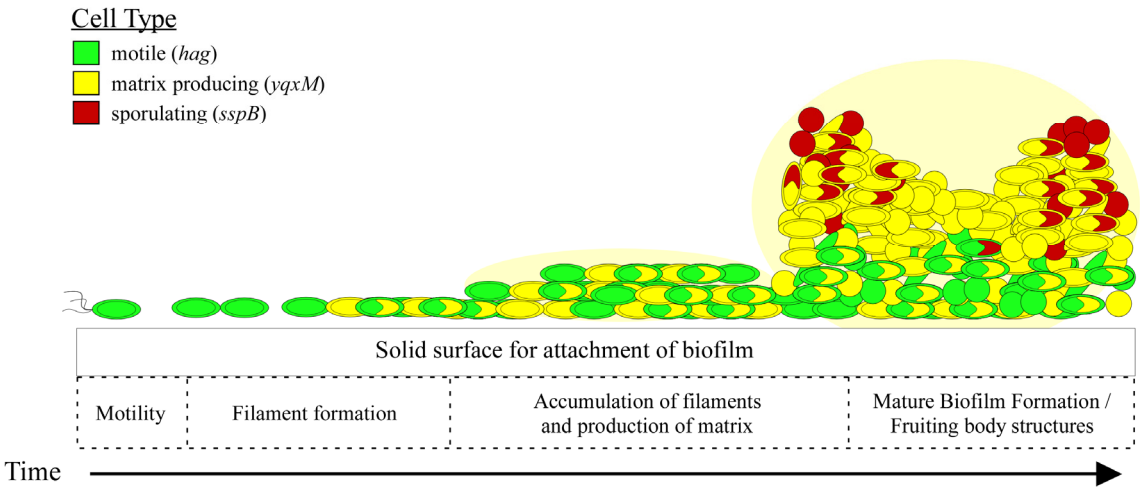


**Figure 1-6: Cells differentiate during biofilm formation**
Schematic representation of biofilm formation over time, highlighting the differentiation of cells during different phases of biofilm growth. Green cells indicate motile cell type, yellow cells indicate matrix forming cells, and red cells indicate sporulating cells. Cells coloured green and yellow indicate the differentiation from a motile cell to a matrix producing cell. Cells coloured yellow and red indicate the differentiation from a matrix producing cell to a sporulating cell. A single cell coloured green and red indicates that very rarely do motile cells differentiate into sporulating cells. Light peach coloured dome indicates the presence of the biofilm matrix. Diagram based on results detailed by Vlamakis *et al.* (Vlamakis, Aguilar et al. 2008).

Biofilm formation is subject to spatial and temporal control and an important step in the initiation of biofilm formation is the switching from growth in a planktonic state to a sessile state (Figure 1-6). In the planktonic state most of the cells are motile and non-chained; whereas in the sessile state a proportion of the population switches to become chained and produce the biofilm matrix. The switching between these two very distinct cell states is governed by a complex regulatory circuit involving SinR, its antagonist SinI and a relatively recently identified protein called SlrR. Spo0A~P is the driving force which acts on SinI, SinR and SlrR and initiates the move towards cell chaining and matrix production (Figure 1-10). In the following sections I will discuss the roles of SinR, SinI and SlrR during biofilm formation and will detail the mechanism by which Spo0A~P drives the switch from motile cells to sessile cells as mediated by SinR and SlrR.

### *1.2.2.4 SinR represses biofilm formation*

SinR is a transcription regulator that was originally identified as an inhibitor of sporulation (Gaur, Dubnau et al. 1986). It was subsequently demonstrated that SinR regulates a number of other multicellular behaviours including biofilm formation (Kearns, Chu et al. 2005). SinR represses biofilm formation by directly repressing the transcription of the *epsA-O* and *yqxM-sipW-tasA* operons which are required for matrix production (Kearns, Chu et al. 2005; Branda, Chu et al. 2006; Chu, Kearns et al. 2006; Kobayashi 2007). The activity of SinR is indirectly inhibited by low levels of Spo0A~P. The mechanism of this repression will be discussed in the following sections.

#### 1.2.2.4.1 SinI acts to derepress the transcription of SinR targets

SinR is encoded by the gene *sinR*, which is located within a two gene operon known as *sinIR* (Figure 1-7). The *sinIR* operon contains three distinct promoter regions; two domains direct transcription of both *sinI* and *sinR*, and a separate promoter which directs transcription of the downstream *sinR* gene alone (Gaur, Cabane et al. 1988).

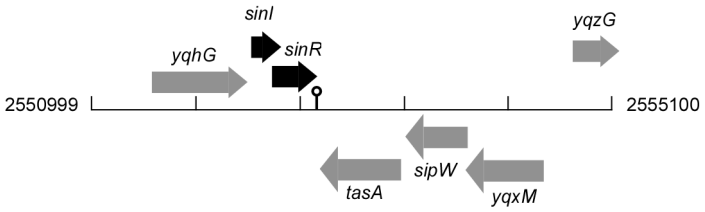


**Figure 1-7: Schematic representation of the *sinIR* operon**
Organisation of *sinIR* operon on the chromosome is depicted to scale; genes flanking the *sinIR* operon are depicted in grey. The stalked circle indicates the transcriptional terminator. The numbers represent the location on the chromosome with respect to the origin of replication.

SinR is subjected to post-translational regulation by the SinR-antagonist SinI (Bai, Mandic-Mulec et al. 1993; Sanchez and Olmos 2004). SinI binds to SinR, thus inhibiting the DNA binding capability of SinR. SinI therefore indirectly activates biofilm formation by de-repressing SinR-repressed genes (Kearns, Chu et al. 2005) (Figure 1-8). Consistent with biofilm formation being activated before sporulation the transcription of *sinI* is directly activated by mid-levels of Spo0A~P (Shafikhani, Mandic-Mulec et al. 2002; Molle, Fujita et al. 2003; Fujita, Gonzalez-Pastor et al. 2005).

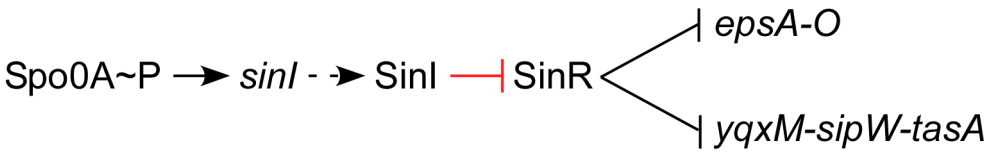


**Figure 1-8: SinR inhibits transcription from the *epsA-O* and *yqxM-sipW-tasA* operons**
Genes are depicted by lowercase italics. Proteins are depicted by uppercase letters. Arrows indicate activation of a gene. Dashed arrows indicate production of a protein. Black T-bars indicate transcriptional inhibition. Red T-bars indicate inhibition by protein-protein interaction.

#### 1.2.2.4.2 SlrR transitions cells from a motile to a matrix producing state

SlrR (previously known as Slr) is a transcription regulator which, in partnership with SinR (see section 1.2.2.4.4), represses swarming motility (Kobayashi 2007; Chai, Norman et al. 2010) and autolysin production (Chai, Norman et al. 2010). SlrR also activates biofilm formation (Chu, Kearns et al. 2008; Kobayashi 2008; Murray, Strauch et al. 2009; Chai, Norman et al. 2010). Consistent with this, SlrR is seen as a key regulator during the transition from a motile state to a matrix producing state.

With respect to its role during biofilm formation, Chu *et al.* demonstrated that SlrR activates the transcription of the *yqxM-sipW-tasA* operon, which is essential for producing the protein component of the biofilm matrix, TasA (Chu, Kearns et al. 2008). However, the authors noted that deletion of *slrR* did not affect the transcription of the *epsA-O* operon, which produces the polysaccharide component of the biofilm matrix (Chu, Kearns et al. 2008). This is in contrast to the findings of Kobayashi who noted that deletion of *slrR* decreased the transcription of both operons (Kobayashi 2008) and Murray *et al*. who noted that overexpression of *slrR* increased transcription of both operons (Murray, Strauch et al. 2009). However, it must be noted that the study by Chu *et al*. utilised a β-galactosidase assay where the promoter region of *eps* was fused to the gene encoding LacZ. This technique assesses the level of transcription from the *eps* promoter, taking the population as a whole. As the *epsA-O* operon is transcribed in a small subpopulation of cells and the experiments were conducted under planktonic conditions (Chai, Chu et al. 2008) perhaps this technique was unable to detect the subtle, yet significant, differences in the transcription of the *epsA-O* operon between the wild type strain and the *slrR* mutant. Thus in summary, SlrR activates biofilm formation by influencing the transcription of both the *yqxM-sipW-tasA* operon and the *epsA-O* operon which are required for biosynthesis of the biofilm matrix. The mechanism by which SlrR activates the transcription from the *yqxM-sipW-tasA* and *epsA-O* operons will be discussed in detail in section 1.2.2.4.4. SlrR represses key operons that are required for swarming and complete separation of daughter cells, however this relies on an interaction with SinR. The mechanism by which SlrR mediates the repression of these operons will also be detailed in section 1.2.2.4.4.

1.2.2.4.3 Transcriptional regulation of *slrR*

The gene *slrR* is located directly downstream, and in the opposite direction, from the *epsA-O* operon (Figure 1-9) and the transcription of *slrR* is directly repressed by AbrB and SinR (Kearns, Chu et al. 2005; Chu, Kearns et al. 2008; Murray, Strauch et al. 2009), and activated indirectly by the transcriptional regulator Abh (Murray, Strauch et al. 2009).

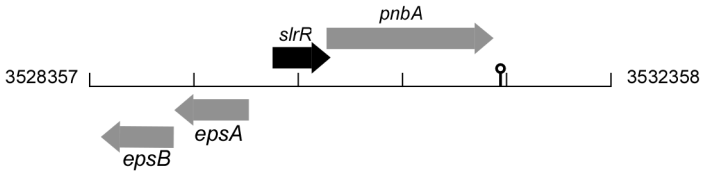


**Figure 1-9: Schematic representation of the *slrR* gene locus**
The location of the *slrR* gene on the chromosome is depicted to scale; genes flanking *slrR* are depicted in grey. The stalked circle indicates the transcriptional terminator. The numbers represent the location on the chromosome with respect to the origin of replication.

Under biofilm activating conditions when Spo0A becomes phosphorylated, the transcription of *abrB* decreases. Additionally, the transcription of *sinI* increases which leads to the production of SinI and subsequent inhibition of the DNA-binding ability of SinR (see section 1.2.2.4.1). Therefore, under these conditions the level of SlrR will increase, due to de-repression of SinR and AbrB binding to the *slrR* promoter. On top of this, *slrR* transcription is regulated by a self-reinforcing positive feedback loop, as increased levels of SlrR lead to binding of SlrR to SinR (Chai, Norman et al. 2010) (Figure 1-10). Binding of SlrR to SinR inhibits the ability of SinR to repress the

transcription from the *slrR* promoter region, thus increasing the level of SlrR in the cell (Chai, Norman et al. 2010).

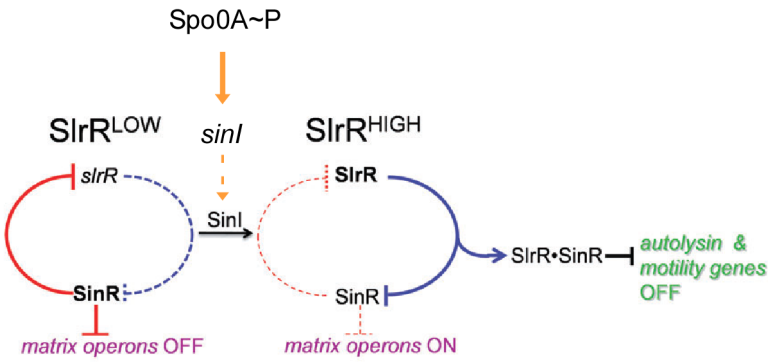


**Figure 1-10: Spo0A~P leads to the switch from motile cells to matrix producing cells.**
Adapted from a figure published by (Chai, Norman et al. 2010). Dashed arrow indicates translation. Solid red or blue lines indicate the dominant pathway of repression. Black T-bars indicate transcriptional repression. SlrR·SinR denotes the SinR-SlrR complex. Genes are signified by italics.

#### 1.2.2.4.4 Spo0A~P drives the switch from motile cells to matrix producers

During the initiation of biofilm formation *B. subtilis* cells can exist in two distinct states. Firstly, they can exist as motile cells which are repressed for the production of matrix operons. In this state, the level of SlrR in the cell is low, due to the repression of *slrR* transcription by SinR (Figure 1-10). However, as the level of Spo0A~P in the cell rises in response to environmental signals, the level of SinI increases. SinI is then able to inhibit SinR from repressing its target genes, including *slrR*. The de-repression of *slrR* mediated by SinI causes the level of SlrR in the cell to rise triggering the switch to the production of matrix and onset of cell chaining (Figure 1-10).

Under high levels of SlrR, matrix genes are de-repressed and autolysins are repressed as follows. First, SlrR acts in a similar way to SinI and binds to SinR, thus inhibiting SinR

from repressing the transcription of the *epsA-O* and *yqxM-sipW-tasA* operons. Secondly, SlrR and SinR form a complex which regulates a distinct subset of genes which neither SinR nor SlrR can regulate individually. The novel group of genes repressed by the SinR: SlrR complex includes the *lytABC* operon and *lytF*, which code for autolysin production (Kobayashi 2008; Chai, Norman et al. 2010). The repression of autolysins is a crucial step in the switch from single to chained cells as autolysins act to remodel the peptidoglycan at the cell poles after cell division to complete the separation of the daughter cells (Smith, Blackman et al. 2000).

In addition to the *lyt* genes, the SlrR: SinR complex also represses the transcription of *hag* (Chai, Norman et al. 2010), which encodes for flagellin. The repression of the bacterial flagella further reinforces the importance of the SlrR: SinR complex in the switch between motile, single cells to sessile matrix producing cells. Thus upon activation of Spo0A~P, a complex regulatory network is put in motion to control single cell fate and promote biofilm formation.

#### *1.2.2.5 DegU regulates biofilm formation*

Biofilm formation is regulated by DegU, a response regulator belonging to the DegS-DegU two-component regulatory system (Stanley and Lazazzera 2005; Kobayashi 2007; Verhamme, Kiley et al. 2007). DegU, formerly known as SacU, was originally identified during a screen for genes required for exoprotease production (Steinmetz, Kunst et al. 1976). However since 1976, DegU has been studied extensively and has been shown to regulate a number of other multicellular behaviours displayed by *B. subtilis* including swarming and swimming motility (Kobayashi 2007; Verhamme, Kiley et al. 2007), and genetic competence (Hamoen, Van Werkhoven et al. 2000).

Much like Spo0A~P, DegU is controlled by phosphorylation and is able to integrate the control of these multicellular behaviours according to the level of DegU~P in the cell (Figure 1-12). However of particular relevance to this work is the role of DegU during the activation and inhibition of biofilm formation at low and high levels of DegU~P, respectively. In the sections below I will discuss how the transcription of DegU is controlled and the way in which the level of DegU~P in the cell is regulated. I will also discuss some of the key targets of DegU during biofilm formation.

#### 1.2.2.5.1 Transcriptional activation of the *degS-degU* operon

The concentration of DegU in the cell is controlled at the level of transcription. The gene encoding DegU is located in an operon along with the gene encoding for the sensor kinase DegS (Figure 1-11). The promoter region of the *degS-degU* operon has been studied in detail. The *degS-degU* operon contains three promoters which direct the transcription of the operon. The promoters are located *1)* upstream of *degS*, *2)* within the coding sequence of *degS* and *3)* in the intergenic region between the coding sequences for DegS and DegU (Figure 1-11). Promoter 1 ensures a basal level of *degS-degU* transcription at all times. Promoter 2 responds to nitrogen-starvation (Yasumura, Abe et al. 2008), while promoter 3 is under the control of the phosphorylated form of DegU (DegU~P) (Veening, Igoshin et al. 2008).

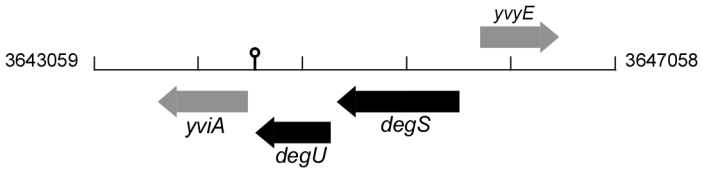


**Figure 1-11: Schematic representation of the *degS-degU* operon**
Organisation of *degS-degU* operon on the chromosome is depicted to scale; genes flanking the *degS-degU* operon are depicted in grey. The stalked circle indicates the transcriptional terminator. The numbers represent the location on the chromosome with respect to the origin of replication.

#### 1.2.2.5.2 DegS phosphorylates DegU

DegS, the cognate sensor kinase encoded by the *degS-degU* operon, responds to increased osmolarity (Mukai, Kawata et al. 1990; Tanaka, Kawata et al. 1991). In response to osmotic changes, DegS autophosphorylates upon the histidine residue at position 189 (Macek, Mijakovic et al. 2007) and transfers a phosphate moiety to DegU. In addition to the autophosphorylation of DegS at position 189, DegS can also be phosphorylated on a serine residue at position 76, however the effects of this modification remain to be established (Macek, Mijakovic et al. 2007).

DegS is subject to post-translational regulation which affects its ability to phosphorylate DegU. Firstly, a kleisin essential for chromosome partitioning known as ScpA interacts with DegS during growth. ScpA, which belongs to the SMC-ScpA-ScpB complex acts to inhibit the kinase activity of DegS (Dervyn, Noirot-Gros et al. 2004). This inhibition is relieved during stationary phase due to a decrease in the SMC-ScpA-ScpB complex, which coincides with the requirement of increased levels of DegU~P for biofilm formation. An additional factor effecting the level of DegU~P in the cell is the fact that, in addition to its role as a kinase, DegS is also a phosphatase and is responsible for dephosphorylating DegU~P (Tanaka, Kawata et al. 1991).

#### 1.2.2.5.3 Additional proteins affecting the level of DegU~P in the cell

Three additional proteins significantly affect the level of DegU~P in the cell and these are DegQ, DegR and RapG. Firstly, DegQ acts to increase the transfer of the phosphate moiety of DegS to DegU, thus positively influencing the level of DegU~P (Kobayashi 2007). The transcription of *degQ* is activated by DegU~P, however very high levels of DegU~P lead to transcriptional inhibition (Msadek, Kunst et al. 1990). The *B. subtilis* domesticated strain, JH642, was shown to contain a point mutation within the promoter region of *degQ* which results in a lower level of *degQ* transcription compared with undomesticated strains (Stanley and Lazazzera 2005). Secondly, the level of DegU~P in the cell is affected by the 60 amino acid protein DegR, which acts to stabilise DegU in its phosphorylated form by inhibiting the dephosphorylation capability of DegS (Msadek, Kunst et al. 1990; Mukai, Kawata-Mukai et al. 1992). Finally, the ability of phosphorylated DegU to bind to its targets is modulated by the response regulator aspartyl phosphatase RapG. RapG binds to DegU and it has been proposed that RapG interferes with the DNA-binding capacity of DegU rather than dephosphorylating it (Ogura, Shimane et al. 2003). Thus the binding of RapG to DegU~P lowers the level of DegU~P in the cell that is capable of transcriptional regulation.

#### 1.2.2.5.4 Putative DegU recognition sequence

The recognition sequence that DegU binds to is dependent on the phosphorylation state of DegU. In 2004, the first identification of a predicted recognition sequence for DegU was discovered (Shimane and Ogura 2004). In this study, Shimane and Ogura suggested that the different phosphorylation states of DegU (DegU and DegU~P)

possessed distinct preferential binding patterns. It was predicted that unphosphorylated DegU would bind to an inverted repeated sequence, such as observed in the promoter region of *comK*, while DegU~P would bind preferentially to a tandem repeated sequence, as observed in the *aprE* promoter region (Shimane and Ogura 2004). This hypothesis was strengthened further in 2007 when Tsukahara *et al*. demonstrated that DegU was able to bind a 3-part tandem repeated sequence located within the promoter region of *bpr*, a bacillopeptidase F activated by DegU~P (Tsukahara and Ogura 2007). Tsukahara *et al*. later conducted footprint analysis in order to confirm that DegU and DegU~P preferentially bound inverted and tandem repeated sequences, respectively (Tsukahara and Ogura 2008). It must be noted that while the ability of DegU to bind to *comK* and DegU~P to bind to *bpr* and *aprE* has been demonstrated, the ability to predict potential targets of DegU/DegU~P based on this predicted recognition sequence is less robust.

#### 1.2.2.5.5 Multiple behaviours are controlled according to the level of DegU~P

The DegU regulon includes genes which are required for a range of physiologically different activities. DegU coordinates the regulation of these behaviours depending on the overall phosphorylation state of DegU in the cell (Figure 1-12). By setting thresholds in which different groups of genes are regulated, DegU can integrate the regulation of physiologically distinct behaviours. For example, a known target of DegU is the promoter region of the *fla/che* operon, which is involved in the development of flagella and chemotactic components (Amati, Bisicchia et al. 2004). Flagella are required for swarming motility (Kearns and Losick 2003) and additionally the production of flagella is a requirement for the initial stages pellicle formation

(Kobayashi 2007). Swarming is activated by low levels of DegU~P and inhibited by higher levels (Kobayashi 2007; Verhamme, Kiley et al. 2007).

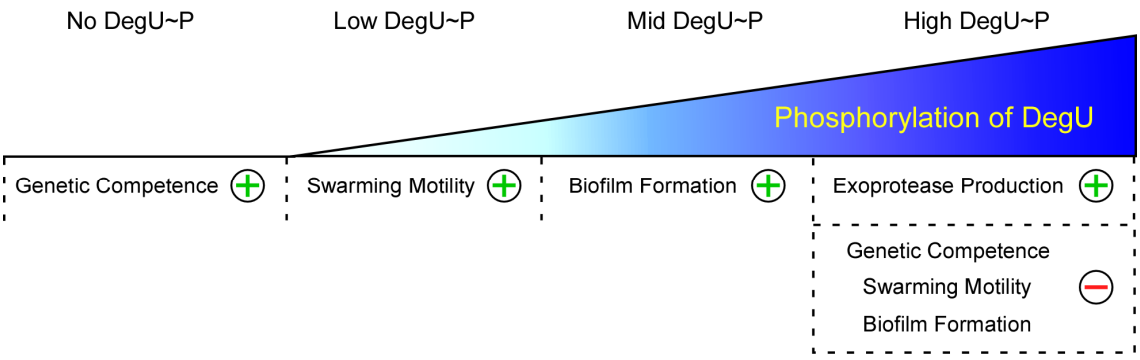


**Figure 1-12: DegU regulates different behaviours depending on its phosphorylation state**
A simplified schematic representation of the effects of increasing levels of DegU~P in the cell and its ability to regulate different multicellular behaviours. Green crosses indicate that the behaviour is activated at the level of DegU~P shown. Red minus symbols indicate that the behaviour is inhibited at the level of DegU~P shown.

In contrast to swarming, mid-levels of DegU~P activate biofilm formation while very high levels of DegU~P inhibit biofilm formation (Kobayashi 2007; Verhamme, Kiley et al. 2007). Indeed, mid-levels of DegU~P have previously been shown to activate the transcription of at least two genes required for biofilm formation which are *yvcA*, which encodes a putative lipoprotein (Verhamme, Kiley et al. 2007), and *yuaB*, which encodes a predicted secreted protein known to be involved in latter stages of pellicle formation and biofilm formation (Kobayashi 2007; Verhamme, Murray et al. 2009) (see section 1.2.1.3 ). High levels of DegU~P activate exoprotease production yet inhibit biofilm formation, genetic competence and swarming motility. This is thought to represent an escape mechanism for the cells contained within the biofilm (Verhamme, Kiley et al. 2007). In this thesis, I will introduce additional genes belonging to the DegU regulon that I identified as influencing biofilm formation by *B. subtilis*.

### *1.2.3 Regulation of multicellular behaviours by post-translational modification*

In addition to the complex network of transcriptional regulators that govern the formation of robust biofilms by *B. subtilis*, the work conducted during this study has identified that post-translational modification by phosphorylation also plays a significant role (Kiley and Stanley-Wall 2010). More specifically, the work shown here demonstrates that *B. subtilis* utilises a bacterial tyrosine kinase and phosphatase pair for the modification of a target protein(s) during the formation of a biofilm. In this section I will provide a general overview to bacterial tyrosine phosphorylation and will also detail specific proteins encoded within the *B. subtilis* genome which, as I will demonstrate in later sections, contribute to the post-translational regulation of biofilm formation.

#### *1.2.3.1 Modification of proteins by phosphorylation in bacteria*

It is now accepted that bacterial proteins can be phosphorylated on histidine, aspartic acid, tyrosine, threonine and serine residues. Modulation of protein activity using phosphorylation of serine/threonine/tyrosine (Ser/Thr/Tyr) residues was initially believed to be confined to eukaryotes (Deutscher and Saier 2005). Prokaryotes were thought to be limited to phosphorylation of histidine and aspartic acid residues; a key signalling feature of two-component signal transduction systems (Hoch 2000). However, this paradigm was revoked in the late 1970's by the identification of Ser/Thr phosphorylation in bacteria (Wang and Koshland 1978; Manai and Cozzone 1979) and again when tyrosine phosphorylation was detected in the mid 1990's (Duclos,

Grangeasse et al. 1996). Serine, threonine, and tyrosine phosphorylation has subsequently emerged as an important mechanism for mediating the dynamic control of diverse cellular processes in bacteria, including polysaccharide biosynthesis (Morona, Paton et al. 2000; Vincent, Duclos et al. 2000; Soulat, Grangeasse et al. 2007), DNA metabolism (Petranovic, Michelsen et al. 2007), cell division (Wu, Ohta et al. 1999), and resistance to antimicrobial compounds (Lacour, Bechet et al. 2008).

### *1.2.3.2 Protein tyrosine phosphorylation by bacteria*

The modification of tyrosine residues by the addition of a phosphate moiety is a reversible process that is controlled by specific kinases and phosphatases. Phosphorylation can alter the activity, and possibly the localisation, of the target protein in the cell (Jers, Pedersen et al. 2010). Tyrosine phosphorylation of bacterial proteins is a very important tool used by bacteria in order to control a wide range of different cellular processes. For example, DivL of *Caulobacter crescentus* is a tyrosine kinase which contributes to the regulation of cellular division (Wu, Ohta et al. 1999). The human pathogen *Streptococcus pneumoniae* encodes the tyrosine kinase CpsD and phosphatase CpsB which are essential for capsule formation and virulence (Bender and Yother 2001; Morona, Miller et al. 2004). This is in line with the most common role of tyrosine phosphorylation during capsule formation (Grangeasse, Cozzone et al. 2007).

A novel group of non-eukaryotic-like tyrosine kinases was identified in prokaryotes and have since been named as bacterial tyrosine kinases (hereafter referred to as BY-kinase). BY- kinases are structurally different from their eukaryotic counterparts and given the range of cellular processes that are regulated by this group of kinases, BY-

kinases have been proposed as novel targets for antimicrobial compounds (Lee, Zheng et al. 2008; Olivares-Illana, Meyer et al. 2008; Grangeasse, Terreux et al. 2009). Therefore, understanding the mechanism(s) and role(s) of modification of tyrosine residues by phosphorylation in bacteria is very important. Like eukaryotic tyrosine kinases, BY-kinases are nucleotide-dependent but the active site of ATP/GTP binding and hydrolysis is not conserved between the eukaryotic and prokaryotic proteins (Lee and Jia 2009). Furthermore, BY-kinases possess unique conserved motifs that are needed for catalytic activity which are absent from the eukaryotic tyrosine kinases and could represent potential targets for small molecule inhibitors (Grangeasse, Terreux et al. 2009; Lee and Jia 2009). Further details regarding the unique features of BY-kinases will be presented in section 1.2.3.3.

### *1.2.3.3 Bacterial tyrosine kinases*

#### 1.2.3.3.1 Common features of bacterial tyrosine kinases

BY- kinases represent a novel class of protein tyrosine kinase which differ substantially from their eukaryotic counterparts. For example, BY-kinases do not possess the characteristic Hanks domains. Hanks domains are 11 highly conserved sequences located within eukaryotic tyrosine kinases that are essential for nucleotide binding and kinase activity (Hanks, Quinn et al. 1988; Hovens, Stacker et al. 1992). In contrast BY-kinases are more closely related to ATPases, yet it must be clarified that ATPases do not possess kinase activity (Lee and Jia 2009). In fact BY-kinases and ATPases share such similarity at the protein sequence level (Figure 1-13) that the bacterial ATPase MinD belonging to *Pyrococcus horikoshii* OT3 has been used to solve the crystal

structure of the BY-kinase Cap5B2 from *Staphylococcus aureus* (Olivares-Illana, Meyer et al. 2008).

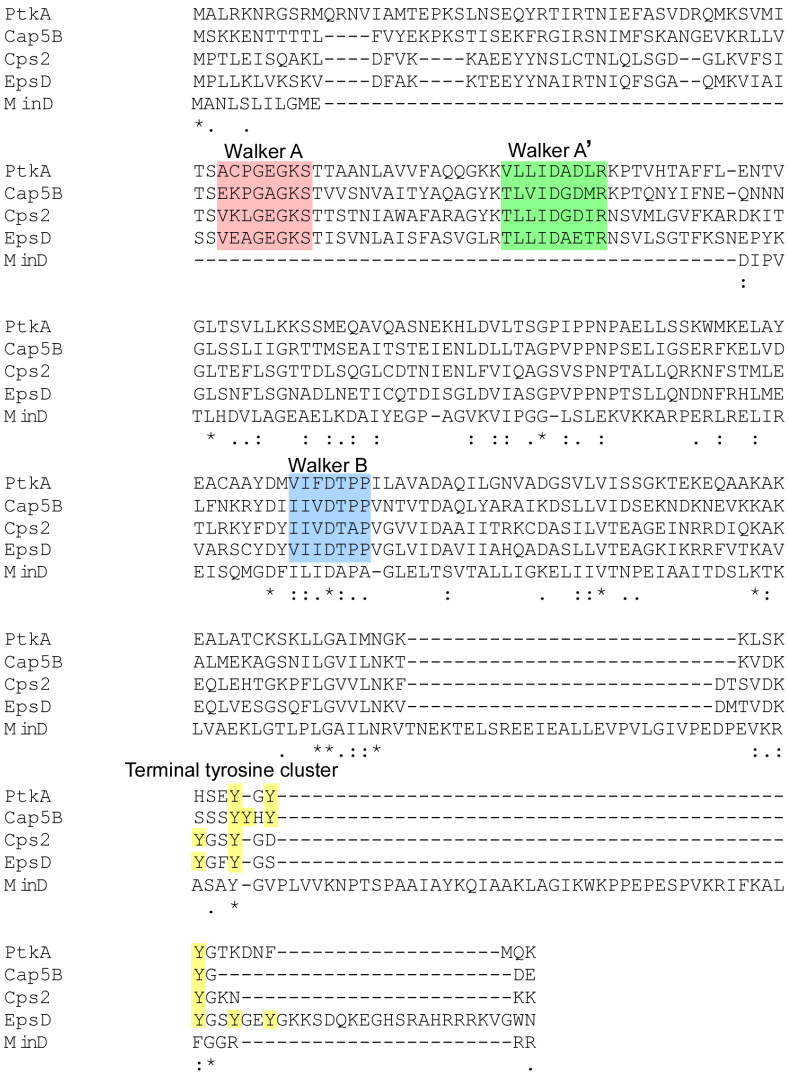


**Figure 1-13: Protein sequence alignment of confirmed BY-kinases and MinD from *Pyrococcus horikoshii OT3***

Alignment was conducted using CLUSTAL W (1.83) multiple sequence alignment software. Protein sequences were obtained from the NCBI protein database (http://www.ncbi.nlm.nih.gov/protein/). Sequences from the following proteins were assessed: PtkA, belonging to *B.subtilis* 168; Cap5B, belonging to *Staphylococcus aureus* Mu50; Cps2, belonging to *Streptococcus pneumoniae* D39; EpsD, belonging to *Streptococcus thermophilus* CNRZ1066; and MinD belonging to *Pyrococcus horikoshii* OT3. Conserved motifs associated with bacterial tyrosine kinases are highlighted as follows: Walker A (red box), Walker A' (also referred to as the DxD motif) (green box), Walker B (blue box), residues comprising the terminal tyrosine cluster (yellow boxes) and proline rich motif (purple box). Asterisks indicate complete sequence conservation, colons indicate closely related amino acid residue substitutions, and a full stop indicates a semi-conserved amino acid substitution.

BY-kinases from Gram-positive and Gram-negative bacteria share several common features. Firstly, an important distinguishing feature of a BY-kinase is the presence of three Walker motifs which are necessary for the binding of either ATP or GTP (Lee and Jia 2009). These are *i)* the Walker A motif ([G/A]XXXXGK[S/T]), also known as a P-loop, which was first identified in ATPases as an essential motif for the binding of the γ-phosphate of ATP/GTP (Walker, Saraste et al. 1982), *ii)* the Walker A' motif ([ILVFM]XXXDXDXR) which is also referred to as the 'DxD' motif due to the conservation of the double aspartic acid residues in its sequence (Grangeasse, Terreux et al. 2009) and *iii)* the Walker B motif ([ILVFM]XXXDXPP) which is necessary for the binding of the cationic co-factor $Mg^{2+}$ and for hydrolysis of ATP/GTP (Walker, Saraste et al. 1982). The Walker B motif also possesses two conserved proline residues which are important for maintaining the open conformation of the active pocket and thus are necessary for allowing substrates to enter and become phosphorylated (Lee and Jia 2009).

BY-kinases possess a C-terminal tyrosine rich region known as the terminal tyrosine cluster (Figure 1-13). While the structure of the terminal tyrosine cluster is far less conserved between BY-kinases than the Walker motifs (Lee and Jia 2009), the terminal tyrosine cluster is nonetheless an important distinguishing feature of a BY-kinase. Indeed, the terminal tyrosine cluster is the site of autophosphorylation (Grangeasse, Doublet et al. 2002; Mijakovic, Poncet et al. 2003). However, it must be noted that the effect of autophosphorylation of the terminal tyrosine cluster on the activity of the BY-kinase is not well conserved or well understood. For example, in the case of Wzc, a BY-kinase from *Escherichia coli*, both autophosphorylation and dephosphorylation of the terminal tyrosine cluster is necessary for colanic acid production (Obadia, Lacour et al. 2007). Whereas mutation of the terminal tyrosine cluster of CpsD from

*Streptococcus pneumoniae* results in a reduction of capsular biosynthesis (Morona, Morona et al. 2003) and can also mildly affect virulence (Morona, Miller et al. 2004). In terms of the autophosphorylation reaction, some BY-kinases such as Cap5B2 from *Staphylococcus aureus* do not autophosphorylate their terminal tyrosine cluster residues in any particular order, but this is not the case for all BY-kinases (Olivares-Illana, Meyer et al. 2008). The BY-kinase PtkA belonging to *B. subtilis* preferentially phosphorylates the tyrosine at position 228 (Mijakovic, Poncet et al. 2003). The reason for the selectivity of the *B. subtilis* BY-kinase during autophosphorylation is currently unknown and an *in vivo* role for the terminal tyrosine cluster is yet to be shown.

#### 1.2.3.3.2 BY-kinases of Gram-positive and –negative bacteria are different

Significant differences can be observed between bacterial tyrosine kinases of Gram-positive and Gram-negative bacteria. In Gram-negative bacteria BY-kinases consist of a single membrane bound polypeptide where the kinase catalytic activity and modulator domains are fused (Mijakovic, Petranovic et al. 2005) (Figure 1-14). As mentioned previously, a key feature of BY-kinases is the ability to autophosphorylate and some Gram-negative bacteria display a mechanism of phosphorylation that is specific to Gram-negative BY-kinases. In the case of *Escherichia coli* K12, it was identified that Wzc, a BY-kinase which regulates colanic acid production (Vincent, Duclos et al. 2000), autophosphorylates in a two-step phosphorylation mechanism (Grangeasse, Doublet et al. 2002). First, intramolecular phosphorylation allows phosphorylation of an internal conserved tyrosine residue at position 569, located between the conserved Walker A and Walker B motifs. The phosphorylation of tyrosine-569 subsequently

enhances the intermolecular phosphorylation of the terminal tyrosine clusters of neighbouring Wzc proteins, thus contributing to colanic acid production (Grangeasse, Doublet et al. 2002). It must be noted however that not all Gram-negative BY-kinases which possess this internal tyrosine residue rely on intramolecular phosphorylation in order to enhance autophosphorylation (Wugeditsch, Paiment et al. 2001). An additional conserved feature of Gram-negative BY-kinases is the highly conserved arginine-lysine rich cluster of unknown function located at the N-terminal end of the C-terminal cytoplasmic domain (Grangeasse, Terreux et al. 2009).

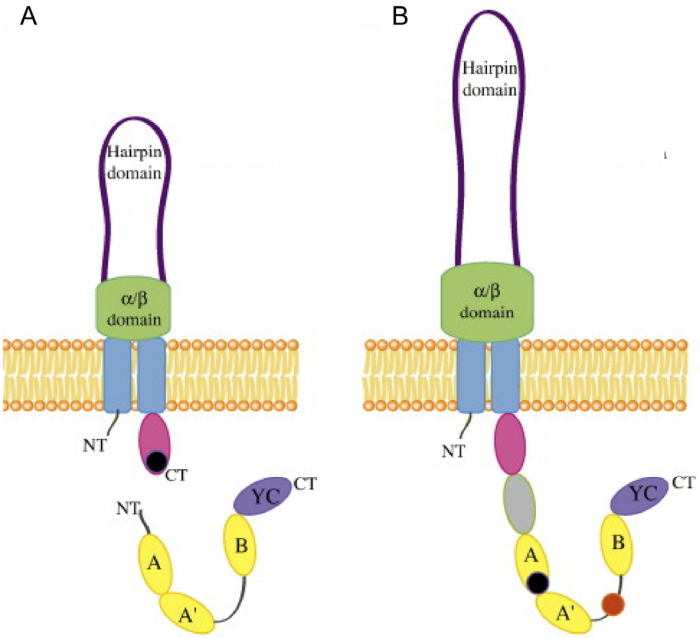


**Figure 1-14: BY- kinases from Gram-positive and Gram-negative bacteria differ in structure.** Schematic representation of the structural differences of BY-kinases from Gram-positive (**A**) and Gram-negative bacteria (**B**). Features of BY-kinases are highlighted as follows: NT, N-terminal; CT, C-terminal; A, Walker A motif; A', Walker A' motif; B, Walker B motif; YC, terminal tyrosine cluster; grey oval, RK rich cluster; black circle, hydrophobic residue which participates in nucleotide binding; orange circle, internal phospho-tyrosine residue which participates in enhancing interphosphorylation of BY-kinases. Figure taken from review by Grangeasse *et al.* (Grangeasse, Terreux et al. 2009).

In contrast to the structure of the Gram-negative BY-kinases, in Gram-positive bacteria the BY-kinase is split into two proteins where the genes encoding the modulator and kinase domains are co-located on the chromosome and co-transcribed (Grangeasse, Cozzone et al. 2007) (Figure 1-14). By separating the kinase domain from the

transmembrane bound modulator domain, there is the potential for Gram-positive BY-kinases to dissociate from their cognate modulators. It is possible that when dissociated from their modulator partners, BY-kinases may possess additional roles in the absence of the kinase modulator. Furthermore, the splitting of the kinase and modulator in Gram-positive bacteria allows for the potential of spatial regulation. In contrast, as BY-kinases from Gram-negative bacteria are anchored to the membrane, they do not possess the potential for spatial regulation.

Gram-positive BY-kinases lack internal phosphorylated tyrosine residues, and consequently an alternative mechanism for phosphorylation exists. In Gram-positive bacteria, kinase activity is stimulated by interaction of the C-terminal domain of the membrane bound modulator protein with the N-terminal region of the cytoplasmic kinase (Mijakovic, Poncet et al. 2003; Grangeasse, Terreux et al. 2009). More specifically, it has been demonstrated that the presence of a hydrophobic residue (such as the phenylalanine at position 221 of the modulator CapA from *S. aureus*) within the C-terminal of the modulator protein stimulates the affinity of the BY-kinase for ATP (Soulat, Jault et al. 2006; Olivares-Illana, Meyer et al. 2008), thus providing a source of phosphate with which target proteins may be modified.

#### *1.2.3.4 Bacterial tyrosine phosphatases*

Bacterial tyrosine phosphatases have been identified within a number of different families, including the manganese-dependent superfamily and the protein tyrosine phosphatase superfamily. Manganese-dependent protein phosphatases have been categorised into three major groups which are called the phosphoprotein phosphatases

(PPP), the $Mg^{2+}$ or $Mn^{2+}$ dependent protein phosphatases (PMP) and the polymerase and histidinol phosphatases (PHP) (Shi 2004). Members of the PPP family were originally identified in eukaryotes, but bacterial members have since been identified. These phosphatases can be identified according to their signature motif (GDXHG – GDXXDRG – GNH[D/E]) (Shi 2004). Members of this group, such as PrpE from *B. subtilis*, have been found to target tyrosine residues (Iwanicki, Herman-Antosiewicz et al. 2002). Members of the PMP group were also originally identified in eukaryotes. As with the PPP group, the activity of members of the PMP group is dependent on the presence of metallo-co-factors. However, to date members of the PMP group have been shown to target phosphorylated threonine and serine residues only, and not tyrosine residues (Cozzone, Grangeasse et al. 2004; Shi 2004). Members of the PHP group have only been identified in prokaryotes, and more specifically only in Gram-positive bacteria. Furthermore, members of this group have been found only to target phosphorylated tyrosine residues (Cozzone, Grangeasse et al. 2004; Shi 2004). Phosphatases belonging to the PHP group are defined by their signature motif containing 5 conserved histidine residues and 2 aspartic acid residues (Shi 2004; Mijakovic, Musumeci et al. 2005). Deletion of any of the conserved amino acids results in a significant loss of phosphatase activity (Mijakovic, Musumeci et al. 2005). Members of the PHP group include CapC from *S. aureus* (Cozzone, Grangeasse et al. 2004), PtpZ from *B. subtilis* (Mijakovic, Poncet et al. 2003; Mijakovic, Musumeci et al. 2005) and CpsB from *S. pneumoniae* (Morona, Morona et al. 2002). Although members of the PHP group appear to exclusively target phosphorylated tyrosine residues, they must not be confused with the protein tyrosine phosphatase (PTP) group. Members of the PTP group are characterised by the presence of the $CX_5R$ motif, and in addition they are not susceptible to the same phosphatase inhibitors that can target members of the

PHP group (Mijakovic, Musumeci et al. 2005). A sub-class of the PTP group has also been described. These are known as the low-molecular weight tyrosine phosphatases (LMW-PTP). These phosphatases also possess the characteristic $CX_5R$ motif, however as the name suggests, these proteins are of a low molecular weight (Shi 2004). Members of this family have been shown to regulate the production of polysaccharides, for example Wzb from *E. coli* which regulates colanic acid production (Vincent, Duclos et al. 2000).

#### *1.2.3.5 Bacterial tyrosine phosphorylation by* B. subtilis

*B. subtilis* encodes one confirmed and one predicted BY-kinase known as PtkA and EpsB, respectively. PtkA is a confirmed and promiscuous BY-kinase (Mijakovic, Poncet et al. 2003; Jers, Pedersen et al. 2010). Consistent with the fact that *B. subtilis* is a Gram-positive organism, PtkA must interact with the bacterial tyrosine modulator TkmA in order to phosphorylate its specific targets (Mijakovic, Poncet et al. 2003). *B. subtilis* also possesses three bacterial protein tyrosine phosphatases. First, there is PtpZ which, as previously mentioned, belongs to the polymerase and histidinol phosphatase (PHP) family and functions to dephosphorylate the targets of PtkA (Mijakovic, Poncet et al. 2003; Mijakovic, Musumeci et al. 2005). Second, *B. subtilis* possesses two tyrosine phosphatases belonging to the LMW-PTP family known as YwlE and YfkJ. It should be noted that YwlE and YfkJ modulate a distinct set of targets from PtpZ (Mijakovic, Petranovic et al. 2005; Musumeci, Bongiorni et al. 2005).

It has been previously demonstrated that PtkA (in partnership with TkmA) and PtpZ act to modulate the activity of a UDP-glucose dehydrogenase, called Ugd (Mijakovic,

Poncet et al. 2003). Furthermore, PtkA and PtpZ are also able to regulate the activity of TuaD, a homologue of Ugd which is active under phosphate limiting conditions (Mijakovic, Poncet et al. 2003) (Figure 1-15). The regulation of Ugd influences the production of teichuronic acid; a component of the cell wall.

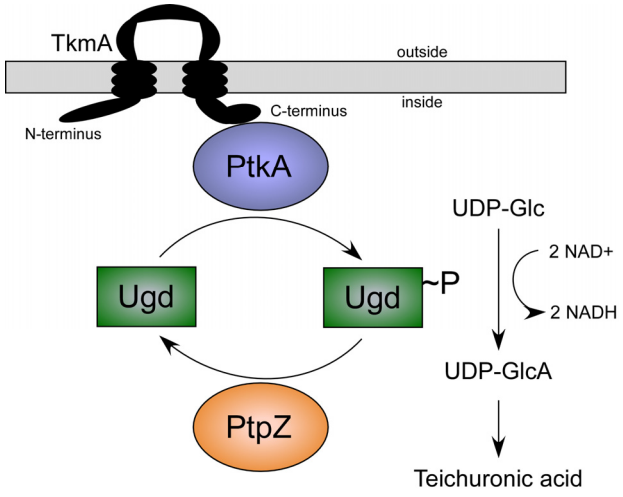


**Figure 1-15: PtkA and PtpZ regulate teichuronic acid biosynthesis**
Schematic representation of the regulation of Ugd activity through phosphorylation. Cell membrane is depicted by a grey bar. UDP-Glc, UDP-glucose; UDP-GlcA, UDP-glucuronate.

In addition to PtkA, *B. subtilis* also encodes a predicted BY-kinase called EpsB (also known as PtkB and previously as YveL). EpsB is encoded by the 15 gene operon *epsA-O* that is required for the production of a secreted exopolysaccharide needed for biofilm formation (Figure 1-1) (Branda, Gonzalez-Pastor et al. 2001; Mijakovic, Poncet et al. 2003). When over-expressed in *E. coli*, phosphorylated tyrosine could be detected within EpsB (Mijakovic, Poncet et al. 2003); however, EpsB was unable to accumulate detectable levels of phosphorylation when incubated with radiolabelled ATP (Mijakovic, Poncet et al. 2003). In addition, an *in vivo* role for EpsB is yet to be established. Thus it is unclear whether EpsB is a functional BY-kinase like its homologue PtkA.

## *1.3 Project Aims*

The overall aim of my project was to understand at the molecular level how DegU controls biofilm formation by *B. subtilis*. Initial experiments led to the discovery that DegU and SinR co-regulate a novel group of genes during biofilm formation. As such, I investigated their impact on biofilm formation and surface adhesion. Through this initial study, it was discovered that *ptpZ*, a DegU and SinR co-regulated gene encoding a protein tyrosine phosphatase, was required for the formation of robust biofilms by *B. subtilis*. From this point forward, the aim of my project was to understand the involvement of post-translational modifications, in particular protein tyrosine phosphorylation, during biofilm formation.

# 2 Materials and Methods

## 2.1 Bacterial strains used in this study

**Table 2-1 Bacterial strains used in this study**

| Strain | Relevant Genotype [a] | Source / Construction [b] |
|---|---|---|
| NCIB3610 | Prototroph | Bacillus Genetic Stock Center |
| JH642 | *trpC2 pheA1* | (Hoch and Anagnostopoulos 1970) |
| 168 | *trpC2* | (Burkholder and Giles 1947) |
| 3610 derived strains | | |
| NRS1389 | *ywfB*::pNW33 (*cml*) | SPP1 NRS1377 → NCIB3610 |
| NRS1499 | Δ*degSU* (*spc*) | (Kiley and Stanley-Wall 2010) |
| NRS1684 | Δ*sinR* (*cml*) | SPP1 BAL2423 → NCIB3610 |
| NRS1686 | Δ*sinR* (*cml*) Δ*degSU* (*spc*) | SPP1 BAL2423 → NRS1499 |
| NRS1808 | *yvyE*::pBL193 (*cml*) | (Stanley and Lazazzera 2005) |
| NRS1826 | *yueH*::pNW300 (*cml*) | SPP1 NRS1815 → NCIB3610 |
| NRS1827 | *ptpZ*::pNW301 (*cml*) | SPP1 NRS1816 → NCIB3610 |
| NRS1828 | *ybfP*::pNW302 (*cml*) | SPP1 NRS1817 → NCIB3610 |
| NRS1829 | *yomI*::pNW303 (*cml*) | SPP1 NRS1818 → NCIB3610 |
| NRS1830 | *yvfO*::pNW304 (*cml*) | SPP1 NRS1819 → NCIB3610 |
| NRS1831 | *ywbC*::pNW305 (*cml*) | SPP1 NRS1820 → NCIB3610 |
| NRS1832 | Δ*yfmH* (*cml*) | SPP1 NRS1821 → NCIB3610 |
| NRS1833 | Δ*yulD* (*cml*) | SPP1 NRS1822 → NCIB3610 |
| NRS1842 | Δ*yvfG* (*cml*) | SPP1 NRS1825 → NCIB3610 |
| NRS1843 | Δ *degSU* (*spc*) + yvyE::pBL193 (*cml*) | SPP1 NRS1243 → NRS1499 |
| NRS1844 | Δ *degSU* (*spc*) + *yueH*::pNW300 (*cml*) | SPP1 NRS1815 → NRS1499 |
| NRS1845 | Δ *degSU* (*spc*) + *ptpZ*::pNW301 (*cml*) | SPP1 NRS1816 → NRS1499 |
| NRS1846 | Δ *degSU* (*spc*) + *ybfP*::pNW302 (*cml*) | SPP1 NRS1817 → NRS1499 |
| NRS1847 | Δ *degSU* (*spc*) + *yomI*::pNW303 (*cml*) | SPP1 NRS1818 → NRS1499 |

| Strain | Relevant Genotype [a] | Source / Construction [b] |
|---|---|---|
| NRS1848 | Δ *degSU* (*spc*) + *yvfO*::pNW304 (*cml*) | SPP1 NRS1819 → NRS1499 |
| NRS1849 | Δ*degSU* (*spc*) + *ywbC*::pNW305 (*cml*) | SPP1 NRS1820 → NRS1499 |
| NRS1851 | Δ *degSU* (*spc*) + Δ*yulD* (*cml*) | SPP1 NRS1822 → NRS1499 |
| NRS1852 | Δ *degSU* (*spc*) + Δ*yvfG* (*cml*) | SPP1 NRS1825 → NRS1499 |
| NRS1857 | Δ *degSU* (*spc*) + Δ*yfmH* (*cml*) | SPP1 NRS1821 → NRS1499 |
| NRS1859 | Δ*sinR* (*kan*) | (Kiley and Stanley-Wall 2010) |
| NRS1860 | Δ*sinR* (*kan*) Δ*degSU* (*spc*) | (Kiley and Stanley-Wall 2010) |
| NRS1874 | Δ *degSU* (*spc*) + *yueH*::pNW300 (*cml*) + Δ*sinR* (*kan*) | SPP1 NRS1858 → NRS1844 |
| NRS1875 | Δ *degSU* (*spc*) + *ptpZ*::pNW301 (*cml*) + Δ*sinR* (*kan*) | SPP1 NRS1858 → NRS1845 |
| NRS1876 | Δ *degSU* (*spc*) + *ybfP*::pNW302 (*cml*) + Δ*sinR* (*kan*) | SPP1 NRS1858 → NRS1846 |
| NRS1877 | Δ *degSU* (*spc*) + *yomI*::pNW303 (*cml*) + Δ*sinR* (*kan*) | SPP1 NRS1858 → NRS1847 |
| NRS1878 | Δ *degSU* (*spc*) + *yvfO*::pNW304 (*cml*) + Δ*sinR* (*kan*) | SPP1 NRS1858 → NRS1848 |
| NRS1879 | Δ *degSU* (*spc*) + *ywbC*::pNW305 (*cml*) + Δ*sinR* (*kan*) | SPP1 NRS1858 → NRS1849 |
| NRS1880 | Δ *degSU* (*spc*) + Δ*yulD* (*cml*) + Δ*sinR* (*kan*) | SPP1 NRS1858 → NRS1851 |
| NRS1881 | Δ *degSU* (*spc*) + Δ*yvfG* (*cml*) + Δ*sinR* (*kan*) | SPP1 NRS1858 → NRS1852 |
| NRS1883 | Δ *degSU* (*spc*) + Δ*yfmH* (*cml*) + Δ*sinR* (*kan*) | SPP1 NRS1858 → NRS1857 |
| NRS2222 | Δ*ptpZ* | (Kiley and Stanley-Wall 2010) |
| NRS2227 | Δ*ytcA* (*kan*) | (Kiley and Stanley-Wall 2010) |
| NRS2467 | Δ*ptpZ* + *amyE*::$P_{spank-hy}$- *ptpZ-lacI* (*spc*) | (Kiley and Stanley-Wall 2010) |
| NRS2468 | Δ*ptpZ* + *amyE*::$P_{spank-hy}$- *ptpZ* ($H^{196}A$)-*lacI* (*spc*) | (Kiley and Stanley-Wall 2010) |
| NRS2471 | Δ*ugd* | (Kiley and Stanley-Wall 2010) |
| NRS2544 | Δ*ptkA* | (Kiley and Stanley-Wall 2010) |
| NRS2795 | *ptkA* $D^{83}A$ | (Kiley and Stanley-Wall 2010) |
| NRS2796 | *ptkA* $D^{81}A$-$D^{83}A$ | (Kiley and Stanley-Wall 2010) |
| NRS2799 | *ptkA* $Y^{225}A$-$Y^{227}A$-$Y^{228}A$ | (Kiley and Stanley-Wall 2010) |
| NRS2804 | Δ*ptkA* + *amyE*::$P_{spank-hy}$-*ptkA-lacI* (*spc*) | (Kiley and Stanley-Wall 2010) |
| NRS2807 | *ptkA* $D^{81}A$-$D^{83}A$ + *amyE*::$P_{spank-hy}$-*ptkA-lacI* (*spc*) | (Kiley and Stanley-Wall 2010) |
| NRS2810 | *ptkA* $Y^{225}A$-$Y^{227}A$-$Y^{228}A$ + *amyE*::$P_{spank-hy}$-*ptkA-lacI* (*spc*) | SPP1 NRS2801→ NRS2799 |
| NRS2821 | Δ*ugd* + Δ*ytcA* (*kan*) | SPP1 NRS2059 → NRS2471 |

| Strain | Relevant Genotype [a] | Source / Construction [b] |
|---|---|---|
| NRS3076 | *sacA*::$P_{hag}$-*yfp* (*kan*) | SPP1 NRS3070 → NCIB3610 |
| NRS3201 | *ahpF*::pNW361(*cml*) | SPP1 NRS2858→ NCIB3610 |
| NRS3205 | *icd*::pNW365 (*cml*) | SPP1 NRS2862→ NCIB3610 |
| NRS3210 | *lctE*::pNW370 (*cml*) | SPP1 NRS2867→ NCIB3610 |
| NRS3211 | *oppA*::pNW558 (*cml*) | SPP1 NRS2868→ NCIB3610 |
| NRS3212 | *rocA*::pNW371 (*cml*) | SPP1 NRS2869→ NCIB3610 |
| NRS3213 | *yjoA*::pNW372 (*cml*) | SPP1 NRS2870→ NCIB3610 |
| NRS3214 | *ynfE*::pNW560 (*cml*) | SPP1 NRS3197→ NCIB3610 |
| NRS3215 | *yorK*::pNW559 (*cml*) | SPP1 NRS3198→ NCIB3610 |
| NRS3216 | *yvyG*::pNW373 (*cml*) | SPP1 NRS3199→ NCIB3610 |
| NRS3229 | Δ*ugd* + *tuaD*::pNW377 (*cml*) | SPP1 NRS3227→ NRS2471 |
| NRS3230 | Δ*ytcA* (*kan*) + *tuaD*::pNW377 (*cml*) | SPP1 NRS3227→ NRS2227 |
| NRS3231 | Δ*ugd* + Δ*ytcA* (*kan*) + *tuaD*::pNW377 (*cml*) | (Kiley and Stanley-Wall 2010) |
| NRS3232 | *tuaD*::pNW377 (*cml*) | (Kiley and Stanley-Wall 2010) |
| NRS3241 | Δ*ptkA* + *sacA*::$P_{hag}$-*yfp* (*kan*) | SPP1 NRS3070→ NRS2544 |
| NRS3243 | *ptkA* $D^{81}A$-$D^{83}A$ + *sacA*::$P_{hag}$-*yfp* (*kan*) | SPP1 NRS3070→ NRS2796 |
| NRS3244 | *ptkA* $Y^{225}A$-$Y^{227}A$-$Y^{228}A$ + *sacA*::$P_{hag}$-*yfp* (*kan*) | SPP1 NRS3070→NRS2799 |
| NRS3248 | *ptkA* $Y^{225}A$-$Y^{227}A$-$Y^{228}A$ + *amyE*::$P_{spank-hy}$-*ptkA -lacI* (*spc*) + *sacA*::$P_{hag}$-*yfp* (*kan*) | SPP1 NRS3070→NRS2810 |
| NRS3528 | Δ*tkmA*Δ*ptkA* | (Kiley and Stanley-Wall 2010) |
| NRS3535 | Δ*tkmA*Δ*ptkA* + *amyE*::$P_{spank-hy}$-*tkmA -lacI* (*spc*) | (Kiley and Stanley-Wall 2010) |
| NRS3536 | Δ*tkmA*Δ*ptkA* + *amyE*::$P_{spank-hy}$-*tkmA ptkA-lacI* (*spc*) | (Kiley and Stanley-Wall 2010) |
| NRS3537 | Δ*tkmA*Δ*ptkA* + *amyE*::$P_{spank-hy}$-*ptkA -lacI* (*spc*) | (Kiley and Stanley-Wall 2010) |
| NRS3541 | Δ*tkmA* | (Kiley and Stanley-Wall 2010) |
| NRS3544 | Δ*tkmA* + *amyE*::$P_{spank-hy}$-*tkmA-lacI* (*spc*) | (Kiley and Stanley-Wall 2010) |
| NRS3557 | *ptkA* $Y^{225}E$- $Y^{227}E$- $Y^{228}E$ | pNW391 → NCIB3610 |
| NRS3563 | *ptkA* $Y^{225}E$- $Y^{227}E$- $Y^{228}A$ | pNW390 → NCIB3610 |
| NRS3566 | *ptkA* $Y^{225}F$- $Y^{227}F$- $Y^{228}F$ | pNW393 → NCIB3610 |
| NRS3570 | Δ*yvyG* | pNW399 → NCIB3610 |
| NRS3571 | *yvyG* $Y^{49}A$ | pNW801 → NCIB3610 |
| NRS3573 | *ptkA* $Y^{225}A$- $Y^{227}A$- $Y^{228}E$ | pNW396→ NCIB3610 |

| Strain | Relevant Genotype [a] | Source / Construction [b] |
|---|---|---|
| NRS3576 | *ptkA* $Y^{225}F$- $Y^{227}F$- $Y^{228}F$ + *amyE*::$P_{spank\text{-}hy}$-*ptkA* - *lacI* (*spc*) | SPP1 NRS2801 → NRS3566 |
| NRS3577 | *ptkA* $Y^{225}F$- $Y^{227}F$- $Y^{228}F$ + *amyE*::$P_{spank\text{-}hy}$-*ptkA* $Y^{225}A$- $Y^{227}A$- $Y^{228}A$ - *lacI* (*spc*) | SPP1 NRS3221 → NRS3566 |
| NRS3578 | Δ*yvyG* + *amyE*::$P_{spank\text{-}hy}$-*yvyG* - *lacI* (*spc*) | SPP1 NRS3256 → NRS3570 |
| NRS3579 | *ptkA* $Y^{225}F$- $Y^{227}F$- $Y^{228}F$ + *amyE*::$P_{spank\text{-}hy}$-*ptkA* $D^{81}A$ – $D^{83}A$ - *lacI* (*spc*) | SPP1 NRS3220 → NRS3566 |
| NRS3585 | *ptkA* $Y^{225}E$- $Y^{227}A$- $Y^{228}A$ | pNW803→ NCIB3610 |
| JH642 derived strains | | |
| BAL1806 | Δ*degSU* (*spc*) | (Stanley and Lazazzera 2005) |
| NRS1377 | *ywfB*::pNW33 (*cml*) | pNW33 → JH642 |
| NRS1815 | *yueH*::pNW300 (*cml*) | pNW300 → JH642 |
| NRS1816 | *ptpZ*::pNW301 (*cml*) | pNW301 → JH642 |
| NRS1817 | *ybfP*::pNW302 (*cml*) | pNW302 → JH642 |
| NRS1818 | *yomI*::pNW303 (*cml*) | pNW303 → JH642 |
| NRS1819 | *yvfO*::pNW304 (*cml*) | pNW304 → JH642 |
| NRS1820 | *ywbC*::pNW305 (*cml*) | pNW305 → JH642 |
| NRS1821 | Δ*yfmH* (*cml*) | *yfmH* (*cml*) PCR → JH642 [c] |
| NRS1822 | Δ*yulD* (*cml*) | *yulD* (*cml*) PCR → JH642 [c] |
| NRS1825 | Δ*yvfG* (*cml*) | *yvfG* (*cml*) PCR→ JH642 [c] |
| NRS1858 | Δ*sinR* (*kan*) | Δ*sinR* PCR → JH642[c] |
| NRS2059 | Δ*ytcA* (*kan*) | *ytcA* (*kan*) PCR→ JH642 [c] |
| NRS2173 | *amyE*::$P_{spank\text{-}hy}$-*ptpZ* - *lacI* (*spc*) | pNW312 → JH642 |
| NRS2193 | *amyE*::$P_{spank\text{-}hy}$-*ptpZ* (H196A) - *lacI* (*spc*) | pNW316 → JH642 |
| 168 derived strains | | |
| NRS2535 | pNW341 | pNW341 → 168 |
| NRS2540 | pNW349 | pNW349 → 168 |
| NRS2541 | pNW348 | pNW348 → 168 |
| NRS2801 | *amyE*::$P_{spank\text{-}hy}$- *ptkA* - *lacI* (*spc*) | pNW351 → 168 |
| NRS2858 | *ahpF*::pNW361 (*cml*) | pNW361 → 168 |
| NRS2862 | *icd*::pNW365 (*cml*) | pNW365 → 168 |
| NRS2867 | *lctE*::pNW370 (*cml*) | pNW370 → 168 |

| Strain | Relevant Genotype [a] | Source / Construction [b] |
|---|---|---|
| NRS2868 | *oppA*::pNW558 (*cml*) | pNW558 → 168 |
| NRS2869 | *rocA*::pNW371 (*cml*) | pNW371 → 168 |
| NRS2870 | *yjoA*::pNW372 (*cml*) | pNW372 → 168 |
| NRS3070 | *sacA*::$P_{hag}$-*yfp* (*kan*) | pNW546 → 168 |
| NRS3197 | *ynfE*::pNW560 (*cml*) | pNW560 → 168 |
| NRS3198 | *yorK*::pNW559 (*cml*) | pNW559 → 168 |
| NRS3199 | *yvyG*::pNW373 (*cml*) | pNW373 → 168 |
| NRS3227 | *tuaD*::pNW377 (*cml*) | pNW377 → 168 |
| NRS3255 | *amyE*::$P_{spank-hy}$- *tkmA* - *lacI* (*spc*) | pNW382 → 168 |
| NRS3256 | *amyE*::$P_{spank-hy}$- *yvyG* - *lacI* (*spc*) | pNW382 → 168 |
| NRS3265 | *amyE*::$P_{spank-hy}$-*tkmA ptkA* - *lacI* (*spc*) | pNW388 → 168 |

[a] Antibiotic resistance cassettes are indicated as follows: *cml*, Chloramphenicol resistance; *spc*, Spectinomycin resistance; *kan*, Kanamycin resistance.
[b] Arrow indicates direction of strain construction. Plasmids (DNA) and SPP1 (phage) were used to transform or transduce the recipient strain noted above.
[c] Strains containing double-crossover mutations were constructed by transformation with PCR fragment.

## 2.2 *Table of Oligonucleotides*

**Table 2-2 Oligonucleotides used in this study.**

| Primer | Target | Sequence[a] | Position[b] |
|---|---|---|---|
| RT-PCR analysis of novel DegU/SinR co-regulated genes | | | |
| NSW122 | *yomI* | CGATGGATCCCTCAACTCCCTCAAGCTC | +100 → +117 |
| NSW123 | *yomI* | CGATGGATCCCCTGTCCTAGTTTCTCAGTGG | +380 → +400 |
| NSW126 | *yvfO* | CGATGGATCCCAGAGCTTCGGGCAGA | +101 → +116 |
| NSW127 | *yvfO* | CGATGGATCCTGAGATTAGCCCAGG | +464 → +479 |
| NSW128 | *ywbC* | CGATGGATCCGACCATACAGGCATCATGG | +16 → +34 |
| NSW129 | *ywbC* | CGATGGATCCGCTCGATTACACCGTTCG | +110 → +127 |

| Primer | Target | Sequence[a] | Position[b] |
|---|---|---|---|
| NSW130 | *ptpZ* | CGATGGATCCGCGACACCTCATCAT | +115 → +129 |
| NSW131 | *ptpZ* | CGATGGATCCACAGCAAGGACGGGT | +437 → +451 |
| RT-PCR analysis of *tkmA* operon | | | |
| NSW57 | *veg* | CGAAGACGTTGTCCGATATTAAAAG | +5 → +29 |
| NSW58 | *veg* | CAACAGTCTCAGTCAAAATATCAGC | +193 → +217 |
| NSW130 | *ptpZ* | As above | As above |
| NSW131 | *ptpZ* | As above | As above |
| NSW163 | *tkmA* | GGGAGAATCTACAAGCTTAAAAGAG | +3 → +27 |
| NSW164 | *tkmA* | CGTTTTCATCCCTGACTGATATGTT | +355 → +379 |
| NSW165 | *ugd* | TCTCTTTCTGAGATTGGACATCATG | +52 → +76 |
| NSW166 | *ugd* | CTATAAAAATGATGTCTGCCTGTGC | +223 → +247 |
| *tkmA* operon analysis | | | |
| NSW163 | *tkmA* | As above | As above |
| NSW164 | *tkmA* | As above | As above |
| NSW165 | *ugd* | As above | As above |
| NSW195 | *ptpZ* | GGCTAGGACATGATCGCTATTCACTGTCACATT | -9 → +24 |
| NSW220 | *ugd* | GCATCCCGGGCACTGTGCTTTTCGTTACCAC | +346 → +366 |
| NSW249 | *ptpZ* | CCGGGAGCTCGAATTCTTTCTCTAGAACATAAAGAGCCTCTTGA | +615 → +625 |
| *tkmA* 5'RACE analysis | | | |
| NSW227 | *tkmA* | GGGCTCTTAATGATGACA | +234 → +251 |
| NSW228 | *tkmA* | GGGTGTAAGTGCGAAGAAA | +108 → +126 |
| NSW367 | Poly-C tail | GGCCACGCGTCGACTAGTACGGGUGGGUGGGUG | N/A |
| EMSA analysis of tkmA promoter region | | | |
| NSW146 | *tkmA* | CGATGAATTCCTAAAAAAGGACATAAAA | -500 → -479 |

| Primer | Target | Sequence[a] | Position[b] |
|---|---|---|---|
| NSW147 | *tkmA* | CGATGGATCCTAACGTTGATAATATC | +27 → +42 |
| NSW163 | *tkmA* | As above | As above |
| NSW164 | *tkmA* | As above | As above |
| NSW61 | *aprE* | GGTAAAGCCTATGAATTCTC | -620 → - 601 |
| NSW654 | *aprE* | GATCCACAATTTTTTGCT | +87 → +104 |
| NSW50 | *yqxM* | TGGCGAATTCATAGACAAATCACACATTGTTTGATCA | -312 → - 276 |
| NSW51 | *yqxM* | GCCAGAATTCGGATCCATCTTACCTCCTGTAAAACACTGTAA | -26 → +16 |
| Construction of insertional mutations | | | |
| NSW33 | *ywfB* | CGAGGCGAATTCACAAGCAGTGAGTACGCA | +91 → +108 |
| NSW34 | *ywfB* | GTCTCTGAATTCAAAATCAGGACGAACAGC | +325 → +354 |
| NSW120 | *ybfP* | CGATGGATCCCGGCATGTCGGTT | +138 → +150 |
| NSW121 | *ybfP* | CGATGGATCCTGTTCGGTATGCTCCTGG | +298 → +315 |
| NSW122 | *yomI* | As above | As above |
| NSW123 | *yomI* | As above | As above |
| NSW124 | *yueH* | CGATGGATCCCGCAAACCGGAATGATC | +29 → +45 |
| NSW125 | *yueH* | CGATGGATCCCAGGCAGAGTTGATTTAT | +140 → +157 |
| NSW126 | *yvfO* | As above | As above |
| NSW127 | *yvfO* | As above | As above |
| NSW128 | *ywbC* | As above | As above |
| NSW129 | *ywbC* | As above | As above |
| NSW130 | *ptpZ* | As above | As above |
| NSW131 | *ptpZ* | As above | As above |
| NSW132 | *yvfG* | GGAGTTTTGCCAAAACAGCCTCCG | -505 → -484 |
| NSW133 | *yvfG* | GTTATCCGCTCACAATTCAGACATTTCTTTGGC | -9 → +6 |
| NSW134 | *yvfG* | CGTCGTGACTGGGAAACAATCAAAATAAACCTTCC | +209 → +226 |

| Primer | Target | Sequence[a] | Position[b] |
|---|---|---|---|
| NSW135 | *yvfG* | TTTTCTCCAAACGCTGAACGTCTTGA | +510 → +535 |
| NSW136 | *yfmH* | CACCATAGAGGCGATGGTTGTCGAATTGG | -326 → -298 |
| NSW137 | *yfmH* | GTTATCCGCTCACAATTCCTCATGGTTTTCCC | -9 → +5 |
| NSW138 | *yfmH* | CGTCGTGACTGGGAAACGAAAAATGGTAAACACTTAG | +61 → +80 |
| NSW139 | *yfmH* | GAAACTAAATCATCCGGATCCCTGGGTTAGATTGA | +435 → +454 |
| NSW140 | *yulD* | GCCATCATCTATGCGATAGCCATCAAAGA | -356 → -328 |
| NSW141 | *yulD* | GTTATCCGCTCACAATTCGGCTTTTCTTTTCAAACCTT | -5 → +15 |
| NSW142 | *yulD* | CGTCGTGACTGGGAAACGGATTGAAAAAC | +309 → +320 |
| NSW143 | *yulD* | CGCATGCAGGTTTACGCGGTGC | +601 → +622 |
| NSW148 | *sinR* | CAGGCGCTGAAAACCTTGTATCAACC | -479 → -454 |
| NSW149 | *sinR* | ATCACCTCAAATGGTTCGCTGCCAATCAATGTCATCACCTTCC | -14 → +9 |
| NSW150 | *sinR* | CGAGCGCCTACGAGGAATTTGTATCGGGCGTAGTGCCTGAGCA GAG | +331 → +349 |
| NSW151 | *sinR* | GATGCAGCGGCTGCTGAAAAATC | +756 → +779 |
| NSW298 | *ahpF* | CGAT CTGCAG ACC AAA AAG TCA TTG ATC AGG | +310 → +331 |
| NSW299 | *ahpF* | CGAT GAATTC TTT GTC AGC AAA CTC AGA TGC | +598 → +618 |
| NSW602 | *ytcA* | GGCAAAAGGCTGTCCTCCTGC | -540 → -520 |
| NSW603 | *ytcA* | ATCACCTCAAATGGTTCGCTCACACAAATTTTCATCACCTGA | -7 → +15 |
| NSW604 | *ytcA* | CGAGCGCCTACGAGGAATTTGTATCGGCGTCCATGAAAATACTC GTCACA | +1279 → +1301 |
| NSW605 | *ytcA* | GCCGGTGAAAAGCCATATC | +1842 → +1860 |
| NSW904 | *sdhA* | GCAT CTGCAG AGA ATT CAT TCA AAT CCA CCC G | +690 → +711 |
| NSW905 | *sdhA* | GCAT GGATCC AAG CTT AAT ATC AAG CTC TTT CGG | +952 → +975 |
| NSW906 | *icd* | GCAT CTGCAG ATATTTCATCGCGATTAAAGGCC | +255 → +277 |
| NSW907 | *icd* | GCAT GGATCC TCG ATC GCA TAA TCA ATG GC | +610 → +629 |
| NSW916 | *lctE* | GCAT CTGCAG ATC GTT AGT GAA GTC ATG GC | +316 → +355 |

| Primer | Target | Sequence[a] | Position[b] |
|---|---|---|---|
| NSW917 | *lctE* | GCATGGATCCTTCTCAATGATATGGTAAGCTGC | +664 → +686 |
| NSW918 | *oppA* | GCATGTCGACAATGATTCAGTATCAGGCGG | +175 → +194 |
| NSW919 | *oppA* | GCATGGATCCCAGTGAAATATGGAGTCGGG | +528 → +547 |
| NSW920 | *rocA* | GCATCTGCAGCTGGAAAAAACAAAGACCGG | +263 → +283 |
| NSW921 | *rocA* | GCATGGATCCGTAATGATATTGATTGACCTCGC | +485 → +506 |
| NSW922 | *yjoA* | GCATCTGCAGCAATCCAATCAAATTGTCAGCC | +7 → +28 |
| NSW923 | *yjoA* | GCATGGATCCATGTCAGATCAATTTCTCTGTCC | +303 → +325 |
| NSW924 | *ynfE* | GCATGTCGACGAAATACTGAAACAGTATATGGTGC | +7 → +31 |
| NSW925 | *ynfE* | GCATGGATCCGTGTTGTCAATCCATAATAAACGG | +230 → +253 |
| NSW926 | *yorK* | GCATGTCGACTGCAGATTGTCTTATCAGGC | +153 → +172 |
| NSW927 | *yorK* | GCATGGATCCCTGTGCCTCTCTTATTAAGAGC | +400 → +420 |
| NSW928 | *yvyG* | GCATCTGCAGGGCAATTATTGAACAATTGAAGCG | +12 → +35 |
| NSW929 | *yvyG* | GCATGGATCCGTATAGTTGTTCCAGCTCTTCC | +264 → +285 |
| NSW930 | *yxxG* | GCATCTGCAGGTATAGAACTTGAATTAACACCGAG | +23 → +47 |
| NSW931 | *yxxG* | GCATGGATCCCGAACAAGTTGGAGTTCGAC | +318 → +337 |
| NSW934 | *tuaD* | CCCTGAATTCCTTCGGGAAG | +450 → +469 |
| NSW935 | *tuaD* | CGATGGATCCGATCGTATGCTTTTACATGGGCG | +1029 → +1051 |
| Complementation of mutant strains | | | |
| NSW172 | *ptpZ* | GGATGTCGACCATCGTGAAAGTTATTTATTT | -44 → -24 |
| NSW173 | *ptpZ* | GGATGCATGCGAATCGGCTGTTAAAAAAACC | +754 → +775 |
| NSW258 | *ptkA* | GCATGTCGACGAAAACAGCAAAGACCTTACAGGG | -56 → +33 |
| NSW259 | *ptkA* | GCATGCATGCGCACGTTATTTATTTTTGCATGAAATTGTCC | +693 → +723 |
| NSW940 | *yvyG* | GCATGTCGACAAGCAATAAAAAAGGAGAAAGCCC | -34 → -1 |
| NSW941 | *yvyG* | GCATGCATGCAATTCCTTTCTGCTAAGCTTTTGAATC | +469 → +505 |
| NSW948 | *tkmA* | GCATGTCGACCTGTCAACACAGTAAATATAGCGC | -167 → -134 |

| Primer | Target | Sequence[a] | Position[b] |
|---|---|---|---|
| NSW949 | *tkmA* | GCATGCATGCGAGCCTCTGTTTTTTCTAAGCG | +741 → +772 |
| Construction of in-frame deletion strains | | | |
| NSW218 | *ptpZ* | GCATGTCGACATCGATCATGTCCTAGCCCCC | -12 → +9 |
| NSW219 | *ptpZ* | GCATGTCGACGGTTTTTTTTAACAGCCGATTCTC | +754 → +777 |
| NSW220 | *ptpZ* | GCATCCCGGGCACTGTGCTTTTCGTTACCAC | +1305 → +1325 |
| NSW221 | *ugd* | GCATGGATCCGGCAAGCAGCTGAAAGCA | -446 → -429 |
| NSW222 | *ugd* | GCATGTCGACGACTGTTATATTCATTGTTTCCCTCCA | -12 → +15 |
| NSW223 | *ugd* | GCATGTCGACGGTGCAATTCAATAGATGAAAAAG | +1309 → +1332 |
| NSW225 | *ptpZ* | GCATGGATCCGGAGTGGACATTTTGGCGCT | -776 → 759 |
| NSW226 | *ugd* | GCATCCCGGGGCGTATCCGCCAATTTTAT | +2092 → +2110 |
| NSW246 | *ptkA* | GGGCGATATCGGATCCGCATACTTTTGATTATGATTGTAACCGCG | -697 → -659 |
| NSW247 | *ptkA* | GCATAAGCTTCAAAATGTCCACTCCCCGTTTTTT | -21 → +13 |
| NSW248 | *ptkA* | CGATAAGCTTCAAAAATAAATAACGTGCATCGTGCCC | +696 → +732 |
| NSW249 | *ptkA* | CCGGGAGCTCGAATTCTTTCTCTAGAACATAAAGAGCCTCTTGA | +1381 → +1418 |
| NSW936 | *yvyG* | GCATGGATCCATCAGGCAGAAGCGAATTCAG | -588 → -558 |
| NSW937 | *yvyG* | GCATTCTAGAAATAATTGCCTTCGCTGACATG | +92 → +123 |
| NSW938 | *yvyG* | GCATTCTAGACTGTTTGATTCAAAAGCTTAGCAGAAAG | +453 → +490 |
| NSW939 | *yvyG* | GCATGTCGACCAACACAGTTGTATTTAGCTCTGC | +1104 → +1137 |
| NSW944 | *tkmA* | GCATGAATTCTTAACTGTTCAGCAGATGCCAG | -645 → -614 |
| NSW945 | *tkmA* | GCATAAGCTTTGTAGATTCTCCCATGATACCTCC | -9 → +25 |
| NSW950 | *tkmA* | GCATGGATCCTTGCTTTTGCACGTTGCAAG | +1340 → +1369 |
| NSW961 | *tkmA* | TCGAAAGCTTTAGTGAAAAAACGGGGAGTGGACATTTTGGCG | +701 → +742 |
| Construction of Point Mutations | | | |
| NSW205 | *ptpZ* $H^{196}A$ | GTAGCCTCAGATGCCGCTAATGTGAAAACGAGA | +571 → +603 |
| NSW206 | *ptpZ* $H^{196}A$ | TCTCGTTTTCACATTAGCGGCATCTGAGGCTAC | +603 → +571 |

| Primer | Target | Sequence[a] | Position[b] |
|---|---|---|---|
| NSW246 | *ptkA*[c] | As above | As above |
| NSW249 | *ptkA*[c] | As above | As above |
| NSW250 | *ptkA* $D^{81}A$-$D^{83}A$ | AAAGTGCTCCTGATTGCTGCTGCTTTGCGAAAACCAACA | +226 → +264 |
| NSW251 | *ptkA* $D^{81}A$-$D^{83}A$ | TGTTGGTTTTCGCAAAGCAGCAGCAATCAGGAGCACTTT | +264 → +226 |
| NSW252 | *ptkA* $Y^{225}A$-$Y^{227}A$- $Y^{228}A$ | TCGAAGCACTCTGAAGCCGGAGCTGCCGGAACCAAGGACAAT | +658 → +699 |
| NSW253 | *ptkA* $Y^{225}A$-$Y^{227}A$- $Y^{228}A$ | ATTGTCCTTGGTTCCGGCAGCTCCGGCTTCAGAGTGCTTCGA | +699 → +658 |
| NSW942 | *yvyG* $Y^{49}A$ | ACAAAAGAGCAAAAAGCAATTCAAGCAATCACG | +130 → +162 |
| NSW943 | *yvyG* $Y^{49}A$ | CGTGATTGCTTGAATTGCTTTTTGCTCTTTTGT | +162 → +130 |
| NSW951 | *ptkA* $Y^{225}E$-$Y^{227}A$- $Y^{228}A$ | TCGAAGCACTCTGAAGAAGGAGCTGCCGGAACCAAGGACAAT | +658 → +699 |
| NSW952 | *ptkA* $Y^{225}E$-$Y^{227}A$- $Y^{228}A$ | ATTGTCCTTGGTTCCGGCAGCTCCTTCTTCAGAGTGCTTCGA | +699 → +658 |
| NSW953 | *ptkA* $Y^{225}E$-$Y^{227}E$- $Y^{228}A$ | TCGAAGCACTCTGAAGAAGGAGAAGCCGGAACCAAGGACAAT | +658 → +699 |
| NSW954 | *ptkA* $Y^{225}E$-$Y^{227}E$- $Y^{228}A$ | ATTGTCCTTGGTTC CGGCTTCTCCTTCTTCAGAGTGCTTCGA | +699 → +658 |
| NSW955 | *ptkA* $Y^{225}E$-$Y^{227}E$- $Y^{228}E$ | TCGAAGCACTCTGAAGAAGGAGAAGAAGGAACCAAGGACAAT | +658 → +699 |
| NSW956 | *ptkA* $Y^{225}E$-$Y^{227}E$- $Y^{228}E$ | ATTGTCCTTGGTTCCTTCTTCTCCTTCTTCAGAGTGCTTCGA | +699 → +658 |
| NSW957 | *ptkA* $Y^{225}A$-$Y^{227}A$- $Y^{228}E$ | TCGAAGCACTCTGAAGCCGGAGCCGAAGGAACCAAGGACAAT | +658 → +699 |
| NSW958 | *ptkA* $Y^{225}A$-$Y^{227}A$- $Y^{228}E$ | ATTGTCCTTGGTTCCTTCGGCTCCGGCTTCAGAGTGCTTCGA | +699 → +658 |
| NSW959 | *ptkA* $Y^{225}F$-$Y^{227}F$- $Y^{228}F$ | TCGAAGCACTCTGAATTTGGATTTTTTGGAACCAAGGACAAT | +658 → +699 |

| Primer | Target | Sequence[a] | Position[b] |
|---|---|---|---|
| NSW960 | *ptkA* $Y^{225}F$-$Y^{227}F$- $Y^{228}F$ | ATTGTCCTTGGTTCCAAAAAATCCAAATTCAGAGTGCTTCGA | +699 → +658 |
| Antibiotic resistance markers | | | |
| NSW107 | *cml*$^R$ | GTTTTCCCAGTCACGACG | |
| NSW108 | *cml*$^R$ | GAATTGTGAGCGGATAAC | |
| NSW152 | *kan*$^R$ | CAGCGAACCATTTGAGGTGATAGG | |
| NSW153 | *kan*$^R$ | CGATACAAATTCCTCGTAGGCGCTCGG | |

Antibiotic resistance genes are indicated as follows: *cml*, Chloramphenicol resistance; *kan*, Kanamycin resistance.
[a] Underlined sequences indicate endonuclease restriction cut sites.
[b] Position of primer is indicated in relation to the translational start site (noted as +1) of the named gene.

## 2.3 *Plasmids used in this study*

**Table 2-3: Plasmids used in this study**

| Plasmid | Description | Reference |
|---|---|---|
| pBL132 | *cml*$^R$ cassette in pUC19 | (Stanley, Britton et al. 2003) |
| pBL193 | *yvyE* in pBL132 | (Stanley and Lazazzera 2005) |
| pDR111 | *amyE* integration plasmid | (Britton, Eichenberger et al. 2002) |
| pET*degS* | *degS*-$_{His6}$ in pET28b | (Kobayashi 2007) |
| pMAD | In-frame markerless mutation plasmid | (Arnaud, Chastanet et al. 2004) |
| pNW33 | *ywfB* in pBL132 | (Kiley and Stanley-Wall 2010) |
| pNW43 | degU-$_{His6}$ in pQE60 | (Verhamme, Kiley et al. 2007) |
| pNW90 | *sinR*-$_{His6}$ in pET28a (+) | (Verhamme, Murray et al. 2009) |
| pNW300 | *yueH* in pBL132 | (Kiley and Stanley-Wall 2010) |
| pNW301 | *ptpZ* in pBL132 | (Kiley and Stanley-Wall 2010) |
| pNW302 | *ybfP* in pBL132 | (Kiley and Stanley-Wall 2010) |

| Plasmid | Description | Reference |
|---|---|---|
| pNW303 | yomI in pBL132 | (Kiley and Stanley-Wall 2010) |
| pNW304 | *yvfO* in pBL132 | (Kiley and Stanley-Wall 2010) |
| pNW305 | *ywbC* in pBL132 | (Kiley and Stanley-Wall 2010) |
| pNW312 | *amyE* ::$P_{spank-hy}$ - *ptpZ* - *lacI* in pDR111 | (Kiley and Stanley-Wall 2010) |
| pNW316 | *amyE* ::$P_{spank-hy}$ - *ptpZ* $H^{196}A$ - *lacI* in pDR111 | (Kiley and Stanley-Wall 2010) |
| pNW330 | *ptpZ* in pMAD | (Kiley and Stanley-Wall 2010) |
| pNW331 | *ugd* in pMAD | (Kiley and Stanley-Wall 2010) |
| pNW341 | *ptkA* in pMAD | (Kiley and Stanley-Wall 2010) |
| pNW348 | *ptkA* $D^{81}A$ - $D^{83}A$ in pMAD | (Kiley and Stanley-Wall 2010) |
| pNW349 | *ptkA* $Y^{225}A$ - $Y^{227}A$ - $Y^{228}A$ in pMAD | (Kiley and Stanley-Wall 2010) |
| pNW351 | *amyE* ::$P_{spank-hy}$ - *ptkA* - *lacI* in pDR111 | (Kiley and Stanley-Wall 2010) |
| pNW361 | *ahpF* in pBL132 | (Kiley and Stanley-Wall 2010) |
| pNW365 | *icd* in pBL132 | (Kiley and Stanley-Wall 2010) |
| pNW370 | *lctE* in pBL132 | (Kiley and Stanley-Wall 2010) |
| pNW371 | *rocA* in pBL132 | (Kiley and Stanley-Wall 2010) |
| pNW372 | *yjoA* in pBL132 | (Kiley and Stanley-Wall 2010) |
| pNW373 | *yvyG* in pBL132 | (Kiley and Stanley-Wall 2010) |
| pNW377 | *tuaD* in pBL132 | (Kiley and Stanley-Wall 2010) |
| pNW380 | *amyE* ::$P_{spank-hy}$ -*yvyG* - *lacI* in pDR111 | This study |
| pNW382 | *amyE* ::$P_{spank-hy}$ - *tkmA* - *lacI* in pDR111 | (Kiley and Stanley-Wall 2010) |
| pNW387 | *tkmA ptkA* in pMAD | (Kiley and Stanley-Wall 2010) |
| pNW388 | *amyE* ::$P_{spank-hy}$ -*tkmA ptkA* - *lacI* in pDR111 | (Kiley and Stanley-Wall 2010) |
| pNW390 | *ptkA* $Y^{225}E$ - $Y^{227}E$ - $Y^{228}A$ in pMAD | This study |
| pNW391 | *ptkA* $Y^{225}E$ - $Y^{227}E$ - $Y^{228}E$ in pMAD | This study |
| pNW393 | *ptkA* $Y^{225}F$ - $Y^{227}F$ - $Y^{228}F$ in pMAD | This study |
| pNW396 | *ptkA* $Y^{225}A$ - $Y^{227}A$ - $Y^{228}E$ in pMAD | This study |
| pNW395 | *tkmA* in pMAD | (Kiley and Stanley-Wall 2010) |
| pNW399 | *yvyG* in pMAD | This study |
| pNW546 | $P_{hag}$-*yfp* in pSac-Kan | Constructed by N. Stanley-Wall |

| Plasmid | Description | Reference |
|---|---|---|
| pNW558 | *oppA* in pBL132 | (Kiley and Stanley-Wall 2010) |
| pNW559 | *yorK* in pBL132 | (Kiley and Stanley-Wall 2010) |
| pNW560 | *ynfE* in pBL132 | (Kiley and Stanley-Wall 2010) |
| pNW801 | *yvyG* $Y^{49}A$ in pMAD | This study |
| pNW803 | *ptkA* $Y^{225}E$ - $Y^{227}A$ - $Y^{228}A$ in pMAD | This study |
| pQE60 | C-terminal $_{His6}$- tag expression vector | Qiagen ™ |

Antibiotic resistance genes are indicated as follows: *cml*, Chloramphenicol resistance

## 2.4 Media and antibiotics

### 2.4.1 Growth Media

*E. coli* and *B. subtilis* strains were routinely grown in Luria-Bertani (LB) medium (10 g NaCl, 5 g yeast extract, and 10 g tryptone per litre) at 37°C unless otherwise stated. *E. coli* strain MC1061 (*F'lacIQ lacZM15 Tn10* (*tet*)) was used for the routine construction and maintenance of plasmids. For analysis of biofilm formation MSgg medium was used (5 mM potassium phosphate and 100 mM MOPS at pH 7.0 supplemented with 2 mM $MgCl_2$, 700 µM $CaCl_2$, 50 µM $MnCl_2$, 50 µM $FeCl_3$, 1 µM $ZnCl_2$, 2 µM thiamine, 0.5% (v/v) glycerol, 0.5% (w/v) glutamate) (Branda, Gonzalez-Pastor et al. 2001). For phage transduction, TY media was used (10 g NaCl, 5 g yeast extract, and 10 g tryptone per litre supplemented with 10mM $MgSO_4$ and 1µM $MnSO_4$) (Kearns and Losick 2003). Transduced cells were plated on selective TY media supplemented with 10mM sodium citrate. Media was solidified with up to 1.5% (w/v) agar as required.

### *2.4.2 B. subtilis competence media*

In order to generate genetically competent *B. subtilis* cells, an overnight lawn of exponentially growing cells was collected using wash buffer (see Appendix A: Buffers and Solutions) and the $OD_{600}$ measured. The cells were used to inoculate 12.5 ml of SpC media (1 x T-base (see Appendix A: Buffers and Solutions) supplemented with 1 mM $MgSO_4$, 0.5% (w/v) glucose, 0.2% (w/v) yeast extract, 0.025% (w/v) caseamino acids and 40 μg $ml^{-1}$ tryptophan) to a final $OD_{600}$ of 0.01. When generating JH642 competent cells the media was also supplemented with 40 μg $ml^{-1}$ phenylalanine. Cells were shaken at 37˚C until 2 hours after the onset of stationary phase. The cells were diluted 10-fold into prewarmed SPII media (1 x T-base, 3.5 mM $MgSO_4$, 0.5% (w/v) glucose, 0.1% (w/v) yeast extract, 0.01% (w/v) caseamino acids and 40 μg $ml^{-1}$ tryptophan and phenylalanine as required) and shaken for 90 minutes at 37˚C. Finally the cells were concentrated 10-fold in the SPII media and glycerol was added to a final concentration of 10% (v/v) (for cells to be stored at -80˚C for future use).

### *2.4.3 Selection media supplements*

The antibiotics used in this work are detailed in Table 2-4.

**Table 2-4 : Antibiotics used in this work**

| | | | *B. subtilis* | *E. coli* |
|---|---|---|---|---|
| Antibiotics | Stock concentration (mg $ml^{-1}$) | Dissolved in | Final concentration (μg $ml^{-1}$) | |
| Ampicillin | 100 | $H_20$ | - | 100 |
| Chloramphenicol | 5 | 100% ethanol | 5 | - |
| Erythromycin | 1 | 95% ethanol | 1 | - |
| Lincomycin | 25 | 50% ethanol | 25 | - |
| Kanamycin | 50 | $H_20$ | 25 | 50 |
| Spectinomycin | 100 | $H_20$ | 100 | - |

As required, IPTG was added to the media up to a final concentration of 100 μM for *B. subtilis* or 500 μM for *E.coli*.

## 2.5 General molecular biology methods

### 2.5.1 DNA methods

#### 2.5.1.1 Agarose gel electrophoresis

Separation of DNA fragments ranging from 100bp - 12kb in size was achieved by running through 1-1.5% (w/v) horizontal agarose gels. 1X TAE buffer (see Appendix A: Buffers and Solutions) was used to dissolve the agarose powder, and was also used as running buffer. DNA samples were mixed with 0.16 volumes of a 6X loading buffer (see Appendix A: Buffers and Solutions) prior to being loaded into the wells. The gels were run at 120V for approximately 25 minutes. Gels were stained in an ethidium bromide solution (0.004% v/v) for approximately 20 minutes before exposure to UV light in order to visualise the DNA and photography.

#### 2.5.1.2 Plasmid purification

To purify plasmids from MC1061 cells, we used the QIAprep Miniprep Kit® (Qiagen) according to the manufacturer's instructions. This method is based on the original alkaline lysis method detailed by Birnboim and Doly (Birnboim and Doly 1979). Typically, 3 ml of cells from an overnight culture were collected by centrifugation and resuspended in a lysis buffer containing RNaseA. After lysis, the cell debris was

removed by centrifugation at 16,000 g for 10 minutes. DNA was selectively captured by application to a silica membrane under high salt conditions. As MC1061 is *endA*+ an additional wash step was used to remove this endonuclease. RNA and cellular proteins were removed by washing the column with additional high salt buffer. The purified plasmid DNA was then eluted by applying 30-50 µl of a low-salt buffer to the column.

### *2.5.1.3 Purification of* B. subtilis *genomic DNA*

Extraction of purified genomic DNA for PCR purposes was conducted essentially as described by Harwood *et al*. (Harwood and Cutting 1990). The method utilises the classic phenol/chloroform method for extraction of nucleic acids. Essentially, cells are incubated with 1.2 mg $ml^{-1}$ lysozyme for 30 minutes at 37°C in order to lyse the cells. This is followed by the addition of the detergent sarkosyl at a final concentration of 0.9% (w/v) which assists with cell disruption. Tris buffered phenol is added to the lysed cell mixture and vortexed well in order to dissolve cellular proteins. The mixture is then centrifuged in order to separate the aqueous DNA-containing phase from phenol containing organic phase. The aqueous phase is removed and chloroform: isoamyl alcohol (24:1 v/v) is added to the mixture, vortexed and centrifuged as before. The aqueous phase containing the DNA is removed from the organic lipid-containing chloroform phase. The DNA is then precipitated by the addition of sodium acetate to a final concentration of 850 mM and ethanol. The precipitated DNA is pelleted and washed with 70% (v/v) ethanol, prior to resuspension in $H_20$.

### *2.5.1.4 Extraction of DNA from agarose gels*

Purification of DNA from agarose gels after electrophoresis was conducted using the QIAquick Gel Extraction Kit® (Qiagen), in accordance with manufacturer's instructions. Essentially, DNA embedded within an agarose gel was removed and the gel was dissolved in QG buffer (Qiagen) at 50˚C for approximately 10 minutes, with shaking. As for the purification of plasmid DNA detailed above, this method involves the capturing of DNA by application of the gel-DNA mixture to a silica membrane under high-salt conditions. Contaminants, such as the agarose, were removed from the column by washes with a high-salt buffer. Elution of the DNA was achieved by applying a low-salt buffer to the column.

### *2.5.1.5 Polymerase chain reaction*

Polymerase chain reaction (PCR) is a method by which regions of DNA are amplified by a thermostable DNA polymerase in the presence of free deoxynucleotides. Essentially, the process begins by denaturing the DNA template by exposing it to high temperatures (typically 95˚C). Then, the temperature is reduced to allow oligonucleotides homologous to the region of interest to bind to the DNA template. Finally the temperature is increased to 72˚C or 68˚C (depending on the variety of Taq used), the optimum temperature for enabling the extension of the homologous strand by the DNA polymerase. The procedure is repeated for approximately 30 cycles. Qiagen Taq DNA polymerase (Qiagen), Phusion DNA polymerase (Finnzymes) and *Pfu* Turbo Polymerase (Stratagene) were used in this work. Qiagen Taq DNA polymerase was predominantly used for screening of potential clones and for use in sQRT-PCR analysis,

whereas PCR fragments required for the construction of new strains and plasmids were amplified using Phusion. *Pfu* Turbo polymerase was used for the introduction of site-directed mutations according to the QuikChange protocol (Stratagene). Reactions contained 1X reaction buffer, up to 200 μM of each dNTP, 0.5 μM each primer and 0.02 U/μl enzyme. Genomic DNA or 1/50 dilution of plasmid DNA served as a template for amplification.

### *2.5.1.6 Restriction endonuclease digests*

All restriction enzymes were supplied by New England Biolabs®. Digests were performed using the supplied endonuclease buffer. Digests typically contained 20 U of each enzyme in a 50 μl reaction. Reactions were carried out at the recommended temperature for the enzymes used and incubated for up to 7 hours for PCR products or up to 4 hours for vectors. Restriction enzymes were removed from products destined for cloning using the QIAquick Gel Extraction Kit® (Qiagen) (see section 2.5.1.4).

### *2.5.1.7 Phosphatase treatment of digested vectors*

As required digested DNA vectors were dephosphorylated using calf intestinal alkaline phosphatase (CIP) (NEB). CIP acts by removing the 5' phosphate group from DNA, thus preventing self-ligation. Reactions were performed according to manufacturer's instructions, with the exception that the reactions were incubated for only 30 minutes at 37°C and the enzyme was removed using the QIAquick Gel Extraction Kit® (Qiagen) (see section 2.5.1.4).

#### *2.5.1.8 Ligation*

The generation of plasmids was achieved using T4 ligase (NEB). T4 ligase acts by reconstructing the phosphodiester bond between 5' phosphate and 3' hydroxyl termini of compatible restriction digested DNA ends. Reactions totalling 20 µl contained 1X T4 ligase buffer and 400 U of T4 ligase. The reactions were incubated at 22˚C for at least 1 hour prior to transformation into competent *E. coli* cells.

#### *2.5.1.9 Long flanking homology for the construction of double crossover deletions*

Long flanking homology was used for the construction of double crossover mutations in the genes *sinR* (NRS1858), *yulD* (NRS1822), *yfmH* (NRS1821), *yvfG* (NRS1825) and *ytcA* (NRS2059). The method was conducted as described by Mascher *et al*. (Mascher, Margulis et al. 2003). Essentially, primer pairs are designed to amplify approximately 1000 bp at the 5’ and 3’ ends of the gene. Additionally a PCR product corresponding to an antibiotic resistance cassette is also amplified. A key feature of the method is the extended 5’ ends of the primers designed to amplify the flanking regions of the gene to be deleted. These extensions are homologous to the antibiotic resistance sequence, thus allowing for annealing of the primer extensions to the antibiotic resistance gene and enabling joining of the three PCR products. The resulting PCR product was used in a transformation reaction with competent *B. subtilis* cells and colonies were selected based on the antibiotic resistance cassette.

#### *2.5.1.10 Construction of plasmids for the insertion of genes at the* amyE *locus under the control of an inducible promoter*

Plasmid pNW312 used to introduce the *ptpZ* gene under the control of the IPTG inducible promoter, $P_{spank\text{-}hy}$ at the non-essential *amyE* locus is a derivative of plasmid pDR111 (Britton, Eichenberger et al. 2002). The *ptpZ* coding region, including ribosome binding site, was amplified from genomic DNA isolated for NCIB3610 using primers NSW172 (5'- GGATGTCGACCATCGTGCCCGTTATTTATTT-3') and NSW173 (5'- GGATGCATGCGAATCGGCTGTTAAAAAAAACC -3'). The PCR product was cloned into the *Sal*I and *Sph*I sites of pDR111 using the restriction sites engineered into the primers (underlined in the primer sequence). The insert was sequenced to ensure that PCR generated errors were not introduced into *ptpZ*. Additional plasmids were constructed in an identical manner using the primers and plasmids detailed in Table 2-2 and Table 2-3.

#### *2.5.1.11 Construction of complementation plasmids containing point mutations*

Plasmid pNW316 was used to introduce the *ptpZ* gene containing a point mutation encoding for a substitution of histidine at position 196 to an alanine, under the control of the IPTG inducible promoter, $P_{spank\text{-}hy}$ at the non-essential *amyE* locus. It is a derivative of plasmid pNW312. The point mutation was introduced using primers NSW205 (5'- GTAGCCTCAGATGCCGCTAATGTGAAAACGAGA -3') and NSW206 (5'- TCTCGTTTTCACATTAGCGGCATCTGAGGCTAC -3') using the QuikChange™ mutagenesis kit (Stratagene). QuikChange™ involves the incorporation of point mutations by amplification of a PCR product using primers which contain the

mutated bases in their DNA sequence. Following PCR of methylated template DNA the reaction was digested using *Dpn*I (NEB). Using this method, template plasmid DNA is removed by digestion, whereas the PCR product containing the desired point mutation(s) remains intact. The remaining DNA was transformed into *E. coli* MC1061 cells. Plasmids containing the insert were sequenced. Additional point mutations were inserted in an identical manner for *ptkA* and *yvyG*, using the primers and plasmids detailed in Table 2-2 and Table 2-3.

#### *2.5.1.12 Construction of mutants using an adapted pMAD method.*

The construction of in-frame antibiotic-minus mutations was conducted using a method based on the original detailed by Arnaud *et al*. (Arnaud, Chastanet et al. 2004). Essentially, pMAD derived plasmids were transformed into competent domesticated *B. subtilis* cells at 30°C for 1 hour. At 30°C the temperature sensitive origin of replication present on the pMAD plasmid will initiate replication, thus the plasmid will be maintained outwith the chromosome. Colonies were selected for resistance to erythromycin and lincomycin, antibiotics which belong to the macrolide-lincosaminde-streptogramin (MLS) group. A pool of MLS resistant colonies was collected and used to inoculate 5 ml TY media plus antibiotic. The culture was grown with agitation at 30°C for 16 hours. This culture was then used to harvest phage containing the pMAD derived plasmid (see section 2.5.2.1). Undomesticated NCIB3610 was then transduced using the harvested phage, ensuring the temperature was kept to 30°C. After growth for 2 days at 30°C, colonies were selected for on TY media supplemented with sodium citrate and MLS. Next, a pool of NCIB3610 transduced colonies were collected and used to

inoculate LB media supplemented with MLS. The culture was grown at 37°C for 16 hours with agitation. Growth of the cells at 37°C prevents initiation from the temperature sensitive origin of replication, thus in the presence of antibiotics, maintenance of the resistance cassette requires integration of the plasmid into the chromosome. Post-integration colonies were selected for on LB supplemented with MLS. Next, a pool of colonies were collected and used to inoculate a culture of LB media. The culture was grown without agitation for 16 hours at 30°C, after which the culture was shaken for a further 4 hours at 30°C. Growth at 30°C in the absence of antibiotics encourages removal of the plasmid from the chromosome. The loci which the plasmid was first integrated into is left either as wildtype or will contain the plasmid engineered mutation, thus selection for mutations is necessary.

*2.5.1.13 Construction of plasmids for in-frame and markerless deletions*

Plasmid pNW330 used for the construction of an in-frame, antibiotic-minus deletion of *ptpZ* was constructed as follows. Primers NSW225 (5'-GCATGGATCCGGAGTGGACATTTTGGCGCT-3') and NSW218 (5'-GCATGTCGACATCGATCATGTCCTAGCCCCC-3') were used to amplify the region located upstream from the coding sequence of *ptpZ.* The PCR product was cloned into pMAD (Arnaud, Chastanet et al. 2004) using the restriction sites engineered into the primers (underlined in the primer sequence) resulting in pNW328. Primers NSW219 (5'- GCATGTCGACGGTTTTTTTTAACAGCCGATTCTC -3') and NSW220 (5'-GCATCCCGGGCACTGTGCTTTTCGTTACCAC -3') were used to amplify the region located downstream from the coding sequence of *ptpZ* which was cloned into pNW328 using the restriction sites engineered into the primers (underlined in the primer

sequence) resulting in pNW330. To introduce the mutation into NCIB3610, pNW330 was first transformed into 168. SPP1 phage was harvested and was used to transduce NCIB3610. NRS2222 was constructed by integration and curing of pNW330 in NCIB3610, according to the method detailed in section 2.5.1.12. Further plasmids were constructed for in-frame mutations in an identical manner for *tkmA*, *ptkA, ugd*, *yvyG* and for *tkmA* and *ptkA* using the primers and plasmids detailed in Table 2-2 and Table 2-3.

#### *2.5.1.14 Generation of competent* B. subtilis *cells and transformation*

Transformation of competent *B. subtilis* cells with genetic material was performed based on the method described by Harwood *et al.* (Harwood and Cutting 1990). Essentially 100 µl of competent cells were placed in a sterile test tube with 100 µl of sterile transformation buffer (seeAppendix A: Buffers and Solutions). Up to 10 µl of purified gDNA or 30 µl plasmid DNA was added to the test tube prior to incubation on a roller drum. All transformations were incubated for 30 minutes at 37˚C, with the exception of temperature sensitive plasmids (pMAD derived constructs) which were incubated at 30˚C for 1 hour. Transformed cells were then plated onto selective media and incubated at the appropriate temperature.

### *2.5.2 Generation of competent E. coli cells and transformation*

Chemically competent *E. coli* cells were generated using the classic $CaCl_2$ method. Essentially, an overnight culture of *E. coli* cells was diluted 10-fold into LB liquid media. The cells were then shaken at 37˚C until an $OD_{600}$ of approximately 0.3 was

reached. The cells were chilled on ice for 30 minutes prior to centrifugation at 3000g for 15 minutes. The cell pellets were then resuspended in 0.1 volume ice cold 0.1 M $CaCl_2$. The cells were pelleted as before, then resuspended in 0.04 volumes ice cold 0.1 M $CaCl_2$ and then incubated overnight on ice. Glycerol was added to a final concentration of 10 % before the cells were stored at -80˚C. Prior to transformation, *E. coli* cells were thawed on ice. Genetic material was added to the cells and allowed to incubate on ice for 30 minutes. The cells were then heat shocked for 2 minutes at 37˚C. The cells were chilled on ice for 15 minutes and then plates on selective media. Alternatively, plasmids carrying a kanamycin resistance cassette were incubated with 1 ml of LB for 1 hour at 37˚C prior to plating on selective media.

#### *2.5.2.1 Phage transduction of undomesticated* B. subtilis

SPP1 phage (Yasbin and Young 1974) was used for the transfer of genetic information from donor to recipient *B. subtilis* cells. The harvest of SPP1 phage containing *B.subtilis* DNA fragments and subsequent phage transductions into undomesticated *B.subtilis* was conducted following the method established by Kearns *et al*. (Kearns and Losick 2003). Harvesting phage was conducted as follows: essentially, 200 µl of an overnight donor-culture grown in TY media was incubated with TY media and a range of concentrations of SPP1 phage. The mixture was incubated at either 37˚C or, in the case of temperature sensitive strains, 30˚C for up to 15 minutes. The phage-cell culture mix was then added to molten TY media supplemented with 0.7% (w/v) agar. The mixtures were then plated onto thick, fresh TY plates and monitored for plaque formation. The 0.7% (w/v) agar containing the lysed cell and phage mixture was removed from the plate, vortexed with additional TY media and passed through a 0.22-

μm syringe filter. In order to conduct the phage transduction recipient cells were grown until late stationary phase. 900 μl of recipient cells was added to 9 ml of TY media with or without the addition of up to 100 μl of SPP1 phage containing DNA from the donor strain. The mixture was incubated for either 30 minutes at 37˚C or 1 hour at 30˚C. The cells were collected by centrifugation at 3000g for 10 minutes. 100 μl of supernatant was retained and used to resuspend the cell pellet prior to plating onto selective TY media supplemented with 10 mM sodium citrate. Colonies were then streak purified on LB agar plates supplemented with the appropriate antibiotic.

#### *2.5.2.2 DNA sequencing*

DNA sequencing was utilised to ensure that all new constructs were free from unwanted mutations. Additionally, the identification of the transcriptional start site of the *tkmA* operon was conducted using DNA sequencing. All sequencing was performed by the DNA sequencing department at the University of Dundee (http://www.dnaseq.co.uk/).

### *2.5.3 RNA methods*

#### *2.5.3.1 Purification of total RNA from* B. subtilis

Cells for RNA isolation were inoculated into 25 ml of LB at an $OD_{600}$ of 0.01 from an overnight lawn plate and grown at 37$^{o}$C with shaking at 200 rpm in 250 ml flasks. When an $OD_{600}$ of 1 was reached, 3 ml of cells were harvested by centrifugation at 13,000g for 1 minute and immediately processed for RNA extraction using the RiboPure ™-Bacteria RNA extraction kit (Ambion®) according to the manufacturer's

instructions. RNA was checked for quality by running on an agarose gel and quantified using a Nanodrop ™.

### *2.5.3.2 DNA Microarray Analysis*

*B. subtilis* microarrays consisting of 4105 gene specific oligonucleotides (Compugen) were printed at the Research Technology Support Facility at Michigan State University. Five oligonucleotides that have no significant similarity to the *B. subtilis* genome were used as negative controls. To identify the genes that were up-regulated in the absence of both SinR and DegU, RNA was extracted from a *degSU* (NRS1499) and a *degSU sinR* (NRS1686) mutant strain. For the DNA array analysis two independent RNA samples were used for each strain and two technical DNA array replicates were conducted. cDNA was synthesised using either 3 or 6 μg of total RNA by reverse transcribed with Superscript III (Invitrogen) for 2 hours at 50$^{o}$C in the presence of amino-allyl-dUTP (Sigma). RNA was degraded by hydrolysis using 15 μl of 0.1 M NaOH and incubation at 70$^{o}$C for 10 minutes. The sample was neutralised by the addition of 15 μl of 0.1M HCl and the cDNA purified using a MinElute PCR purification kit (Qiagen) and eluted in 10 μl $H_20$. To fluorescently label the cDNA, 0.5 μl of fresh 1M $NaHCO_3$ was added to the cDNA and was used to hydrate an aliquot of either GE Healthcare Fluorolink Cy3 dye (*degSU* cDNA) or GE Healthcare Fluorolink Cy5 dye (*degSU sinR* cDNA). After 1-hour incubation at room temperature unincorporated dye was removed using the MinElute PCR purification kit. Both labelled cDNA populations were applied onto a microarray and hybridized overnight at 42˚C for 16-18 hours. After washing, hybridized microarray slides were analysed using

a GenePix™ 4100A array scanner (Axon Instruments). Images were processed using the GenePix Pro 5.0 software which generates red-green fluorescent intensity values for each spot. The fluorescent signal intensities were imported into Microsoft Excel (available from http://www.dundee.ac.uk/lifesciences/Stanley-Wall/Home.html). The microarray datasets were filtered to remove those genes that were expressed at levels less than two standard deviations above the average background values in both channels. The intensity values were normalised relative to the ratio generated by dividing the total value of Cy3 fluorescence with that of the total value of Cy5 fluorescence measure per array. The average value from the four spots per gene was calculated and those genes with an expression level of greater than 2.0 after normalization were selected. At this point the genes that had previously been identified as directly repressed by SinR were eliminated (Chu, Kearns et al. 2006), e.g. genes in the *epsA-O* operon and the *yqxM-sipW-tasA* operon (Table 3-1). This resulted in a group of 11 genes that had an average expression value of >2.0 and that had previously not been demonstrated to be SinR repressed. This work was conducted by Dr. Nicola Stanley-Wall.

#### *2.5.3.3 Semi-quantitative RT-PCR*

RNA was isolated from cultures of NCIB3610, *degSU* (NRS1499), *sinR* (NRS1859) and *degSU sinR* (NRS1860) as described above. The harvested RNA was DNAse treated and cDNA was synthesised as previously published (Stanley and Lazazzera 2005). Essentially, cDNA synthesis was achieved by incubation of purified, DNase-treated RNA with the reverse transcriptase enzyme, Superscript III (Invitrogen). The RNA is first incubated at 70°C in order to remove secondary structures which would

disrupt progression of the Superscript III. The temperature is then lowered to allow binding of random hexamers. These short primers are designed to possess very low specificity and coupled with their random sequences, they bind at various positions along the length of the purified RNA. This increases the chance of the Superscript III converting a high proportion of the harvested RNA to cDNA. Elongation was performed once for 50 minutes to ensure maximal cDNA synthesis. To ensure that the original RNA samples were free from contaminant DNA, samples of RNA lacking Superscript III (Invitrogen) were treated in parallel with samples intended for cDNA synthesis. After cDNA synthesis, RNA-cDNA hybrid nucleic acid is present. To remove the contaminating RNA, the mixture is incubated with RNAse H (Invitrogen) for 20 minutes at 37°C. To assess the level of transcription of target genes, cDNA was amplified as follows. 1 µl of synthesised cDNA was used in a standard 20 µl PCR reaction using Qiagen Taq DNA polymerase with the addition of 3.5 mM $MgCl_2$ and 8.3 nl $ml^{-1}$ SyberGreen (Sigma). PCR samples were held at 95˚C for 10 minutes prior to a 25-cycle PCR reaction involving a melting step at 95˚C, followed by an annealing step at 50˚C and then an elongation step at 72˚C. Each PCR step was held for the duration of 25 seconds. The genes *tkmA*, *ugd, ptpZ, yomI, ywbC* and *yvfO* were amplified using gene-specific primers detailed in Table 2-2. To determine the melting temperatures of the PCR products the set point temperature was increased in 40 cycles (10 s each) by 1°C per cycle, starting from 50°C. Expression of *tkmA*, *ugd, ptpZ, yomI, ywbC,* and *yvfO,* was calculated as fold changes relative to the wild type strain using the formula: Fold change = $2^{-\Delta\Delta Ct}$; with $-\Delta\Delta Ct = (Ct_{(gene\ x)} - Ct_{(constitutive\ gene)})_{condition\ I} - (Ct_{(gene\ x)} - Ct_{(constitutive\ gene)})_{condition\ II}$ (Talaat *et al.*, 2002). The level of transcription of each gene was measured using Corbett qPCR reader, run using Rotorgene 8 software (Corbett) with expression of *veg* monitored as a reference gene (Hamon, Stanley et al. 2004).

### *2.5.3.4 RT-PCR as a tool for validating operon structure*

RNA was isolated from NCIB3610 grown in LB to an $OD_{600}$ of 0.01, as described above. cDNA was synthesised using an adapted method to the procedure detailed in section 2.5.3.3. Instead of random hexamers, a reverse primer specific to *ugd* (NSW220) was used. If a single transcript was produced by the *tkmA* operon, elongation of cDNA synthesis initiated from within the *ugd* gene would produce a cDNA strand containing all four genes downstream of the *tkmA* promoter. The following primer pairs were used for amplification of an internal region of *ptkA* (NSW225 and NSW254), *ptpZ* (NSW195 and NSW249), or *ugd* (NSW165 and NSW220) (See Table 2-2 for primer sequences). The resulting PCR products were analysed by gel electrophoresis and visualised by ethidium bromide staining and exposure to UV light.

### *2.5.3.5 5'Rapid amplification of complementary DNA ends (RACE)*

The transcription start site of *tkmA* was determined using 5'RACE conducted using DNAse treated RNA harvested from NCIB3610 as described in section 2.5.3.3. To synthesise cDNA corresponding to the promoter region of the *tkmA* gene, 5 μg of DNAse treated RNA was incubated with 2.5 pmol NSW227 (5' – GGGCTCTTAATGATGACA – 3') at 70°C for 10 minutes. The reaction mixture was made up to a total volume of 25 μl with the addition of 1x first strand buffer, 11.2 μM dithiothreitol (DTT) and 0.4 mM dNTPs. The mixture was incubated at 42°C for 1 minute prior to the addition of 200 U of Superscript II (Invitrogen ™) and then

incubated for a further 50 minutes. The reverse transcriptase was heat inactivated by incubation at 70°C for 15 minutes. To remove any remaining RNA template, RNAse H (Invitrogen). 500 ng of synthesised cDNA was 5' dC-tailed using 20 units of terminal transferase (Tdt) (New England Biolabs ™), supplemented with 1X Terminal Transferase Reaction Buffer (20 mM Tris-acetate, 50 mM potassium acetate and 10 mM Magnesium Acetate), 0.25 mM $CoCl_2$ and 200 μM dCTP. The reaction was incubated at 37°C for 10 minutes and then 10 minutes at 65°C for to heat inactivate the Tdt. Touchdown PCR was used to amplify the *tkmA* promoter region using primers NSW367 (5' – GGCCACGCGTCGACTAGTACGGGUUGGGUUGGGUUG – 3') and NSW228 (5' – GGGTGTAAGTGCGAAGAAA - 3). The standard PCR reaction mixture included 1.5 mM $MgCl_2$ , 5 μl of dC-tailed cDNA, 0.4 mM each primer, 1 HotStart Taq bead and 1X PCR buffer (Promega). Annealing temperature was gradually reduced from 58°C to 48°C in 0.5 increments, with a final 20 cycles at 48°C. The resulting PCR product was visualised by gel electrophoresis and staining prior to recombination into the TOPO-TA vector pCR2.1 (Invitrogen ™). The inserts cloned were sequenced and the transcription start site identified.

### *2.5.4 Protein methods*

#### *2.5.4.1 SDS-polyacrylamide gel electrophoresis*

The Bio-Rad protein gel electrophoresis mini-gel system was used for the running of SDS-PAGE gels. The resolving gels for SDS-PAGE contained the following: 375 mM Tris-HCl (pH 8.8), 0.1 % (w/v) SDS, 0.1% (w/v) APS, 0.1% (v/v) TEMED. Polyacrylamide was added to reach a final concentration of either 12 or 15% (v/v). The

resolving gel was poured to approximately 2 cm from the top between two glass plates. Ethanol was applied to the top of the resolving gel to ensure a level gel. The ethanol was removed after polymerisation was achieved. The stacking gels for SDS-PAGE contained the following: 125 mM Tris-HCl (pH 6.8), 0.1 % (w/v) SDS, 0.1% (w/v) APS, 0.1% (v/v) TEMED and 6% (v/v) polyacrylamide. The gels were run in 1X SDS running buffer (seeAppendix A: Buffers and Solutions) for approximately 1 hour at 200V (constant voltage). Samples were run against 5 µl of SeeBlue®Plus2 protein marker (Invitrogen).

#### *2.5.4.2 Coomassie staining of polyacrylamide gels*

Detection of proteins separated by electrophoresis through polyacrylamide gels was achieved by staining with coomassie stain (see Appendix A: Buffers and Solutions). The gels were incubated for approximately 20 minutes in the stain at room temperature with gentle shaking. To remove non-specifically bound stain, the gels were then transferred to destain solution (seeAppendix A: Buffers and Solutions). Saturated destain was changed for fresh destain periodically until non-specific staining was sufficiently removed. Gels were then photographed.

#### *2.5.4.3 Protein detection by Western blotting*

A western blot was conducted in order to detect the histidine tag of the DegS construct. Cells sampled prior to and 3 hours after induction of DegS-$_{His6}$ expression were collected by centrifugation. The cell pellets were resuspended in SDS loading dye (seeAppendix A: Buffers and Solutions), normalised according to the $OD_{600}$

measurement at the time of sampling. The samples were boiled for 10 minutes, and then cell debris was removed by centrifugation. 10 µl of the prepared samples was loaded into a 12% (v/v) SDS-PAGE gel. The gels were run for approximately 1 hour at 200V. The proteins were subsequently transferred onto a nitrocellulose membrane which was then incubated for >1 hour at room temperature in 1X TBS supplemented with 5% (w/v) skimmed milk powder. To detect the histidine tag, the membrane was incubated for 1 hour at room temperature with the primary antibody, α-His antibody raised in rabbit used at a dilution of 1:1000 (AbCam). The membrane was thoroughly washed with TBST (seeAppendix A: Buffers and Solutions), then incubated with ImmunoPure Goat α Rabbit IgG antibody conjugated to horseradish peroxidase used at a dilution of 1:5000 (Pierce). The membrane was washed again, prior to development with ECL reagents and exposure to X-ray film.

#### *2.5.4.4 Protein quantification by Bradford method*

To quantify the amount of purified protein, the Coomassie (Bradford) Protein Assay Kit was used (Pierce). The kit contains modified ready-to-use components of the classic Bradford coomassie-protein binding colourimetric method. Following the manufacturer's instructions, a number of samples containing increasing concentrations of bovine serum albumin (BSA) or the test protein were prepared. The coomassie reagent was added to the samples, the samples were read at 595 nm and a standard curve was plotted. In parallel, the concentration of test protein was measured using a spectrophotometer ND-1000 (Nanodrop) with the ability to in put the specific molar extinction co-efficient ($m^{-1}$ $cm^{-1}$) (details the degree to which a substance absorbs light

at a given wavelength) and molecular weight of the test protein, which allows for the calculation of the concentration of protein from the absorbance at 280 nm. As the results from the Bradford and Nanodrop were in agreement with one another, future protein quantification was routinely carried out using the Nanodrop.

#### *2.5.4.5 Protein purification*

##### 2.5.4.5.1 DegS

For the overproduction of DegS-$_{His6}$, plasmid pET28b-degS-$_{His6}$ (Kobayashi 2007), was induced by the addition of 500 μM IPTG at $OD_{600}$ 0.4. Growth was continued for 3 hours prior to collection by centrifugation at 4˚C. Cells were washed with ice cold 10 mM Tris-HCl (pH 7.6). DegS-$_{His6}$ was purified from inclusion bodies according to the BugBuster protocol (Novagen). BugBuster is a gentle detergent which has been designed to disrupt *E. coli* cell walls for the purification of proteins. In addition to purification of soluble proteins, BugBuster can be used to wash cell debris from inclusion body pellets. After purification by BugBuster, the DegS-$_{His6}$ inclusion body pellet was resuspended in denaturing buffer (50 mM Tris-HCl (pH 7.6), 150 mM NaCl, 8 M urea and 10 mM imidazole) and incubated on ice for 2 hours before the protein solution was applied to a HisTrap FF column (GE healthcare). DegS-$_{His6}$ was slowly renatured by gradual removal of the urea over the course of 90 minutes at room temperature with the use of an AKTA purifier FPLC machine (GE Healthcare). DegS-$_{His6}$ was eluted from the column by the addition of 500 mM imidazole and was dialysed in 50 mM Tris-HCl (pH 7.6), 200 mM KCl, 10 mM $MgCl_2$, 0.1 mM EDTA, 1 mM DTT and 50% (v/v) glycerol.

#### 2.5.4.5.2 DegU

DegU-$_{His6}$ was purified as described previously (Verhamme, Kiley et al. 2007). Essentially, BL21 (λDE3) carrying pNW43 were grown to an $OD_{600}$ of 0.5 at which point the expression of DegU–$_{His6}$ production was induced by the addition of 50 mM IPTG. The induced cells were allowed to grow for 16 hours at 26°C. The cells were harvested and washed twice in ice cold 500 ml of 20 mM Tris-HCl pH 8.0 and 200 mM NaCl. The washed cells were suspended in 3.5 ml lysis buffer per 1 g wet weight cells (20 mM Tris-HCl pH 8.0, 10 mM imidazole, 2 mM benzamidine, 1.0% (v/v) Triton X-100, 200 mM NaCl, and one Roche EDTA minus protease inhibitor cocktail tablet per 7 ml). The suspended cells were incubated in the presence of 1 mg $ml^{-1}$ lysozyme on ice for 30 minutes prior to lysis by French press. Following immobilised metal ion affinity chromatography (IMAC) purification DegU-$_{His6}$ was purified from contaminating DNA by application to a DEAE-FF column (GE Healthcare ™). Purified DegU-$_{His6}$ was dialysed before use (20 mM Tris-HCl (pH 8.0) 50 mM NaCl).

#### 2.5.4.5.3 SinR

SinR-$_{His6}$ was purified based on the original method established by Kearns *et al* (Kearns, Chu et al. 2005). The following alterations were made to the method: BL21 cells containing plasmid pNW90 were grown in 500 ml LB + 25 μg $ml^{-1}$ kanamycin to an OD600 of 0.5. The expression of SinR-$_{His6}$ was initiated by the addition of 100 μM IPTG. The cells were then grown for 16 hours at 26˚C. The cells were lysed using the Novagen BugBuster Master Mix (Novagen) in accordance with manufacturer's instructions. SinR-$_{His6}$ was purified by application through a HisTrap HP (GE

Healthcare) using an AKTA purifier FPLC machine (GE Healthcare). The histidine tag used for purification was removed using a thrombin cleavage capture kit in accordance with manufacturer's instructions (Novagen).

## 2.6 *Analytical methods*

### *2.6.1 Complex colony analysis*

Analysis of biofilm formation was performed as described (Branda et al., 2001, Verhamme et al., 2007). *B. subtilis* strains were inoculated from a fresh LB plate and grown to mid-late exponential phase in LB. 10 µl of the undiluted culture was spotted onto an MSgg plate containing 1.5% (w/v) agar (containing IPTG as required) and incubated at 37$^{o}$C for the time period indicated. Images of the bacterial colonies were captured using a Leica MZ16 FA stereoscope using LAS software version 2.7.1. Due to slight changes in the appearance of colonies between different rounds of experiments, figures have been made by taking representative colonies from a single experiment. In all cases, colonies were spotted with the wild type *B. subtilis* strain NCIB3610 on the same plate. Subtle changes in the overall complexity of the wild type *B.subtilis* colonies which may be observed between different figures are within the accepted levels of natural variability.

### *2.6.2 Pellicle formation*

Analysis of pellicle formation was performed as described (Branda et al., 2001). *B. subtilis* strains were inoculated from a fresh LB plate and grown to mid-late exponential phase in LB. For pellicle formation the culture was diluted 1000-fold into 1.5 ml MSgg

media in a 24-well plate and was incubated for 16 hours at 37°C. Images of the pellicles were captured using a Leica MZ16 FA stereoscope using LAS software version 2.7.1.

### *2.6.3 Sporulation Analysis*

Sporulation analysis was conducted as described previously (Vlamakis, Aguilar et al. 2008). Essentially, colonies were grown on solid MSgg media for 24 or 72 hours at 37°C prior to cell collection. Liquid cultures were prepared by growing cells in 10 ml MSgg media inoculated with cells from an $OD_{600}$ of 0.01. Cultures were grown for 24 or 72 hours with shaking at 37°C. Colonies were collected in 500 µl 1X PBS, whereas 1ml of cells grown in liquid media was collected by centrifugation and resuspended in 500 µl 1X PBS. Cells were gently sonicated in order to remove the matrix material from the cells without lysing the cells. The cells were then serial diluted in 1X PBS and 100 µl of diluted cells were plated on LB agar plates. The dilution was then heated to 95°C to kill all non-sporulated cells and 100 µl of the heat treated diluted cells were plated on LB agar plates. The plates were incubated for 16 hours at 37°C and sporulation efficiencies were calculated.

### *2.6.4 Electrophoretic mobility shift analysis (EMSA)*

For the assessment of DegU~P binding to the *tkmA* promoter, a PCR product corresponding to the promoter region of *tkmA* ($P_{tkmA}$) was amplified using primers NSW146 and NSW147 and purified by gel extraction. Additionally, a PCR product corresponding to the promoter region of *aprE* ($P_{aprE}$) was amplified using primers NSW61 and NSW654 and purified as above (see Table 2-2 for sequences). The

promoter DNA was labelled using 50 μCi [γ-$^{32}$P] ATP (Perkin-Elmer) and T4 polynucleotide kinase (New England Biolabs). Unincorporated ATP was removed from the labelled DNA using an Illustra Microspin G-25 column (GE Healthcare). Phosphorylated purified DegU was produced essentially as described previously (Gueriri, Bay et al. 2008), with the exception that a final concentration of 10 μM purified DegU~P and 0.78 μM purified DegS were added to the phosphorylation reaction. The reaction was incubated for 30 minutes at 25˚C. EMSA binding mixtures were prepared containing 15 mM Tris-HCl (pH 7.6), 0.2% (v/v) Tween-20, 1 mM $MgCl_2$, 60 mM NaCl, 4% (v/v) glycerol, 15 mM DTT, 0.5 mg ml$^{-1}$ bovine serum albumin, 1 μg poly (dI-dC), and a range of concentrations of DegU~P, made up to a total volume of 30 μl. The reactions were initiated by the addition of 2 ng of $^{32}$P-labelled DNA probe. 15 μl of the reaction mixtures were loaded onto a prewarmed 5% (v/v) Polyacrylamide (AccuFLOWGel; Acrylamide:Bis-Acrylamide solution 29:1) Tris Glycine gel (50 mM Tris-HCl, 400 mM glycine, 1.75 mM EDTA) which was run at 100V for ~1-2 hours. Dried gels were exposed to X-ray film overnight at -70° C prior to development.

For the assessment of SinR binding to the *tkmA* promoter, labelled *tkmA* PCR product was produced as described above. Additionally, a PCR product corresponding to the promoter region of *yqxM* ($P_{yqxM}$) was amplified using primers NSW50 and NSW51 and purified as described above (see Table 2-2 for sequences). The SinR EMSA reaction mixture contained 1X SinR EMSA buffer (10mM Tris-HCL (pH 7.6), 1 mM $MgCl_2$, 50 mM NaCl, 5% (v/v) glycerol, 1mM EDTA, 1mM DTT, 50 ng ml$^{-1}$ BSA and 50 ng ml$^{-1}$ Poly (dI-dC)) and a range of concentrations of SinR, made up to a total volume of 30 μl. The reactions were initiated by the addition of 2 ng of $^{32}$P-labelled DNA probe. 15 μl of

the reaction mixtures were loaded onto a prewarmed 5% (v/v) Polyacrylamide (AccuFLOWGel; Acrylamide:Bis-Acrylamide solution 29:1) 0.5X TBE gel (45 mM Tris-borate and 1 mM EDTA) which was run at 140V for ~1-2 hours. Dried gels were exposed to X-ray film overnight at -70° C prior to development.

### *2.6.5 Protease analysis*

Secreted proteases were monitored using LB agar plates supplemented with 1.5% (w/v) skimmed milk. *B. subtilis* cultures to be tested were grown to mid-late exponential phase in LB from a freshly streaked LB plate and subsequently diluted to an $OD_{600}$ of 0.01 in fresh LB medium. In total, 10 µl of the diluted culture was spotted onto a 1.5% (w/v) milk plate and incubated at 37°C for 16 hours. The diameter of the halo surrounding protease-positive strains was measured, and the diameter of the colony was subtracted. The experiment was conducted on at least three independent occasions and plotted as the mean ± SEM.

### *2.6.6 Motility analysis*

Swimming and swarming analysis was conducted using low-salt LB medium (5 g NaCl, 5 g yeast extract, and 10 g tryptone per litre) supplemented with 0.3% (w/v) and 0.7% (w/v) agar, respectively (Kearns and Losick 2003). For swarming assays, cultures were grown in 3ml LB media at 37°C, with shaking, until $OD_{600}$ ~1.0 was reached. The cultures were then concentrated to an $OD_{600}$ 10, and 10 µl of culture was spotted onto the swarming media. The swarming media plates were prepared directly prior to

inoculation. Plates were poured in a laminar flow, and allowed to dry for 20 minutes prior to spotting. The inoculated plates were then dried for a further 10 minutes before the plates were incubated at 37°C. For swimming assays, media was prepared prior to use and the swimming plates were not dried. Cell material was picked using a sterile pipette tip, and this was used to stab the centre of the swimming plate. The plates were incubated at 37°C. The extent of swimming and swarming was noted for each plate at defined intervals.

### *2.6.7 Microscopy*

Strains for nucleoid number analysis or for fluorescent reporter fusion visualisation were grown in LB at 37$^{o}$C with shaking to an $OD_{600}$ of 0.3. Cells were collected by centrifugation and were concentrated 5-fold by resuspension in wash buffer (Appendix A: Buffers and Solutions). Cells to be analysed for nucleoid number were by stained using Hoechst 33342 (10 ng ml$^{-1}$) (Invitrogen ™) for 5 minutes and were washed twice in wash buffer. 2 µl of cell suspension was spotted onto thin 1.5% (w/v) agarose slides and viewed using an Axio Imager M1 microscope (Zeiss). Hoechst 33342 excitation is at wavelength 361 nm and emission is at wavelength 486 nm. The peak excitation and emission wavelengths of YFP are 514 nm and 527 nm, respectively. Images were analysed using AxioVision Rel. version 4.6 image capture software (Zeiss).

# 3 Characterisation of the *tkmA* operon

## *3.1 Introduction*

As discussed in Chapter 1, DegU and SinR regulate a number of multicellular behaviours displayed by *B. subtilis* including biofilm formation [for DegU see (Stanley and Lazazzera 2005; Kobayashi 2007; Verhamme, Kiley et al. 2007) and for SinR see (Kearns, Chu et al. 2005; Branda, Chu et al. 2006)]. To further understand the molecular basis of the co-regulation of biofilm formation by DegU and SinR, experiments were designed to determine whether they functioned via parallel pathways or if they were members of the same regulation cascade. Epistasis analysis presented in this chapter supports the conclusion that DegU and SinR operate using separate pathways to control biofilm formation. Later in this chapter, I went on to identify a novel DegU and SinR regulated operon that is required for biofilm formation and I characterised the structure of this operon at the genetic level.

## *3.2 DegU and SinR regulate biofilm formation via separate pathways*

I aimed to test whether DegU and SinR were part of the same or parallel pathways that regulates biofilm formation by *B. subtilis*. Mutations in *sinR* and *degSU* were introduced separately, and in combination, into the *B. subtilis* isolate NCIB3610. Colony architecture and pellicle formation were used as two independent measures of the capability to form a biofilm (Branda, Gonzalez-Pastor et al. 2001). The phenotype exhibited by the following strains was assessed with respect to the wild type parental strain (NCIB3610); *degSU* (NRS1499), *sinR* (NRS1859), and *degSU sinR* (NRS1860).

The *degSU sinR* (NRS1860) double mutant, exhibited a colony morphology that was distinct from the wild type strain and was dissimilar from either of the previously characterised single mutant strains, *degSU* (NRS1499) and *sinR* (NRS1859) (Figure 3-1A). Consistent with previous findings, the *degSU* mutant strain was unable to form a robust stable pellicle (Stanley and Lazazzera 2005; Kobayashi 2007; Verhamme, Kiley et al. 2007) and the *sinR* mutant formed a very robust rugose pellicle (Figure 3-1B) (Kearns, Chu et al. 2005). The *degSU sinR* double mutant formed a pellicle that was distinct from either single mutant strain or wild-type strain (Figure 3-1B).

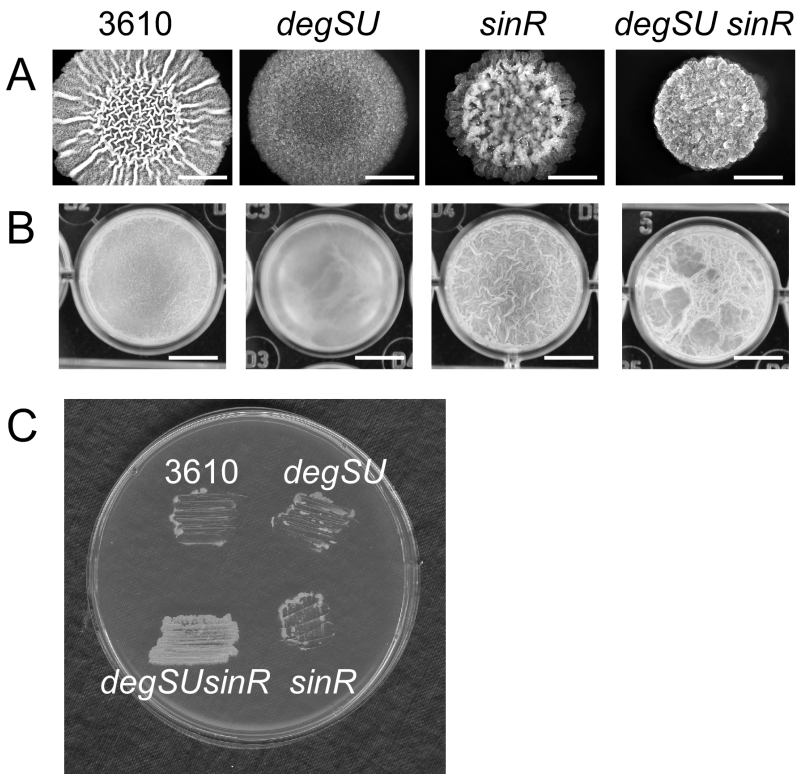


**Figure 3-1: Epistasis analysis of DegSU and SinR.**
Complex colony architecture assay of *B. subtilis.* (**A**) Strains NCIB3610, *degSU* (NRS1499), *sinR* (NRS1859), and *degSU sinR* (NRS1860) were grown on MSgg agar plates for 40 hours at 37˚C prior to photographing. Scale bar represents 5 mm. (**B**) Pellicles were allowed to grow in MSgg media overnight at 37˚C prior to photography. (**C**) Strains as detailed above were patched onto an LB agar plate and grown for 16 hours at 37˚C prior to scraping and photography.

## *3.3 Identification of novel targets of DegU and SinR*

It was noted that by comparison with both the wild type and single mutant strains, the double *degSU sinR* mutant (NRS1860) tightly adhered to the surface of an agar plate (Figure 3-1C). This led to the hypothesis that a novel set of DegU and SinR co-regulated genes existed and that one (or more) was responsible for the enhanced adhesion phenotype. It also provided a possible mechanism to identify novel loci involved in the control of biofilm formation. To identify these potential gene(s), DNA microarray analysis was used. As the number of genes controlled by DegU is significantly greater than those controlled by SinR, the expression profile of the *degSU* strain was compared to that of the *degSU sinR* strain (Dartois, Debarbouille et al. 1998; Ogura, Yamaguchi et al. 2001; Tsukahara and Ogura 2008) (Kearns, Chu et al. 2005; Chu, Kearns et al. 2006; Kodgire, Dixit et al. 2006). By identifying loci that were up-regulated >2-fold in the *degSU sinR* strain compared to the *degSU* strain, a combination of putative DegU and SinR co-regulated genes, and known SinR-regulated genes, was generated (Table 3-1). A finalised list of eleven DegU & SinR co-regulated genes was compiled by removing known SinR-repressed genes (highlighted in red) (Table 3-1).

| Gene | Putative Operon Structure | Ratio [a] | Putative/Known Function |
|---|---|---|---|
| *yvfO* | *yvfO* | 5.48 ± 1.77 | similar to arabinogalactan endo-1,4-beta-galactosidase |
| *yfmH* | *yfmH* | 4.79 ± 0.55 | unknown function – no known homologues |
| *yvfG* | *yvfG* | 4.23 ± 0.55 | inverse direction to *epsA-O* operon |
| *ptpZ* | *tkmA-ptkA-ptpZ-ugd* | 3.66 ± 0.26 | protein tyrosine phosphatase |
| *ywfD* | *ywfBCDEFG* | 3.53 ± 0.22 | similar to glucose 1-dehydrogenase |
| *ywbC* | *ywbC* | 3.24 ± 0.29 | glyoxylase family protein |
| *yomI* | *yomI* | 3.01 ± 0.27 | potential lytic transglycosylase |
| *yvyE* | *yvyE-yvhJ* | 2.80 ± 0.3 | unknown function - potential peptidase |
| *ybfP* | *ybfP* | 2.56 ± 0.31 | similar to transcriptional regulator (AraC/XylS family) |
| *yueH* | *yueH-yueI* | 2.54 ± 0.08 | unknown function – no known homologues |
| *leuD* * | *ilvBHC-leuABCD* | 2.30 ± 0.24 | leucine biosynthesis |
| *yulD* | *yuxG-yulBCDE* | 2.17 ± 0.12 | potential L-rhamnose 1-epimerase |
| *epsA* | *epsABCDEFGHIJKLMNO* | 3.45 ± 0.54 | Required for polysaccharide biosynthesis |
| *epsC* | *epsABCDEFGHIJKLMNO* | 2.81 ± 0.18 | Required for polysaccharide biosynthesis |
| *epsH* | *epsABCDEFGHIJKLMNO* | 3.68 ± 0.28 | Required for polysaccharide biosynthesis |
| *epsI* | *epsABCDEFGHIJKLMNO* | 2.32 ± 0.51 | Required for polysaccharide biosynthesis |
| *epsJ* | *epsABCDEFGHIJKLMNO* | 4.68 ± 0.96 | Required for polysaccharide biosynthesis |
| *epsK* | *epsABCDEFGHIJKLMNO* | 3.19 ± 0.66 | Required for polysaccharide biosynthesis |
| *epsL* | *epsABCDEFGHIJKLMNO* | 8.27 ± 0.59 | Required for polysaccharide biosynthesis |
| *epsO* | *epsABCDEFGHIJKLMNO* | 2.89 ± 0.68 | Required for polysaccharide biosynthesis |
| *tasA* | *yqxM-sipW-tasA* | 5.08 ± 0.89 | Protein component of spore coat and biofilm matrix |

**Table 3-1: Genes identified as up-regulated in the absence of *sinR* and *degSU*.**
[a.] The value represents the average ratio of expression identified via DNA array analysis for the *degSUsinR* strain versus *degSU* strain. A value greater than 1 represents a higher level of expression in the *degSUsinR* strain. The errors represent the standard error of the mean from 3 independent experiments. Genes highlighted in red indicate confirmed SinR regulated genes. **leuD* was not included in the study as deletion would result in a growth defect.

For a subset of the genes (*ptpZ, yomI, ywbC,* and *yvfO*) semi-quantitative RT-PCR was used to verify the DNA microarray results. An increase in transcription that was at least 3-fold higher in the *degSU sinR* mutant *versus* the wild type strain ($p<0.05$) was observed confirming that transcription was elevated in the absence of DegU and SinR (Figure 3-2).

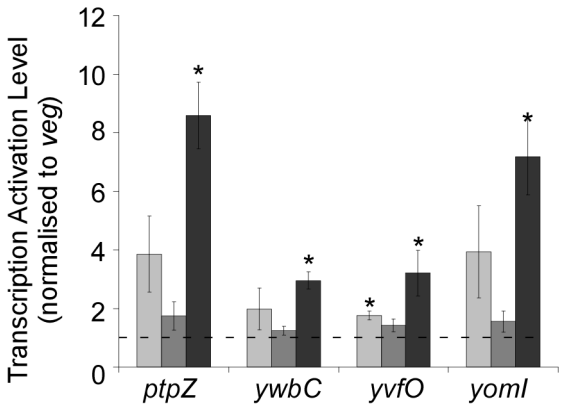


**Figure 3-2 : RT-PCR analysis of targets of DegU and SinR**
RT-PCR analysis in *degSU* (NRS1499) (light-grey bars), *sinR* (NRS1684) (mid-grey bars) and *degSUsinR* (NRS1686) (black bars). Dashed line represents the transcriptional level of 1 in the wild type strain, NCIB3610. Asterisks indicate where transcription was significantly different from wild type (p-value $< 0.05$ for $n \geq 3$). Error bars represent standard error of the mean.

## *3.4 Screening novel SinR DegU co-regulated genes for a role in biofilm formation*

Genes identified through the DNA microarray analysis were tested to see if they were responsible for the enhanced surface adhesion exhibited by the *degSU sinR* strain. To do this, a mutation in each gene was constructed and introduced into the wild-type and *degSU sinR* mutant strains (Table 2-1). None of the mutations screened were successful in relieving the enhanced cell-surface adhesion phenotype (data not shown). It is likely that a combination of mutations would be required to relieve this phenotype but this was not tested. In parallel, taking into account the role that DegU and SinR have in controlling biofilm formation (Kearns, Chu et al. 2005; Kobayashi 2007; Verhamme, Kiley et al. 2007) the impact of deleting each gene on biofilm formation was assessed. Biofilm morphology was monitored after 40 hours incubation. Mutation of ten of the eleven genes identified by DNA microarray analysis did not affect biofilm formation but deletion of *ptpZ* (NRS1827) altered the architecture of the biofilm by comparison

with the wild-type strain (Figure 3-3). For the remainder of this study, focus was devoted to the characterisation of the *tkmA* operon and its members to which *ptpZ* was shown to belong.

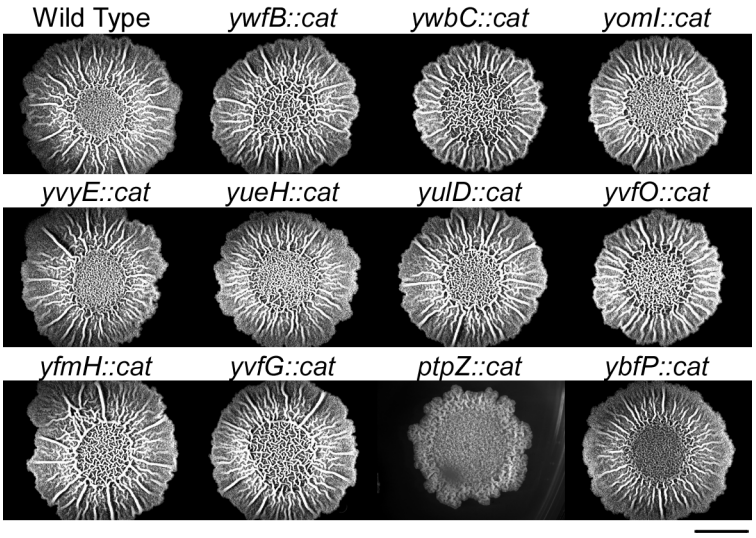


**Figure 3-3 : Assessing the impact on biofilm formation of mutations in the novel DegU and SinR co-repressed genes.**
NCIB3610 (wild type) and strains mutant for *yvfO* (NRS1830), *yfmH* (NRS1832), *yvfG* (NRS1842), *ybfP* (NRS1828), *ywfB* (NRS1389), *ywbC* (NRS1831), *yvyE* (NRS1808), *yulD* (NRS1833), *ptpZ* (NRS1827), *yomI* (NRS1829) and *yueH* (NRS1826) were grown on MSgg agar for 40 hours at 37°C. Scale bar represents 5 mm.

## *3.5 Transcriptional analysis of the tkmA operon.*

The gene encoding PtpZ is found within a region of the chromosome including *tkmA, ptkA,* and *ugd*. The initial aim was to establish if these four genes formed an operon. This was necessary as *i)* the DNA microarray analysis only identified *ptpZ* as differentially expressed, *ii) ugd* is not co-located in the same region of the genome in other Gram-positive bacteria (data not shown), *iii)* and there is a 198-bp gap between the stop codon of *ptpZ* and the start codon of *ugd* that could conceivably contain a

promoter element (see Figure 3-5 for schematic drawing of the *tkmA* operon). We tested whether, as seen for *ptpZ* (Figure 3-2), transcription of *tkmA* and *ugd* was up-regulated in the absence of DegU and SinR. We used RT-PCR analysis with cDNA synthesised from RNA isolated from the wild type (NCIB3610) and the *degSUsinR* mutant strain. For *tkmA, ptpZ* and *ugd* respectively a 10-fold, 7-fold and 3-fold increase in transcription was observed in the absence of SinR and DegU by comparison to the wild-type strain (Figure 3-4). These findings are consistent with the genes being co-regulated and suggest that the DNA microarray analysis was the limiting factor in the identification of *tkmA*, *ptkA* and *ugd* as differentially expressed in the absence of *degU* and *sinR*.

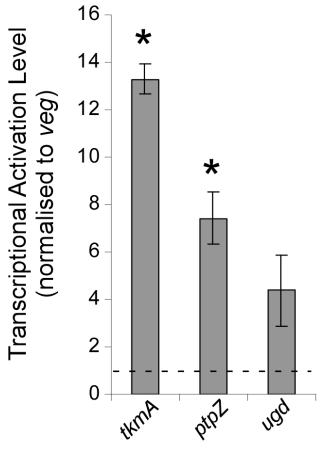


**Figure 3-4: sQRT-PCR analysis of the *tkmA* operon.**
Semi quantitative RT-PCR analysis of the *tkmA* operon. cDNA synthesised from *degSUsinR* (NRS1860) RNA was compared to cDNA synthesised from NCIB3610. The level of transcription shown was obtained by comparison with wild type levels of transcription and normalised to the transcription of the control gene *veg*. The dashed line represents the transcriptional level of 1 in the wild type strain, NCIB3610. The asterisks indicate genes whose transcription is significantly different from wild type transcription levels (p-value < 0.05) where $n \geq 3$. The error bars represent standard error of the mean.

### *3.5.1 Identification of the transcriptional start site of the tkmA operon.*

To determine the transcription start site of the *tkmA* operon 5'-RACE was used. The start site was localised to either -33 bp or -32bp upstream of the *tkmA* coding sequence initiation codon (Figure 3-5). It was not possible to distinguish this more specifically as the anchor primer that is needed for the 5'RACE (NSW367) contains a series of guanine residues which cannot be distinguished from guanine residues in the amplified promoter region (Figure 3-5). However, the favoured nucleotide is the guanine located at -33bp upstream from the initiation codon of *tkmA* for the transcriptional start site. The reasoning being that there is a perfect -10 binding site (TATAAT) for the housekeeping RNA polymerase sigma factor A centred 10bp upstream from this nucleotide (Figure 3-5). Additionally, a sequence with a four out of six base pair match (TGGAGA) to the canonical -35 binding site (TTGACA) for the housekeeping RNA polymerase Sigma-A is centred at 35-bp upstream from the nucleotide (Figure 3-5) (Moran, Johnson et al. 1982). When 5'RACE was applied to the region upstream from the *ugd* translation start site, no transcription initiation site could be identified (data not shown). Taken together the simplest explanation is that the *tkmA-ptkA-ptpZ-ugd* operon is a single transcript that is up-regulated in the absence of DegU and SinR and driven from a single transcriptional start site at 33-bp upstream from the translation initiation codon of *tkmA* (Figure 3-5).

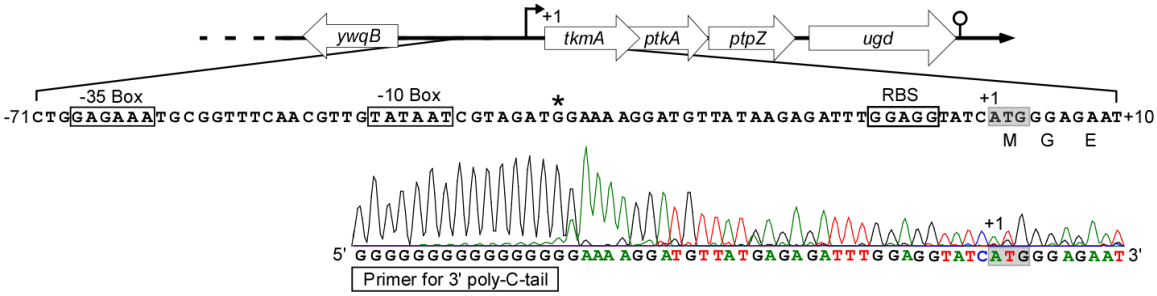


**Figure 3-5: Identifying the transcriptional start of the *tkmA* operon**
5'RACE analysis was used to identify the transcriptional start site of the *tkmA* operon. Genes are represented by hollow arrows containing the gene name in italics. A black, stalked arrow schematically indicates the start position of transcription. A stalked, hollow circle indicates the translational stop site. A section of the *tkmA* promoter sequence can be found directly below the operon structure schematic. Positive and negative numbers refer to the position of the nucleotide with reference to the translational start site, designated as +1. The translational start codon ATG is highlighted by a grey box. Conserved sequences, including the ribosome binding site (RBS), -10 TATAA box and -35 box, are outlined in black. The proposed transcriptional start site (-33bp downstream of the translational start site) is highlighted by an asterisk. The capital letters M, G, E indicate the translated sequence of TkmA. A DNA sequencing readout showing the predicted transcriptional start site preceded by an engineered poly-G tail can be seen directly below the DNA sequence of *tkmA*.

### *3.5.2 The tkmA operon is transcribed as a single transcript.*

To determine if *tkmA, ptkA, ptpZ,* and *ugd* were encoded on a single transcript, mRNA was isolated from wild-type *B. subtilis* and cDNA was synthesised using a reverse *ugd* gene specific primer (Figure 3-6). The cDNA generated corresponded to the *ugd* transcript and was used as a template for PCR with three primer pairs that were specific to the internal coding regions of *tkmA*, *ptpZ* and *ugd*. As a negative control, a sample that had been subjected to the same treatment but which lacked the reverse transcriptase was used to ensure that the PCR products were not the result of any contaminating genomic DNA (data not shown). As a positive control, genomic DNA was used to

ensure the product amplified was the correct size (Figure 3-6). All three gene-specific PCR products were amplified from the cDNA indicating that *tkmA, ptkA, ptpZ and ugd* are co-transcribed (Figure 3-6).

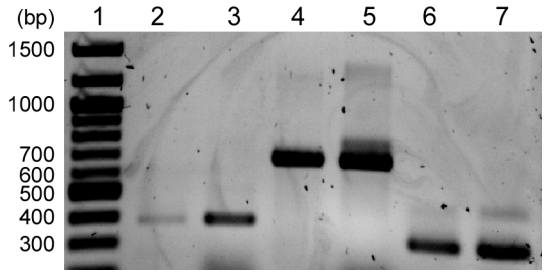


**Figure 3-6: *tkmA*, *ptkA*, *ptpZ* and *ugd* are co-transcribed.**
Regions of DNA internal to *tkmA, ptpZ* and *ugd* were amplified from cDNA generated using an *ugd*-specific reverse primer. Lane 1 contains 100bp ladder (NEB Biolabs™). Lanes 2 and 3 contain *tkmA*; lanes 4 and 5 contain *ptpZ*; and lanes 6 and 7 contain *ugd* PCR product. Lanes 2, 4 and 6 show PCR products amplified from cDNA template, while lanes 3, 5 and 7 show PCR products amplified from gDNA template. Primer combinations used for amplification of *tkmA*, *ptpZ* and *ugd* can be found in Table 2-2.

## *3.6 Electrophoretic mobility shift analysis of the* tkmA *promoter.*

### *3.6.1 Purification of DegS*

We wanted to establish whether DegU and/or SinR directly regulated transcription from the *tkmA* promoter. To test this we conducted electrophoretic mobility shift assays with purified and phosphorylated DegU-$_{His6}$ and purified SinR-$_{His6}$. It has been shown previously that the phosphorylated form of DegU (hereafter referred to as DegU~P) is required for biofilm formation (Verhamme, Kiley et al. 2007). Therefore DegS was also purified as it is the cognate sensor kinase responsible for the phosphorylation of DegU.

Initial attempts to purify DegS in its native and active conformation were based on a method established by the Msadek research group (Dubrac and Msadek 2004). The expression vector pETdegS, carried by BL21 λDE3 pRep4 GroESL, designed for the over-expression of DegS-$_{His6}$ was kindly provided by Prof. Msadek (NRS2219). Unfortunately, purification of soluble DegS could not be achieved using this approach. In an attempt to overcome this, NRS2219 was grown at a range of different temperatures in the hope that lowering the temperature of the cells during growth would allow DegS-$_{His6}$ to fold more slowly, and thus increase the chance that DegS-$_{His6}$ would be produced in its active form. However despite extensive attempts to purify soluble DegS, this could not be achieved (Figure 3-7).

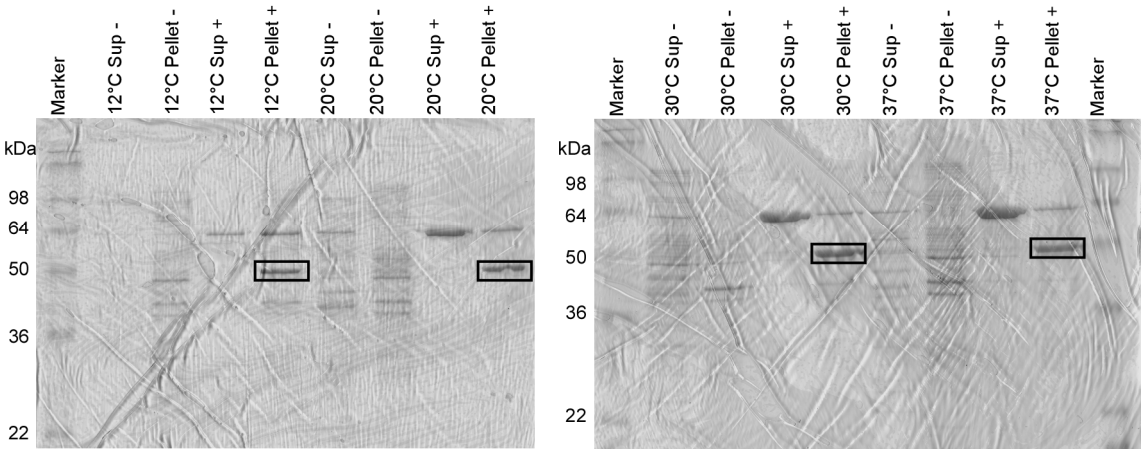


**Figure 3-7: Solubility testing of DegS-$_{His6}$ at a range of growth temperatures.**
Cells were grown at the temperatures stated in the figure overnight. Cells were lysed by sonication and centrifuged to separate soluble and insoluble proteins. Samples were normalised according to the $OD_{600}$ measurement of the culture. 10 µl of pellet (Pellet) or supernatant (Sup) boiled in SDS loading buffer was run on a 12% SDS polyacrylamide gel. 'Marker' refers to 5 µl SeeBlue Plus2 protein marker. A 'plus' symbol denotes samples in which the expression of DegS-$_{His6}$ was induced by the addition of 500 µM IPTG, whereas a 'minus' symbol identified samples which were not induced. Black boxes indicate presence of DegS-$_{His6}$. See materials and methods for details.

As we were unable to purify DegS-$_{His6}$ in its native conformation directly from the cells, a different method was used. The alternative method, which is based on a method from

Dr. K. Kobayashi (Kobayashi 2007), involves the denaturation of insoluble inclusion bodies containing over-expressed DegS-$_{His6}$. Essentially, the inclusion bodies are purified from contaminating proteins, and then the purified protein is renatured slowly alowing the protein to re-fold into its active conformation. A new plasmid, pETdegS, constructed for the purpose of over-expressing DegS-$_{His6}$ was kindly provided by Dr. K. Kobayashi (Kobayashi 2007). Cells containing the pETdegS construct were grown until an $OD_{600}$ of 0.38 was reached. At this point DegS-$_{His6}$ expression was induced by the addition of 500 μM IPTG. Samples of cells were taken prior to induction of DegS-$_{His6}$ expression and at 3 hours after induction. The samples were then assessed using SDS-PAGE in order to confirm that DegS-$_{His6}$ was expressed. Additionally, a western blot was conducted in order to detect the histidine tag of the DegS construct. This was done to ensure that the histidine tag had not been degraded and could therefore still be used for the purification of DegS–$_{His6}$ (Figure 3-8).

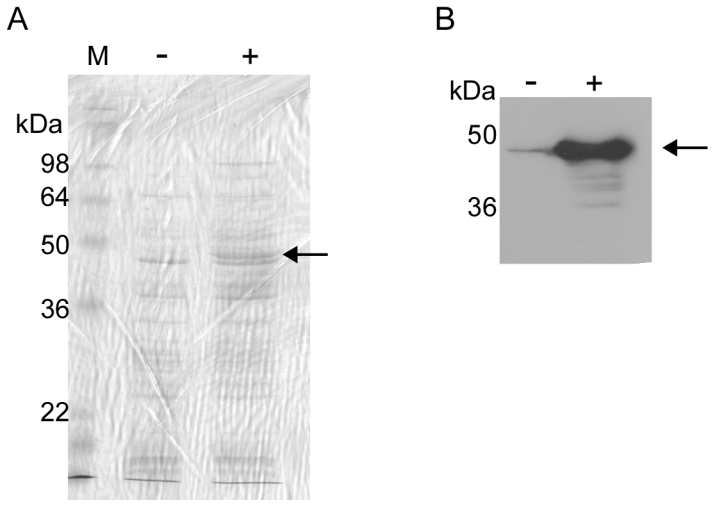


**Figure 3-8: SDS-PAGE and western blot analysis of DegS-$_{His6}$ expression.**
(**A**) Cell samples before (-) and after (+) induction were resuspended in SDS loading buffer. 10 μl of each sample was run on a 12% SDS polyacrylamide gel. 5μl of SeeBlue Plus2 (Invitrogen) protein marker was also run on gel (M). (**B**) Western blot analysis for the detection of DegS-$_{His6}$. Arrows on both (**A**) and (**B**) indicate the size that DegS-$_{His6}$ is expected to run to (45.73 kDa).

Expression of DegS-$_{His6}$ was confirmed (Figure 3-8A) and the histidine tag was found to be intact (Figure 3-8B). The cells containing DegS-$_{His6}$ were pelleted and lysed using BugBuster (Novagene) (see Material and Methods section 2.5.4.5.1). DegS-$_{His6}$ inclusion bodies were then purified and finally resuspended in denaturation buffer (Figure 3-9).

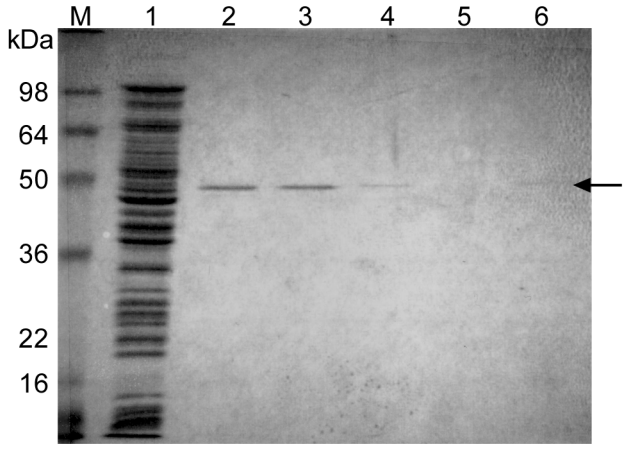


**Figure 3-9: Purification of DegS-$_{His6}$ inclusion bodies.**
Samples were run on a 12% SDS polyacrylamide gel. Samples were boiled in SDS loading buffer. Lanes were loaded as follows: M, 5 µl SeeBlue Plus2 protein marker; 1, whole cell lysis; 2, supernatant from wash 1 ; 3, supernatant from wash 2 ; 4, supernatant from wash 3 ; 5, supernatant from wash 4 ; 6, purified inclusion bodies resuspended in the denaturation buffer (see Materials and Methods). Arrow indicates the presence of DegS-$_{His6}$ in the denaturation buffer sample. Expected size of DegS-$_{His6}$ is 45.73 kDa.

After denaturation, the protein was applied to a HisTrap column, in which the $_{His6}$-tagged-protein was captured by the Ni-NTA beads. Other contaminating proteins were washed from the column. Next, the protein was refolded while still attached to the HisTrap column. In contrast to the Kobayashi method, this step was performed using a FPLC machine. This allowed for a more gradual removal of the denaturing urea from

the bound DegS-$_{His6}$, and it was felt that this would improve the quality of the re-folded DegS protein. After refolding of the protein was complete, elution of DegS-$_{His6}$ was achieved by adding increasing amounts of imidazole (Figure 3-10).

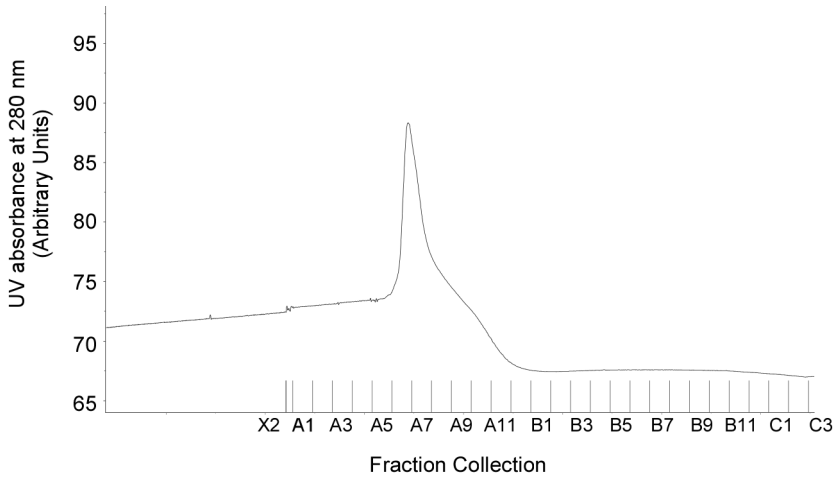


**Figure 3-10: Elution trace of renatured DegS-$_{His6}$ from HisTrap column.**
Trace shows the elution profile of DegS-His6 protein after purification through a HisTrap column. Protein was detected by UV absorbance at 280 nm. Fractions were collected in 1ml volumes and were labelled as A1-A12, B1-B12 and C1-C3. The X2 fraction indicates the flow through collection from the stringent wash step.

Assessment of the elution trace showed a strong peak correlating with the A7 fraction collection, indicating the presence of protein in this sample. In order to verify that the peak observed in the trace was due to the presence of DegS-$_{His6}$, samples of collection fractions A5 to A10 were tested for the presence of DegS-$_{His6}$ by running the samples on a 12% SDS polyacrylamide gel and staining with coomassie blue stain (Figure 3-11).

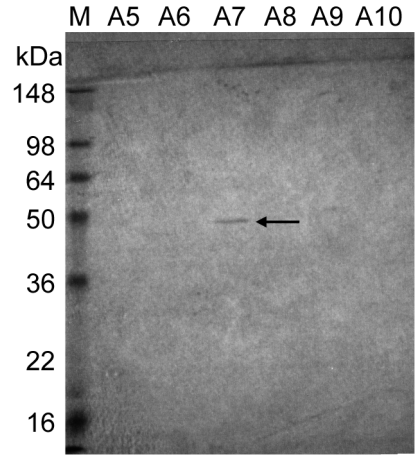


**Figure 3-11: SDS-PAGE analysis of eluted DegS-$_{His6}$ fractions**
Samples were run on a 12% SDS polyacrylamide gel. Samples were added to SDS loading buffer. Lanes were loaded as follows: M, 5 µl SeeBlue Plus2 protein marker; A5 to A10, 10 µl of each eluted fraction mixed with SDS loading buffer. Arrow indicates the presence of DegS-$_{His6}$ in sample A7. Expected size of DegS-$_{His6}$ is 45.73 kDa.

Assessment of the SDS polyacrylamide gel revealed a band correlating to the expected size of Degs-$_{His6}$ in the A7 fraction collection. From this we can assume with a level of certainty that the protein present is DegS-$_{His6}$. Protein from this fraction was dialysed against DegS dialysis buffer (Materials and Methods) and concentrated prior to use.

### *3.6.2 Purification of DegU*

DegU-$_{His6}$ was purified as described previously (Verhamme, Kiley et al. 2007). Plasmid pNW43 (*degU-$_{His6}$* in pQE60) was transformed into M15 *E. coli* cells containing the pRep4 vector. pRep4 encodes a repressor of the IPTG inducible promoter located within pNW43, thus ensuring that induction of *degU-$_{His6}$* occurs only in the presence of IPTG . The cells were then grown at 37 ˚C until an $OD_{600}$ of 1.0 was reached. Cells were sampled and then induced by adding IPTG to a final concentration of 100 µM IPTG. Growth was continued at 26˚C for 16 hours prior to harvesting the cells. Cells containing DegU-$_{His6}$ were lysed using a French press and the cell debris removed by

centrifugation at 4˚C prior to application to a Ni-NTA HisTrap column for protein capture. Protein purification and elution was achieved by gradually increasing the concentration of imidazole present in the elution buffer, controlled by an Akta Prime FPLC machine.

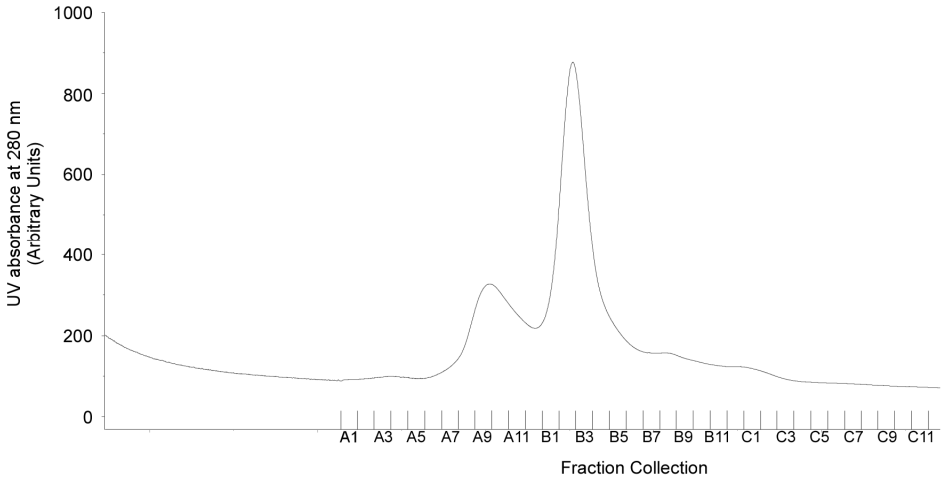


**Figure 3-12: Elution trace of DegU-$_{His6}$ from HisTrap column**
Trace shows the elution profile of DegU-$_{His6}$ protein after purification through a HisTrap column. Protein was detected by UV absorbance at 280 nm. Fractions were collected in 1ml volumes and were labelled as A1-A12, B1-B12 and C1-C11.

Assessment of the elution trace showed two peaks ranging from fractions A9 to B6, indicating the presence of protein in these samples. In order to identify if DegU-$_{His6}$ was present in either of these groups of fractions, samples of the above mentioned collection fractions were tested for the presence of DegU-$_{His6}$ by running the samples on a 12% (v/v) SDS polyacrylamide gel and staining with coomassie blue stain (Figure 3-13).

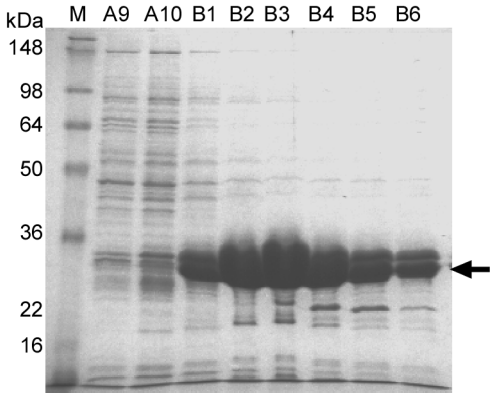


**Figure 3-13: SDS-PAGE analysis of DegU-$_{His6}$ fractions eluted from a HisTrap column**
Samples were run on a 12% (v/v) SDS polyacrylamide gel. Samples were added to SDS loading buffer prior to running. Lanes were loaded as follows: M, 5 µl SeeBlue Plus2 protein marker; A9 to B6, 10 µl of each eluted fraction mixed with SDS loading buffer. Arrow indicates the expected size of DegU-$_{His6}$ which is 26.64 kDa.

By assessing the SDS polyacrylamide gel together with the FPLC elution tract, we could determine that the second, larger peak correlating with fraction collection B3 most likely contained DegU-$_{His6}$. Following IMAC purification fraction collections B1-B6 were pooled and DegU-$_{His6}$ was purified from contaminating DNA by application to a DEAE-FF column (GE Healthcare ™). It is necessary to remove contaminating DNA from the purified DegU-$_{His6}$ prior to EMSA application, as DNA binding cannot occur otherwise. Elution fractions containing DegU-$_{His6}$ were collected by FPLC machine (Figure 3-14).

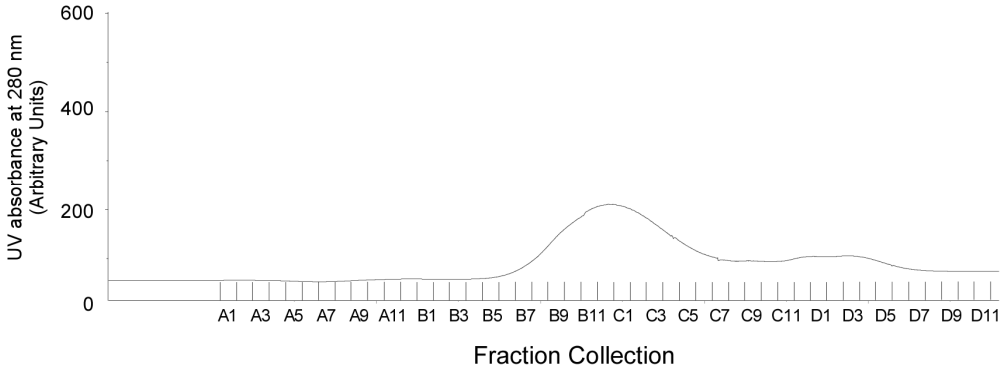


**Figure 3-14: Elution trace of DegU-$_{His6}$ from DEAE column**
Trace shows the elution profile of DegU-$_{His6}$ protein after purification through a DEAE column. Protein was detected by UV absorbance at 280 nm. Fractions were collected in 1ml volumes and were labelled as A1-A12, B1-B12, C1-C12 and finally D1-D11.

Assessment of the elution trace showed a single peak ranging from fractions B6 to C7, indicating the presence of protein in these samples. In order to assess the purity of DegU-$_{His6}$ present in this group of fractions, samples of the above mentioned collection fractions were tested for the presence of DegU-$_{His6}$ by running the samples on a 12% (v/v) SDS polyacrylamide gel and staining with coomassie blue stain (Figure 3-15).

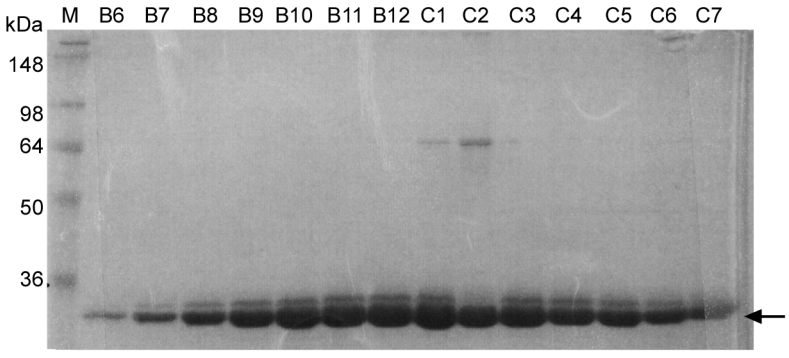


**Figure 3-15: SDS-PAGE analysis of DegU-$_{His6}$ fractions eluted from a DEAE column**
Samples were run on a 12% (v/v) SDS polyacrylamide gel. Samples were added to SDS loading buffer prior to running. Lanes were loaded as follows: M, 5 µl SeeBlue Plus2 protein marker; B6 to C7, 10 µl of each eluted fraction mixed with SDS loading buffer. Arrow indicates the expected size of DegU-$_{His6}$ which is 26.64 kDa.

A strong band correlating to the expected size of DegU-$_{His6}$ could be seen on the SDS-polyacrylamide gel. In addition, present in all lanes except B6 and C2 is a band which corresponds to a protein which has a slightly higher molecular weight than DegU-$_{His6}$. The identity of the additional band is unknown, and may be a minor contaminant. However it is important to note that the presence of this additional band does not impact on the ability of DegU-$_{His6}$ to bind to its DNA targets (Figure 3-17 and Figure 3-18). Additionally, bands of a higher molecular weight were observed in lanes C1 and C2. Based on the size of DegU-$_{His6}$ and the approximate size of the observed band, it is possible that these bands correspond to DegU-$_{His6}$ trimers. All samples (B6-C7) were pooled and dialysed before use (20 mM Tris-HCl (pH 8.0) 50 mM NaCl).

### *3.6.2.1 DegS phosphorylates DegU* in vitro.

Prior to EMSA analysis we confirmed that purified DegS-$_{His6}$ was capable of phosphorylating DegU-$_{His6}$ *in vitro* using γ-$^{32}$P-ATP (Figure 3-16). Interestingly, an additional band was detected that ran to ~98 kDa. We predict that this may be a DegS-dimer complex as it runs at approximately twice the molecular weight of a single DegS-$_{His6}$ protein. This additional band does not impair the ability of DegS-$_{His6}$ to phosphorylate DegU-$_{His6}$. As we were able to achieve successful phosphorylation of DegU by purified DegS *in vitro*, we decided to proceed with the electrophoretic mobility shift analysis of the *tkmA* promoter region.

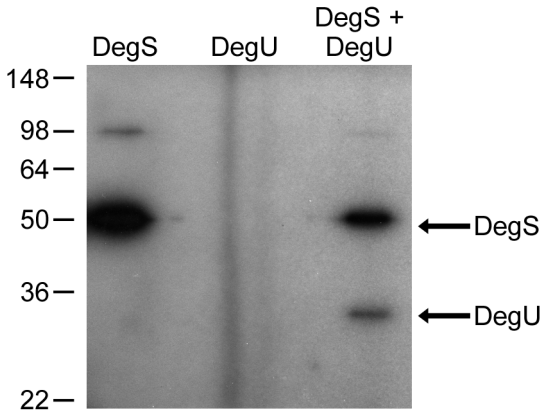


**Figure 3-16: Phosphorylation of DegU-$_{His6}$ by purified DegS-$_{His6}$.**
Purified DegU-$_{His6}$ and DegS-$_{His6}$ were incubated with $^{32}$P γ-ATP, separately and in combination. 1μg of each protein, as required, was added to each reaction mixture. Proteins were mixed with SDS loading buffer before they were loaded onto a 12% SDS polyacrylamide gel. Gel was dried and exposed to X-ray film for 20 hours at -70˚C. Arrows indicate the size that DegU (26.64 kDa) and DegS (45.73 kDa) are expected to run to.

### *3.6.2.2 DegU directly regulates the transcription of the* tkmA *operon.*

The activity of purified and phosphorylated DegU-$_{His6}$ protein was established by the presence of a positive interaction between the known DegU~P regulated promoter, $P_{aprE}$ and the freshly phosphorylated DegU-$_{His6}$ (Figure 3-17). The promoter region of *aprE* was amplified using primers NSW61 and NSW654 (see Table 2-2 for full sequences). Additional non-sifting bands were observed. It is highly unlikely that these bands correspond to PCR products which are not $P_{aprE}$. This is because prior to radio-labelling, the PCR product was run through an agarose gel and a band corresponding to the expected size of $P_{aprE}$ was cut from the gel. During the optimisation of the DegU EMSA protocol, several different buffering systems were tested. Interestingly, multiple radiolabelled bands were only detected when the $P_{aprE}$ product was run through a Tris-Glycine polyacrylamide gel. Thus the presence of the multiple bands may be simply due to the conditions in which the EMSA was run. It is important to stress that under

these conditions freshly phosphorylated DegU-$_{His6}$ is able to shift $P_{aprE}$. Therefore we felt it was appropriate to continue using these conditions during our investigation into the interaction between $P_{tkmA}$ and phosphorylated DegU-$_{His6}$.

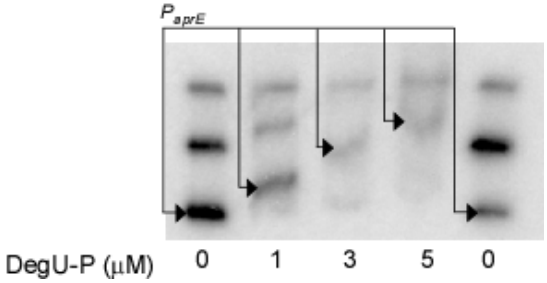


**Figure 3-17: Electrophoretic mobility shift analysis of the *aprE* promoter using purified DegU~P**
DNA binding reactions were conducted with γ-$^{32}$P labelled DNA corresponding to the region -620 to +24bp surrounding the start of *aprE*. 1 ng labelled DNA was loaded into each lane, with increasing amounts of purified DegU~P-$_{His6}$. Arrows indicate labelled DNA corresponding to the promoter region of *aprE*.

A 542-bp region of DNA upstream from the translation start site of *tkmA* was amplified by PCR using primers NSW146 and NSW147 (See Table 2-2 for full sequences). The results showed that the mobility of the promoter region of *tkmA* was impeded by the addition of 1 μM DegU~P during gel electrophoresis (Figure 3-18). Greater retention was seen with increasing amounts of DegU~P (3 μM). Unlabelled DNA corresponding to the *tkmA* promoter was able to out-compete radio-labelled DNA for access to the binding domain of DegU~P, indicating that the interaction was specific (Figure 3-18). Consistent with this a region of DNA corresponding to the internal coding region of *tkmA* was not able to compete for the binding domain of DegU~P (Figure 3-18).

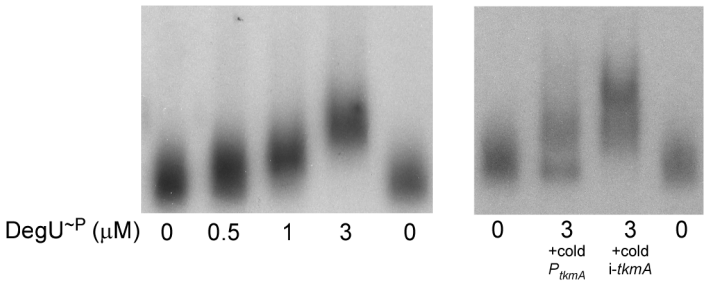


**Figure 3-18: Electrophoretic mobility shift analysis of the *tkmA* promoter using purified DegU~P.** DNA binding reactions were conducted with γ-$^{32}$P labelled DNA corresponding to the region -500 to +42 bp. 1 ng labelled DNA was loaded into each lane, with or without purified DegU~P-$_{His6}$. Further binding reactions include the addition of 100 ng of unlabelled *tkmA* promoter region PCR product ($P_{tkmA}$) (-500 to +42 bp fragment) or unlabelled internal *tkmA* (*i-tkmA*) (+3 to +379 bp) to the EMSA reaction.

### *3.6.3 Purification of SinR*

SinR-$_{His6}$ was purified as previously described (Verhamme, Murray et al. 2009). The histidine tag used for purification was removed using Novagen's thrombin cleavage capture kit. The purification of SinR was monitored at various stages by running samples on a 15% SDS polyacrylamide (Figure 3-19).

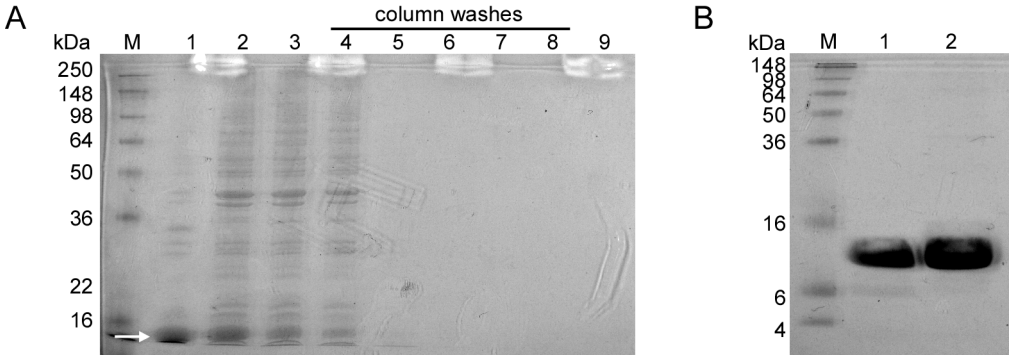


**Figure 3-19: SDS-PAGE analysis of SinR purification**
(**A**) Samples collected during the purification of SinR were assessed by SDS PAGE in order to determine the purity of SinR. White arrow indicates expected position of SinR-$_{His6}$. Samples were normalised by volume and 10 μl of each sample was loaded onto the gel. Lanes were loaded as follows: lane 1, lysed, cell debris; lane 2. ultra centrifuge supernatant; lane 3, flow through from Ni-NTA column; lanes 4-8, series of washes with 20 mM imidazole; lane 9, liquid phase of Ni- beads prior to His tag cleavage (SinR-His should be attached to the beads). (**B**) Samples of purified SinR before (1) and after (2) removal of thrombin after cleavage.

The activity of purified SinR-$_{His6}$ protein was established by the presence of a positive interaction between the known SinR regulated promoter, $P_{yqxM}$ and the purified SinR-$_{His6}$ (Chu, Kearns et al. 2006) (Figure 3-20). Under the conditions used, SinR was able to inhibit the progression of the *yqxM* promoter region through the gel. This test confirmed that SinR was active and under these conditions SinR would bind to its targets *in vitro*.

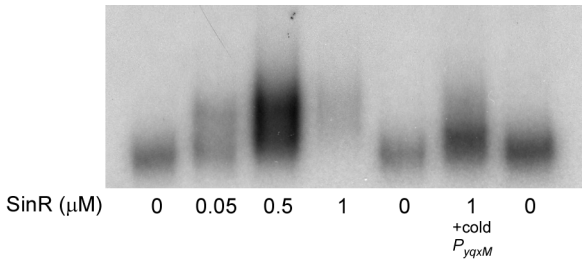


**Figure 3-20: Electrophoretic mobility shift analysis of the *yqxM* promoter using purified SinR.** DNA binding reactions were conducted with γ-$^{32}$P labelled DNA corresponding to the region -312 to +16 bp surrounding the start of *yqxM*. 1 ng labelled DNA was loaded into each lane, with increasing amounts of purified SinR. Further binding reactions include the addition of 100 ng of unlabelled *yqxM* promoter region PCR product to the EMSA reaction.

### *3.6.3.1 SinR indirectly regulates the transcription of the* tkmA *operon.*

In contrast to DegU-$_{His6}$, SinR-$_{His6}$ did not interact with the *tkmA* promoter DNA (Figure 3-21). These results were as anticipated as *in silico* analysis of the *tkmA* promoter region did not identify any DNA sequences corresponding to the SinR consensus binding (Chu, Kearns et al. 2006). The inhibitory action exerted by SinR on transcription from the *tkmA* promoter is therefore unlikely to be directly mediated (Figure 3-2 and Figure 3-21).

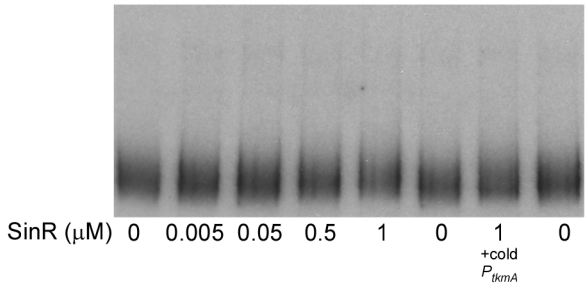


**Figure 3-21: Electrophoretic mobility analysis of the *tkmA* promoter using purified SinR.**
DNA binding reactions were conducted with γ-$^{32}$P labelled DNA corresponding to the region -500 to +42 bp. 1 ng labelled DNA was loaded into each lane, with or without purified SinR-$_{His6}$. Further binding reactions include the addition of 100 ng of unlabelled *tkmA* promoter region PCR product ($P_{tkmA}$) (-500 to +42 bp fragment).

## *3.7 Discussion*

In summary the results from this investigation confirmed that DegU and SinR regulate biofilm formation via parallel pathways. Furthermore, a novel group of 11 genes were found to be upregulated in the absence of DegU and SinR. Given the involvement of DegU and SinR during biofilm formation, mutations were made in these 11 genes and their impact on biofilm formation was investigated. The results demonstrated that only mutation of one target, *ptpZ*, resulted in an altered colony phenotype (Figure 3-3). While the remaining 10 genes did not alter biofilm formation, based on the known functions of the genes identified, it is possible that DegU and SinR may regulate an even wider range of behaviours and cellular functions. It must be noted that false positives are common occurrences with large scale screens such as DNA microarrays, and as only a selection of genes were double checked as being upregulated in the absence of DegU and SinR by semi-quantitative RT-PCR (Figure 3-2), the overlapping

targets of DegU and SinR remain to be validated. However as the focus of this study was to investigate the impact of DegU and SinR during biofilm formation, this was not included in the scope of this investigation and as such our attention was devoted to investigating the role of *ptpZ* during biofilm formation.

The results from our investigation of the *tkmA* operon have shown that the transcription of this operon is under the control of the transcriptional regulators DegU and SinR. Recently we hypothesised that DegU and SinR were part of two separate but converging pathways that are required for biofilm formation by *B. subtilis* (Verhamme, Murray et al. 2009) and the work shown here supports this original hypothesis. Moreover, this study has demonstrated that DegU directly regulates the transcription of the *tkmA* operon as it binds directly to the *tkmA* promoter region. In order to identify the exact binding site of DegU within the 500 bp region of DNA used during the EMSA analysis, future experiments would include DNA footprinting analysis.

It must be noted that limitations of the EMSA analysis do exist. A major limitation is that the extent to which the pool of DegU was phosphorylated by DegS cannot be determined. It must be stressed that under the conditions used, it is clear that DegS was able to phosphorylate DegU (Figure 3-16). Yet to conclusively determine which form of DegU was able to bind to the promoter region of *tkmA*, future experiments would include EMSA analysis using a form of DegU which could not become phosphorylated (DegU $D^{56}N$) (Dahl, Msadek et al. 1991). Using the information that is available, it is highly likely that the phosphorylated form of DegU was able to bind the promoter region of *tkmA*. Under the conditions used, DegU that was phosphorylated by DegS was able to shift the promoter region of *aprE* (Figure 3-17), a known target of DegU~P (Ogura, Shimane et al. 2003). Given that the phosphorylated form of DegU is required to regulate biofilm formation by *B. subtilis* (Kobayashi 2007; Verhamme, Kiley et al.

2007) and that mutating *tkmA*, *ptkA* and *ptpZ* affect biofilm formation, it is most likely that the phosphorylated form of DegU binds to the promoter region of the *tkmA* operon. Taking into consideration that transcription from the *tkmA* promoter is up-regulated in the absence of *degU* (Figure 3-2) this suggests that DegU~P therefore functions as an inhibitor, and not an activator, of transcription from the *tkmA* operon. It is important to note that while mid-levels of DegU~P activate biofilm formation (Stanley and Lazazzera 2005; Kobayashi 2007; Verhamme, Kiley et al. 2007), high levels of DegU~P in the cell inhibit biofilm formation (Verhamme, Kiley et al. 2007). Furthermore, these findings add to the loci regulated by DegU~P during the formation of a biofilm (Kobayashi 2007; Verhamme, Kiley et al. 2007; Verhamme, Murray et al. 2009).

In contrast to the results for DegU, it was determined that the transcriptional regulator SinR does not directly regulate the transcription of *tkmA* operon. However, we cannot exclude the possibility that the increase in transcription may be due to pleiotropic effects on gene expression that occur when *sinR* and *degU* are deleted in combination. In addition, we cannot rule out the possibility that SinR may require an additional transcriptional regulator in order to exert its regulatory effect on the transcription of the *tkmA* operon. Such a situation exists for the *lytABC* operon where SlrR and SinR are required for a protein-DNA interaction to be established (Chai, Norman et al. 2010). Finally, it is also interesting to note that transcription of the *tkmA* operon is also directly regulated by Spo0A~P (Fawcett, Eichenberger et al. 2000; Molle, Fujita et al. 2003). This provides the second example of a locus involved in biofilm formation where the Spo0A and DegU regulatory cascades converge; the first being the promoter element of *yuaB* (Verhamme, Murray et al. 2009).

# 4 Investigating the role of tyrosine phosphorylation during biofilm formation

## *4.1 Introduction*

The *tkmA* operon identified and characterised in Chapter 3 encodes the proteins TkmA, PtkA and PtpZ which are involved in regulating the activity of target proteins through tyrosine phosphorylation (Mijakovic, Poncet et al. 2003; Mijakovic, Petranovic et al. 2006; Jers, Pedersen et al. 2010). The products of the *tkmA* operon were first identified as regulators of the conversion of UDP-glucose to UDP-glucuronate, which is used as a precursor of the cell wall associated polysaccharide, teichuronic acid (Figure 1-15) (Mijakovic, Poncet et al. 2003). Specifically, PtkA is a BY-kinase that activates the UDP-glucose dehydrogenase Ugd (Mijakovic, Poncet et al. 2003) by phosphorylation of the tyrosine residue at position 70 (Petranovic, Grangeasse et al. 2009). Conversely, PtpZ is a tyrosine phosphatase which acts by dephosphorylating Ugd~P, thus inactivating it (Mijakovic, Poncet et al. 2003).

In addition to the role of PtkA as an activator of Ugd, it has additional target proteins and thus is described as a promiscuous BY-kinase (Mijakovic, Poncet et al. 2003; Jers, Pedersen et al. 2010). To date PtkA has been shown to phosphorylate 13 proteins (Ugd and TuaD (Mijakovic, Poncet et al. 2003), SsbA and SsbB (YwpH) (Mijakovic, Petranovic et al. 2006), and YorK, Asd, Eno, YjoA, YnfE, YvyG, InfA, Ldh and OppA (Jers, Pedersen et al. 2010)), and thus is an important regulator of a wide range of cellular processes.

In this chapter, I aimed to investigate, in detail, the role of tyrosine phosphorylation during biofilm formation. I began by using a more sophisticated approach to introduce marker-less and in-frame mutations on the chromosome. I addressed whether the other

proteins encoded by the *tkmA* operon namely, TkmA, PtkA and Ugd, participated in the regulation of biofilm formation. Using this method, I also repeated the construction of the *ptpZ* mutant and confirmed the participation of PtpZ during the regulation of biofilm formation (Figure 3-3).

## 4.2 Characteristic features of PtkA

### *4.2.1 Assessing the impact of deleting ptkA*

Having defined the structure of the *tkmA* operon (Figure 3-5 and Figure 3-6) I wanted to establish the role of tyrosine phosphorylation during the formation of a biofilm. As *tkmA-ptkA-ptpZ-ugd* form an operon (Figure 3-4 and Figure 3-6), an in-frame deletion in *ptkA* was made to circumvent downstream effects on transcription and/or the stoichiometry of the remaining proteins (see Materials and Methods). It has been reported that PtkA and PtpZ play a role in controlling DNA replication (Petranovic, Michelsen et al. 2007) and that a *ptpZ* mutant exhibits a severe growth defect (Petranovic, Michelsen et al. 2007). A growth defect would render interpretation of biofilm formation ambiguous; therefore I first tested whether the Δ*ptkA* strain had a reduced growth rate. In both MSgg liquid medium and LB (data not shown), the Δ*ptkA* mutant had a doubling time equal to that of the parental strain (Figure 4-1).

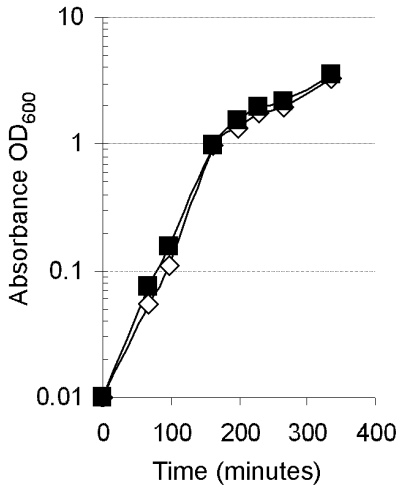


**Figure 4-1: Δ*ptkA* does not have a reduced growth rate**
Growth NCIB3610 (white triangles) and Δ*ptkA* (black squares) was monitored for several hours in MSgg liquid media. At various time points, the absorbance of the culture was assessed by reading the sample at wavelength $OD_{600}$. The graph displayed is representative of 3 independent rounds.

Absence of PtkA has been shown to have deleterious effects on cell length and nucleoid number (Petranovic, Michelsen et al. 2007). Therefore we analysed cell length and nucleoid distribution of our Δ*ptkA* strain using microscopy. In contrast to the previously published data, our preliminary findings suggested that there was no significant difference between the cell length of a *ptkA* mutant compared with wild type. Furthermore, under the conditions used in this study, deletion of *ptkA* did not appear to significantly alter nucleoid number (Figure 4-2). Several reasons may explain this discrepancy. Firstly, it must be noted that the Hoechst stain was not uniformly taken up by both the wild type NCIB3610 strain and the Δ*ptkA* mutant (Figure 4-2). Secondly, we did not test the original *ptkA* mutant used in the Petranovic study to see the impact of the mutation under our conditions. It is possible that differences in either the method of strain construction or the genetic background may explain why we were unable to observe the effects on cell length and nucleoid number that was observed by Pertranovic *et al*. However, in our hands these results tentatively suggest that in NCIB3610, deletion

of *ptkA* does not result in a gross growth defect and that our *ptkA* mutant is unlikely to possess a defect in DNA replication.

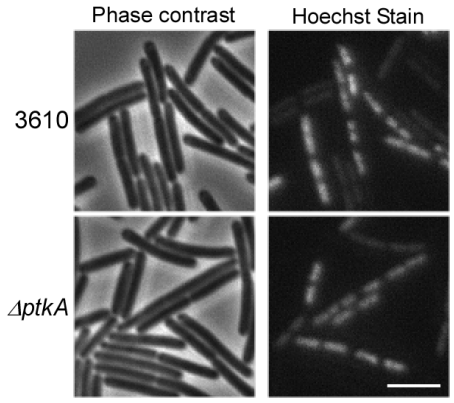


**Figure 4-2: Staining of nucleoids in Δ*ptkA* cells compared to NCIB3610 using Hoechst 33342.**
Phase contrast and fluorescent images of NCIB3610 and Δ*ptkA* collected using Zeiss Axio Imager M1. Scale bars represent 5 μm.

Having established that Δ*ptkA* (NRS2544) did not exhibit a growth defect, the impact of deleting *ptkA* on biofilm formation was tested. Three independent indicators of biofilm formation were assessed; namely complex colony architecture, pellicle formation and the ability to form environmentally resistant spores (Branda, Gonzalez-Pastor et al. 2001; Vlamakis, Aguilar et al. 2008). All of these processes have been linked with the biosynthesis and assembly of the extracellular matrix. Starting with complex colony architecture; we determined that Δ*ptkA* was unable to develop the complex radial structures typical of the mature *B. subtilis* biofilm on semi-solid agar (Figure 4-3). To confirm that the biofilm morphology of the Δ*ptkA* mutant was specific to the absence of PtkA, a wild-type copy of *ptkA* was introduced into the *amyE* locus under the control of a heterologous promoter; $P_{spank\text{-}hy}$-*ptkA-lacI* (NRS2804). The biofilm architecture was fully restored compared to that shown by the wild-type strain both in the absence of IPTG and in the presence of 10 μM IPTG (compare Figure 4-3B to Figure 4-3C). These

findings confirm that the altered biofilm phenotype was specific to the disruption of *ptkA*.

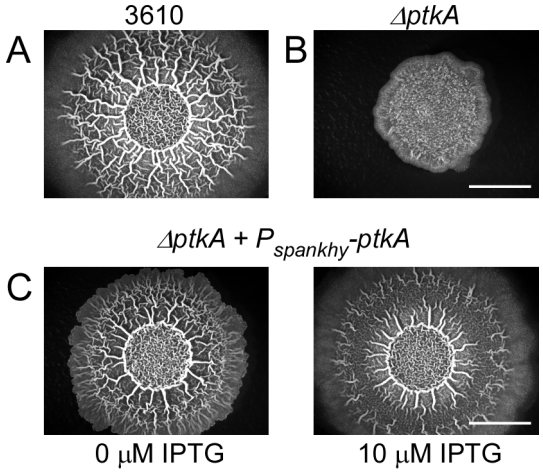


**Figure 4-3: Complex colony architecture of Δ*ptkA* and Δ*ptkA* complemented with wild type *ptkA*.**
Strains (**A)** NCIB3610 and **(B)** Δ*ptkA* (NRS2544) were assessed as described in Figure 3-1. (**C**) Mutant Δ*ptkA* + *amyE*-$P_{spank\text{-}hy}$-*ptkA*-*lacI* (NRS2804) was grown on MSgg agar with and without the addition of 10 μM IPTG. The scale bar represents 5 mm.

Next, we tested the effect of mutating *ptkA* on the ability of the strain to form robust pellicles. In contrast to the reduction in colony architecture complexity (Figure 4-3B), the pellicle formed by the Δ*ptkA* strain showed extensive three dimensional structural complexity but it entirely lacked the "fruiting body structures" that are present on the wild-type pellicle (compare Figure 4-4C to Figure 4-4D).

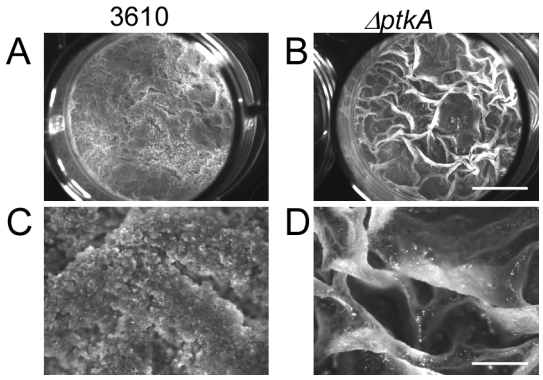


**Figure 4-4: Pellicle morphology of Δ*ptkA* compared to NCIB3610.**
Strains (**A**) NCIB3610 and (**B**) Δ*ptkA* (NRS2544) were assessed as described in Figure 3-1. The scale bar represents 5 mm (**A** and **B**) and 1mm (**C** and **D**).

Taken together, the altered colony morphology and lack of "fruiting body" formation on the pellicle, we decided to investigate whether or not the Δ*ptkA* strain was able to sporulate. After 24 hours incubation under biofilm formation conditions 13±2.5% of the Δ*ptkA* mutant population had sporulated by comparison to the wild-type that exhibited 25±4% sporulation (n=3; $p<0.06$ 2-way students t-test). After 72 hours the difference in the sporulation efficiency widened such that only 37±10 % of the Δ*ptkA* cells in the colony had sporulated by comparison with 103±9% of the wild-type strain (n=3; $p<0.01$ students 2-way t-test). In contrast after 72 hours planktonic growth there was no difference between the sporulation levels of the wild-type strain and that of the Δ*ptkA* mutant indicating that the decrease in sporulation did not reflect a reduction in the sporulation efficiency *per se* (data not shown) (Vlamakis, Aguilar et al. 2008). From the results of our investigation into colony architecture, pellicle formation and sporulation ability, it is clear that *ptkA* plays an important role in the development of structurally complex and robust biofilms.

### *4.2.2 Characterisation of the PtkA terminal tyrosine cluster*

The conserved C-terminal tyrosine domain serves as the site of autophosphorylation on PtkA, a process that is dependent on the catalytic activity of PtkA (Mijakovic, Poncet et al. 2003). The results from an i*n vitro* assay suggest that the C-terminal tyrosine residues are not needed for phosphorylation of substrate proteins (Mijakovic, Poncet et al. 2003) but structural analysis of a PtkA homologue demonstrates that the C-terminal tyrosine domain interacts with the neighbouring kinase active site (Olivares-Illana,

Meyer et al. 2008). Taken together, these findings render the role of the conserved tyrosine residues ambiguous. The influence that PtkA has on colony morphology presents a robust and simple route to clarify if the terminal tyrosine residues play a role *in vivo* during biofilm formation. To investigate the role of the terminal tyrosine cluster of PtkA during biofilm formation we constructed a strain in which the three terminal tyrosine residues were mutated to alanine (PtkA $Y^{225}A$; $Y^{227}A$; $Y^{228}A$; NRS2799). Substitution of the terminal tyrosine cluster however did not impact on biofilm formation (Figure 4-5). From these results we can conclude that the terminal tyrosine cluster does not appear to be required for the activity of PtkA during biofilm formation. A more detailed analysis is provided in Chapter 5.

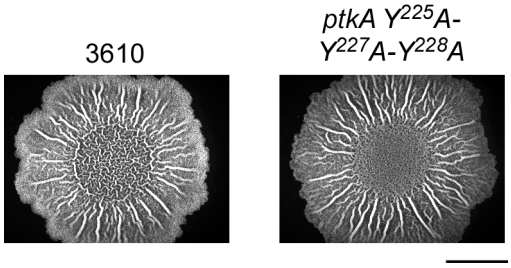


**Figure 4-5: Alanine substitution of the PtkA terminal tyrosine cluster does not impact on biofilm formation.**
Strains NCIB3610 and *ptkA* $Y^{225}A$-$Y^{227}A$-$Y^{228}A$ (NRS2799) were grown on MSgg agar plates for 40 hours at 37˚C prior to photographing. Scale bar represents 5 mm.

### *4.2.3 Assessing the requirement of the kinase activity of PtkA during biofilm formation*

Bacterial tyrosine kinases (BY-kinase) share a strong degree of sequence conservation (Figure 1-13). Structural analysis of a PtkA homologue, Cap5B belonging to *Staphylococcus aureus*, showed that the Walker A, the 'DxD' motif and the Walker B

motifs are required to coordinate and stabilise four water molecules and an $Mg^{2+}$ ion into the active site where hydrolysis of a bound nucleotide occurs (Figure 1-13) (Olivares-Illana, Meyer et al. 2008). Therefore the activity of PtkA is dependent on binding and hydrolysis of ATP coupled to the transfer of the released phosphate moiety onto a target substrate protein(s) (Mijakovic, Poncet et al. 2003).

We aimed to confirm whether or not the catalytic kinase activity of PtkA was needed during biofilm formation. To achieve this, two strains were made that resulted in substitutions on the chromosome leading to alterations in the PtkA amino acid sequence: *1)* an amino acid point mutation in the second of the aspartic acid residues in the conserved 'DxD' motif required for ATP hydrolysis catalysis; (PtkA $D^{83}A$; NRS2795); and *2)* a dual 'DxD' aspartic acid to alanine substitution; (PtkA $D^{81}A$ and $D^{83}A$; NRS2796). The nucleotide substitutions were introduced into the chromosome using pMAD (Arnaud, Chastanet et al. 2004) and in each case an isolate that had been subjected to the mutagenesis but had retained the wild-type sequence was retained as a control (see Materials and Methods). Each of the negative control strains exhibited wild-type morphology (data not shown). Consistent with the 'DxD' motif being required for the activity of PtkA, mutation to 'AxA' resulted in a biofilm morphology that was indistinguishable from the complete in-frame Δ*ptkA* strain (NRS2544) (compare Figure 4-3B to Figure 4-6C).

To confirm that the biofilm morphologies of the *ptkA* point mutation strains were specific to the point mutations introduced at the native locus, a wild-type copy of *ptkA* was introduced the *ptkA* $D^{81}A$-$D^{83}A$ mutant at the *amyE* locus in under the control of a heterologous promoter; $P_{spank\text{-}hy}$-*ptkA-lacI* (NRS2804). The biofilm architecture was fully restored compared to that shown by the wild-type strain both in the absence of IPTG and in the presence of 10 μM IPTG (compare Figure 4-6C to Figure 4-6D). These

findings confirm that the altered biofilm phenotype was specific to the disruption of *ptkA*.

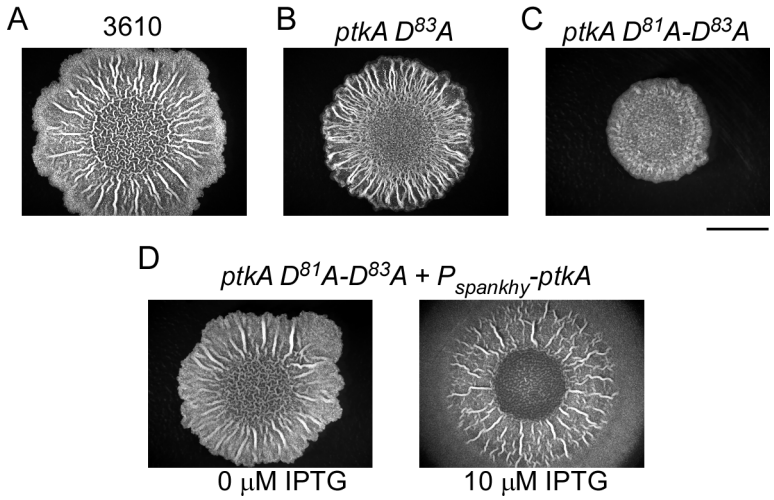


**Figure 4-6: Complex colony architecture of *ptkA* 'DxD' motif point mutation strains.**
Strains were grown on MSgg agar plates with and without the addition of 10 μM IPTG as required for 40 hours at 37˚C prior to photographing. Scale bar represents 5 mm.

The data presented here enables us to conclude that the 'DxD' motif of PtkA is necessary for its role during biofilm formation. The 'DxD' motif is essential for hydrolysis of nucleotides and is needed for autophosphorylation of the terminal tyrosine cluster of PtkA. Establishing the requirement of the 'DxD' motif during biofilm formation is an important step in determining whether or not the kinase activity of PtkA is required during biofilm formation. However these results alone cannot specifically confirm that the kinase activity of PtkA is necessary for its role during biofilm formation. To achieve our goal of understanding if the kinase activity of PtkA is required for its role in biofilm formation, further experiments were conducted. These experiments are detailed in section 4.3.

## 4.3 *Characterisation of TkmA*

In addition to its role as a kinase, PtkA also exhibits ATPase activity (Mijakovic, Poncet et al. 2003). To (indirectly) distinguish whether the ATPase or kinase activity of PtkA was responsible for its role in biofilm formation, an in-frame deletion of *tkmA* was constructed (NRS3541) (Figure 4-7B). As the translational start site of PtkA is located within the coding sequence of TkmA, an artificial *ptkA* ribosomal binding site and PtkA translational start site were engineered into the chromosome (Figure 4-7B). TkmA is the cognate BY-kinase modulator that interacts with PtkA allowing it to phosphorylate its target proteins (Mijakovic, Poncet et al. 2003; Jers, Pedersen et al. 2010). Thus in the absence of TkmA, PtkA is unable to exhibit kinase activity and can no longer phosphorylate substrate proteins but its ATPase activity remains intact (Mijakovic, Poncet et al. 2003).

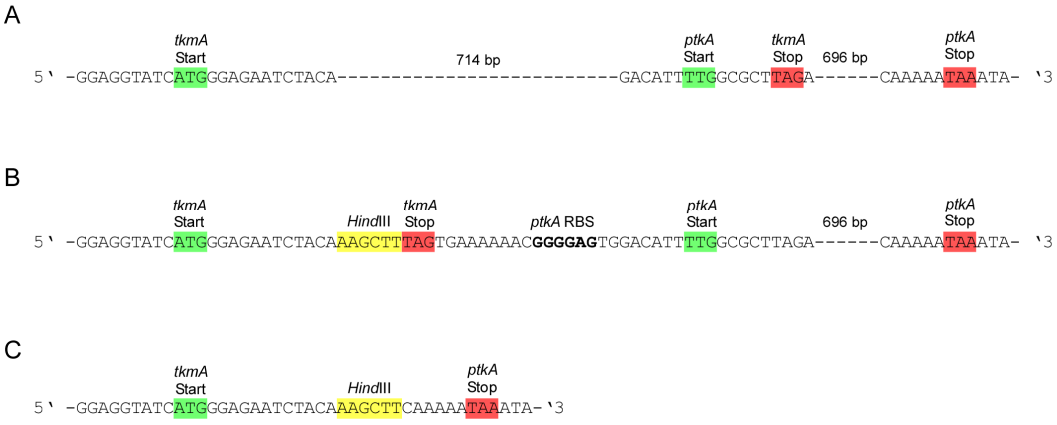


**Figure 4-7: Representation of *tkmA* and *tkmAptkA* mutations constructed on the chromosome.** Schematic representation of Δ*tkmA* and Δ*tkmA*Δ*ptkA* deletion strains. (**A**) Wild type *tkmA* and *ptkA*. Translational start and stop codons are highlighted in green and red, respectively. (**B**) Deletion of *tkmA*. Translational start and stop codons are highlighted as mentioned in (**A**). Primer engineered restriction site for *hin*dIII is highlighted in yellow. Primer engineered replacement of the native *ptkA* ribosome binding site (RBS) is in bold text. (**C**) Deletion of *tkmA* and *ptkA*. Translational start and stop codons are highlighted as mentioned in (**A**) and the restriction site is highlighted as mentioned in (**B**).

### *4.3.1 Assessing the impact of deleting tkmA on biofilm formation*

Upon deletion of *tkmA* we observed a reduction in colony complexity and a loss of complex aerial structures and fruiting bodies (Figure 4-8C), consistent with TkmA being required for biofilm formation. The heterologous expression of *tkmA* under the control of the $P_{spank\text{-}hy}$ promoter was able to complement the *tkmA* mutation (in the absence of IPTG) (Figure 4-8D). Taken together this demonstrates that TkmA is required for biofilm formation and supports the hypothesis that the kinase activity of PtkA is essential for its role during biofilm formation.

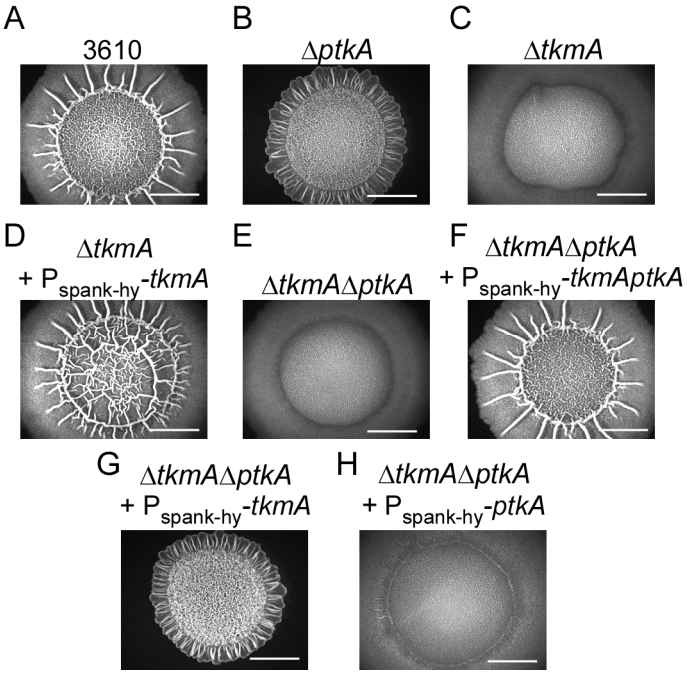


**Figure 4-8: Complex colony architecture of Δ*tkmA* and Δ*tkmA* Δ*ptkA* deletion strains**
Strains (**A**) NCIB3610, (**B**) Δ*ptkA* (NRS2544), (**C**) Δ*tkmA* (NRS3541), (**D**) Δ*tkmA*+ $P_{spank\text{-}hy}$-*tkmA* (NRS3544), (**E**) Δ*tkmA*Δ*ptkA* (NRS3528), (**F**) Δ*tkmA*Δ*ptkA*+ $P_{spank\text{-}hy}$-*tkmA- ptkA* (NRS3536), (**G**) Δ*tkmA*Δ*ptkA*+ $P_{spank\text{-}hy}$-*tkmA* (NRS3535), and (**H**) Δ*tkmA*Δ*ptkA*+ $P_{spank\text{-}hy}$-*ptkA* (NRS3537) were grown on MSgg agar plates without the addition IPTG for 40 hours at 30˚C prior to photographing. Scale bar represents 5 mm.

### *4.3.2 TkmA remains active in the absence of PtkA*

Interestingly, deletion of *tkmA* did not phenocopy the Δ*ptkA* strain (NRS2544) (compare Figure 4-8B to Figure 4-8C). Therefore we hypothesised that TkmA retained activity in the absence of PtkA and that TkmA was capable of interacting with other proteins. To test this we constructed a strain lacking both *tkmA* and *ptkA* (NRS3528) (Figure 4-7C). We predicted that if our hypothesis was correct restoration of *tkmA* expression in the strain mutant for both *tkmA* and *ptkA* would return the colony phenotype to that of a *ptkA* mutant. When grown on MSgg media Δ*tkmA*Δ*ptkA* (NRS3528) displayed a complex colony architecture that was indistinguishable to the Δ*tkmA* mutant (NRS3541) (compare Figure 4-8C with Figure 4-8E). We confirmed that addition of both the *tkmA* and *ptkA* coding regions (NRS3536) under the control of an inducible promoter was necessary and sufficient to return the mutant phenotype back to that of wild type *B. subtilis* (Figure 4-8F). From this we conclude that both TkmA and PtkA are required for biofilm formation and that TkmA is epistatic to PtkA.

Next, only the *tkmA* coding region was introduced into the Δ*tkmA*Δ*ptkA* mutant strain (NRS3535). The complex colony architecture of this strain was indistinguishable from the Δ*ptkA* mutant (NRS2544) (compare Figure 4-8G with Figure 4-8B). As a change to colony architecture was observed upon expression of *tkmA*, this indicated that, as hypothesized above, TkmA can function (at least in part) in the absence of PtkA. In contrast, expression of only the *ptkA* coding region in the Δ*tkmA*Δ*ptkA* mutant strain (NRS3537) had no impact on complex colony architecture (Figure 4-8H). This further supports the conclusion that substrate phosphorylation by PtkA during biofilm formation relies on activation of its kinase activity through interaction with TkmA.

When taken together we conclude that the kinase activity of PtkA is required for its role during biofilm formation, whereas the ATPase activity of PtkA is not.

## *4.4 Characterisation of PtpZ*

As for the deletion of PtkA, we aimed to establish the role of tyrosine phosphorylation during the formation of a biofilm by deleting *ptpZ,* the gene encoding the tyrosine phosphatase PtpZ. The initial *ptpZ* mutant that was constructed as part of the screening process was generated using single-crossover disruption (Figure 3-3). As *tkmA-ptkA-ptpZ-ugd* form an operon (Figure 3-5 and Figure 3-6), an in-frame deletion of *ptpZ* was made to circumvent downstream effects on transcription and/or the stoichiometry of the remaining proteins (see Materials and Methods). It was first necessary to establish if the in-frame *ptpZ* mutant exhibited a severe growth defect, as has been previously reported (Petranovic, Michelsen et al. 2007). A growth defect would render interpretation of biofilm formation ambiguous; therefore we tested whether the Δ*ptpZ* strain had a reduced growth rate. In both LB (data not shown) and MSgg liquid medium the Δ*ptpZ* mutant had a doubling time equal to that of the parental strain (Figure 4-9).

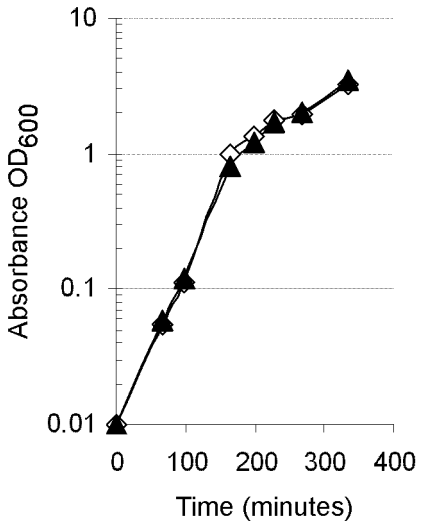


**Figure 4-9: Growth of Δ*ptpZ* mutants compared to NCIB3610**
Growth of NCIB3610 (white diamonds) and Δ*ptpZ* (NRS2222) (black triangles) in MSgg media. Results are representative of >3 independent rounds.

Absence of PtkA has been shown to have deleterious effects on cell length and nucleoid number (Petranovic, Michelsen et al. 2007). Therefore we analysed cell length and nucleoid distribution at the single cell level using microscopy of the *ptpZ* mutant strain in comparison to the wild type NCIB3610 strain. Our preliminary findings suggested that there was no significant difference between the cell length of a *ptpZ* mutant compared with wild type. Furthermore, under the conditions used in this study, deletion of *ptpZ* did not appear to significantly alter nucleoid number (Figure 4-10). However, as for *ptkA,* it must be noted that the Hoechst stain was not uniformly taken up by both the wild type NCIB3610 strain and the Δ*ptpZ* mutant (Figure 4-10).

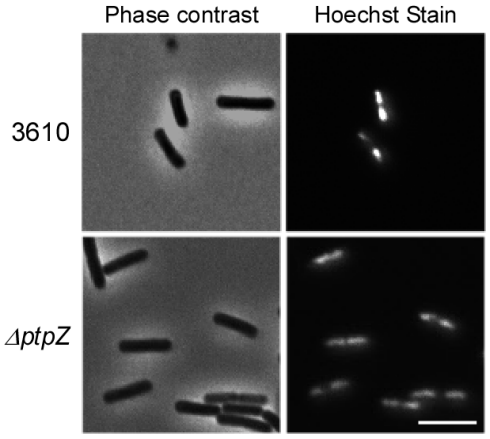


**Figure 4-10: Nucleoid staining of Δ*ptpZ* compared to NCIB3610 using Hoechst 33342**
Phase contrast and fluorescent images of NCIB3610 and Δ*ptpZ* collected using Zeiss Axio Imager M1. Scale bars represent 5 μm.

However when taken together, these results tentatively suggest that in NCIB3610, deletion of *ptpZ* does not result in a gross growth defect and that our *ptpZ* mutant is unlikely to possess a defect in DNA replication.

### *4.4.1 Impact of deletion of ptpZ on biofilm formation*

An approach similar to that used for PtkA was taken to assess the impact of deleting *ptpZ* on biofilm formation. As determined for the Δ*ptkA* mutant, the Δ*ptpZ* mutant was unable to develop the complex radial structures typical of the maturing *B. subtilis* biofilm at 24 hours (Figure 4-11B). To ensure that the Δ*ptpZ* mutant phenotype was specific to the absence of PtpZ, a wild type copy of *ptpZ* was introduced to the *amyE* locus in the Δ*ptpZ* mutant under the control of a heterologous promoter; $P_{spank\text{-}hy}$-*ptpZ-lacI* (NRS2467). In the presence of 100 μM IPTG biofilm architecture was comparable to that of the wild-type strain (Figure 4-11B compared to Figure 4-11C). These findings confirm that the altered biofilm phenotype was specific to the disruption of *ptpZ*.

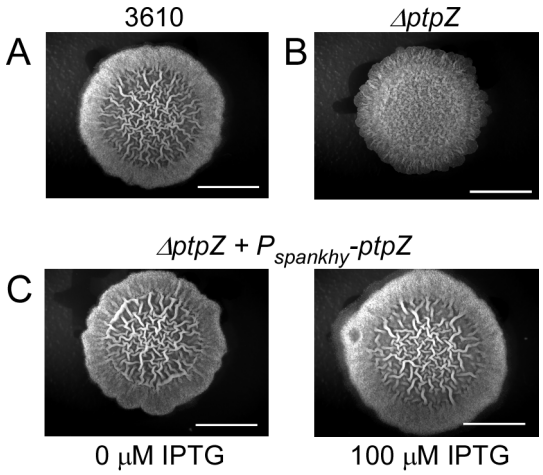


**Figure 4-11: Complex colony architecture of *ptpZ* mutants**
(**A**) Strains NCIB3610, (B) Δ*ptpZ* (NRS2222) and (C) Δ*ptpZ* + $P_{spank\text{-}hy}$-*ptpZ* (NRS2467) were grown on MSgg media with or without the addition of 100μM IPTG for 24h at 37˚C. Scale bar represents 5 mm.

Again, in contrast to the reduction in colony architecture complexity (Figure 4-11B) the pellicle formed by the Δ*ptpZ* strain showed extensive three dimensional structural complexity but entirely lacked the "fruiting bodies" that are present on the wild-type pellicle (compare Figure 4-12A and C with Figure 4-12B and D).

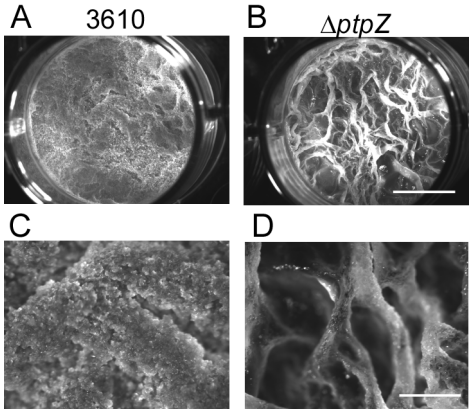


**Figure 4-12: Pellicle morphology of Δ*ptpZ* compared to NCIB3610**
Strains NCIB3610 (**A** + **C)** and Δ*ptpZ* (**B** + **D)** (NRS2222) were assessed as described in Figure 3-1. The scale bar represents 5 mm (A and B) and 1mm (C and D).

These alterations in colony morphology and pellicle morphology were accompanied by a reduction in the level of sporulation from ~25 ±4% in the wild-type strain to ~8± 3.6

% in the Δ*ptpZ* mutant (n=3; p<0.05 2-way students t-test). The decrease in sporulation was found to be specific to cells growing in the biofilm colony as after 24 hours growth in liquid medium the wild type strain and the Δ*ptpZ* mutant had sporulated at a frequency of ~33±1.5% and ~40±9%, respectively. However in contrast to the Δ*ptkA* mutant, the impact of deleting Δ*ptpZ* became less apparent over time; such that by 48 hours the lack of PtpZ had only a minor impact on the ability to form a biofilm (data not shown). The sporulation analysis confirmed this conclusion. After 72 hours of incubation ~65±3% of the *ptpZ* mutant population had sporulated, a value that was not significantly different from the wild-type strain (n=3; p=0.09 2-way students t-test).

### *4.4.2 Assessing the requirement of the phosphatase activity of PtpZ during biofilm formation*

The phosphatase activity of PtpZ has been shown to be reduced by ~95% when the histidine residue at position 196 was mutated to alanine (Mijakovic, Musumeci et al. 2005). Therefore to establish whether the phosphatase activity of PtpZ was required to control biofilm formation a mutant allele of *ptpZ* (PtpZ-$H^{196}$A) was introduced into the *amyE* locus under the control of a heterologous promoter; $P_{spankhy}$-*ptpZ*-$H^{196}$A-*lacI* (NRS2468). In contrast to the wild-type allele of PtpZ, the mutant PtpZ-$H^{196}$A protein was not capable of restoring wild-type colony morphology (compare Figure 4-13C to Figure 4-11C). These findings support the conclusion that the phosphatase activity of PtpZ is required for its role during biofilm formation.

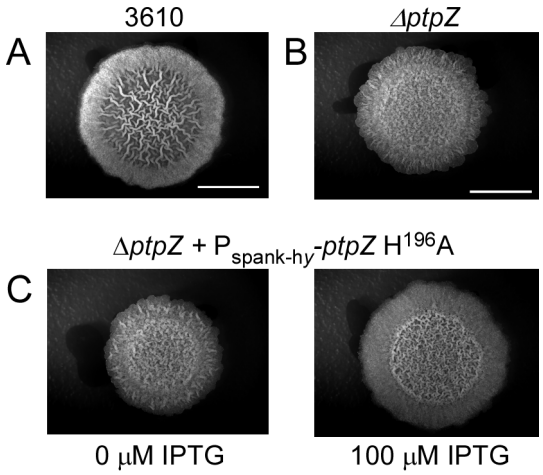


**Figure 4-13: Complex colony architecture of a *ptpZ* point mutation strain.**
(**A**) Strains NCIB3610, (B) Δ*ptpZ* (NRS2222) and (C) Δ*ptpZ* + $P_{spank\text{-}hy}$-*ptpZ* $H^{196}A$ (NRS2468) were grown on MSgg media with or without the addition of 100μM IPTG for 40h at 37˚C. Scale bar represents 5 mm.

## *4.5 Influence of known and predicted targets of PtkA and PtpZ on biofilm formation*

We wanted to identify the downstream target(s) of PtkA that is phosphorylated during biofilm formation. *In vitro* analysis currently indicates that PtkA has 13 confirmed substrates (Mijakovic, Poncet et al. 2003; Mijakovic, Petranovic et al. 2006; Jers, Pedersen et al. 2010). Additionally, using phosphoproteome analysis a further 8 proteins have been identified as tyrosine phosphorylated (Levine, Vannier et al. 2006; Eymann, Becher et al. 2007; Macek, Mijakovic et al. 2007) (Table 4-1). When investigating potential targets of PtkA during biofilm formation we set two criteria: *1)* the protein must be able to become phosphorylated on a tyrosine residue and *2)* biofilm formation must be affected when the gene encoding the protein is mutated. With these criteria in mind, we began by investigating the impact on biofilm formation of known PtkA targets.

### *4.5.1 Mutation of known targets of PtkA and PtpZ have no impact on biofilm formation*

One obvious potential target of PtkA during biofilm formation was Ugd. Ugd is regulated by both PtkA and PtpZ (Mijakovic, Poncet et al. 2003; Mijakovic, Musumeci et al. 2005) and is co-transcribed with *ptkA* and *ptpZ* (Figure 3-6). Ugd is a uridine-5'-diphosphoglucose (UDP-glucose) dehydrogenase (Mijakovic, Poncet et al. 2003). When phosphorylated on tyrosine-70 by PtkA, Ugd is activated and can catalyse the oxidation of UDP-glucose to UDP-glucuronate (Petranovic, Grangeasse et al. 2009). UDP-glucuronate is subsequently used as a precursor for the production of teichuronic acid which is a component of the cell wall (Soldo, Lazarevic et al. 1999). It has been postulated that Ugd may be required for biofilm formation (Mijakovic, Petranovic et al. 2005; Hung, Chien et al. 2007). To test whether Ugd was required for biofilm formation we constructed an in-frame deletion in *ugd* (NRS2471). The Δ*ugd* mutant exhibited a colony morphology that was indistinguishable from the parental strain biofilm (Figure 4-14), indicating that Ugd is not needed. However encoded on the *B. subtilis* chromosome is an additional proven and one putative UDP-glucose dehydrogenase called *tuaD* and *ytcA,* respectively (Mijakovic, Poncet et al. 2003; Mijakovic, Petranovic et al. 2005). Functional redundancy between these proteins is a possibility, therefore a series of single, double and triple mutant strains were constructed and the ability to form a robust biofilm was tested. None of the strains tested had an influence on colony architecture (Figure 4-14). Taken together these findings indicate that Ugd, YtcA and TuaD are not the downstream substrates of PtpZ and PtkA regulated during post-translational control of biofilm formation by *B. subtilis*.

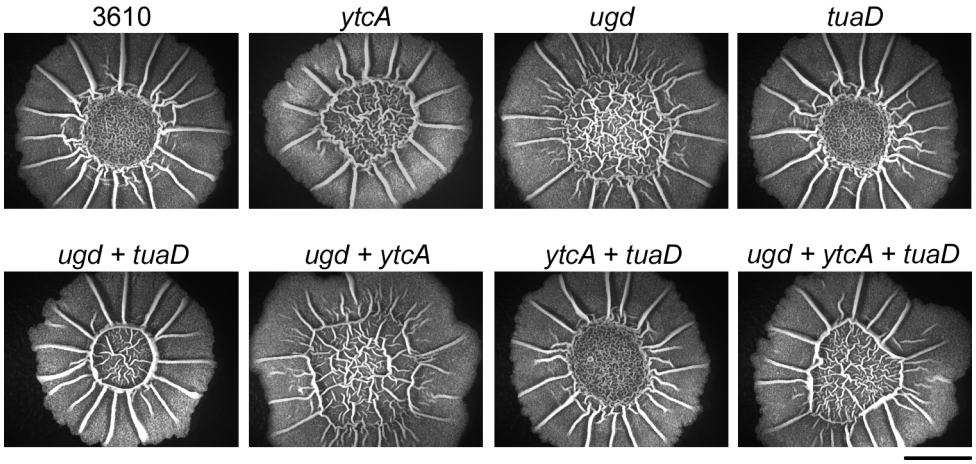


**Figure 4-14: Complex colony architecture of *ugd*, *tuaD* and *ytcA* mutants**
Strains Δ*ugd* (NRS2471), *tuaD::*pNW377 (NRS3232), Δ*ytcA* (NRS2227), Δ*ugd* + *tuaD::*pNW377 (NRS3229), Δ*ugd* + Δ*ytcA* (NRS2821), Δ*ytcA* + *tuaD::*pNW377 (NRS3230) and Δ*ugd* + Δ*ytcA* + *tuaD::*pNW377 (NRS3231) were grown on MSgg agar for 40 hours at 30°C. Scale bar represents 5 mm.

### *4.5.2 The target of PtkA during biofilm formation remains unidentified*

Having eliminated Ugd, TuaD, and YtcA as targets of PtkA during biofilm formation, we widened our search. Global phosphoproteome analyses have broadened our understanding of the processes that are regulated by tyrosine phosphorylation in bacteria (Levine, Vannier et al. 2006; Eymann, Becher et al. 2007; Macek, Mijakovic et al. 2007). We therefore chose to take a systematic mutagenesis approach to try and identify the target of PtkA during biofilm formation. After removing Ugd and TuaD (Figure 4-14), 19 proteins have been identified as tyrosine phosphorylated and therefore represent potential targets of PtkA (Table 4-1). 7 genes are known to encode essential proteins (*asd, aspS, yaaD, yurY, infA, ssbA* and *eno*) and thus were excluded from our analysis. The gene *ssbB* was also excluded from the analysis as SsbB shares 63% identity and 81% similarity to SsbA, an essential protein. This left 11 proteins (AhpF, CitC, Ldh, OppA, RocA, YjoA, YvyG, YnfE, SdhA, YxxG, and YorK) of which

mutations could be constructed in 9 of the corresponding genes (*ahpF, citC, ldh, oppA, rocA, yjoA, yvyG, ynfE* and *yorK*).

| *Gene Name* | *Essential* [a] | *Function* [b] | *Position of Phosphorylated Tyrosine* [c] | Reference |
|---|---|---|---|---|
| *ahpF* | No | Alkyl hydroperoxide reductase (large subunit) | Y393 | (Macek, Mijakovic et al. 2007) |
| *asd* | Yes | Aspartate-semialdehyde dehydrogenase | Y146 | (Macek, Mijakovic et al. 2007) |
| *aspS* | Yes | Aspartyl-tRNA synthetase | Y70 or Y194 | (Levine, Vannier et al. 2006) |
| *sdhA (citF)* | Yes† | Succinate dehydrogenase (flavoprotein subunit) | Y146/ Y270 /Y276 /Y279 / Y310 / Y332 | (Levine, Vannier et al. 2006) |
| *icd (citC)* | No | Isocitrate dehydrogenase | Y207 | (Levine, Vannier et al. 2006) |
| *pdxS (yaaD)* | Yes | Pyridoxal-5'-phosphate synthase (synthase domain) | Y193 | (Levine, Vannier et al. 2006) |
| *sufC (yurY)* | Yes | ABC transporter (ATP-binding protein) | Y243 | (Levine, Vannier et al. 2006) |
| *eno* | Yes | Enolase | Y281* | (Macek, Mijakovic et al. 2007) |
| *ldh (lctE)* | No | L-lactate dehydrogenase | Y224 | (Macek, Mijakovic et al. 2007) |
| *spo0KA (oppA)* | No | Oligopeptide ABC transporter (binding protein) | Y301 | (Macek, Mijakovic et al. 2007) |
| *rocA (ipa-76d)* | No | 3-hydroxy-1-pyrroline-5-carboxylate dehydrogenase | Y5* | (Macek, Mijakovic et al. 2007) |
| *yjoA* | No | Unknown | Y150 | (Macek, Mijakovic et al. 2007) |
| *ynfE* | No | Unknown | Y12 | (Macek, Mijakovic et al. 2007) |
| *yorK* | No | Unknown | Y473 | (Macek, Mijakovic et al. 2007) |
| *yvyG (yviC)* | No | Unknown | Y49 | (Macek, Mijakovic et al. 2007) |
| *yxxG* | Yes† | Unknown | Y102* | (Macek, Mijakovic et al. 2007) |
| *ugd* | No | UDP-glucose dehydrogenase | Y70 | (Petranovic, Grangeasse et al. 2009) |
| *tuaD* | No | UDP-glucose dehydrogenase | Unknown | (Mijakovic, Poncet et al. 2003) |
| *ssbA* | Yes | Single-strand DNA-binding protein | Y82 | (Mijakovic, Petranovic et al. 2006) |
| *ssbB* | No | Single-strand DNA-binding protein | Y82 | (Mijakovic, Petranovic et al. 2006) |
| *infA* | Yes | Initiation factor IF-1 | Y60 | (Macek, Mijakovic et al. 2007) |

**Table 4-1: Tyrosine modulated proteins identified by literature review**
[a] Genes were designated as essential or non-essential based on previously published data (Kobayashi, Ehrlich et al. 2003) or our own findings †.
[b] Protein functions were designated according to previously published data.
[c] The proteins AspS and SdhA (CitF) contain several tyrosine residues. The techniques used to identify these proteins as modulated by phosphorylation were not capable of identifying the specific phosphorylated residue. * Indicates instances when the phosphorylated residue could not be specifically confirmed as a tyrosine.

Mutation of two genes (*sdhA* and *yxxG*) resulted in a severe growth defect (Figure 4-15). As a consequence of this growth impairment, interpretation of the effect of the mutation on biofilm formation would be very difficult. As a result *sdhA* and *yxxG* were

also removed from the screen. SdhA (previously known as CitF) is a succinate dehydrogenase and is involved in the TCA cycle (Hederstedt and Rutberg 1980), while *yxxG* encodes for a protein of unknown function. Neither protein has previously been shown to be essential.

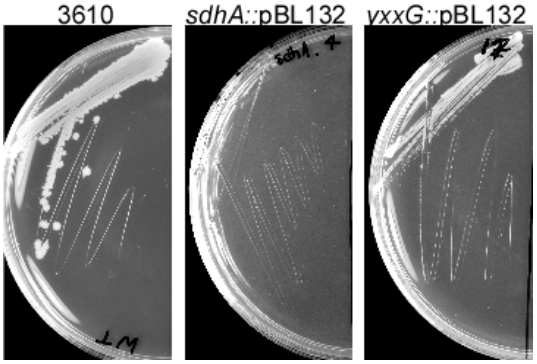


**Figure 4-15: Mutation of *sdhA* and *yxxG* results in a severe growth defect**
Growth of the mutant strains *sdhA*::pBL132 and *yxxG*::pBL132 were compared with wild type strain NCIB3610. Strains were streaked out for single colonies on LB media and incubated for 16 hours at 37˚C.

After construction and verification of the mutant strains the impact on colony morphology was tested. Unfortunately, none were found to influence colony formation (Figure 4-16).

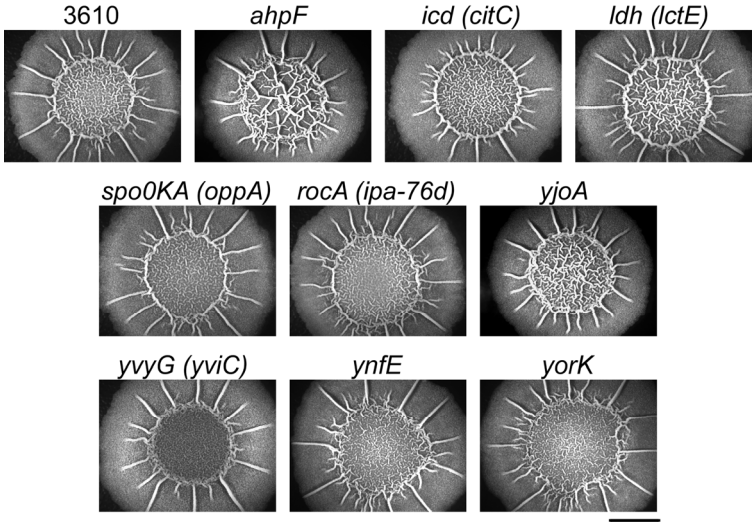


**Figure 4-16: Impact on biofilm formation of mutations in non-essential tyrosine modulated proteins.**
Strains mutant for *ahpF* (NRS3201), *icd (citC)* (NRS3205), *ldh (lctE)* (NRS3210), *spo0KA (oppA)* (NRS3211), *rocA (ipa-76d)* (NRS3212), *yjoA* (NRS3213), *ynfE* (NRS3216), *yorK* (NRS3214) and *yvyG (yviC)* (NRS3215) were grown on MSgg agar for 40 hours at 30°C. Scale bar represents 5 mm.

Therefore despite extensive efforts to identify the substrate phosphorylated by PtkA it remained elusive. It is of course possible that one, or more, of the essential proteins is (are) the target of PtkA. However it is important to remember that the *B. subtilis* strain NCIB3610 is the progenitor of the *B. subtilis* 168 strain that was used in the phosphoproteome analyses and they contain several single nucleotide polymorphisms (Srivatsan, Han et al. 2008) (Levine, Vannier et al. 2006; Eymann, Becher et al. 2007; Macek, Mijakovic et al. 2007). Some of these genome level differences alter the ability of the two strains to form a biofilm (Branda, Gonzalez-Pastor et al. 2001; Kobayashi 2008). The NCIB3610 strain also contains a plasmid of ~85 kbp which could conceivably encode proteins that are tyrosine phosphorylated and required for biofilm formation (Earl, Losick et al. 2007). Therefore it will be necessary to conduct global proteome analyses using NCIB3610 to identify further possible targets of PtkA that are modulated during biofilm formation.

## *4.6 Discussion*

As detailed in the previous chapter, the *tkmA* operon was found to be regulated by the transcriptional regulators DegU and SinR. As both DegU and SinR are involved in the regulation of biofilm formation, I aimed to investigate the impact on biofilm formation of deleting genes belonging to the *tkmA* operon. Before assessing the impact of these mutations on biofilm formation, the effect of mutating *ptkA* and *ptpZ* on growth rate, cell length and nucleoid number were checked. This was done as it was previously demonstrated by Petranovic *et al.*, that disruption of *ptpZ* displayed a severe growth defect when succinate was provided as the sole carbon source (Petranovic, Michelsen et

al. 2007). In contrast, our construction of clean, in-frame Δ*ptkA* and Δ*ptpZ* mutants did not display any growth defect under the conditions tested. Furthermore, the Δ*ptkA* and Δ*ptpZ* mutants were not affected for cell length or nucleoid number, as was also demonstrated for the *ptkA* mutant constructed by Petranovic *et al*. (Petranovic, Michelsen et al. 2007). It is possible that the differences observed in regard to cell length, nucleoid number and growth between our mutant strains and those constructed by Petranovic *et al*. have arisen as a result of the different methods of strain construction or because our study utilised the NCIB3610 *B. subtilis* isolate whereas Petranovic *et al*. utilised the 168 *B. subtilis* isolate. The main aim of these experiments was to ensure that under the conditions tested that no effect on cell growth would occur as this would impair our ability to interpret the effects of deleting the *tkmA* genes during biofilm formation, and this was achieved. It is interesting that no effect on DNA metabolism was detected in our Δ*ptkA* strain constructed in NCIB3610, as there are not thought to be any differences between the sequences of PtkA and the small single stranded DNA binding proteins of the *B. subtilis* isolates 168 and NCIB3610 (Zeigler, Pragai et al. 2008). Perhaps this information suggests significant uncharacterised differences between isolates of *B. subtilis*.

### *4.6.1 PtkA and PtpZ are essential for a structurally complex biofilm*

Next, it was demonstrated that deletion of *ptkA* and *ptpZ* resulted in a biofilm and pellicle formation defect (For *ptkA* mutants see Figure 4-3 and Figure 4-4 and for *ptpZ* mutants see Figure 4-11 and Figure 4-12). Additionally, it was determined that deletion of *ptkA* and *ptpZ* resulted in a decrease in spores harvested from complex colonies (For

*ptkA* mutant see section 4.2.1 and for *ptpZ* mutant see 4.4.1). However, no impact on sporulation was observed in liquid media, thus it was concluded that the impact on sporulation in the *ptkA* and *ptpZ* mutants was a result of the altered complex colony architecture and not a direct effect on the developmental process of sporulation. These results demonstrate the importance of a structurally complex biofilm for the formation of spores by *B. subtilis*. Our results are in agreement with previous reports which demonstrated that disruption to the complex architecture results in a sporulation decrease (Vlamakis, Aguilar et al. 2008). While the target of PtkA and PtpZ was not identified in this study, it is possible that they may act by affecting the production of a component of the extracellular matrix, which is essential for the construction of an architecturally complex colony. Although it is important to note that PtkA and PtpZ most likely will not act on the production of EPS, as the operon encoding the biosynthetic machinery for the production of EPS encodes the putative BY-kinase, EpsB.

### *4.6.2 Kinase activity is essential for biofilm formation*

Further to identifying that PtkA is necessary for biofilm formation, we aimed to assess whether the kinase activity of PtkA was necessary for its role during biofilm formation. To do this, a strain containing alanine substitutions at the 'DxD' motif was made. The kinase activity of BY-kinases is associated with the Walker motifs, including the 'DxD' motif. Disruption of the 'DxD' motif of PtkA has been shown in previous studies to inhibit PtkA from phosphorylating tyrosine residues on GST (when fused to TkmA) (Mijakovic, Poncet et al. 2003). This both demonstrates the requirement of the 'DxD' motif for kinase activity and the loose substrate specificity of PtkA. In our study, the

*ptkA* $D^{81}A$-$D^{83}A$ mutant was unable to form robust complex colonies, which suggested a role for the kinase activity of PtkA during biofilm formation. As mutation of the 'DxD' motif also disrupts ATPase activity of PtkA, we determined whether loss of kinase activity or ATPase activity caused the disruption to biofilm formation. To confirm this hypothesis, the tyrosine kinase modulator TkmA was deleted and biofilm formation was assessed.

In Gram-positive organisms, activation of kinase activity relies on an interaction between the BY-kinase and the cognate bacterial tyrosine kinase modulator (Lee and Jia 2009). Deletion of *tkmA* in the presence of PtkA resulted in a defect to biofilm formation (Figure 4-8C). This demonstrated that, as expected, TkmA was involved in the activation of the kinase activity of PtkA and thus the kinase activity of PtkA was required for its role in biofilm formation. Furthermore it was identified that TkmA possesses targets in addition to its cognate partner PtkA (Figure 4-8). While it is rare to find examples of tyrosine kinase modulators with multiple targets, they do exist. For example, the bacterial tyrosine kinase Cap5B2 belonging to *S. aureus* is co-located on the chromosome along side the gene encoding for the tyrosine kinase modulator Cap5A2 (Olivares-Illana, Meyer et al. 2008). Cap5A2 activates the kinase activity of Cap5B2. However, *S. aureus* also encodes an additional bacterial tyrosine modulator and kinase pair called Cap5A1 and Cap5B1, respectively (Olivares-Illana, Meyer et al. 2008). Studies have demonstrated that the kinase modulator Cap5A1 is able to activate the kinase activity of Cap5B2 more efficiently than Cap5A2 (Soulat, Jault et al. 2006).

The ability of a BY-kinase to dissociate from its cognate kinase modulator is a feature which is specific to Gram positive BY-kinases. In *B. subtilis* previously published data collected using a fluorescent tagged construct of PtkA suggests that PtkA may become dissociated from its kinase modulator during stationary phase (Jers, Pedersen et al.

2010). It should be noted however that this work was conducted using an artificial system where the transcription of PtkA-GFP was active in stationary phase. This is in contrast to the work presented in this thesis which suggests that as levels of DegU~P rise in the cell upon entry into stationary phase, the transcription of the *tkmA* operon will be repressed. Thus further research is required to confirm whether PtkA disssoicates from TkmA under native conditions.

The knowledge that TkmA may be able to activate proteins in addition to PtkA, at least in the absence of PtkA, calls into question the specificity of the response to a specific stimulus. It will be interesting to identify the additional targets of TkmA and to understand what impact they may have in the event that PtkA is not interacting with TkmA. Furthermore, it would be interesting to discover how common this is among Gram-positive bacterial tyrosine kinase-modulator pairs.

### *4.6.3 Deletion of ptkA and ptpZ result in similar phenotypes*

An interesting outcome of this study is that deletion of both the kinase PtkA and the phosphatase PtpZ result in a defect of biofilm and pellicle formation. It may seem counter intuitive that deletion of the kinase and its partner phosphatase would have the same outcome. This however is not an unusual case as deletion of the BY-kinase BceF and phosphatase BceD belonging to *Burkholderia cepacian* result in a decrease in the production of cepacian, the major exopolysaccharide component. Cepacian production is positively correlated with the formation of mature biofilms by *B. cepacian*, thus deletion of either kinase or phosphatase results in a defect to biofilm formation. Additionally, deletion of the BY-kinase Wzc and phosphatase Wzb belonging to the Gram-negative *Acinetobacter lwoffii* RAG-1 result in the formation of colonies which

are emulsan-negative (Nakar and Gutnick 2003); emulsan is an extracellular lipoheteropolysaccharide bioemulsifier. Apoemulsan, the protein-free polysaccharide, inhibits biofilm formation by reducing hydrophobicity (Dams-Kozlowska and Kaplan 2007). Taken together, deletion of both the kinase and phosphatase result in increased biofilm formation. Furthermore, deletion of the BY-kinase CpsB and the phosphatase CpsD belonging to *Streptococcus pneumoniae* D39 both result in the formation of rough colonies (Morona, Miller et al. 2004); the formation of smooth colonies is associated with the production of capsular polysaccharide (CPS), an essential exopolysaccharide required for virulence (Morona, Miller et al. 2004). Thus both kinase and phosphatase are required for polysaccharide production. At least in terms of the regulation of polysaccharides it has been proposed that cycling between a targets' phosphorylated and unphosphorylated state maybe essential for polysaccharide synthesis (Olivares-Illana, Meyer et al. 2008). However as we have demonstrated, the regulation of biofilm formation by PtkA and PtpZ is not mediated by regulating Ugd or TuaD (UDP-glucose dehydrogenases), therefore the production of teichuronic acid is not essential for biofilm formation. The impact of deleting PtkA and PtpZ on total exopolysaccharide production remains to be investigated. In order to fully understand the mechanism by which PtkA and PtpZ regulate biofilm formation, the target of these regulators during biofilm formation must be identified.

### *4.6.4 The target of PtkA and PtpZ remains elusive*

In this chapter we aimed to identify the target of PtkA and PtpZ during biofilm formation. Initial investigations showed that the most likely targets, Ugd, TuaD and YtcA, did not affect biofilm formation (Figure 4-14). A screen of known PtkA targets

and known tyrosine phosphorylated proteins was conducted, however no impact was observed on biofilm formation (Figure 4-16). A significant drawback of using the phosphoproteome screens that were available was that the proteins used were isolated from cells that were not grown under biofilm inducing conditions (Levine, Vannier et al. 2006; Eymann, Becher et al. 2007; Macek, Mijakovic et al. 2007). Future experiments would include a phosphotyrosine proteomic screen conducted under biofilm forming conditions, utilising the *ptkA* and *ptpZ* mutants in order to identify proteins which are phosphorylated in the absence of *ptpZ* and unphosphorylated in the absence of *ptkA* compared to wild type *B. subtilis*.

# 5 Terminal tyrosine cluster extended analysis and YvyG investigation

## *5.1 Extended characterisation of the terminal tyrosine cluster of PtkA*

As discussed in Chapter 4, the bacterial tyrosine kinase PtkA is necessary for the development of architecturally complex biofilms by *B. subtilis*. By constructing strains which contained alanine substitutions at the terminal tyrosine cluster, we aimed to assess whether or not PtkA required the terminal tyrosine cluster in order to regulate biofilm formation. Our results suggested that the terminal tyrosine cluster was not required during biofilm formation (Figure 4-5). As the terminal tyrosine cluster is a well conserved feature of BY-kinases (Figure 1-13), this result came as a surprise. It is unusual to conserve features of a protein which serve no obvious function. With this in mind, we aimed to extend our investigation of the terminal tyrosine cluster of PtkA by replacing the terminal tyrosine cluster with residues which would structurally mimic a tyrosine, but which were either unable to be phosphorylated or mimicked a phosphorylated tyrosine.

To mimic the negative charge associated with a phosphorylated tyrosine residue, the tyrosine residue was replaced with glutamic acid (Figure 5-1). In addition, the tyrosine residues were replaced by phenylalanine in order to simulate a non-phosphorylated tyrosine (Figure 5-1). Phenylalanine and tyrosine share significant structural similarity; however phenylalanine lacks the functional hydroxyl group attached to the end of the 6-carbon aromatic ring, thus preventing phenylalanine from becoming phosphorylated (Figure 5-1).

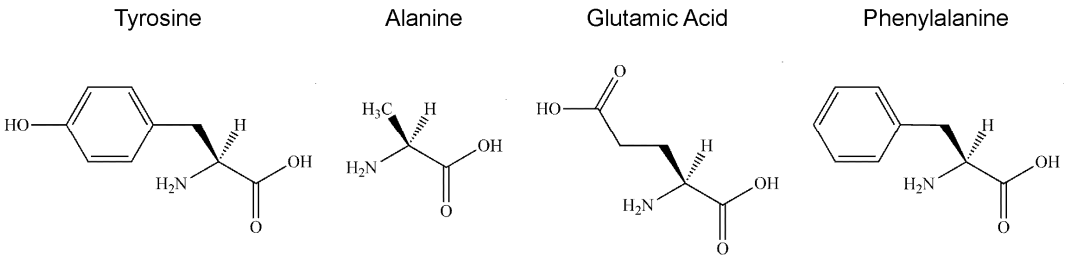


**Figure 5-1: Amino acid structure**
Structures of the amino acids tyrosine, alanine, glutamic acid and phenylalanine were obtained from http://www.chem.ucla.edu/harding/IGOC/A/amino_acid.html.

A collection of strains were constructed in which either 1, 2 or 3 of the tyrosine residues were replaced by glutamic acid, or all 3 were replaced by phenylalanine. In addition one strain was constructed in which only tyrosine at position 228, previously shown to be the preferential site of autophosphorylation, was mutated to a glutamic acid residue (Mijakovic, Poncet et al. 2003). For ease of interpretation, tyrosine residues not mutated to glutamic acid or phenylalanine were replaced by alanine. This allowed us to rule out phosphorylation of the native tyrosine residues. Interestingly, replacement of the native tyrosine residues with glutamic acid residues did not impact on biofilm formation (Figure 5-2D). In sharp contrast, replacement of the tyrosine residues with phenylalanine resulted in a loss of complex colony architecture (Figure 5-2F).

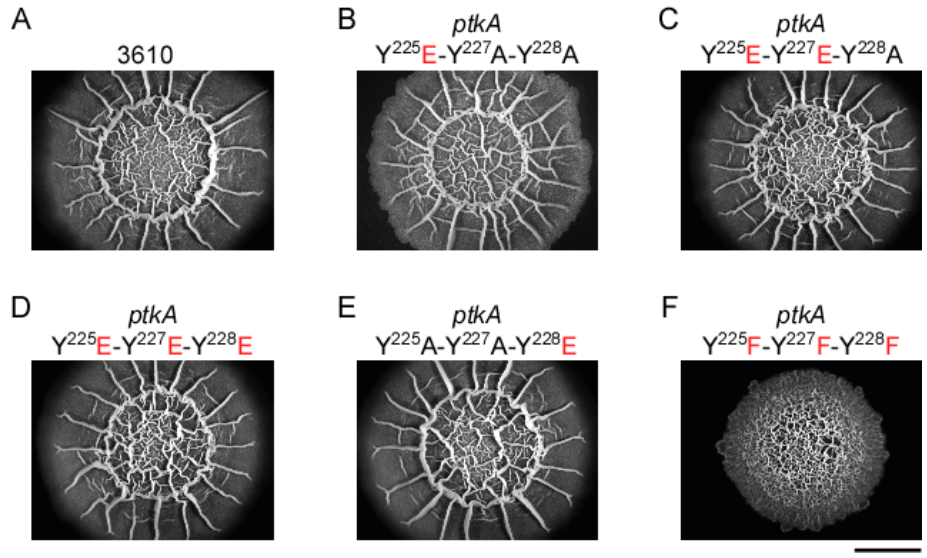


**Figure 5-2: Complex colony architecture of ptkA phosphomimic mutants**
Strains (**A**) NCIB3610, (**B**) Δ*ptkA* $Y^{225}$E-$Y^{227}$A-$Y^{228}$A (NRS3585), (**C**) Δ*ptkA* $Y^{225}$E-$Y^{227}$E-$Y^{228}$A (NRS3563), (**D**) Δ*ptkA* $Y^{225}$E-$Y^{227}$E-$Y^{228}$E (NRS3557), (**E**) Δ*ptkA* $Y^{225}$A-$Y^{227}$A-$Y^{228}$E (NRS3573) and (**F**) Δ*ptkA* $Y^{225}$F-$Y^{227}$F-$Y^{228}$F (NRS3566) were grown on MSgg agar plates for 40 hours at 30˚C prior to photography. Scale bar represents 5 mm.

It was noted that the colony morphology of *ptkA* $Y^{225}$F-$Y^{227}$F-$Y^{228}$F was very similar to that of the Δ*ptkA* and *ptkA* $D^{81}$A-$D^{83}$A mutants (Figure 4-3 and Figure 4-6). In order to rule out the possibility that the *ptkA* $Y^{225}$F-$Y^{227}$F-$Y^{228}$F phenotype was a result of an unintended point mutation at the $D^{81}$A-$D^{83}$A motif, the *ptkA* locus from *ptkA* $Y^{225}$F-$Y^{227}$F-$Y^{228}$F was sequenced. The sequence results confirmed that the 'DxD' motif was wild type. The only mutations detected within the *ptkA* sequence were the phenylalanine substitutions at the terminal tyrosine cluster (data not shown).

To confirm that the biofilm morphology of the *ptkA* $Y^{225}$F-$Y^{227}$F-$Y^{228}$F strain was specific to the point mutations introduced at the native locus, three alleles of *ptkA* were introduced independently into the *amyE* locus under the control of the IPTG inducible promoter $P_{spank\text{-}hy}$; *1)* wild type *ptkA*, *2) ptkA* $D^{81}$A-$D^{83}$A and *3) ptkA* $Y^{225}$A- $Y^{227}$A-$Y^{228}$A. Consistent with the phenotype being specific to the *ptkA* $Y^{225}$F-$Y^{227}$F-$Y^{228}$F mutation, and not a mutation at a heterologous location, biofilm architecture was fully

restored upon induction of wild type *ptkA* (compare Figure 5-3B to Figure 5-3C). Additionally, considerable restoration was achieved by the induction of *ptkA* $Y^{225}$A-$Y^{227}$A-$Y^{228}$A in the *ptkA* $Y^{225}$F-$Y^{227}$F-$Y^{228}$F mutant background (compare Figure 5-3B to Figure 5-3D). In contrast *ptkA* $D^{81}$A-$D^{83}$A was unable to restore the complex colony morphology of *ptkA* $Y^{225}$F-$Y^{227}$F-$Y^{228}$F mutant to that of the wild type colony (compare Figure 5-3B to Figure 5-3E). Taken together, the results tentatively suggest a role for unphosphorylated tyrosine residues within the terminal tyrosine cluster.

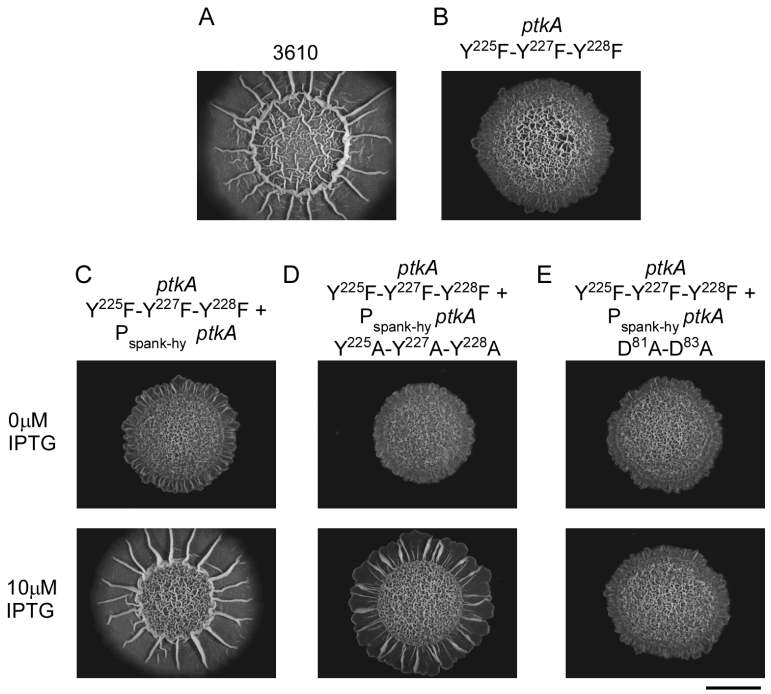


**Figure 5-3: Complex colony architecture of *ptkA* $Y^{225}$F-$Y^{227}$F-$Y^{228}$F complemented with *ptkA***
Strains (**A**) NCIB3610, (**B**) *ptkA* $Y^{225}$F-$Y^{227}$F-$Y^{228}$F (NRS3566), (**C**) *ptkA* $Y^{225}$F-$Y^{227}$F-$Y^{228}$F + $P_{spank-hy}$-*ptkA* (NRS3576), (**D**) *ptkA* $Y^{225}$F-$Y^{227}$F-$Y^{228}$F + $P_{spank-hy}$-*ptkA* $Y^{225}$A-$Y^{227}$A-$Y^{228}$A (NRS3577), and (**E**) *ptkA* $Y^{225}$F-$Y^{227}$F-$Y^{228}$F + $P_{spank-hy}$-*ptkA* $D^{81}$A-$D^{83}$A (NRS3579) were grown on MSgg agar plates with and without the addition of 10μM IPTG as required for 40 hours at 30˚C prior to photographing. Scale bar represents 5 mm.

## *5.2 Investigating the role of PtkA during other multicellular behaviours*

PtkA is a promiscuous BY-kinase (Mijakovic, Petranovic et al. 2005). The work presented here demonstrates that PtkA influences biofilm formation, pellicle formation

and sporulation (Kiley and Stanley-Wall 2010). In addition, it has been shown that PtkA also controls DNA metabolism (Mijakovic, Petranovic et al. 2006; Petranovic, Michelsen et al. 2007) and teichuronic acid production (Mijakovic, Poncet et al. 2003). Furthermore, we have identified that the transcription of the *tkmA* operon, to which *ptkA* belongs, is under the direct control of the transcriptional regulator DegU (Figure 3-18). In addition to its role as an activator of biofilm formation, DegU~P is known to regulate a number of multicellular behaviours including swarming motility (Kobayashi 2007; Verhamme, Kiley et al. 2007) and protease activity (Ogura, Yamaguchi et al. 2001). As DegU~P is a regulator of *ptkA* transcription, we aimed to investigate whether multicellular behaviours known to be regulated by DegU~P are also regulated by PtkA. In particular we aimed to investigate if PtkA was also involved in regulating swarming motility and protease production.

### *5.2.1 PtkA does not influence protease production*

In order to acquire nutrients from the environment many bacteria secrete extracellular proteases (hereafter referred to as exoproteases). In *B. subtilis*, 7 exoproteases have been demonstrated to be secreted in response to high levels of DegU~P (Antelmann, Tjalsma et al. 2001). These include AprE (alkaline serine protease), NprE (neutral protease B), Bpr (bacillopeptidase), Vpr (serine protease), Mpr (metalloproteases), Epr (minor serine protease) and WprA (cell wall-associated protein precursor). The most abundant of the exoproteases are AprE and NprE, whereas Vpr, Bpr, Mpr, Epr and WprA are regarded as minor proteases. DegU was first proposed by Steinmetz *et al*. to activate exoprotease production (Steinmetz, Kunst et al. 1976). Later it was determined

that the over-expression of DegU-$^{HY}$ (which dephosphorylates 7-fold slower) resulted in an increase in exoprotease production (Msadek, Kunst et al. 1990). Moreover, it was shown that exoproteases expression is heterogeneous, in that only a sub-population of cells are switched on for exoprotease production and that in addition to requiring DegU~P, cells also require Spo0A~P, in order to down regulate the repression of *aprE* by AbrB and SinR (Veening, Igoshin et al. 2008). As high levels of DegU~P are required to activate exoprotease production, but high levels of DegU~P also repress biofilm formation, it has been proposed that exoprotease production may also act as a means of releasing cells from a biofilm (Verhamme, Kiley et al. 2007). Thus protease production can be viewed as a multicellular event.

To investigate if PtkA was involved in the regulation of protease production, strains containing mutations in either the 'DxD' motif or the terminal tyrosine cluster were spotted onto agar plates containing 1.5% milk alongside the wild type parental strain. Production of the exoproteases leaves a cleared halo surrounding the colony due to milk digestion. We chose to use strains containing point mutations rather than the Δ*ptkA* strain as it was assumed that the mutant strains would produce the mutant version of the PtkA protein and therefore would be the most comparable. Any change to the level of protease activity of the strain could then be attributed to either the kinase activity of PtkA or may provide additional information about the role of the terminal tyrosine cluster. The results from these experiments showed that upon mutation of the 'DxD' motif or the terminal tyrosine cluster, protease production was unaffected compared with wild type protease production (Figure 5-4). Thus, we can conclude that PtkA is not involved in the production of exoproteases.

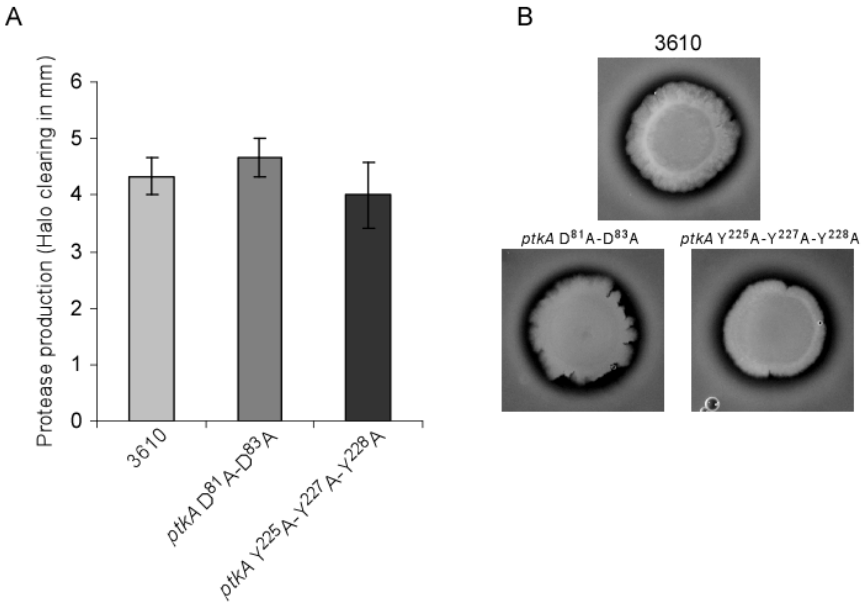


**Figure 5-4: Protease activity is not dependent on PtkA activity**
(A) Bar graph showing average protease production from wild type NCIB3610 (light grey), *ptkA* $D^{81}A$-$D^{83}A$ (dark grey) (NRS2796) and *ptkA* $Y^{225}A$-$Y^{227}A$-$Y^{228}A$ (black) (NRS2799). Error bars represent standard error of the mean. Data represents 3 independent rounds. (**B**) Photograph of digestion of milk protein by wild type NCIB3610, *ptkA* $D^{81}A$-$D^{83}A$ and *ptkA* $Y^{225}A$-$Y^{227}A$-$Y^{228}A$ colonies. Colonies were incubated at 37˚C for 16 hours prior to photography.

### *5.2.2 PtkA influences swarming motility*

Swarming motility is a multicellular behaviour displayed by many different species of bacteria, including *B. subtilis* (Kearns 2010). Swarming motility is defined as the migration of a population of cells over a substrate, and relies on the cooperation of cells belonging to a dense population. In *B. subtilis*, many factors are required to coordinate this complex multicellular behaviour. A key feature of a swarming population is the formation of cell rafts; collections of ordered cells which sit side-by-side in order to achieve rapid and directed movement (Kearns and Losick 2003). Additionally, swarming cells require production of the antibiotic lipopeptide surfactin. The use of a surfactant to reduce surface tension is a common feature among swarming bacteria (Kearns 2010). It is now well established that domesticated *B. subtilis* have lost the

ability to swarm (Kearns and Losick 2003; Patrick and Kearns 2009). The genetic basis for this is a frameshift mutation in the *swrA* gene, which leads to a truncation after tyrosine 13 (Kearns, Chu et al. 2004). The *swrA* gene encodes for an activator of the *fla/che* operon which encodes proteins required for the biosynthesis of the bacterial flagella as well as the *swrB* gene. SwrB activates the transcription of the late flagella genes including *hag*, which codes for flagellin (Kearns and Losick 2005). Moreover, domesticated *B. subtilis* possesses a mutation in the *sfp* gene (Nakano, Corbell et al. 1992) which results in the loss of surfactin production.

The transcriptional regulators DegU and SinR regulate swarming motility (Amati, Bisicchia et al. 2004; Blair, Turner et al. 2008). Firstly, very low levels of DegU~P activate swarming motility in the undomesticated NCIB3610 isolate, whereas high levels inhibit swarming motility (Verhamme, Kiley et al. 2007). Secondly, SinR is able to indirectly regulate the activity of the flagella motor. SinR represses the transcription of the *epsA-O* operon (Kearns, Chu et al. 2005), which encodes EpsE. EpsE has been demonstrated to act as a clutch, thus uncoupling the flagellum from the motor (Blair, Turner et al. 2008).

Integration of these multiple factors contributing to swarming motility must be achieved in order to activate swarming motility. In chapter 4.2, I demonstrated the requirement of PtkA during biofilm formation. With this in mind, I aimed to test whether PtkA also participated in the regulation of other multicellular behaviours, such as swarming motility. To address this, wild type NCIB3610, *ptkA* $D^{81}A$-$D^{83}A$ and *ptkA* $Y^{225}A$-$Y^{227}A$-$Y^{228}A$ were assessed for their ability to swarm under laboratory conditions. As with protease production assay, our intention was to keep the protein present and use the $D^{81}A$-$D^{83}A$ and terminal tyrosine cluster mutations as these will allow us to see if

kinase activity is needed and if a role for the terminal tyrosine cluster could be identified.

Assessment of the motility of the strains was carried out under standard swarming conditions (Kearns and Losick 2003). Cultures of NCIB3610, *ptkA* $D^{81}A$-$D^{83}A$ and *ptkA* $Y^{225}A$-$Y^{227}A$-$Y^{228}A$ were grown to an $OD_{600}$ of 1.0, concentrated to a final $OD_{600}$ of 10 and were spotted onto LB media plates solidified with 0.7% agar. The distance of the swarm was measured at defined time points and photographs of the swarm plates were taken after 6 hours incubation at 37˚C. The results showed that in comparison to wild type cells, the *ptkA* $D^{81}A$-$D^{83}A$ and *ptkA* $Y^{225}A$-$Y^{227}A$-$Y^{228}A$ mutants were unable to swarm (Figure 5-5). These results suggested a role for PtkA during swarming motility and in particular, demonstrated that the kinase activity of PtkA was required during swarming. Additionally, the results indicated that the terminal tyrosine cluster was important for the regulation of this multicellular behaviour.

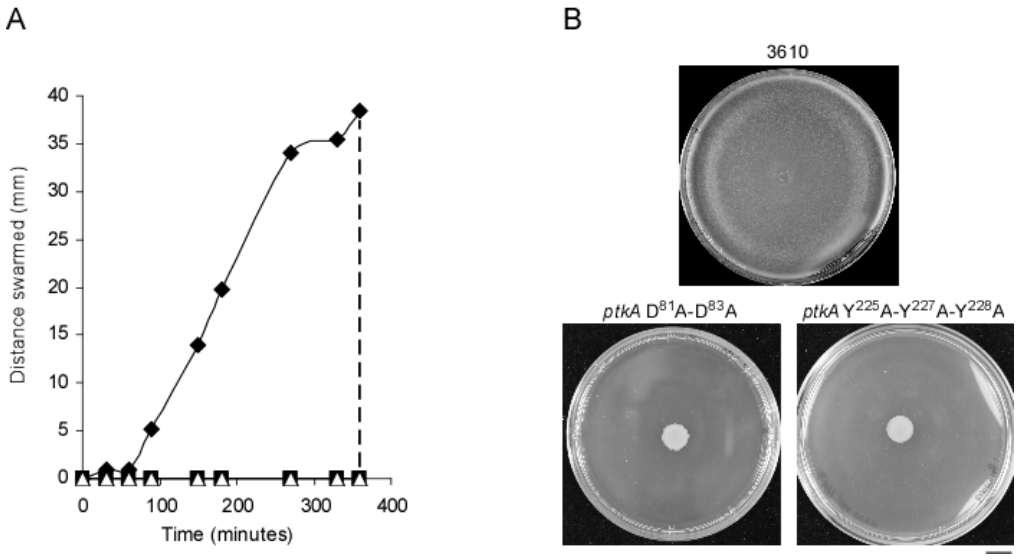


**Figure 5-5: Swarming of *ptkA* $D^{81}A$-$D^{83}A$ and *ptkA* $Y^{225}A$-$Y^{227}A$-$Y^{228}A$.**
(**A**) Strains NCIB3610 (black diamonds), *ptkA* $D^{81}A$-$D^{83}A$ (NRS2796) (black squares) and *ptkA* $Y^{225}A$-$Y^{227}A$-$Y^{228}A$ (NRS2799) (white triangles) were grown in LB until $OD_{600}$ 1.0 prior to being concentrated to $OD_{600}$ 10. LB media solidified with 0.7% agar was spotted with 10 µl of culture and incubated at 37 ˚C for 360 minutes. Dashed line represents time point at which photographs of the swarming plates were taken. (**B**) Photographs of the strains were taken after 6 hours swarming. Scale bar represents 1 cm.

In light of the discovery that PtkA was important for swarming motility, we then decided to further investigate potential targets of PtkA during swarming.

## *5.3 YvyG is a potential target of PtkA during swarming*

To identify the target of PtkA during swarming motility, we decided to first test the most obvious potential target, YvyG (Jers, Pedersen et al. 2010). YvyG is encoded by the *yvyG* gene which is situated upstream of the genes encoding for the transcriptional regulator and cognate sensor kinase pair, DegU and DegS (Figure 5-6).


**Figure 5-6: Schematic representation of the chromosomal region surrounding *yvyG*.**
Arrows indicate open reading frames (ORF), the direction of the arrow indicating the direction of the ORF. The gene *yvyG* is highlighted in red. Black arrows indicate genes which encode proteins essential for swarming and swimming motility. Stalked circles indicate sites of transcriptional termination. Numbers flanking the chromosomal region indicate the position on the chromosome in relation to the origin of replication.

The *yvyG* gene is located on the chromosome between *flgM* and *flgK*, which encode an anti-sigma factor required for inactivating $\sigma^{-D}$ (Mirel, Lauer et al. 1994) and a protein necessary for forming the hook-filament junction (Mirel, Lauer et al. 1994), respectively. YvyG however encodes a protein of unknown function and specific involvement in motility had not been demonstrated. YvyG has been shown to become phosphorylated *in vivo* (Macek, Mijakovic et al. 2007) and *in vitro* (Jers, Pedersen et al. 2010). The bacterial tyrosine kinase that is responsible for the phosphorylation of YvyG is PtkA (Jers, Pedersen et al. 2010). Taken together, we hypothesised that YvyG

plays a role in motility and that the function of YvyG is controlled by phosphorylation mediated by PtkA. To test our hypothesis, we first assessed the impact of mutating *yvyG* on swarming. As a disruption mutant was already available (*yvyG*::pBL132, previously used to assess the impact on colony architecture see Figure 4-16), we used this mutant to get an initial insight into the effect on swarming. The results showed that a disruption to *yvyG* completely inhibited swarming motility (Figure 5-7). As a negative control a strain lacking the gene required to synthesise the flagellin protein (*hag*) was used.

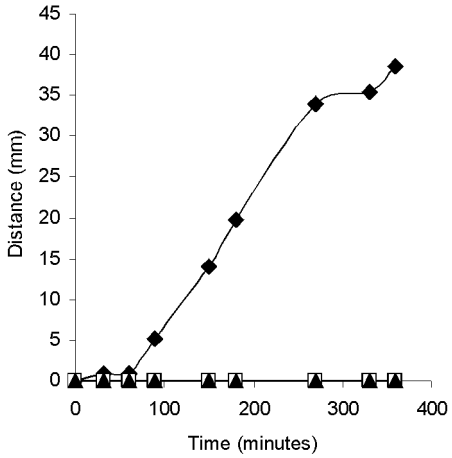


**Figure 5-7: Swarming of *yvyG*::pBL132**
Swarming motility of NCIB3610 (black diamonds), *yvyG*::pBL132 (NRS3216) (white squares), and Δ*hag* (NRS2253) (black triangles). Data is representative of >3 independent rounds.

This strain, however, was constructed by introducing a plasmid into the chromosome at the *yvyG* locus with the aim of disrupting the transcription of the gene. As *yvyG* is located within an operon that is essential for motility (Figure 5-6) this carries the risk that construction of a mutation of this sort will impose polar effects on genes neighbouring *yvyG*, thus indirectly affecting swarming motility. In order to verify if the affect on swarming motility was a result of the disruption to *yvyG* or a disturbance to its neighbouring genes, an in-frame marker-less deletion was constructed at the *yvyG* locus (Figure 5-8).

YvyG is phosphorylated on a single tyrosine residue at position 49 (Macek, Mijakovic et al. 2007). In light of the evidence suggesting a role for PtkA during swarming, the fact that YvyG is a known target of PtkA and the prediction that *yvyG* may also be important for swarming, we proposed that PtkA phosphorylates YvyG at residue $Y^{49}$, thus regulating the activity of YvyG during swarming. For these reasons, a mutant strain containing a tyrosine to alanine substitution at position 49 was also constructed in order to test if the inability to become phosphorylated affected the role of YvyG during swarming.

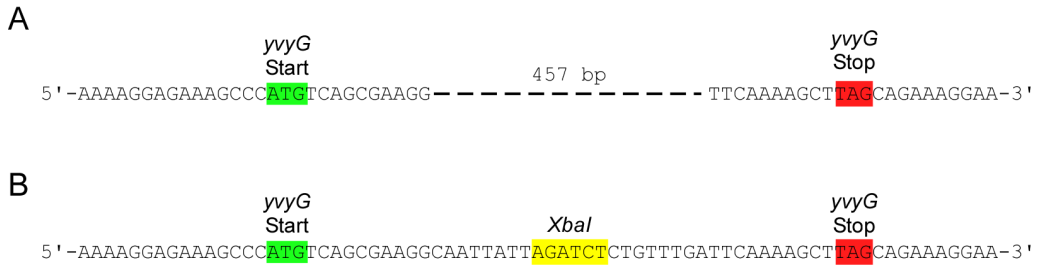


**Figure 5-8: Schematic representation of the Δ*yvyG* mutant construction**
(**A**) Wild type *yvyG*. Translational start and stop codons are highlighted in green and red, respectively. (**B**) Deletion of *yvyG*. Translational start and stop codons are highlighted as noted in (**A**). Primer engineered restriction site for *Xba*I is highlighted in yellow.

After construction of the deletion strain and the *yvyG* $Y^{49}$A point mutant, but prior to assessing the effects of the mutations on swarming motility, colony complexity was assessed to ensure that the morphology of Δ*yvyG* was the same as the original *yvyG*::pBL132 mutant (Compare Figure 4-16 and Figure 5-9 ). The resulting colony of the newly constructed Δ*yvyG* mutant retained its original phenotype, as did the single point mutation of *yvyG* $Y^{49}$A (Figure 5-9). These results are in agreement with the previous experiments (Figure 4-16)

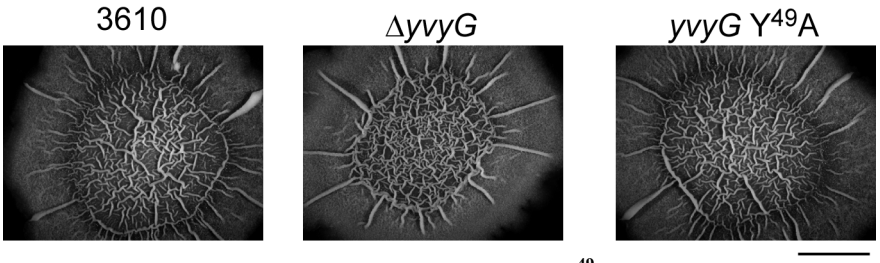


**Figure 5-9: Complex colony morphology of Δ*yvyG* and *yvyG* Y$^{49}$A.**
The strains NCIB3610, Δ*yvyG* (NRS3570) and *yvyG* Y$^{49}$A (NRS3571) were grown on MSgg agar for 40 hours at 30°C. Scale bar represents 5 mm.

Next, swarming and swimming analysis were conducted using the Δ*yvyG* mutant. The strain lacking *yvyG* was unable to swim or swarm (Figure 5-10). Motility could be restored by adding back the wild type copy of *yvyG* at a heterologous location on the chromosome. These results demonstrate for the first time *in vivo* that *yvyG* is required for both swimming and swarming motility. Additionally, these results demonstrate the requirement of higher levels of *yvyG* for swarming motility rather than swimming, since a higher level of complementation could be linked with the higher demand of flagella for swarming than swimming (Fraser and Hughes 1999).

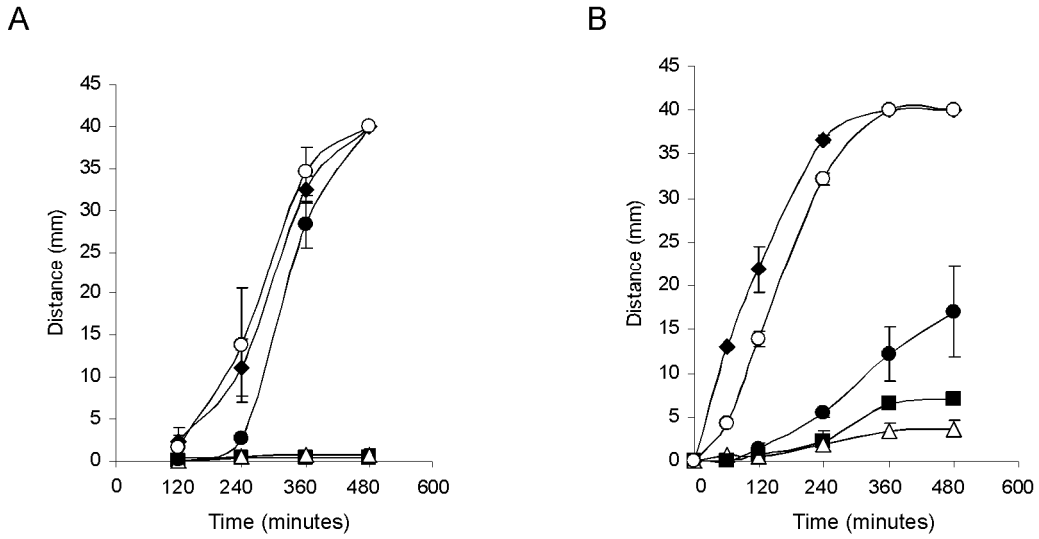


**Figure 5-10: Swimming and swarming motility of Δ*yvyG***
(**A**) Swimming and (**B**) swarming motility of NCIB3610 (black diamonds), Δ*hag* (NRS2253) (black squares), Δ*yvyG* (NRS3570) (white triangles), Δ*yvyG* + $P_{spank\text{-}hy}$ *yvyG* (NRS3578) without the addition of IPTG (black circles) and with the addition of 10 μM IPTG (white circles). Data is representative of >3 independent rounds. Error bars represent the standard error of the mean.

Next, the impact on motility of mutating the tyrosine at position 49 to an alanine was assessed. In contrast to the results obtained for the deletion of *yvyG*, it was discovered that the $Y^{49}A$ mutation did not impact on swimming nor swarming motility (Figure 5-11).

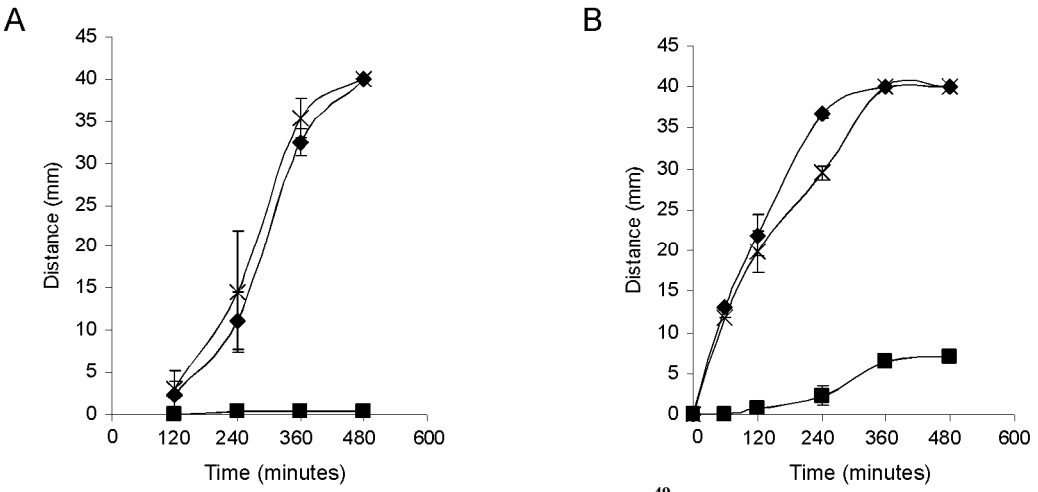


**Figure 5-11: Swimming and swarming motility of *yvyG* $Y^{49}A$.**
(**A**) Swimming and (**B**) swarming motility of NCIB3610 (black diamonds), Δ*hag* (NRS2253) (black squares), and *yvyG* $Y^{49}A$ (NRS3570) (crosses). Data is representative of >3 independent rounds. Error bars represent the standard error of the mean.

Taken together, these results confirm that YvyG participates in swarming and swimming motility. However, contrary to our hypothesis this function is independent of phosphorylation, as the *yvyG* $Y^{49}A$ mutant was unaffected for swarming and swimming motility. The discovery that the role of YvyG during swarming motility is independent of the phosphorylation status of the protein called into question the validity of the results demonstrating that the kinase activity and terminal tyrosine cluster of PtkA are necessary for swarming motility. In order to address this discrepancy, we decided to reassess the impact of the *ptkA* $D^{81}A$-$D^{83}A$ and terminal tyrosine cluster mutations on swarming motility.

## *5.4 Reassessment of PtkA involvement during swarming and swimming motility*

To begin reassessing the impact of mutating *ptkA* on motility, we aimed to test whether the addition of wild type *ptkA* could restore swarming motility to the *ptkA* $D^{81}A$-$D^{83}A$ mutant.

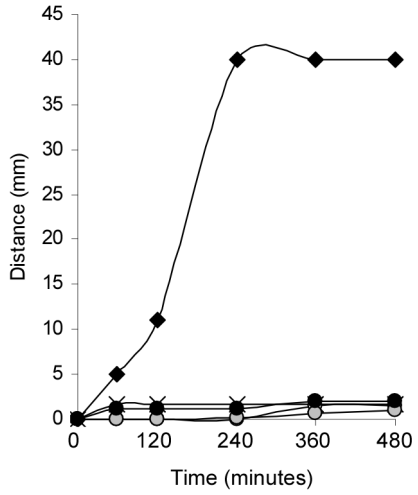


**Figure 5-12: Swarming motility of *ptkA* $D^{81}A$-$D^{83}A$ + $P_{spank\text{-}hy}$ *ptkA***
Swarming was assayed using the strains NCIB3610 (black diamonds), *ptkA* $D^{81}A$-$D^{83}A$ (NRS2796) (crosses), and *ptkA* $D^{81}A$-$D^{83}A$ + $P_{spank\text{-}hy}$ *ptkA* (NRS2807) in the absence of IPTG (white circles), in the presence of 1 μM IPTG (grey circles), and the presence of 10 μM IPTG (black circles). Graph is representative of > 3 independent rounds.

The results showed that upon artificial induction of *ptkA* expression from a heterologous location on the chromosome, swarming motility did not return to the *ptkA* $D^{81}A$-$D^{83}A$ mutant. The inability of this mutation to be complemented raised the concern that the phenotype observed was not caused by the $D^{81}A$-$D^{83}A$ mutation, despite biofilm formation being restored with this same construct (Figure 4-6). In order to ascertain what could have caused the lack of swarming motility in the $D^{81}A$-$D^{83}A$ mutant, the level of transcription from the promoter of the *hag* gene was assessed. The *hag* gene encodes for the flagellin structural protein component of the *B. subtilis* flagella and is

transcribed by the alternative sigma factor, $\sigma^D$ RNA polymerase (Mirel and Chamberlin 1989). The expression of *hag* is essential for motility. A strain was constructed which contained the promoter region of *hag* fused to the gene coding for YFP. The level of $P_{hag}$-YFP observed in the *ptkA* $D^{81}A$-$D^{83}A$ mutant was indistinguishable from the level observed in wild type cells (Figure 5-13).

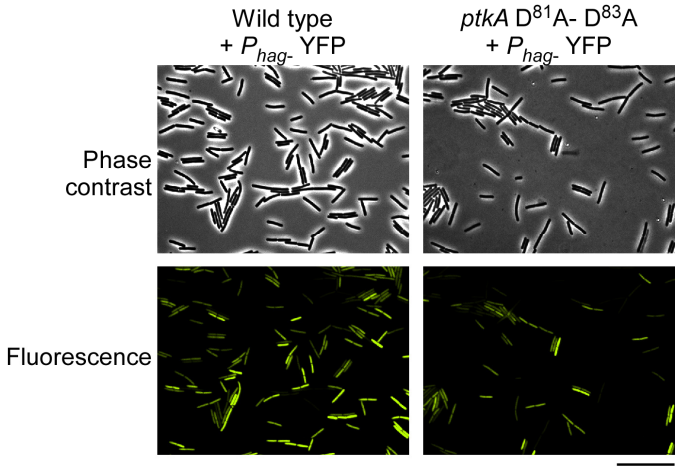


**Figure 5-13: Transcription of $P_{hag}$-YFP in *ptkA* $D^{81}A$-$D^{83}A$**
Phase contrast and fluorescent images of wild type (NRS3076) and *ptkA* $D^{81}A$-$D^{83}A$ (NRS3243) collected using Zeiss Axio Imager M1. Both strains contain $P_{hag}$ reporter fusions with *yfp*. Scale bars represent 20 μm.

Based on the results of the experiment above, we are unable to determine the cause of the lack of motility observed in the $D^{81}A$-$D^{83}A$ mutant. As *ptkA* $D^{81}A$-$D^{83}A$ was constructed using the pMAD method, which uses transduction to transfer a large region of DNA into the cell for homologous recombination, it is possible that an undesired mutation(s) was carried over during the transduction of the *ptkA* $D^{81}A$-$D^{83}A$ mutation into NCIB3610. Complementation of the *ptkA* $D^{81}A$-$D^{83}A$ mutation by addition of a wild type copy of *ptkA* at a heterologous location was unable to restore motility, however complex colony architecture was restored using this construct (Figure 4-6).

Taken together, we can conclude that the lack of swarming motility in the *ptkA* $D^{81}A$-$D^{83}A$ mutant is not the cause of the altered colony morphology.

In parallel to investigating the validity of the non-swarming phenotype displayed by the *ptkA* $D^{81}A$-$D^{83}A$ mutant, we also assessed the non-swarming phenotype of the terminal tyrosine cluster mutant. As for the *ptkA* $D^{81}A$-$D^{83}A$ mutant, we attempted to complement the terminal tyrosine cluster mutant by introducing a wild type copy of *ptkA* at a heterologous location on the chromosome under the control of an IPTG inducible promoter. Again upon addition of IPTG, swarming motility could not be restored to the *ptkA* $Y^{225}A$-$Y^{227}A$-$Y^{228}A$ mutant (Figure 5-14).

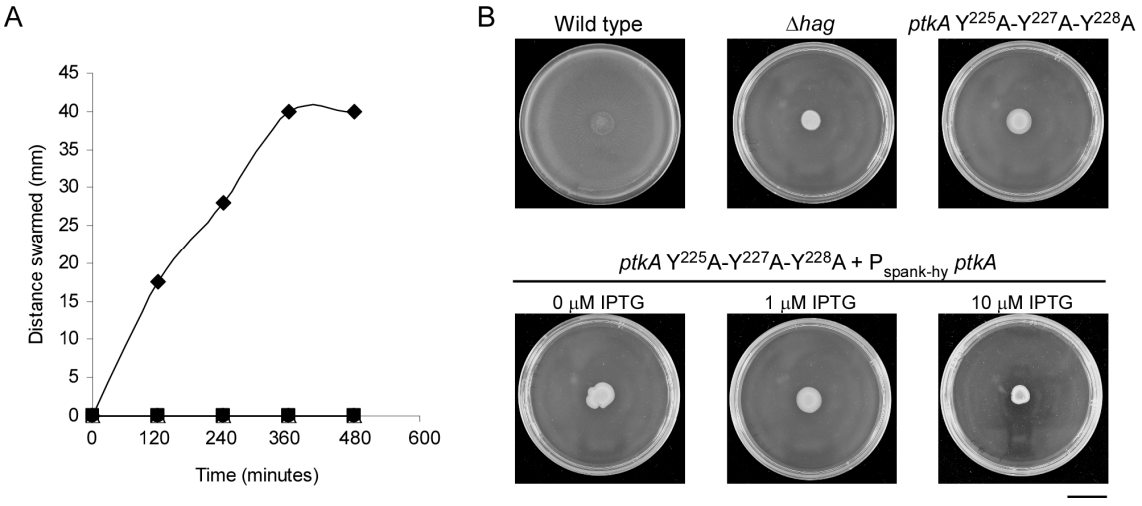


**Figure 5-14: Swarming of *ptkA* $Y^{225}A$-$Y^{227}A$-$Y^{228}A$ + $P_{spank\text{-}hy}$ *ptkA***
(A) Swarming was assayed using the strains NCIB3610 (black diamonds), Δ*hag* (black square), *ptkA* $Y^{225}A$-$Y^{227}A$-$Y^{228}A$ (white triangles), and *ptkA* $Y^{225}A$-$Y^{227}A$-$Y^{228}A$ in the absence of IPTG (white circles), in the presence of 1 μM IPTG (grey circles), and the presence of 10 μM IPTG (black circles). (B) Photographs of swarming plates taken at 8 hours incubation. Scale bar represents 2cm.

As for the *ptkA* $D^{81}A$-$D^{83}A$ mutant, we also decided to test if the lack of motility displayed by the terminal tyrosine cluster mutant was caused by an unanticipated

mutation within the *hag* gene or (indirectly) a regulator of the *fla/che* operon. To achieve this, we again utilised the *hag* reporter fusion construct. The results showed that *hag* transcription was significantly lower in the terminal tyrosine cluster mutant than in the wild type cells (Figure 5-15). Attempts were made to restore *hag* expression by adding back in a wild type copy of *ptkA* at a heterologous location; however this was not successful (Figure 5-15). This was anticipated since induction of expression did not restore swarming motility itself (Figure 5-14).

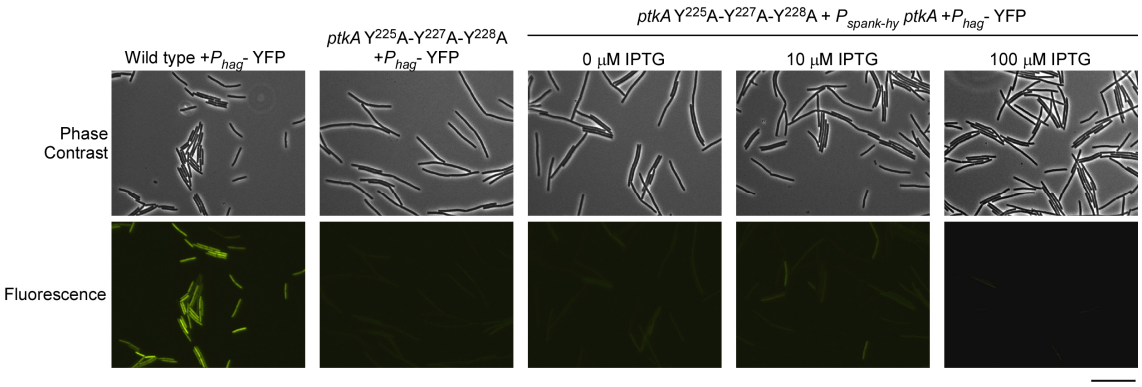


**Figure 5-15: Transcription of $P_{hag}$ in *ptkA* $Y^{225}A$-$Y^{227}A$-$Y^{228}A$ and *ptkA* $Y^{225}A$-$Y^{227}A$-$Y^{228}A$ + $P_{spank-hy}$ *ptkA***
Phase contrast and fluorescent images of wild type (NRS3076), *ptkA* $Y^{225}A$-$Y^{227}A$-$Y^{228}A$ (NRS3244) and *ptkA* $Y^{225}A$-$Y^{227}A$-$Y^{228}A$ + $P_{spank-hy}$*ptkA* (NRS3248) collected using Zeiss Axio Imager M1. Scale bar represents 20 μm.

As the lack of swarming motility and *hag* transcription in the *ptkA* $Y^{225}A$-$Y^{227}A$-$Y^{228}A$ could not be complemented, we must conclude that this phenotype is not a result of the terminal tyrosine cluster mutation. The cause of the unusual phenotype may be explained by the fact that the *ptkA* $Y^{225}A$-$Y^{227}A$-$Y^{228}A$ displays unusually long chains of cells compared to wild type cells, a phenotype which could also not be complemented. Hyper-chaining phenotypes have been associated with mutations in the *swrA* gene (formerly *yvzD*), responsible for the regulation of swarming-dependent

genes, including *hag* (Kearns and Losick 2005). The *swrA* gene of *ptkA* $Y^{225}A$-$Y^{227}A$-$Y^{228}A$ was sequenced in order to determine if the phenotype of *ptkA* $Y^{225}A$-$Y^{227}A$-$Y^{228}A$ could be accounted for by a mutation in the *swrA* gene. The sequencing results showed that *swrA* was wild type in the *ptkA* $Y^{225}A$-$Y^{227}A$-$Y^{228}A$ mutant (data not shown). In conclusion, the cause of the unusual hyper chained phenotype displayed by the *ptkA* $Y^{225}A$-$Y^{227}A$-$Y^{228}A$ mutant remains to be determined, and as such this remains a point of work which is on going.

As verification of the non-swarming phenotypes of the *ptkA* $Y^{225}A$-$Y^{227}A$-$Y^{228}A$ and *ptkA* $D^{81}A$-$D^{83}A$ mutants failed to confirm the role of *ptkA* during swarming, it was decided that the *ptkA* $Y^{225}A$-$Y^{227}A$-$Y^{228}A$ mutant would be remade. The *ptkA* $Y^{225}A$-$Y^{227}A$-$Y^{228}A$ strain was remade in an identical manner to the original mutant; using the standard pMAD protocol. Prior to assessing the strains' ability to swarm, the colony morphology phenotype was assessed in order to ensure that the phenotype of the new mutant was the same as the original *ptkA* $Y^{225}A$-$Y^{227}A$-$Y^{228}A$ mutation (NRS2799). The new replacement *ptkA* $Y^{225}A$-$Y^{227}A$-$Y^{228}A$ mutant (NRS3559) displayed a phenotype that was indistinguishable from wild type (Figure 5-16). This is in agreement with the colony architecture analysis results for the original *ptkA* $Y^{225}A$-$Y^{227}A$-$Y^{228}A$ mutant.

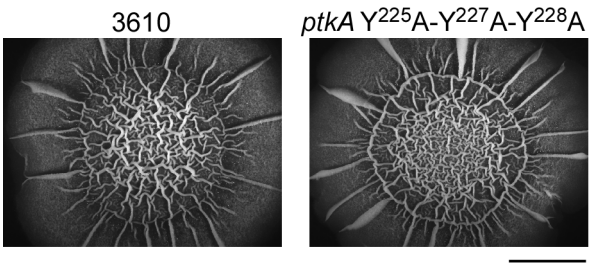


**Figure 5-16: Colony architecture analysis of remade *ptkA* $Y^{225}A$-$Y^{227}A$-$Y^{228}A$ mutant**
Strains NCIB3610 and replacement *ptkA* $Y^{225}A$-$Y^{227}A$-$Y^{228}A$ mutant (NRS3559) were grown on MSgg agar for 40 hours at 30°C. Scale bar represents 5 mm.

Next, the replacement remade *ptkA* $Y^{225}A$-$Y^{227}A$-$Y^{228}A$ mutant was assessed for its ability to swarm. Swarming motility of the remade *ptkA* $Y^{225}A$-$Y^{227}A$-$Y^{228}A$ mutant was indistinguishable from the wild type cells, thus we can conclude that the terminal tyrosine cluster in not involved in the regulation of swarming motility.

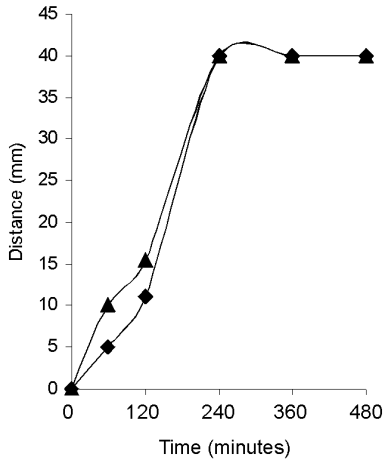


**Figure 5-17: Swarming motility analysis of remade ptkA $Y^{225}A$-$Y^{227}A$-$Y^{228}A$**
Swarming was assayed using the strains NCIB3610 (black diamonds) and ptkA $Y^{225}A$-$Y^{227}A$-$Y^{228}A$ (NRS3559) (black triangles). Graph is representative of > 3 independent rounds.

As the replacement *ptkA* $Y^{225}A$-$Y^{227}A$-$Y^{228}A$ mutant showed no impact on swarming motility, this raised the question as to whether or not *ptkA* was at all involved in swarming motility. To address this concern, the swarming ability of the Δ*ptkA* mutant was tested. The results clearly showed that there was no impact of deleting *ptkA* on swarming motility (Figure 5-18). These results are now consistent with our findings that the phosphorylation of YvyG is not required for swarming and we can conclude that PtkA is not involved in swarming motility.

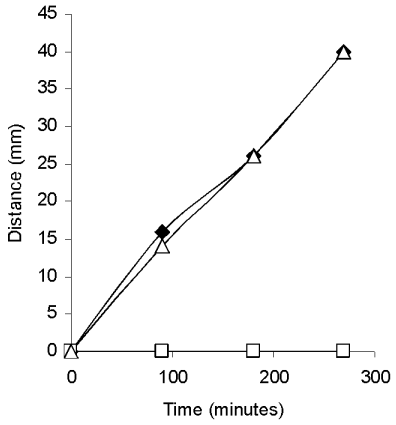


**Figure 5-18: Swarming analysis of Δ*ptkA***
Swarming was assayed using the strains NCIB3610 (black diamonds), Δ*hag* (NRS2253) (white squares) and Δ*ptkA* (NRS2544) (white triangles). Graph is representative of > 3 independent rounds.

## *5.5 Discussion*

### *5.5.1 Phenylalanine substitutions suggest a role for the PtkA terminal tyrosine cluster*

In this section I aimed to further investigate the role of the terminal tyrosine cluster of PtkA. To do this, amino acids that are structurally similar to tyrosine and mimic either a phosphorylated or unphosphorylated state were substituted into the terminal tyrosine cluster of PtkA (see Figure 5-2). Analysis of the data led to the conclusion that mutation of the terminal tyrosine cluster may affect biofilm formation. While it was noted that replacement of the tyrosine with glutamic acid (mimicking a phosphorylated state) did not cause a disruption to biofilm formation, replacement of the terminal tyrosine residues with phenylalanine did (Figure 5-2). Additionally, it was noted that complementation of a *ptkA* $Y^{225}F$-$Y^{227}F$-$Y^{228}F$ mutant was less successful with *ptkA* $Y^{225}A$-$Y^{227}A$-$Y^{228}A$ than a wild type copy of *ptkA*. This outcome was unexpected as no

difference was first observed between the complex colony of the *ptkA* $Y^{225}$A-$Y^{227}$A-$Y^{228}$A mutant and wild type *B. subtilis*. It is important to note that the effects observed upon substitution of the terminal tyrosine cluster for phenylalanines may be due to an impairment of protein stability rather than a loss of tyrosine residues. Future experiments will aim to address this issue.

In summary, the results of the extended investigation of the terminal tyrosine cluster of PtkA have tentatively suggested a role for the terminal tyrosine cluster during biofilm formation. This is the first study which has suggested that replacement of the terminal tyrosine cluster of PtkA with phenylalanines may affect the function of the protein. In fact, other studies have demonstrated that a mutant form of PtkA possessing substitutions to phenylalanines at the terminal tyrosine cluster remained active, in the sense that it was able to phosphorylate Ugd (Mijakovic, Poncet et al. 2003). It is important to keep in mind that Ugd is not required for biofilm formation and the ability of PtkA $Y^{225}$F-$Y^{227}$F-$Y^{228}$F to phosphorylate other target proteins is unknown. A key difference between our study and that of Prof. Mijakovic is that the work presented here involves constructing in-frame mutations on the chromosome, the effects of which were subsequently assessed *in vivo*, whereas the Mijakovic study assayed the kinase activity of purified mutated PtkA *in vitro*. These differences perhaps highlight the need to observe mutations in their native environments in addition to studying the impact of mutations *in vitro*.

### *5.5.2 The terminal tyrosine cluster of PtkA may act like a gate*

Presuming that all of the mutant alleles of PtkA are stable, it is interesting to note the differences between the impacts of substituting the terminal tyrosine cluster residues with a range of different amino acids. X-ray crystal studies of the PtkA homologue Cap5B2, from the Gram-positive bacterium *S. aureus,* demonstrated that the terminal tyrosine cluster of a form of Cap5B2 that is unable to autophosphorylate is positioned in the active pocket of the kinase (Olivares-Illana, Meyer et al. 2008). It is mentioned that substitution of the terminal tyrosine cluster to glutamic acids (mimicking a phosphorylated state) allows Cap5B2 to phosphorylate the cognate partner CapO. Furthermore, deletion of the terminal tyrosine cluster region did not inhibit phosphorylation of CapO (Olivares-Illana, Meyer et al. 2008).

Taken together, it appears that the terminal tyrosine cluster of BY-kinases may act like a gate; when phosphorylated the gate is open, thus allowing substrates to enter the active pocket of the kinase and become phosphorylated. In contrast when unphosphorylated, the gate is closed, and substrates are prevented from becoming phosphorylated. Therefore, as the R-group of the amino acid alanine is significantly smaller than that of a tyrosine, it is tempting to hypothesise that the reason why no impact on complex colony architecture was originally observed upon substitution with alanines was because the amino acid was unable to block entry to the active site, and thus the ‘gate’ remained open.

### *5.5.3 Investigating the role of YvyG regulated by PtkA*

The role of PtkA during swarming and protease production was also explored. In summary, the results showed that PtkA does not regulate protease production or swarming motility. However, while investigating the role of PtkA during swarming motility, this study highlighted a protein called YvyG. YvyG is required for swarming and swimming motility by *B. subtilis* (Figure 5-10). PtkA has been shown to phosphorylate YvyG *in vitro* (Jers, Pedersen et al. 2010). Indeed the localisation of YvyG changes depending on the presence or absence of PtkA, thus the authors concluded that the location of YvyG is controlled by its phosphorylation state. Interestingly the function of YvyG during motility is not dependent on being phosphorylated (Figure 5-11). To expand on these initial findings, I intended to test whether the localisation of YvyG was due to a protein-protein interaction with PtkA (as they shared identical localisation patterns), or, as the authors suggest, the localisation of YvyG was due to becoming phosphorylated by PtkA. Thus, I aimed to test the impact of the YvyG $Y^{49}A$ mutation, which cannot become phosphorylated, on the localisation of the protein. However, a translational fusion of YvyG-GFP was unable to complement a *yvyG* mutant and restore swarming motility (data not shown) and therefore I felt that any data interpreted would be unreliable. As the translational fusion proteins constructed by Jers *et al.* were not tested to ensure they were functional, this perhaps casts doubt on the conclusions drawn by the authors. Overall, the effect of phosphorylation on YvyG by PtkA is very interesting, as this study has demonstrated that YvyG is able to fulfil an uncharacterised function in addition to motility.

YvyG was predicted to act as a chaperone as it was suggested to be a homologue of FlgN (Pallen, Penn et al. 2005). FlgN is an export chaperone encoded by *E. coli* that is

involved in flagellar synthesis (Pallen, Penn et al. 2005). However, it must be noted that YvyG and FlgN share very little protein sequence similarity (2 protein BLAST alignment shows that only a 6 amino acid run is shared by both proteins; YvyG is 160 amino acids long). Indeed, the designation of YvyG as a homologue of FlgN was based on two points: *1)* that *yvyG* is located on the chromosome upstream of *flgM* (which mirrors the chromosomal location of *flgN* and *flgM* in *E. coli*); and *2)* that the protein sequences of YvyG and FlgN are roughly the same length (Pallen, Penn et al. 2005). Therefore the function of YvyG as a chaperone remains to be confirmed. It will be interesting to further understand the role of YvyG at the molecular level during flagella synthesis and motility. An interesting outcome of this work has been the discovery that PtkA may able to regulate a novel and as of yet undefined function mediated through the phosphorylation of YvyG. Furthermore this work may suggest that, in addition to its role controlling motility, YvyG possesses a further function(s), which is subject to regulation via phosphorylation.

# 6 Concluding remarks

## *6.1 Novel functions are assigned to PtkA and PtpZ*

Biofilm formation by *B. subtilis* has been investigated in detail and, as such, a great deal is known about the complex regulatory network controlling biofilm formation at the level of transcription. The work presented here adds to our knowledge of this complex regulatory network. An initial aim of this project was to investigate the relationship between two key regulators of biofilm formation by *B. subtilis*; SinR and DegU. The results of the epigenetic study demonstrated that SinR and DegU regulate biofilm formation via parallel pathways (see section 3.2). However, a novel group of genes were identified as DegU and SinR co-regulated targets (see section 3.3) and from this initial investigation, the gene *ptpZ*, encoding a bacterial tyrosine phosphatase, was found to be required for robust biofilm formation (see Figure 3-3). Following on from this, the genes *tkmA*, encoding a tyrosine kinase modulator, and *ptkA*, encoding a bacterial tyrosine kinase, were also found to be required for biofilm formation by *B. subtilis* (see sections 4.2 and 4.3). These findings allowed novel functions to be assigned to the bacterial tyrosine kinase, PtkA, and phosphatase, PtpZ. Furthermore, the work presented here demonstrates for the first time in *B. subtilis* that biofilm formation is subject to regulation at the post-translational level.

An interesting outcome of this work was that the UDP-glucose dehydrogenase Ugd, which is encoded by the gene *ugd* located within the same operon as *tkmA*, *ptkA* and *ptpZ*, is not the physiological target of PtkA and PtpZ during biofilm formation (see section 4.5.1). Ugd had been predicted to have a role in biofilm formation due to its role in the biosynthesis of teichuronic acid (Pagni, Lazarevic et al. 1999; Mijakovic,

Petranovic et al. 2004). Despite extensive attempts to identify the target of PtkA and PtpZ during biofilm formation, a target was not identified. To identify the target of PtkA, future work will include the identification of proteins phosphorylated in the absence of PtpZ and unphosphorylated in the absence of PtkA using gas chromatography-mass spectrometry (GC-MS) coupled with enrichment for tyrosine phosphorylated proteins. Cells would be cultured under biofilm forming conditions, and if a target of PtkA and PtpZ is identified, then further experiments would be conducted in order to identify the mechanism by which PtkA and PtpZ regulate biofilm formation.

## 6.2 *Potential role for phosphorylation of the terminal tyrosine cluster of PtkA*

Using a site directed mutagenesis approach, work presented in this thesis has tentatively suggested a role for the C-terminal tyrosine cluster of PtkA. It was determined that substitution of the terminal tyrosine residues with the structurally similar amino acid phenylalanine had a significant impact on the biofilm architecture (see Figure 5-2). Conversely, substitution of the terminal tyrosine cluster with either glutamic acid (mimicking a phosphorylated state) (see Figure 5-2) or alanine (see Figure 4-5) did not effect biofilm formation. *In toto*, the results detailed in sections 5.5.2 and 4.2.2 support the hypothesis that the terminal tyrosine cluster acts like a gate, whereby targets of PtkA would be able to enter the active site and become phosphorylated when the terminal tyrosine cluster itself is phosphorylated, as this displaces the C-terminal domain from its position blocking the active site (Lee, Zheng et al. 2008; Olivares-Illana, Meyer et al. 2008). This model is supported by other studies that investigated the role of the

terminal tyrosine cluster of BY-kinases. Firstly, it was demonstrated that a mutant variant of Cap5B2, from *S. aureus*, in which the terminal tyrosine cluster residues were substituted for glutamic acid, was still able to phosphorylate its target CapO (Olivares-Illana, Meyer et al. 2008). This is consistent with the finding that mutation of the C-terminal tyrosine cluster in PtkA to glutamic acid did not affect biofilm formation (Figure 5-2). The authors were also able to demonstrate that a variant of Cap5B2, in which the terminal tyrosine cluster was completely removed, could still phosphorylate CapO (Olivares-Illana, Meyer et al. 2008), indicating that access to the active site of the kinase was still possible. Secondly, it was demonstrated that a mutant variant of the BY-kinase Wzc, from *E. coli*, which lacked the terminal tyrosine cluster domain, was still able to phosphorylate its target Ugd (Grangeasse, Obadia et al. 2003). Once more indicating that the active site of the kinase was accessible. Thus, the data presented here, and the results from other studies, support an 'open/closed gate' hypothesis. This may represent a generalised regulatory mechanism by which endogenous targets of BY-kinases are phosphorylated. This of course remains to be experimentally proven and the assessment of protein stability and X-ray crystal structures of PtkA and the PtkA mutant variants would be highly informative in establishing if this hypothesis is correct.

## 6.3 *Do BY-kinases represent a valid target for the development of antimicrobials?*

It has been suggested that BY-kinases may provide a novel target for antibacterial therapeutic compounds (Cozzone 2009; Grangeasse, Terreux et al. 2009). This is based on a number of reasons: *1)* BY-kinases are structurally different from eukaryote-like kinases and include unique features such as the conserved terminal tyrosine cluster. This

would ensure drug specificity for a prokaryotic target; *2)* BY-kinases regulate a wide range of cellular processes which include the regulation of polysaccharide production and thus are implicated in the regulation of virulence in pathogenic bacteria; *3)* BY-kinases are encoded in a wide range of bacteria including pathogenic isolates suggesting that compounds developed would be effective across different species. However, in my opinon it remains to be established whether BY-kinases actually do represent a valid target for anti-microbial compounds. The proposed mechanism for blocking BY-kinase function centres on disrupting the oligomeric structure which is predicted for BY-kinases from both Gram-positive (Olivares-Illana, Meyer et al. 2008) and Gram-negative species (Lee, Zheng et al. 2008) during the regulation of polysaccharide production. It is thought that fusing an artificial C-terminal tyrosine cluster domain to a compound will target the molecule to the BY-kinase (Cozzone 2009). Once the artificial C-terminal tyrosine cluster is positioned in the active site of the targetted BY-kinase this will inhibit oligomerisation of neighbouring kinases. This would subsequently inhibit their function. It is unclear how stable these compounds will be, since it is possible that the artificial terminal tyrosine clusters fused to the compounds could become phosphorylated. This could conceivably dissociate the artificial terminal tyrosine cluster from the active pocket and render the compound ineffective. Additionally, there is the chance of developing resistance to potential compounds via co-evolution, which would naturally render the antimicrobial compound ineffective. It also needs to be recognised that blocking the active site of BY-kinases may have various impacts depending on the specific kinase. Indeed, substitution of the terminal tyrosine cluster of PtkA with phenylalanines (thus mimicking an unphosphorylated state in which the cluster is thought to sit in the active site) had a significant impact of colony morphology (see Figure 5-2). However, phenylalanine substitution of the terminal

tyrosine cluster of CpsD from *S. pneumonia* did not significantly affect capsular polysaccharide production or virulence (Morona, Miller et al. 2004). Examples like this raise the question of how useful compounds designed to target BY-kinases will be in controlling their function. Therefore it can be concluded that a significant amount of research remains to be conducted before BY-kinases should be proposed as novel anti-bacterial targets.

# 7 References

Aguilar, C., H. Vlamakis, et al. (2010). "KinD is a checkpoint protein linking spore formation to extracellular-matrix production in *Bacillus subtilis* biofilms." mBio **1**(1): e00035-00010.

Amati, G., P. Bisicchia, et al. (2004). "DegU-P represses expression of the motility fla-che operon in Bacillus subtilis." J Bacteriol **186**(18): 6003-6014.

Antelmann, H., H. Tjalsma, et al. (2001). "A proteomic view on genome-based signal peptide predictions." Genome Res **11**(9): 1484-1502.

Arnaud, M., A. Chastanet, et al. (2004). "New vector for efficient allelic replacement in naturally nontransformable, low-GC-content, gram-positive bacteria." Appl Environ Microbiol **70**(11): 6887-6891.

Bai, U., I. Mandic-Mulec, et al. (1993). "SinI modulates the activity of SinR, a developmental switch protein of Bacillus subtilis, by protein-protein interaction." Genes Dev **7**(1): 139-148.

Banse, A. V., A. Chastanet, et al. (2008). "Parallel pathways of repression and antirepression governing the transition to stationary phase in Bacillus subtilis." Proc Natl Acad Sci U S A **105**(40): 15547-15552.

Bender, M. H. and J. Yother (2001). "CpsB is a modulator of capsule-associated tyrosine kinase activity in Streptococcus pneumoniae." J Biol Chem **276**(51): 47966-47974.

Birnboim, H. C. and J. Doly (1979). "A rapid alkaline extraction procedure for screening recombinant plasmid DNA." Nucleic Acids Res **7**(6): 1513-1523.

Blair, K. M., L. Turner, et al. (2008). "A molecular clutch disables flagella in the Bacillus subtilis biofilm." Science **320**(5883): 1636-1638.

Branda, S. S., F. Chu, et al. (2006). "A major protein component of the Bacillus subtilis biofilm matrix." Mol Microbiol **59**(4): 1229-1238.

Branda, S. S., J. E. Gonzalez-Pastor, et al. (2001). "Fruiting body formation by Bacillus subtilis." Proc Natl Acad Sci U S A **98**(20): 11621-11626.

Branda, S. S., J. E. Gonzalez-Pastor, et al. (2004). "Genes involved in formation of structured multicellular communities by Bacillus subtilis." J Bacteriol **186**(12): 3970-3979.

Britton, R. A., P. Eichenberger, et al. (2002). "Genome-wide analysis of the stationary-phase sigma factor (Sigma-H) regulon of *Bacillus subtilis*." Journal of Bacteriology **184**(17): 4881-4890.

Burkholder, P. R. and N. H. Giles (1947). "Induced biochemical mutations in *Bacillus subtilis*." Amer. J. Bot. **34**: 345.

Chai, Y., F. Chu, et al. (2008). "Bistability and biofilm formation in Bacillus subtilis." Mol Microbiol **67**(2): 254-263.

Chai, Y., T. Norman, et al. (2010). "An epigenetic switch governing daughter cell separation in Bacillus subtilis." Genes Dev **24**(8).

Chu, F., D. B. Kearns, et al. (2006). "Targets of the master regulator of biofilm formation in Bacillus subtilis." Mol Microbiol **59**(4): 1216-1228.

Chu, F., D. B. Kearns, et al. (2008). "A novel regulatory protein governing biofilm formation in Bacillus subtilis." Mol Microbiol **68**(5): 1117-1127.

Chu, F., D. B. Kearns, et al. (2008). "A novel regulatory protein governing biofilm formation in Bacillus subtilis." Mol Microbiol.

Costerton, J. W., Z. Lewandowski, et al. (1995). "Microbial biofilms." Annu Rev Microbiol **49**: 711-745.

Cozzone, A. J. (2009). "Bacterial tyrosine kinases: novel targets for antibacterial therapy?" Trends Microbiol **17**(12): 536-543.

Cozzone, A. J., C. Grangeasse, et al. (2004). "Protein phosphorylation on tyrosine in bacteria." Arch Microbiol **181**(3): 171-181.

Dahl, M. K., T. Msadek, et al. (1991). "Mutational analysis of the Bacillus subtilis DegU regulator and its phosphorylation by the DegS protein kinase." J Bacteriol **173**(8): 2539-2547.

Dams-Kozlowska, H. and D. L. Kaplan (2007). "Protein engineering of wzc to generate new emulsan analogs." Appl Environ Microbiol **73**(12): 4020-4028.

Dartois, V., M. Debarbouille, et al. (1998). "Characterization of a novel member of the DegS-DegU regulon affected by salt stress in *Bacillus subtilis*." J Bacteriol **180**(7): 1855-1861.

Dervyn, E., M. F. Noirot-Gros, et al. (2004). "The bacterial condensin/cohesin-like protein complex acts in DNA repair and regulation of gene expression." Mol Microbiol **51**(6): 1629-1640.

Deutscher, J. and M. H. Saier, Jr. (2005). "Ser/Thr/Tyr protein phosphorylation in bacteria - for long time neglected, now well established." J Mol Microbiol Biotechnol **9**(3-4): 125-131.

Drobniewski, F. A. (1993). "Bacillus cereus and related species." Clin Microbiol Rev **6**(4): 324-338.

Dubrac, S. and T. Msadek (2004). "Identification of genes controlled by the essential YycG/YycF two-component system of Staphylococcus aureus." J Bacteriol **186**(4): 1175-1181.

Duclos, B., C. Grangeasse, et al. (1996). "Autophosphorylation of a bacterial protein at tyrosine." J Mol Biol **259**(5): 891-895.

Earl, A. M., R. Losick, et al. (2007). "Bacillus subtilis genome diversity." J Bacteriol **189**(3): 1163-1170.

Emmert, E. A. and J. Handelsman (1999). "Biocontrol of plant disease: a (gram-) positive perspective." FEMS Microbiol Lett **171**(1): 1-9.

Eymann, C., D. Becher, et al. (2007). "Dynamics of protein phosphorylation on Ser/Thr/Tyr in Bacillus subtilis." Proteomics **7**(19): 3509-3526.

Farber, J. M. and P. I. Peterkin (1991). "Listeria monocytogenes, a food-borne pathogen." Microbiol Rev **55**(3): 476-511.

Fawcett, P., P. Eichenberger, et al. (2000). "The transcriptional profile of early to middle sporulation in *Bacillus subtilis*." Proceedings National Academy Sciences USA **97**(14): 8063-8068.

Ferrari, E., D. J. Henner, et al. (1988). "Transcription of *Bacillus subtilis* subtilisin and expression of subtilisin in sporulation mutants." Journal of Bacteriology **170**(1): 289-295.

Flemming, H. C. and J. Wingender (2010). "The biofilm matrix." Nat Rev Microbiol **8**(9): 623-633.

Fraser, G. M. and C. Hughes (1999). "Swarming motility." Curr Opin Microbiol **2**(6): 630-635.

Fujita, M., J. E. Gonzalez-Pastor, et al. (2005). "High- and low-threshold genes in the Spo0A regulon of Bacillus subtilis." J Bacteriol **187**(4): 1357-1368.

Gaur, N. K., K. Cabane, et al. (1988). "Structure and expression of the Bacillus subtilis sin operon." J Bacteriol **170**(3): 1046-1053.

Gaur, N. K., E. Dubnau, et al. (1986). "Characterization of a cloned Bacillus subtilis gene that inhibits sporulation in multiple copies." J Bacteriol **168**(2): 860-869.

Grangeasse, C., A. J. Cozzone, et al. (2007). "Tyrosine phosphorylation: an emerging regulatory device of bacterial physiology." Trends Biochem Sci **32**(2): 86-94.

Grangeasse, C., P. Doublet, et al. (2002). "Tyrosine phosphorylation of protein kinase Wzc from Escherichia coli K12 occurs through a two-step process." J Biol Chem **277**(9): 7127-7135.

Grangeasse, C., B. Obadia, et al. (2003). "Autophosphorylation of the Escherichia coli protein kinase Wzc regulates tyrosine phosphorylation of Ugd, a UDP-glucose dehydrogenase." J Biol Chem **278**(41): 39323-39329.

Grangeasse, C., R. Terreux, et al. (2009). "Bacterial tyrosine-kinases: structure-function analysis and therapeutic potential." Biochim Biophys Acta **1804**(3): 628-634.

Greene, E. A. and G. B. Spiegelman (1996). "The Spo0A protein of Bacillus subtilis inhibits transcription of the abrB gene without preventing binding of the polymerase to the promoter." J Biol Chem **271**(19): 11455-11461.

Gueriri, I., S. Bay, et al. (2008). "The Pta-AckA pathway controlling acetyl phosphate levels and the phosphorylation state of the DegU orphan response regulator both play a role in regulating *Listeria monocytogenes* motility and chemotaxis." Molecular Microbiology **70**(6).

Gupta, R., Q. K. Beg, et al. (2002). "Bacterial alkaline proteases: molecular approaches and industrial applications." Appl Microbiol Biotechnol **59**(1): 15-32.

Guttenplan, S. B., K. M. Blair, et al. (2010). "The EpsE flagellar clutch is bifunctional and synergizes with EPS biosynthesis to promote Bacillus subtilis biofilm formation." PLoS Genet **6**(12): e1001243.

Hamoen, L. W., A. F. Van Werkhoven, et al. (2000). "The pleiotropic response regulator DegU functions as a priming protein in competence development in Bacillus subtilis." Proc Natl Acad Sci U S A **97**(16): 9246-9251.

Hamon, M. A. and B. A. Lazazzera (2001). "The sporulation transcription factor Spo0A is required for biofilm development in Bacillus subtilis." Mol Microbiol **42**(5): 1199-1209.

Hamon, M. A., N. R. Stanley, et al. (2004). "Identification of AbrB-regulated genes involved in biofilm formation by Bacillus subtilis." Mol Microbiol **52**(3): 847-860.

Hanks, S. K., A. M. Quinn, et al. (1988). "The protein kinase family: conserved features and deduced phylogeny of the catalytic domains." Science **241**(4861): 42-52.

Harwood, C. R. and S. M. Cutting (1990). "Molecular biological methods for *Bacillus*. John Wiley &Sons Ltd. Chichester, England."

Hederstedt, L. and L. Rutberg (1980). "Biosynthesis and membrane binding of succinate dehydrogenase in Bacillus subtilis." J Bacteriol **144**(3): 941-951.

Hoch, J. A. (2000). "Two-component and phosphorelay signal transduction." Curr Opin Microbiol **3**(2): 165-170.

Hoch, J. A. and C. Anagnostopoulos (1970). "Chromosomal location and properties of radiation sensitivity mutations in Bacillus subtilis." J Bacteriol **103**(2): 295-301.

Hoiby, N., T. Bjarnsholt, et al. (2010). "Antibiotic resistance of bacterial biofilms." Int J Antimicrob Agents **35**(4): 322-332.

Hovens, C. M., S. A. Stacker, et al. (1992). "RYK, a receptor tyrosine kinase-related molecule with unusual kinase domain motifs." Proc Natl Acad Sci U S A **89**(24): 11818-11822.

Hung, R. J., H. S. Chien, et al. (2007). "Comparative analysis of two UDP-glucose dehydrogenases in Pseudomonas aeruginosa PAO1." J Biol Chem **282**(24): 17738-17748.

Irnov, I. and W. C. Winkler (2010). "A regulatory RNA required for antitermination of biofilm and capsular polysaccharide operons in Bacillales." Mol Microbiol **76**(3): 559-575.

Iwanicki, A., A. Herman-Antosiewicz, et al. (2002). "PrpE, a PPP protein phosphatase from Bacillus subtilis with unusual substrate specificity." Biochem J **366**(Pt 3): 929-936.

Jers, C., M. M. Pedersen, et al. (2010). "Bacillus subtilis BY-kinase PtkA controls enzyme activity and localization of its protein substrates." Mol Microbiol **77**(2): 287-299.

Kearns, D. B. (2010). "A field guide to bacterial swarming motility." Nat Rev Microbiol **8**(9): 634-644.

Kearns, D. B., F. Chu, et al. (2005). "A master regulator for biofilm formation by *Bacillus subtilis*." Mol Microbiol **55**(3): 739-749.

Kearns, D. B., F. Chu, et al. (2004). "Genes governing swarming in Bacillus subtilis and evidence for a phase variation mechanism controlling surface motility." Mol Microbiol **52**(2): 357-369.

Kearns, D. B. and R. Losick (2003). "Swarming motility in undomesticated Bacillus subtilis." Mol Microbiol **49**(3): 581-590.

Kearns, D. B. and R. Losick (2005). "Cell population heterogeneity during growth of Bacillus subtilis." Genes Dev **19**(24): 3083-3094.

Kiley, T. B. and N. R. Stanley-Wall (2010). "Post-translational control of Bacillus subtilis biofilm formation mediated by tyrosine phosphorylation." Mol Microbiol **78**(4): 947-963.

Kobayashi, K. (2007). "Bacillus subtilis pellicle formation proceeds through genetically defined morphological changes." J Bacteriol **189**(13): 4920-4931.

Kobayashi, K. (2007). "Gradual activation of the response regulator DegU controls serial expression of genes for flagellum formation and biofilm formation in Bacillus subtilis." Mol Microbiol **66**(2): 395-409.

Kobayashi, K. (2008). "SlrR/SlrA controls the initiation of biofilm formation in Bacillus subtilis." Mol Microbiol **69**(6): 1399-1410.

Kobayashi, K., S. D. Ehrlich, et al. (2003). "Essential Bacillus subtilis genes." Proc Natl Acad Sci U S A **100**(8): 4678-4683.

Kodgire, P., M. Dixit, et al. (2006). "ScoC and SinR negatively regulate epr by corepression in Bacillus subtilis." J Bacteriol **188**(17): 6425-6428.

Kolodkin-Gal, I., D. Romero, et al. (2010). "D-amino acids trigger biofilm disassembly." Science **328**(5978): 627-629.

Kunst, F., N. Ogasawara, et al. (1997). "The complete genome sequence of the gram-positive bacterium Bacillus subtilis." Nature **390**(6657): 249-256.

Lacour, S., E. Bechet, et al. (2008). "Tyrosine phosphorylation of the UDP-glucose dehydrogenase of Escherichia coli is at the crossroads of colanic acid synthesis and polymyxin resistance." PLoS One **3**(8): e3053.

Lee, D. C. and Z. Jia (2009). "Emerging structural insights into bacterial tyrosine kinases." Trends Biochem Sci **34**(7): 351-357.

Lee, D. C., J. Zheng, et al. (2008). "Structure of Escherichia coli tyrosine kinase Etk reveals a novel activation mechanism." Embo J **27**(12): 1758-1766.

Levine, A., F. Vannier, et al. (2006). "Analysis of the dynamic Bacillus subtilis Ser/Thr/Tyr phosphoproteome implicated in a wide variety of cellular processes." Proteomics **6**(7): 2157-2173.

Lopez, D., M. A. Fischbach, et al. (2009). "Structurally diverse natural products that cause potassium leakage trigger multicellularity in Bacillus subtilis." Proc Natl Acad Sci U S A **106**(1): 280-285.

Lopez, D., H. Vlamakis, et al. (2010). "Biofilms." Cold Spring Harb Perspect Biol **2**(7): a000398.

Macek, B., I. Mijakovic, et al. (2007). "The serine/threonine/tyrosine phosphoproteome of the model bacterium Bacillus subtilis." Mol Cell Proteomics **6**(4): 697-707.

Manai, M. and A. J. Cozzone (1979). "Analysis of the protein-kinase activity of Escherichia coli cells." Biochem Biophys Res Commun **91**(3): 819-826.

Mascher, T., N. G. Margulis, et al. (2003). "Cell wall stress responses in Bacillus subtilis: the regulatory network of the bacitracin stimulon." Mol Microbiol **50**(5): 1591-1604.

McLoon, A. L., I. Kolodkin-Gal, et al. (2010). "Spatial Regulation of Histidine Kinases Governing Biofilm Formation in Bacillus subtilis." J Bacteriol.

Mijakovic, I., L. Musumeci, et al. (2005). "In vitro characterization of the Bacillus subtilis protein tyrosine phosphatase YwqE." J Bacteriol **187**(10): 3384-3390.

Mijakovic, I., D. Petranovic, et al. (2005). "Protein-tyrosine phosphorylation in Bacillus subtilis." J Mol Microbiol Biotechnol **9**(3-4): 189-197.

Mijakovic, I., D. Petranovic, et al. (2004). "How tyrosine phosphorylation affects the UDP-glucose dehydrogenase activity of Bacillus subtilis YwqF." J Mol Microbiol Biotechnol **8**(1): 19-25.

Mijakovic, I., D. Petranovic, et al. (2006). "Bacterial single-stranded DNA-binding proteins are phosphorylated on tyrosine." Nucleic Acids Res **34**(5): 1588-1596.

Mijakovic, I., S. Poncet, et al. (2003). "Transmembrane modulator-dependent bacterial tyrosine kinase activates UDP-glucose dehydrogenases." Embo J **22**(18): 4709-4718.

Mirel, D. B. and M. J. Chamberlin (1989). "The Bacillus subtilis flagellin gene (hag) is transcribed by the sigma 28 form of RNA polymerase." J Bacteriol **171**(6): 3095-3101.

Mirel, D. B., P. Lauer, et al. (1994). "Identification of flagellar synthesis regulatory and structural genes in a sigma D-dependent operon of Bacillus subtilis." J Bacteriol **176**(15): 4492-4500.

Molle, V., M. Fujita, et al. (2003). "The Spo0A regulon of Bacillus subtilis." Mol Microbiol **50**(5): 1683-1701.

Moran, C. P., Jr., W. C. Johnson, et al. (1982). "Close contacts between sigma 37-RNA polymerase and a Bacillus subtilis chromosomal promoter." J Mol Biol **162**(3): 709-713.

Morikawa, M. (2006). "Beneficial biofilm formation by industrial bacteria Bacillus subtilis and related species." J Biosci Bioeng **101**(1): 1-8.

Morona, J. K., D. C. Miller, et al. (2004). "The effect that mutations in the conserved capsular polysaccharide biosynthesis genes cpsA, cpsB, and cpsD have on virulence of Streptococcus pneumoniae." J Infect Dis **189**(10): 1905-1913.

Morona, J. K., R. Morona, et al. (2002). "Streptococcus pneumoniae capsule biosynthesis protein CpsB is a novel manganese-dependent phosphotyrosine-protein phosphatase." J Bacteriol **184**(2): 577-583.

Morona, J. K., R. Morona, et al. (2003). "Mutational analysis of the carboxy-terminal (YGX)4 repeat domain of CpsD, an autophosphorylating tyrosine kinase required for capsule biosynthesis in Streptococcus pneumoniae." J Bacteriol **185**(10): 3009-3019.

Morona, J. K., J. C. Paton, et al. (2000). "Tyrosine phosphorylation of CpsD negatively regulates capsular polysaccharide biosynthesis in streptococcus pneumoniae." Mol Microbiol **35**(6): 1431-1442.

Msadek, T., F. Kunst, et al. (1990). "Signal transduction pathway controlling synthesis of a class of degradative enzymes in Bacillus subtilis: expression of the regulatory genes and analysis of mutations in degS and degU." J Bacteriol **172**(2): 824-834.

Mukai, K., M. Kawata-Mukai, et al. (1992). "Stabilization of phosphorylated Bacillus subtilis DegU by DegR." J Bacteriol **174**(24): 7954-7962.

Mukai, K., M. Kawata, et al. (1990). "Isolation and phosphorylation of the Bacillus subtilis degS and degU gene products." J Biol Chem **265**(32): 20000-20006.

Murray, E. J., M. A. Strauch, et al. (2009). "σX is involved in controlling Bacillus subtilis biofilm architecture through the AbrB homologue Abh." J Bacteriol **191**(22): 6822-6832.

Musumeci, L., C. Bongiorni, et al. (2005). "Low-molecular-weight protein tyrosine phosphatases of Bacillus subtilis." J Bacteriol **187**(14): 4945-4956.

Nagorska, K., K. Hinc, et al. (2008). "Influence of the {sigma}B Stress Factor and yxaB, the Gene for a Putative Exopolysaccharide Synthase under {sigma}B Control, on Biofilm Formation." J Bacteriol **190**(10): 3546-3556.

Nagorska, K., A. Ostrowski, et al. (2010). "Importance of eps genes from Bacillus subtilis in biofilm formation and swarming." J Appl Genet **51**(3): 369-381.

Nakano, M. M., N. Corbell, et al. (1992). "Isolation and characterization of sfp: a gene that functions in the production of the lipopeptide biosurfactant, surfactin, in Bacillus subtilis." Mol Gen Genet **232**(2): 313-321.

Nakar, D. and D. L. Gutnick (2003). "Involvement of a protein tyrosine kinase in production of the polymeric bioemulsifier emulsan from the oil-degrading strain Acinetobacter lwoffii RAG-1." J Bacteriol **185**(3): 1001-1009.

Nishito, Y., Y. Osana, et al. (2010). "Whole genome assembly of a natto production strain Bacillus subtilis natto from very short read data." BMC Genomics **11**: 243.

O'Reilly, M. and K. M. Devine (1997). "Expression of AbrB, a transition state regulator from Bacillus subtilis, is growth phase dependent in a manner resembling that of Fis, the nucleoid binding protein from Escherichia coli." J Bacteriol **179**(2): 522-529.

Obadia, B., S. Lacour, et al. (2007). "Influence of tyrosine-kinase Wzc activity on colanic acid production in Escherichia coli K12 cells." J Mol Biol **367**(1): 42-53.

Ogura, M., K. Shimane, et al. (2003). "Binding of response regulator DegU to the aprE promoter is inhibited by RapG, which is counteracted by extracellular PhrG in Bacillus subtilis." Mol Microbiol **49**(6): 1685-1697.

Ogura, M., H. Yamaguchi, et al. (2001). "DNA microarray analysis of Bacillus subtilis DegU, ComA and PhoP regulons: an approach to comprehensive analysis of B.subtilis two-component regulatory systems." Nucleic Acids Res **29**(18): 3804-3813.

Ohlsen, K. L., J. K. Grimsley, et al. (1994). "Deactivation of the sporulation transcription factor Spo0A by the Spo0E protein phosphatase." Proc Natl Acad Sci U S A **91**(5): 1756-1760.

Olivares-Illana, V., P. Meyer, et al. (2008). "Structural basis for the regulation mechanism of the tyrosine kinase CapB from Staphylococcus aureus." PLoS Biol **6**(6): e143.

Pagni, M., V. Lazarevic, et al. (1999). "Assay for UDPglucose 6-dehydrogenase in phosphate-starved cells: gene tuaD of Bacillus subtilis 168 encodes the UDPglucose 6-dehydrogenase involved in teichuronic acid synthesis." Microbiology **145 ( Pt 5)**: 1049-1053.

Pallen, M. J., C. W. Penn, et al. (2005). "Bacterial flagellar diversity in the post-genomic era." Trends Microbiol **13**(4): 143-149.

Patrick, J. E. and D. B. Kearns (2009). "Laboratory strains of Bacillus subtilis do not exhibit swarming motility." J Bacteriol **191**(22): 7129-7133.

Perego, M., G. B. Spiegelman, et al. (1988). "Structure of the gene for the transition state regulator, *abrB*:regulator synthesis is controlled by the *spo0A* sporulation gene in *Bacillus subtilis*." Molecular Microbiology **2**: 689-699.

Petranovic, D., C. Grangeasse, et al. (2009). "Activation of Bacillus subtilis Ugd by the BY-kinase PtkA proceeds via phosphorylation of its residue tyrosine 70." J Mol Microbiol Biotechnol **17**(2): 83-89.

Petranovic, D., O. Michelsen, et al. (2007). "Bacillus subtilis strain deficient for the protein-tyrosine kinase PtkA exhibits impaired DNA replication." Mol Microbiol **63**(6): 1797-1805.

Phillips, Z. E. and M. A. Strauch (2002). "Bacillus subtilis sporulation and stationary phase gene expression." Cell Mol Life Sci **59**(3): 392-402.

Romero, D., C. Aguilar, et al. (2010). "Amyloid fibers provide structural integrity to Bacillus subtilis biofilms." Proc Natl Acad Sci U S A **107**(5): 2230-2234.

Sanchez, A. and J. Olmos (2004). "Bacillus subtilis transcriptional regulators interaction." Biotechnol Lett **26**(5): 403-407.

Shafikhani, S. H., I. Mandic-Mulec, et al. (2002). "Postexponential regulation of sin operon expression in Bacillus subtilis." J Bacteriol **184**(2): 564-571.

Shapiro, J. A. (1998). "Thinking about bacterial populations as multicellular organisms." Annu Rev Microbiol **52**: 81-104.

Shemesh, M., R. Kolter, et al. (2010). "The biocide chlorine dioxide stimulates biofilm formation in Bacillus subtilis by activation of the histidine kinase KinC." J Bacteriol **192**(24): 6352-6356.

Shi, L. (2004). "Manganese-dependent protein O-phosphatases in prokaryotes and their biological functions." Front Biosci **9**: 1382-1397.

Shimane, K. and M. Ogura (2004). "Mutational analysis of the helix-turn-helix region of Bacillus subtilis response regulator DegU, and identification of cis-acting sequences for DegU in the aprE and comK promoters." J Biochem (Tokyo) **136**(3): 387-397.

Smith, T. J., S. A. Blackman, et al. (2000). "Autolysins of Bacillus subtilis: multiple enzymes with multiple functions." Microbiology **146 ( Pt 2)**: 249-262.

Soldo, B., V. Lazarevic, et al. (1999). "Teichuronic acid operon of Bacillus subtilis 168." Mol Microbiol **31**(3): 795-805.

Sonenshein, A. L. (2000). "Control of sporulation initiation in *Bacillus subtilis*." Curr Opin Microbiol **3**(6): 561-566.

Soulat, D., C. Grangeasse, et al. (2007). "UDP-acetyl-mannosamine dehydrogenase is an endogenous protein substrate of Staphylococcus aureus protein-tyrosine kinase activity." J Mol Microbiol Biotechnol **13**(1-3): 45-54.

Soulat, D., J. M. Jault, et al. (2006). "Staphylococcus aureus operates protein-tyrosine phosphorylation through a specific mechanism." J Biol Chem **281**(20): 14048-14056.

Spencer, R. C. (2003). "Bacillus anthracis." J Clin Pathol **56**(3): 182-187.

Spizizen, J. (1958). "Transformation of Biochemically Deficient Strains of Bacillus Subtilis by Deoxyribonucleate." Proc Natl Acad Sci U S A **44**(10): 1072-1078.

Srivatsan, A., Y. Han, et al. (2008). "High-precision, whole-genome sequencing of laboratory strains facilitates genetic studies." PLoS Genet **4**(8): e1000139.

Stanley, N. R., R. A. Britton, et al. (2003). "Identification of catabolite repression as a physiological regulator of biofilm formation by *Bacillus subtilis* by use of DNA microarrays." J Bacteriol **185**(6): 1951-1957.

Stanley, N. R. and B. A. Lazazzera (2005). "Defining the genetic differences between wild and domestic strains of Bacillus subtilis that affect poly-gamma-dl-glutamic acid production and biofilm formation." Mol Microbiol **57**(4): 1143-1158.

Steinmetz, M., F. Kunst, et al. (1976). "Mapping of mutations affecting synthesis of exocellular enzymes in Bacillus subtilis. Identity of the sacUh, amyB and pap mutations." Mol Gen Genet **148**(3): 281-285.

Stover, A. G. and A. Driks (1999). "Regulation of synthesis of the Bacillus subtilis transition-phase, spore-associated antibacterial protein TasA." J Bacteriol **181**(17): 5476-5481.

Stover, A. G. and A. Driks (1999). "Secretion. localization and antibacterial activity of tasA, a *Bacillus subtilis* spore-associated protein." J. bacteriol. **181**: 1664-1672.

Strauch, M. A., G. B. Spiegelman, et al. (1989). "The transition state transcription regulator abrB of Bacillus subtilis is a DNA binding protein." Embo J **8**(5): 1615-1621.

Sutherland, I. W. (2001). "The biofilm matrix--an immobilized but dynamic microbial environment." Trends Microbiol **9**(5): 222-227.

Tanaka, T., M. Kawata, et al. (1991). "Altered phosphorylation of Bacillus subtilis DegU caused by single amino acid changes in DegS." J Bacteriol **173**(17): 5507-5515.

Tjalsma, H., A. Bolhuis, et al. (1998). "Functional analysis of the secretory precursor processing machinery of Bacillus subtilis: identification of a eubacterial homolog of archaeal and eukaryotic signal peptidases." Genes Dev **12**(15): 2318-2331.

Tjalsma, H., V. P. Kontinen, et al. (1999). "The role of lipoprotein processing by signal peptidase II in the Gram-positive eubacterium bacillus subtilis. Signal peptidase II is required for the efficient secretion of alpha-amylase, a non-lipoprotein." J Biol Chem **274**(3): 1698-1707.

Tsukahara, K. and M. Ogura (2007). "Characterization of DegU-dependent expression of *bpr* in *Bacillus subtilis*." FEMS Microbiol Lett: 1-6.

Tsukahara, K. and M. Ogura (2008). "Promoter selectivity of the Bacillus subtilis response regulator DegU, a positive regulator of the fla/che operon and sacB." BMC Microbiol **8**: 8.

Veening, J. W., O. A. Igoshin, et al. (2008). "Transient heterogeneity in extracellular protease production by Bacillus subtilis." Mol Syst Biol **4**: 184.

Veening, J. W., W. K. Smits, et al. (2008). "Bistability, Epigenetics, and Bet-Hedging in Bacteria." Annu Rev Microbiol **62**: 193-210.

Verhamme, D. T., T. B. Kiley, et al. (2007). "DegU co-ordinates multicellular behaviour exhibited by Bacillus subtilis." Mol Microbiol **65**(2): 554-568.

Verhamme, D. T., E. J. Murray, et al. (2009). "DegU and Spo0A jointly control transcription of two loci required for complex colony development by Bacillus subtilis." J Bacteriol **191**(1): 100-108.

Vincent, C., B. Duclos, et al. (2000). "Relationship between exopolysaccharide production and protein-tyrosine phosphorylation in gram-negative bacteria." J Mol Biol **304**(3): 311-321.

Vlamakis, H., C. Aguilar, et al. (2008). "Control of cell fate by the formation of an architecturally complex bacterial community." Genes Dev **22**(7): 945-953.

Walker, J. E., M. Saraste, et al. (1982). "Distantly related sequences in the alpha- and beta-subunits of ATP synthase, myosin, kinases and other ATP-requiring enzymes and a common nucleotide binding fold." Embo J **1**(8): 945-951.

Wang, J. Y. and D. E. Koshland, Jr. (1978). "Evidence for protein kinase activities in the prokaryote Salmonella typhimurium." J Biol Chem **253**(21): 7605-7608.

Wu, J., N. Ohta, et al. (1999). "A novel bacterial tyrosine kinase essential for cell division and differentiation." Proc Natl Acad Sci U S A **96**(23): 13068-13073.

Wugeditsch, T., A. Paiment, et al. (2001). "Phosphorylation of Wzc, a tyrosine autokinase, is essential for assembly of group 1 capsular polysaccharides in Escherichia coli." J Biol Chem **276**(4): 2361-2371.

Yasbin, R. E. and F. E. Young (1974). "Transduction in Bacillus subtilis by bacteriophage SPP1." J Virol **14**(6): 1343-1348.

Yasumura, A., S. Abe, et al. (2008). "Involvement of nitrogen regulation in Bacillus subtilis degU expression." J Bacteriol **190**(15): 5162-5171.

Zeigler, D. R., Z. Pragai, et al. (2008). "The origins of 168, W23, and other Bacillus subtilis legacy strains." J Bacteriol.

# 8 Appendices

## 8.1 *Appendix A: Buffers and Solutions*

| *General buffers* | Composition |
|---|---|
| *B. subtilis* transformation buffer | 1X T-Base<br>2 mM EGTA |
| 10x PBS | 1.37 M NaCl<br>26.8 mM KCl<br>104.36 mM $NaHPO_4$<br>17.64 mM $KH_2PO_4$ |
| SDS running buffer | 25 mM Tris-HCl (pH 8.3)<br>192 mM Glycine<br>0.1 % (w/v) SDS |
| 10X T-Base | 150 mM $(NH4)_2SO_4$<br>800 mM $K_2HPO_4$<br>440 mM $KH_2PO_4$<br>34 mM Sodium citrate |
| 50X TAE | 2 M Tris-acetate<br>50 mM EDTA (pH 8.0) |
| 10X TBE | 0.9 M Tris-borate<br>0.02 M EDTA (pH 8.0) |
| 20X TBS | 400 mM Tris-HCl (pH 8.0)<br>3 M NaCl |
| TBST (also Western wash buffer) | 1X TBS<br>0.05 % (v/v) Tween 20 |
| 5X Tris-glycine | 250 mM Tris<br>2 M glycine<br>8.75 mM EDTA (pH 8.0) |
| Wash buffer | 1X T-Base<br>1 mM $Mg_2SO_4$ |

| | |
|---|---|
| Western Blocking buffer | 1X TBST<br>5 % (w/v) skimmed milk powder |
| Western Transfer buffer | 25 mM Tris-HCl<br>192 mM Glycine<br>0.2 % (v/v) Tween 20<br>20 % (v/v) Methanol |

*gDNA extraction*

| | |
|---|---|
| Lysis buffer | 0.1 M NaCl<br>0.05 M EDTA (pH 7.5) |

*Protein purification*

| | |
|---|---|
| DegS cell pellet wash buffer | 10 mM Tris-HCl (pH 7.6) |
| DegS Denaturing buffer | 50 mM Tris-HCl (pH 7.6)<br>150 mM NaCl<br>8M Urea<br>10 mM Imidazole |
| DegS Renaturing buffer | 50 mM Tris-HCl (pH 7.6)<br>150 mM NaCl<br>10 mM Imidazole |
| DegS Elution buffer | 50 mM Tris-HCl (pH 7.6)<br>150 mM NaCl<br>500 mM Imidazole |
| DegS Dialysis buffer | 50 mM Tris-HCl (pH 7.6)<br>200 mM KCl<br>10 mM $MgCl_2$<br>0.1 mM EDTA<br>1 mM DTT<br>50% (v/v) Glycerol |
| DegU cell pellet wash buffer | 20 mM Tris-HCl (pH 8.0)<br>200 mM NaCl |
| DegU Cell lysis buffer | 20 mM Tris-HCl (pH 8.0) |

| | |
|---|---|
| | 200 mM NaCl<br>10 mM Imidazole<br>2 mM Benzamidine<br>1.0 % (v/v) Triton X-100<br>1 Roche protease inhibitor EDTA-free tablet / 7ml buffer |
| DegU HisTrap column wash buffer | 20 mM Tris-HCl (pH 8.0)<br>200 mM NaCl<br>30 mM Imidazole |
| DegU Elution buffer | 20 mM Tris-HCl (pH 8.0)<br>200 mM NaCl<br>500 mM Imidazole |
| DegU DEAE binding buffer | 20 mM Tris-HCl (pH 7.6)<br>1 mM EDTA<br>0.5 mM DTT |
| DegU DEAE elution buffer | 20 mM Tris-HCl (pH 7.6)<br>1 mM EDTA<br>0.5 mM DTT<br>1 M NaCl |
| DegU Dialysis buffer | 20 mM Tris-HCl (pH 8.0)<br>50 mM NaCl |
| Novagen Thrombin Cleavage buffer | 20 mM Tris (pH 8.4)<br>150 mM NaCl<br>2.5 mM $CaCl_2$<br>5 % (v/v) Glycerol<br>2 μl $ml^{-1}$ Biotinylated Thrombin |
| SinR cell lysis buffer | Novagen BugBuster Master Mix<br>10 mM Imidazole |
| SinR cell pellet wash buffer | 20 mM Tris-HCl (pH 8.0)<br>200 mM NaCl |
| SinR Dialysis buffer | 10 mM Tris-HCl (pH 8.0)<br>10 mM $MgCl_2$<br>1 mM EDTA<br>0.3 mM DTT |

| | |
|---|---|
| | 1 mM PMSF |
| SinR Elution buffer | 50 mM Tris-HCl (pH 8.0)<br>500 mM NaCl<br>250 mM Imidazole |
| SinR HisTrap column wash buffer | 50 mM Tris-HCl (pH 8.0)<br>500 mM NaCl<br>20 mM Imidazole |

*EMSA*

| | |
|---|---|
| 5X DegU phosphorylation buffer | 500 mM Tris-HCl (pH 7.6)<br>0.5 mM EDTA<br>20 mM $MgCl_2$<br>2.5 mM DTT<br>17.5% (v/v) Glycerol |
| 10X $DegU^{\sim P}$ EMSA reaction buffer | 150 mM Tris-HCl (pH 7.6)<br>2 % (v/v) Tween 20<br>10 mM $MgCl_2$<br>600 mM NaCl<br>5 mM DTT |
| 5X SinR EMSA reaction buffer | 50 mM Tris-HCl (pH 7.6)<br>5 mM $MgCl_2$<br>250 mM NaCl<br>25 % (v/v) Glycerol<br>5 mM EDTA<br>5 mM DTT<br>250 ng $\mu l^{-1}$ BSA<br>250 ng $\mu l^{-1}$ Poly (dI-dC) |

*Dyes*

| | |
|---|---|
| 6X DNA loading dye for EMSA | 0.025 % (w/v) Xylene cyanol<br>0.025 % (w/v) Bromophenol Blue<br>30 % (v/v) Glycerol |
| 2X SDS loading dye | 375 mM Tris-HCl (pH 8.8)<br>20% β-mercaptoethanol |

| | |
|---|---|
| | 4 % (w/v) SDS<br>0.2 % (w/v) Bromophenol Blue<br>20 % (v/v) Glycerol |

*Solutions*

| | |
|---|---|
| Coomassie destain | 50 % (v/v) Methanol<br>10 % (v/v) Acetic Acid |
| Coomassie stain | 50 % (v/v) Ethanol<br>7.5 % (v/v) Acetic Acid<br>0.1 % (w/v) Coomassie Brilliant Blue |
| ECL solution 1 | 100 mM Tris-HCl (pH 8.5)<br>2.5 mM Luminol<br>0.4 mM p-Coumaric Acid |
| ECL solution 2 | 100 mM Tris-HCl (pH 8.5)<br>0.0192 % (v/v) $H_2O_2$ |
| Luminol solution | 250 mM made in DMSO |
| p-Coumaric Acid | 40 mM made in DMSO |

## 8.2 *Appendix B: Papers published from this work*

Molecular Microbiology (2007) doi:10.1111/j.1365-2958.2007.05810.x

# DegU co-ordinates multicellular behaviour exhibited by *Bacillus subtilis*

**Daniël T. Verhamme, Taryn B. Kiley and Nicola R. Stanley-Wall***
*Division of Environmental and Applied Biology, College of Life Sciences, MSI/WTB/JBC Complex, University of Dundee, Dundee DD1 4EH, UK.*

### Summary

**Unicellular organisms use a variety of mechanisms to co-ordinate activity within a community and accomplish complex multicellular processes. Because some of the processes that are exhibited by one species can be physiologically incompatible, it raises the question of how entry into these different pathways is regulated. In the Gram-positive bacterium *Bacillus subtilis*, genetic competence, swarming motility, biofilm formation, complex colony architecture and protease production are all regulated by the response regulator DegU. DegU appears to integrate environmental signals and co-ordinate multicellular behaviours that are subsequently manifested at different levels of DegU phosphorylation. Data are presented which indicate that: (i) swarming motility is activated by very low levels of DegU~P that can be generated independently from its cognate sensor kinase DegS; (ii) complex colony architecture is activated by low levels of DegU~P that are produced in a DegS-dependent manner to activate transcription of *yvcA*, a novel gene required for complex colony architecture; and (iii) high levels of DegU~P inhibit complex colony architecture and swarming motility but are required prior to the activation of exoprotease production. A model is proposed to explain why such a system may have evolved within *B. subtilis* to control these multicellular processes through a single regulator.**

### Introduction

Unicellular organisms, such as bacteria, use a variety of mechanisms to co-ordinate activity within a community and accomplish complex multicellular processes. This strategy is often utilized if the outcome will be more effective when exhibited by the majority of the population, rather than when conducted by an isolated bacterium (Bassler and Losick, 2006). Multicellular behaviour can be exemplified by fruiting body formation by the Gram-negative bacterium *Myxococcus xanthus* (Kaplan, 2003), fruiting body-like assembly formation by the Gram-positive bacterium *Bacillus subtilis* (Branda *et al*., 2001), and aerial hyphae development by the Gram-positive bacterium *Streptomyces coelicolor* (Claessen *et al*., 2006), all which appear to allow the propagation of bacterial spores from the aerial projections.

Given the knowledge that one species of bacterium is capable of accomplishing different, and often incompatible, multicellular states, it raises the question of how entry into the different multicellular behaviour pathways is regulated. *B. subtilis* is able to co-ordinate the multicellular processes of sporulation (Piggot and Hilbert, 2004), uptake of exogenous DNA (known as genetic competence) (Hamoen *et al*., 2003), social motility (known as swarming) (Kearns and Losick, 2003), extracellular protease production (Dahl *et al*., 1992), and biofilm formation/complex colony architecture (Branda *et al*., 2001; Hamon and Lazazzera, 2001). Recent work has begun to establish how these processes are integrated within the population, and has led to the identification of SinR as a regulator of two physiologically distinct states, complex colony architecture and swarming motility (Kearns *et al*., 2005).

The transcription factor DegU, the response regulator of the DegSU two-component system, has a key role in regulating several post-exponential phase processes in *B. subtilis*, including the activation and inhibition of genetic competence (Dubnau *et al*., 1994; Kunst *et al*., 1994; Ogura and Tanaka, 1996), the inhibition of flagellar-based motility (Amati *et al*., 2004), the activation of degradative enzyme production (Msadek *et al*., 1990; Dahl *et al*., 1992), and, as recently demonstrated, the activation of poly-γ-glutamic acid production (Stanley and Lazazzera, 2005). Through activating poly-γ-glutamic acid production, DegU was shown to enhance biofilm formation by the laboratory strain *B. subtilis* JH642, and in addition, control mucoid colony morphology exhibited by wild *B. subtilis* strain RO-FF-1 (Stanley and Lazazzera, 2005). Subsequent analysis using *B. subtilis* wild strains 3610 and B-1, indicated that poly-γ-glutamic acid had an inconsistent role in the formation of sessile communities

Accepted 26 May, 2007. *For correspondence. E-mail n.r.stanleywall@dundee.ac.uk; Tel. (+33) 0 1382 386244; Fax (+33) 0 1382 386375.

(Branda *et al*., 2006; Morikawa *et al*., 2006), thereby raising the question of whether the regulator DegU also had a variable role in controlling biofilm formation in strains of *B. subtilis* other than JH642.

In this paper, a novel mechanism by which the response regulator DegU co-regulates four multicellular behaviour phenomena exhibited by *B. subtilis* is discussed. Previously it was demonstrated that unphosphorylated DegU is required for genetic competence to occur, while phosphorylated DegU (DegU~P) is necessary for degradative enzyme synthesis (exoproteases) (Dahl *et al*., 1992; Hamoen *et al*., 2000). Here, data showing a novel role for DegU~P during the activation of swarming motility and the regulation complex colony architecture are presented, and through subsequent genetic analyses, a model is proposed describing DegU's function as a rheostat to regulate swarming motility, complex colony architecture and exoprotease production at increasing concentrations of phosphorylated DegU. Through comparative DNA microarray analysis and a subsequent systematic mutagenesis approach, a novel gene – *yvcA* – that is required for complex colony architecture by *B. subtilis* was identified. It was subsequently shown that, consistent with the physiological process of complex colony architecture being dependent on DegU~P, transcription from the *yvcA* promoter is activated by DegU~P.

## Results

### *DegU is required for complex colony architecture*

To assess whether the two-component regulatory system DegSU has a role in regulating biofilm formation, or its analogy complex colony architecture, in isolates of *Bacillus subtilis* other than JH642 (Stanley and Lazazzera, 2005), *degSU* was deleted from the chromosome of *B. subtilis* strains 168 (Burkholder and Giles, 1947), RO-FF-1 (Roberts, 1995) and NCBI3610 (hereafter referred to as 3610) (*Bacillus* genetic stock centre). The ability of the *degSU* strains to form sessile communities was assessed by using a crystal violet microtitre plate assay to measure biofilm formation (Stanley and Lazazzera, 2005). It should be noted that the microtitre plate assay could not be used to assess biofilm formation for the 3610 strain for technical reasons (Branda *et al*., 2006); therefore, the ability to form colonies that display a complex architecture, an analogy for biofilm formation (Branda *et al*., 2001), was used.

Using *B. subtilis* strain 3610, it was observed that, on deletion of either *degSU (*data not shown) or *degU,* there was a loss in the gross complex colony architecture exhibited by comparison with the parental strain (Fig. 1). Taken together with the findings that deletion of *degSU* resulted in a 2.2-fold decrease in biofilm formation by strain 168

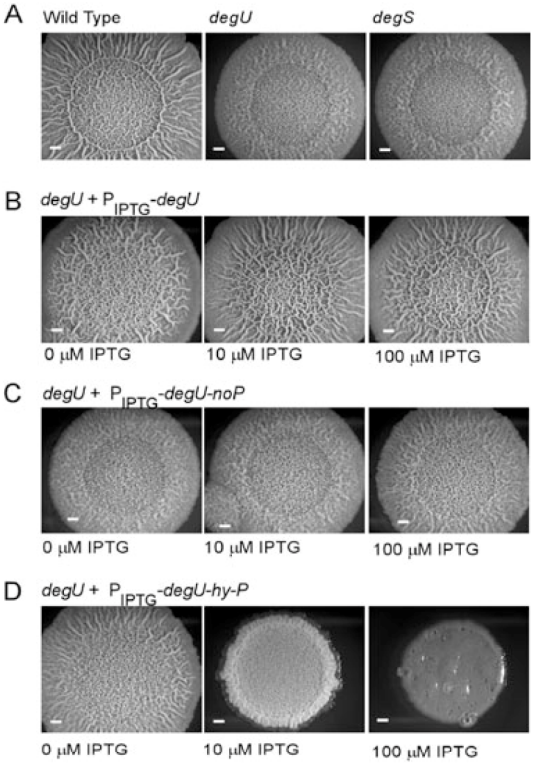


**Fig. 1.** DegU~P regulates complex colony architecture. Representative images showing the complex colony architecture after 40 h incubation at 37°C on MSgg medium of: (A) WT (3610), *degU* (NRS1314) and *degS* (NRS1358); (B) *degU* + $P_{IPTG}$–*degU* (NRS1326); (C) *degU* + $P_{IPTG}$–*degU-noP* (NRS1327); and (D) *degU* + $P_{IPTG}$–*degU-hy-P* (NRS1325). NRS1326, NRS1327 and NRS1325 were grown in the presence of 0, 10 and 100 μM IPTG. The scale bars represent 100 μm.

($P < 0.001$, Student's *t*-test, data not shown) and a 6.8-fold decrease by strain RO-FF-1 (Student's *t*-test = 0.03, data not shown), these data indicate that DegSU has a ubiquitous role in regulating biofilm formation and complex colony architecture exhibited by *B. subtilis*. The role that DegSU plays in controlling complex colony architecture is not that of activating poly-γ-glutamic acid production, because this polymer is not required for complex colony architecture exhibited by strain 3610 (Branda *et al*., 2006). The *degSU* locus in strain 3610 was sequenced and was found not to contain any nucleotide differences by comparison with strain 168 (data not shown). All further experiments were performed with strain 3610.

Upon closer examination of the 3610 *degU* mutant, it was apparent that the central aerial structures observed on colonies formed by the wild-type (WT) strain were not able to protrude into the air and remained flattened

against the agar surface in the *degU* mutant. Additionally, the *degU* mutant did not form fruiting body-like structures that had been observed to form on the parental strain (Fig. 1) (Branda *et al*., 2001). The lipopeptide surfactin produced by *B. subtilis* has recently been assigned a role in raising the aerial structures formed by *B. subtilis* 3610 during complex colony formation (Straight *et al*., 2006). Therefore, to determine whether the lack of complex architecture associated with the *degU* 3610 mutant was a consequence of a defect in surfactin production, it was assessed: (i) whether the exogenous addition of surfactin (for method, see Straight *et al*., 2006) could rescue the *degU* complex colony defect, and (ii) whether the *degU* mutant produced surfactin through direct observation of surfactin production on swarming motility plates (Kearns and Losick, 2003). The presence of exogenously supplied surfactin did not affect the colony morphology exhibited by the *degU* strain (data not shown), and the *degU* mutant was observed to produce surfactin (data not shown). Therefore, it can be concluded that the genes that are regulated by DegU and required for complex colony architecture, are distinct from those involved in surfactin production. These findings are highly consistent with the knowledge that laboratory strains do not produce surfactin (Nakano *et al*., 1992), but that deletion of *degU* from the chromosome of JH642 resulted in an inhibition of cell-surface biofilm formation (Stanley and Lazazzera, 2005).

### *DegU~P activates complex colony architecture*

DegU has been shown to act as a molecular switch to control genetic competence and protease production in its unphosphorylated (DegU) and phosphorylated (DegU~P) form respectively (Dahl *et al*., 1992). Therefore, to determine whether phosphorylation of DegU was necessary to allow complex colony architecture, the following alleles of *degU* were introduced into the *degU* mutant strain at the non-essential *amyE* locus under the control of the IPTG-inducible promoter Pspank-hy (hereafter $P_{IPTG}$) (Britton *et al*., 2002): (i) the WT *degU* allele (hereafter *degU* or DegU); (ii) an allele of *degU* that carries an aspartic acid to asparagine mutation at amino acid number 56 (D56N) that encodes a DegU protein that cannot be phosphorylated (hereafter *degU-noP* or DegU-noP) (Dahl *et al*., 1991); and (iii) an allele of *degU* that carries a histidine to leucine mutation at amino acid number 12 (H12L) that encodes a DegU protein that exhibits a sevenfold slower rate of dephosphorylation by comparison with the WT protein (hereafter *degU-hy-P* or DegU-Hy-P) (Dahl *et al*., 1992).

The addition of either 10 or 100 μM IPTG did not affect the complex colony architecture morphology displayed by the WT (3610) (data not shown), the *degU* mutant (NRS1314) (data not shown), or the *degU* mutant carrying the $P_{IPTG}$–*degU-noP* construct (NRS1327) (Fig. 1C),

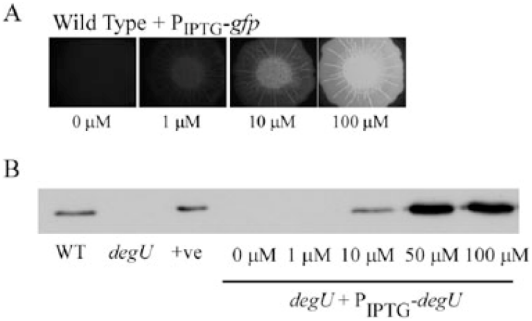


**Fig. 2.** Expression from the $P_{IPTG}$ promoter is IPTG dependent.
A. Fluorescence images of complex colonies of strain 3610 $P_{IPTG}$–*gfp–lacI* (NRS1478) after 40 h incubation at 37°C on MSgg medium containing IPTG as indicated.
B. Immunoblot analysis using an anti-DegU antibody indicating that DegU is expressed in strain NRS1326 (*degU* + $P_{IPTG}$–*degU*) in an IPTG-dependent manner. WT (3610) whole-cell extract and purified DegU–$His_6$ protein (+ ve) were used as positive controls, and *degU* mutant (NRS1314) extract was used as a negative control.

thereby suggesting that DegU~P is required to regulate complex colony architecture. Consistent with these findings, the $P_{IPTG}$–*degU* construct was able to complement the morphology defect exhibited by the 3610 *degU* strain (Fig. 1B). The fact that the *degU* mutant was significantly complemented by the $P_{IPTG}$–*degU* construct even in the absence of inducer implied that only low levels of DegU~P were required to allow complex colony architecture. However, before concluding this, it was first necessary to confirm whether transcription from the $P_{IPTG}$ promoter was regulated in response to the exogenous concentration of IPTG, or whether transcription was uncoupled from the IPTG concentration given the long incubation time (40 h). To test this, a $P_{IPTG}$–*gfp–lacI* fusion was constructed and introduced into *B. subtilis* strain 3610. The fluorescence generated by the strain when grown under complex colony architecture conditions with a range of IPTG concentrations was analysed using fluorescence microscopy (Fig. 2A). From this it was readily apparent that the $P_{IPTG}$ promoter was highly controlled by the external concentration of IPTG. Confirmation that induction of *degU*, like *gfp*, was produced in an IPTG-dependent manner was obtained by Western blot analysis of whole-cell extracts (NRS1326) after exposure to a range of IPTG concentrations (Fig. 2B). Thus, these data support the hypothesis that low levels of DegU~P are sufficient to allow complex colony architecture.

### *High levels of DegU~P inhibit complex colony architecture*

Additional confirmation supporting the role of DegU~P in regulating complex colony architecture was obtained on

the basis of two further experiments. First, deletion of the gene coding for DegU's cognate sensor kinase, *degS*, resulted in a loss in complex colony architecture by comparison with the parental 3610 strain (Fig. 1A). Using Western blot analysis it was observed that the *degS* mutant produced DegU, although at levels lower than the WT (data not shown). Given that only very low levels of DegU are required to partially restore complex colony architecture to the *degU* mutant (Fig. 1B), these findings support the hypothesis that DegU~P is required for complex colony architecture. Second, when the *degU* mutant was complemented with the $P_{IPTG}$–*degU-hy-P* construct, it was observed that in the absence of inducer, there was a partial complementation of the *degU* mutant phenotype (Fig. 1A versus 1D). This represents conditions where there are only low levels of DegU-Hy-P and is in contrast to attempts to complement the *degU* mutant with the $P_{IPTG}$–*degU-noP* construct (Fig. 1C versus 1D). In contrast, the presence of 10 μM IPTG inhibited complex colony architecture, a phenotype that became more apparent when 100 μM IPTG was used to induce transcription (Fig. 1D). It should be noted that induction of the $P_{IPTG}$–*degU-hy-P* construct did not result in a growth defect when analysed under planktonic conditions (data not shown), indicating that high levels of DegU-Hy-P are not intrinsically toxic to *B. subtilis*. These data led to the conclusion that while low levels of DegU~P are required to activate complex colony architecture, high levels of DegU~P inhibit complex colony architecture by *B. subtilis*.

### *Identification of potential DegU~P-regulated targets*

To begin to identify the DegU~P-activated genes that are required for complex colony architecture, the following two criteria were designated: (i) the candidate genes would be upregulated during biofilm formation, and (ii) the candidate genes would be upregulated upon exposure to an increase in osmolarity, because DegS is activated by osmolarity which would therefore result in the phosphorylation of DegU (Kunst and Rapoport, 1995; Steil *et al.*, 2003). By utilizing two previously published DNA microarray analyses (Stanley *et al.*, 2003; Steil *et al.*, 2003), a set of 29 genes located in 24 operons that fulfilled the two criteria was generated (Table S1). Of the 29 genes, 7 genes had previously been identified as regulated by DegU (Ogura *et al.*, 2001; Mader *et al.*, 2002), which provided confidence in the dataset. Here, 16 operons, consisting of 21 of the 29 genes identified through comparative DNA microarray analysis, all coding for proteins of unknown function, along with the *rapG–phrG* locus that has been shown to regulate DegU activity (Ogura *et al.*, 2003), were inactivated in JH642 (Tables S2 and S3) and transferred to strain 3610 by phage transduction. The resulting strains were tested to assess

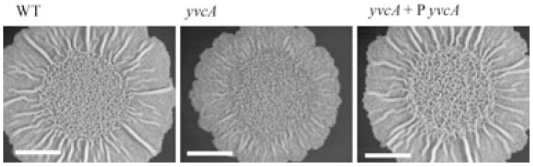


**Fig. 3.** YvcA is required for complex colony architecture. Representative images showing the complex colony architecture of strain 3610 (WT), the *yvcA* mutant (NRS1390) and *yvcA* + PyvcA–*yvcA* (NRS1777) after 40 h incubation at 37°C on MSgg medium. The scale bar is 4 mm in length.

the impact of the mutation on the ability to display a complex architecture. Using this approach, it was identified that one of the insertion mutations located in *yvcA*, the first gene in a three gene operon *yvcA–yvcB–yvzA*, resulted in disrupted complex colony architecture by comparison with the parental strain (Fig. 3). Like the *degU* mutant, the *yvcA* mutant exhibited an overall loss in complex colony architecture, had a lack of fruiting body-like structures (Fig. 3), produced surfactin (data not shown), and did not exhibit a growth defect under planktonic conditions (data not shown).

### *YvcA is required for complex colony architecture*

Because it was highly probable that the *yvcA* insertion in strain NRS1390 could have downstream polar effects on transcription of *yvcB* and *yvzA,* complementation analysis was used to assess which of the three genes was required for WT colony architecture. The *yvcA* coding region, including its native promoter, was introduced into the chromosome at the heterologous *amyE* locus. By assessing the complex colony architecture, it was determined that the introduction of the *yvcA* promoter and coding region was both sufficient and necessary to restore complex colony architecture to the *yvcA* mutant strain (Fig. 3). The *yvcA* gene encodes a 241-amino-acid putative lipoprotein with a predicted signal sequence of 18 amino acids that contains a lipobox motif (Tjalsma *et al.*, 1999). YvcA is designated as of unknown function and has homologies to putative proteins in *B. clausii* and *Oceanobacillus iheyensis*.

### *DegU~P activates* yvcA *transcription*

To determine whether transcription of *yvcA* was in fact regulated by DegU~P, the *yvcA* upstream promoter region ($P_{yvcA}$) was fused to *lacZ* and introduced into the chromosome at the heterologous *thrC* locus. Expression from $P_{yvcA}$ was measured in the WT (NRS1582) and *degU* (NRS1583) mutant strains; these experiments indicated that $P_{yvcA}$ was activated by DegU, because a 6.5-fold reduction in transcription was measured in the *degU* mutant strain by

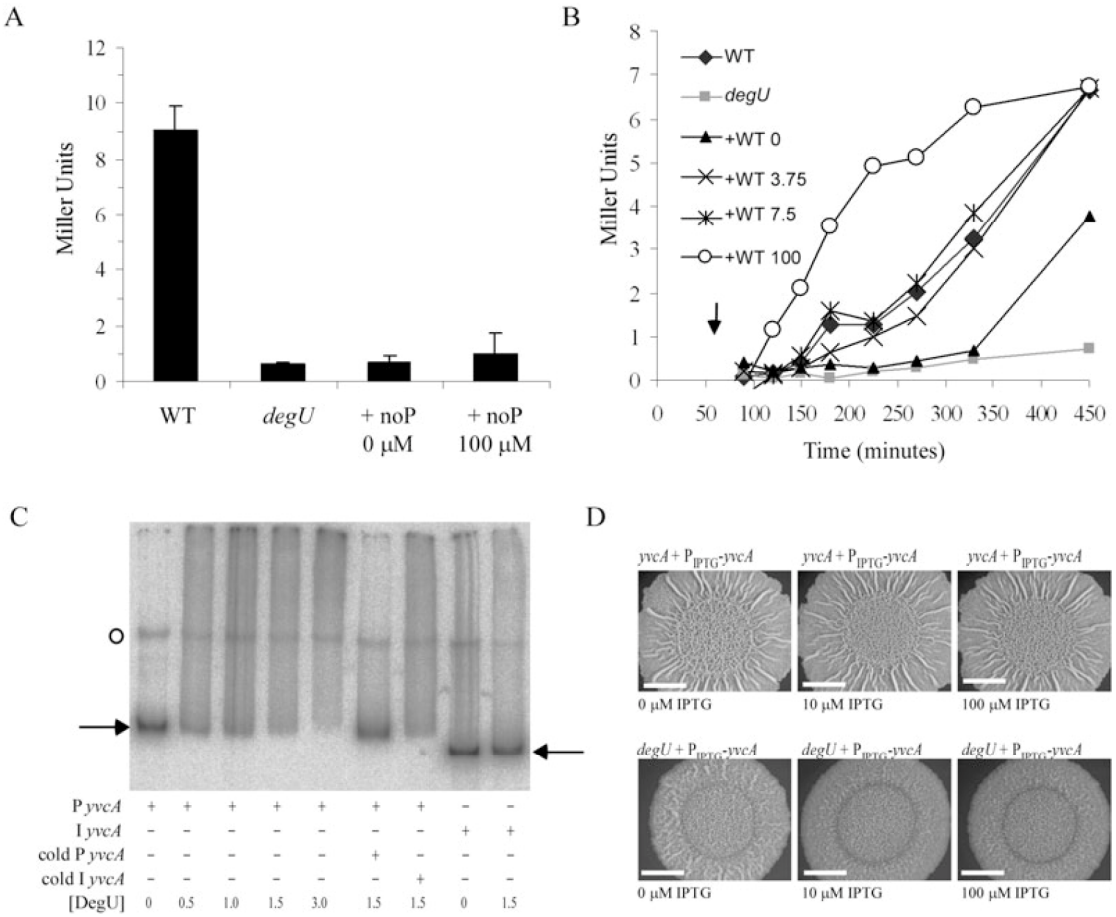


**Fig. 4.** DegU~P regulates expression of *yvcA*.
A. β-Galactosidase assays from the WT (NRS1582), *degU* mutant (NRS1583), and *degU* mutant complemented with the $P_{IPTG}$–*degU-noP* construct in the absence or presence of 100 μM IPTG (NRS1586) carrying the P*yvcA*–*lacZ* fusion.
B. β-Galactosidase assays of the WT (NRS1582), *degU* mutant (*degU*) (NRS1583), and *degU* mutant complemented with the $P_{IPTG}$–*degU* (+WT) (NRS1584) construct carrying the P*yvcA*–*lacZ* fusion over time under planktonic growth conditions. The IPTG concentrations used are as indicated, e.g. '+WT 0' represents the absence of IPTG, and '+WT 100' represents 100 μM IPTG. The IPTG was added at the time point indicated by an arrow.
C. Electrophoretic mobility shift assay. The $^{32}$P-labelled promoter (P*yvcA*) or internal (I*yvcA*) region is indicated by an arrow, and non-*yvcA* labelled DNA (PCR by-product) is indicated by a black circle. DegU–$His_6$ concentrations are in μM, and the '–' and '+' indicate the presence or absence of promoter/internal region labelled DNA and unlabelled (cold) competitor promoter/internal DNA.
D. Representative complex colony images of the *yvcA* mutant + $P_{IPTG}$–*yvcA* (NRS1731) and *degU* mutant + $P_{IPTG}$–*yvcA* (NRS1415), after 40 h incubation at 37°C in the presence of 0, 10 and 100 μM IPTG. The scale bar is 4 mm in length.

comparison with the parental strain (Fig. 4A). Using strain NRS1584, which carried the *degU* mutation and the $P_{IPTG}$–*degU-noP* complementation allele, it was determined that transcription of $P_{yvcA}$ could not be activated even by high levels of DegU-noP (Fig. 4A). The requirement for DegU~P was confirmed by monitoring transcription from the *yvcA* promoter in the *degU* mutant carrying the $P_{IPTG}$–*degU* construct over time where activation of *yvcA* transcription was restored (Fig. 4B). The degree of *yvcA* transcription measured increased, along with increases in the amount of $P_{IPTG}$–*degU* induction, where IPTG concentrations of 3.75 and 7.5 μM allowed near-WT levels of *yvcA* transcription (Fig. 4B).

### *DegU binds to the* yvcA *promoter region*

To determine whether DegU directly regulated *yvcA* transcription, an electrophoretic mobility shift assay using the

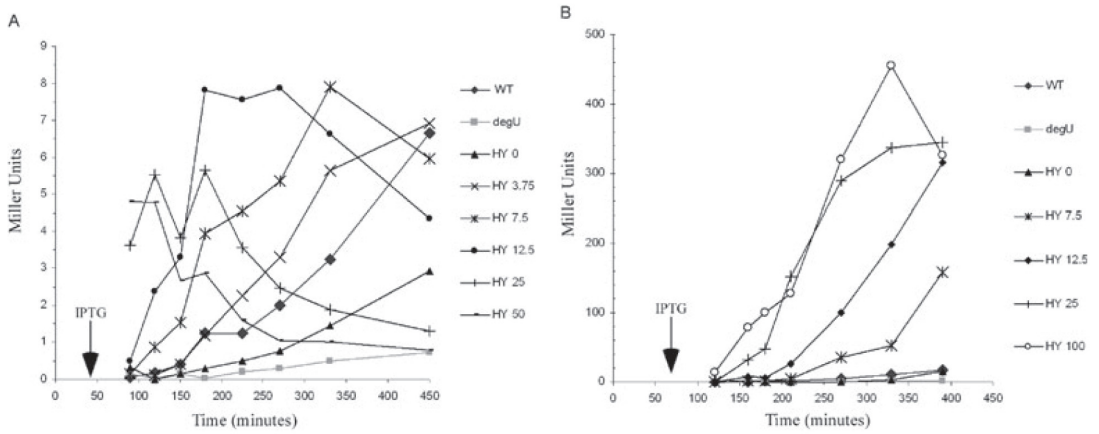


**Fig. 5.** High levels of DegU~P inhibit *yvcA* transcription.
A. β-Galactosidase assays of the WT (NRS1582), *degU* mutant (degU) (NRS1583), and *degU* mutant complemented with the $P_{IPTG}$–*degU-hy-P* (HY) (NRS1585) construct carrying the P*yvcA–lacZ* fusion over time under planktonic growth conditions.
B. β-Galactosidase assays of the WT (NRS1561), *degU* mutant (degU) (NRS1542), and *degU* mutant complemented with the $P_{IPTG}$–*degU-hy-P* (HY) (NRS1543) construct carrying the P*aprE–lacZ* fusion over time under planktonic growth conditions. The IPTG concentrations used are as indicated, e.g. 'HY 0' represents the absence of IPTG, and 'HY 50' represents 50 μM IPTG. The IPTG was added at the time point indicated by an arrow.

*yvcA* promoter region ($P_{yvcA}$) and purified DegU protein was performed. It was observed that at increasing concentrations of DegU, the electrophoretic mobility of the 550 bp $P_{yvcA}$ region was retarded (Fig. 4C). The specificity of the binding interaction was shown using unlabelled $P_{yvcA}$ DNA that was able to out-compete the electrophoretic shift, while non-specific unlabelled competitor DNA, from the internal coding region of *yvcA*, was not (Fig. 4C). Despite numerous attempts, a discrete shifted DNA–protein complex was not observed, suggesting the presence of multiple DegU binding sites. Comparable findings with DegU have been obtained before for the *fla-che* and *aprE* promoter regions (Ogura *et al*., 2003; Amati *et al*., 2004); control reactions with the *comK* promoter region resulted in a discrete band shift similar to previous observations (Hamoen *et al*., 2000; Shimane and Ogura, 2004) (Fig. S1).

### *DegU~P regulates more than one gene during complex colony architecture*

Having demonstrated that *yvcA* was regulated by DegU~P (Fig. 4), it was hypothesized that, if *yvcA* were the sole gene regulated by DegU~P that is required for complex colony architecture, then the artificial induction of *yvcA* transcription in the *degU* mutant strain would be sufficient to restore complex colony architecture. This was tested by placing the *yvcA* coding region and ribosome binding site under the control of the heterologous $P_{IPTG}$ promoter and introducing it into the *degU* mutant strain. While the $P_{IPTG}$–*yvcA* construct was able to fully complement the *yvcA* mutation, even in the absence of IPTG, it was unable to restore complex colony architecture to the *degU* mutant (Fig. 4D). Therefore, it can be concluded that DegU~P regulates at least one further gene that is required for complex colony architecture. The identity of this gene, and the mechanism by which YvcA contributes to complex colony architecture, is not known and is the subject of current investigations.

### *High levels of DegU-Hy-P inhibit* yvcA *transcription*

In this study, it was demonstrated that complex colony architecture exhibited by *B. subtilis* was activated by a low level of DegU~P and inhibited by high levels of DegU~P (Fig. 1). Therefore, it was predicted that transcription of *yvcA*, a gene that is required for complex colony architecture and directly regulated by DegU~P (Fig. 4), may likewise be activated by low levels of DegU~P and inhibited by high levels of DegU~P. To test this, the *degU* mutant carrying the $P_{IPTG}$–*degU-hy-P* construct was utilized (NRS1585). Because the DegU-Hy-P protein exhibits a sevenfold slower rate of dephosphorylation compared with the WT protein (Dahl *et al*., 1992), it allows the effect of high DegU~P levels on the transcription of the *yvcA* promoter to be assessed using a gradient of IPTG induction. It became apparent that, consistent with complex colony architecture being activated by low levels of DegU~P, *yvcA* transcription was activated when the $P_{IPTG}$–*degU-hy-P* construct was induced with 3.75 and 7.5 μM IPTG (Fig. 5A). Subsequently, and consistent with complex colony architecture being inhibited by high levels

of DegU~P, when the $P_{IPTG}$–*degU-hy-P* was induced with 12.5 μM IPTG, transcription of *yvcA* was initially activated but at later time points inhibited (Fig. 5A). Like the process of complex colony architecture formation, the inhibition of *yvcA* transcription became even more apparent when the $P_{IPTG}$–*degU-hy-P* construct was induced with either 25 or 50 μM IPTG (Fig. 5A). These findings indicate that *yvcA* transcription and the global process of complex colony architecture behave in a similar manner, with both being activated by low levels of DegU~P and inhibited by high levels of DegU~P (Figs 1 and 5A).

To confirm whether this profile of transcriptional activation and inhibition was specific to *yvcA,* or whether the inhibition was a non-specific consequence of the high level of DegU-Hy-P in the cell, a P*aprE–lacZ* fusion was constructed and analysed in an identical manner. The *aprE* gene encodes an exoprotease that is known to be activated by DegU~P (Henner *et al.*, 1988). It was observed that the level of transcription from the P*aprE–lacZ* fusion was modulated in direct response to the amount of IPTG added to control the $P_{IPTG}$–*degU-hy-P* construct (Fig. 5B). Additionally, unlike the *yvcA* transcription fusion, the level of transcription from the *aprE* promoter remained high when the $P_{IPTG}$–*degU-hy-P* construct was induced with high levels of IPTG (Fig. 5B). These data strongly support the conclusion that transcription of *yvcA* is activated by low levels of DegU~P and inhibited by high levels of DegU~P.

### *High levels of DegU~P activate exoprotease production*

The transcriptional responses of the *yvcA* and *aprE* promoter regions to induction of the $P_{IPTG}$–*degU-hy-P* construct are different (Fig. 5A versus 5B). When these findings were considered along with the knowledge that protease production, like complex colony architecture, can be considered a 'multicellular behaviour' (i.e. a process that is more effective if co-ordinated and conducted by bacteria in a community), it was hypothesized that the level of DegU~P required to activate protease production may be higher than that required to activate complex colony architecture, and that perhaps the physiological response exhibited by *B. subtilis* was determined, at least in part, by the level of DegU~P in the cell. To test whether this was the case, exoprotease production was assayed using the complemented *degU* strains (NRS1325, NRS1326 and NRS1327) on Luria–Bertani (LB) plates that contained 1.5% milk (Msadek *et al.*, 1990). As expected, no alteration in the level of protease production was observed for the parental 3610 strain when the concentration of IPTG was modulated (Fig. 6); additionally, no exoprotease production was observed for the *degU* mutant (NRS1314) (Fig. 6). Consistent with the previous findings indicating that DegU~P was required for

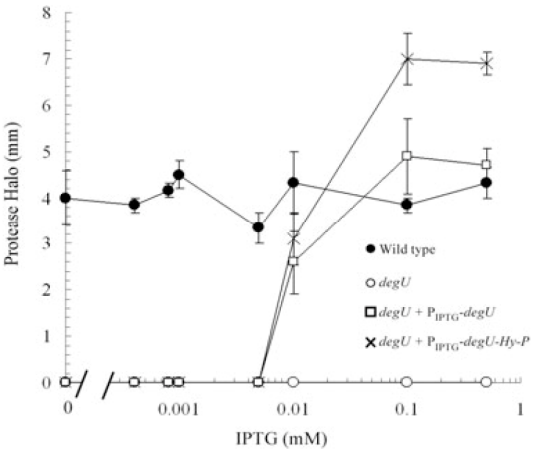


**Fig. 6.** High levels of DegU~P activate exoprotease production. Exoprotease production was monitored on 1.5% milk LB plates, as described in the *Experimental procedures*. Plotted are the average values of 3–5 independent experiments over four orders of magnitude of IPTG concentrations for WT (3610), *degU* mutant (NRS1314), *degU* mutant carrying the $P_{IPTG}$–*degU* allele (NRS1326), and *degU* mutant carrying the $P_{IPTG}$–*degU-hy-P* allele (NRS1325). The error bars represent the SEM.

exoprotease production (Dahl *et al.*, 1992), the *degU-noP* gene, although it was transcribed and translated in an IPTG-dependent manner, was unable to restore exoprotease production in the *degU* mutant (data not shown).

Exoprotease production was partially complemented in the *degU* mutant strain by the $P_{IPTG}$–*degU* allele in the presence of 10 μM IPTG and fully complemented with 100 μM IPTG (Fig. 6). Likewise, exoprotease production was almost fully restored in the *degU* mutant strain carrying the $P_{IPTG}$–*degU-hy-P* allele after induction with 10 μM IPTG. However, in the presence of either 100 or 500 μM IPTG, the level of protease production in this strain exceeded that observed for either the WT strain or the *degU* mutant carrying the $P_{IPTG}$–*degU* construct. It should be noted that under these experimental conditions, the $P_{IPTG}$ promoter responds directly to the external IPTG concentration (data not shown). Taken together with the results from the analysis of complex colony architecture, these findings strongly indicated that a low level of DegU~P is sufficient and necessary to allow complex colony architecture, while a high level of DegU~P is required to allow DegU-activated protease production and, correspondingly, inhibit complex colony architecture.

### *Low levels of DegU~P are required for swarming motility*

While assessing the ability of the *degU* mutant strain to produce surfactin on swarming motility plates (see above), it was observed that DegU was required for

**Table 1.** DegU~P regulates swarming motility.

| Genotype[a] | IPTG (μM) | Swarming[b] | Swimming[c] |
|---|---|---|---|
| WT (3610) | 0 | + | + |
| *degU* (NRS1314) | 0 | – | + |
| *degS* (NRS1358) | 0 | + | + |
| *degU* + $P_{IPTG}$–*degU* | 0 | + | + |
| (NRS1326) | 10 | + | + |
| | 100 | + | + |
| *degU* + $P_{IPTG}$–*degU-noP* | 0 | – | + |
| (NRS1327) | 10 | – | + |
| | 100 | – | + |
| *degU* + $P_{IPTG}$–*degU-hy-P* | 0 | + | + |
| (NRS1325) | 10 | – | – |
| | 100 | – | – |

**a.** The relevant strain genotype is listed, with the strain name provided in brackets.
**b.** The swarming phenotype was assessed on LB 0.7% agar plates, and is indicated by a '+' to represent WT swarming motility and a '–' to indicate a lack of swarming motility. See Fig. S2 for quantitative results.
**c.** The swimming phenotype was assessed on LB 0.3% agar plates, and is indicated by a '+' to represent WT swimming motility and a '–' to indicate a lack of swimming motility.

swarming motility (Table 1 and Fig. S2). Swarming motility is a multicellular behaviour displayed by wild isolates of *B. subtilis* (Kearns and Losick, 2003). It should be noted that on some occasions, the *degU* mutant regained the ability to swarm after prolonged incubation; however, this occurred in an unpredictable manner, and the cells that were contained within the swarm did not retain the antibiotic resistance cassette associated with the *degU* insertion, suggesting that the insertion had been removed from the chromosome (data not shown). In contrast, it was observed that deletion of *degS* did not significantly affect the rate of swarming observed by comparison with the parental 3610 strain (Table 1 and Fig. S2). Using fresh 0.3% agar LB plates, it was confirmed that flagellar-based swimming motility was not affected upon deletion of either *degU* or *degS* in either the 3610 (Table 1) or JH642 strain backgrounds (data not shown).

The finding that *degS* was not required for swarming motility while *degU* was required, suggested that unphosphorylated DegU activated swarming motility. To test this hypothesis, the ability of the $P_{IPTG}$ –*degU-noP* construct to restore swarming motility to the *degU* mutant was tested. Contrary to the proposed hypothesis, the $P_{IPTG}$–*degU-noP* allele was not able to restore swarming even when expressed at a high level (Table 1 and Fig. S2). In contrast, the $P_{IPTG}$–*degU* allele was able to restore full swarming motility by the *degU* mutant even in the absence of IPTG, thereby indicating that DegU~P is required for the activation of swarming motility (Table 1 and Fig. S2). Considering that DegS was found to be dispensable for swarming motility, it is possible that in the *degS* mutant strain, DegU is phosphorylated at a very low level by acetyl phosphate in a manner similar to the mechanism that has been observed previously, e.g. for VanS in *S. coelicolor* and the $\sigma^S$ regulator RssB in *Escherichia coli* (Bouche *et al.*, 1998; Hutchings *et al.*, 2006). Alternatively, DegU could be phosphorylated at a low level in the absence of *degS* by a non-cognate sensor kinase to a level sufficient to activate swarming. Unless the interaction between DegS and DegU can be inhibited, these explanations do not necessarily reflect the *in vivo* situation, because DegS acts both as a phosphatase and as a kinase (Mukai *et al.*, 1990; Dahl *et al.*, 1991; 1992). However, they may represent the mechanism by which DegU is phosphorylated in the absence of *degS* to allow swarming motility to be activated. Taken together, these findings indicate that the generation of DegU~P at a very low level is sufficient to trigger *B. subtilis* to activate swarming motility.

### *High levels of DegU~P inhibit swarming motility*

DegU~P has different roles in the cell at different concentrations; therefore, the impact of the $P_{IPTG}$–*degU-hy-P* construct with respect to swarming motility was assessed. Highly consistent with very low levels of DegU~P activating swarming motility, in the absence of IPTG strain, NRS1325 exhibited swarming at a rate comparable to that observed for the WT 3610 strain (Table 1 and Fig. S2). In contrast, addition of either 10 or 100 μM IPTG completely inhibited the ability of the $P_{IPTG}$–*degU-hy-P* construct to restore swarming motility to the *degU* mutant (Table 1 and Fig. S2). These data indicate that, like complex colony architecture (Fig. 1) and genetic competence (Dahl *et al.*, 1992), swarming motility is inhibited by a high level of DegU~P. High levels of DegU~P have been shown to inhibit flagellar-based motility in domestic strains of *B. subtilis* (Amati *et al.*, 2004), and flagella-based motility has been shown to be required for swarming motility (Kearns and Losick, 2003). Therefore, the impact of the $P_{IPTG}$–*degU-hy-P* construct, with and without induction with IPTG, on swimming motility was tested to ensure that there were not any strain specific differences in the regulation of flagellar biogenesis. Entirely consistent with DegU not being required to activate swimming motility, in the absence of IPTG, swimming motility by strain NRS1325 was comparable to WT (Table 1). In contrast, addition of either 10 or 100 μM IPTG inhibited swimming-based motility (Table 1). The findings detailed above, taken in conjunction with the knowledge that the *degS* mutant strain *does not* exhibit a swarming defect, support a model where very low levels of DegU~P activate swarming and high levels of DegU~P inhibit swarming (Table 1 and Fig. S2). The genes that are regulated by very low levels of DegU~P that are required for swarming motility are currently unknown.

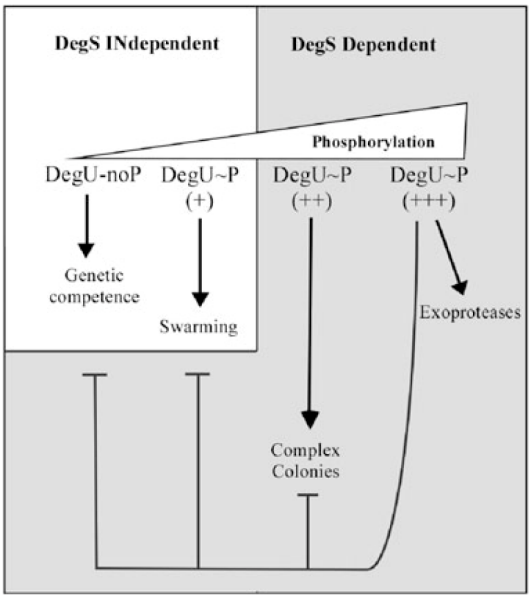


**Fig. 7.** Model for DegU regulation of multicellular behaviour phenomena. Genetic competence (Dahl *et al*., 1992; Hamoen *et al*., 2000), swarming motility, sessile community formation, flagellar motility (Amati *et al*., 2004) and protease production (Dahl *et al*., 1992; Henner *et al*., 1988) are regulated by the DegSU system in a manner that is dependent on the concentration of phosphorylated DegU. '+', '++' and '+++' represent very low, low and high levels of phosphorylated DegU (DegU~P) respectively. Activation is depicted by arrow heads and repression by 'T-bars'.

## Discussion

Here a model where the response regulator DegU controls four multicellular phenomena using a mechanism that is dependent on the level of DegU phosphorylation in the cell is presented (Fig. 7). This study has added further evidence to existing knowledge that DegU and DegU~P act as a molecular switch to control the multicellular processes of genetic competence and exoprotease production (Dahl *et al*., 1992), to indicate that the regulatory control exerted by DegU is more flexible than a simple molecular switch and has the capacity to integrate physiological responses along a gradient of DegU phosphorylation (Fig. 7). Additionally, a novel biological function for DegU as a positive and negative regulator of swarming motility and complex colony architecture, together with a novel gene, *yvcA*, that is directly regulated by DegU~P and required for complex colony architecture, has been identified.

YvcA is a predicted membrane-anchored lipoprotein (Tjalsma *et al*., 1999) that, until this study, had an entirely unknown function in *B. subtilis*. Here it was demonstrated that the presence of YvcA was required to allow *B. subtilis* 3610 to form complex colony architecture (Fig. 3). To our knowledge, this is the first example of a proposed membrane-bound lipoprotein that has been shown to be involved in complex colony architecture by *B. subtilis*. Through reporter fusion analysis, it was demonstrated that transcription from the *yvcA* promoter was activated in the presence of low levels of DegU~P and inhibited by high levels of DegU~P (Fig. 5). Evidence to demonstrate that this is a direct regulatory event is provided (Fig. 4). It is not known, at the current time, how YvcA functions to control complex colony architecture, although it is possible that it could form a structural component of the extracellular matrix or could be involved in a signalling process. However, what is clear is that *yvcA* is not the only gene regulated by DegU~P that is required for complex colony architecture, because the $P_{IPTG}$–*yvcA* construct was unable to restore complex colony architecture to the *degU* mutant strain (Fig. 4). The identity of further DegU~P-regulated genes, and the mechanism by which YvcA functions to control complex colony architecture, are the focus of current investigations.

DegU is a positive and negative regulator of swarming motility (Table 1 and Fig. S2). It was shown that very low levels of DegU~P, which can be generated in a *degS* mutant strain through an atypical pathway, are required to activate swarming motility. Because neither the *degS* nor the *degU* mutant strains exhibited a swimming motility defect, these findings indicate that *degU* is not required for flagellar biogenesis (Table 1). At this point, the mechanism used by DegU~P to activate swarming motility is unknown. In contrast, at high levels of DegU~P, swarming motility is inhibited. This is most likely a consequence of high levels of DegU~P inhibiting transcription of the *flache* operon (Amati *et al*., 2004) that encodes the components for flagella biosynthesis, which is in turn required for swarming motility (Kearns and Losick, 2003).

One must question why a single response regulator has evolved to control at least four distinct physiological behaviours in the one organism. It is possible that *B. subtilis* has evolved so that the progression from motile swarming cells to sessile cells (and back again) is controlled through an increase in the level of DegU phosphorylation, as it may reflect the environmental conditions that are favourable for establishing a sessile community. It is curious that complex colony architecture, a community of sessile cells, and swarming motility are activated by low and very low levels of DegU~P respectively, but that both processes are inhibited by high levels of DegU~P, because they represent apparently physiologically incompatible behaviours. These findings argue that the very low and low levels of DegU~P are most important for triggering entry to swarming and sessile behaviours, and confirm that there is a need for these processes to be tightly and co-ordinately controlled (Kearns *et al*., 2005). Given that SinR is a key regulator of swarming motility and complex colony architecture (Kearns *et al*., 2005), it will be of great

interest in the future to understand how the DegU and SinR regulatory networks interact to control multicellular behaviours exhibited by *B. subtilis*. It is likely that the co-ordinated regulation of swarming motility and capsular polysaccharide production, which can be used as an indication of a sessile lifestyle, will be a common theme used by bacteria to control entry into biofilm formation pathways, because it has been observed in unrelated bacterial species like *Vibrio parahaemolyticus* (Boles and McCarter, 2002) and *Pseudomonas aeruginosa* (Caiazza *et al*., 2007).

An important feature of cells in a sessile community is the ability to leave the community when conditions become undesirable (Webb *et al*., 2004; Barraud *et al*., 2006). Here it was shown that exoprotease production is activated under conditions that generate a high proportion of DegU~P, which correspondingly inhibits both complex colony architecture and swarming motility. Therefore, it seems possible that a sessile lifestyle 'escape mechanism' has been integrated into the DegU regulatory network. When conditions become unfavourable, protease production is activated, and genes that are directly required for complex colony architecture and swarming motility are inhibited (Fig. 7), at least temporarily. The increase in exoprotease production could conceivably enable release of the cells from the extracellular matrix of the biofilm (Branda *et al*., 2005; 2006) through enhanced proteolytic cleavage. Once the bacteria have 'escaped' from the confines of the biofilm or colony, the degree to which DegU is phosphorylated will most likely alter and may decrease to a level that would allow the activation of swarming motility, or one which once more promotes a sessile lifestyle in a more suitable environment. Biofilm 'escape' mechanisms based on signalling through nitric oxide, and the upregulation of bacteriophage genes have previously been reported to aid dispersal from *P. aeruginosa* biofilms (Webb *et al*., 2004; Barraud *et al*., 2006).

The mechanism used by the regulator DegU to control multicellular behaviours exhibited by *B. subtilis* (Fig. 7) appears to be similar to the mechanism used by Spo0A to control biofilm formation, cannibalism and sporulation (Gonzalez-Pastor *et al*., 2003; Molle *et al*., 2003; Fujita *et al*., 2005), where biofilm formation and cannibalism are activated by lower levels of Spo0A~Phosphate than sporulation (Fujita *et al*., 2005). One difference, by comparison with the Spo0A regulatory network, appears to be that DegU can integrate the regulation of at least four distinct physiological processes at what seems to be four distinct levels of DegU~P. When this is considered, the control exerted by DegU and DegU~P appears analogous to that used in *Bordetella* by BvgAS (Cummings *et al*., 2006). The BvgAS phosphorelay system is used by *B. pertussis* and *B. bronciseptica* to control virulence and biofilm formation, among other phenotypes (Beier and Gross, 2006). It was recently determined, using DNA microarray analysis, that the BvgAS regulatory system regulates a large and flexible regulon using a rheostat mechanism to control genes that can be separated into at least five regulatory groups that are activated or repressed, depending on the concentration and phosphorylation status of BvgS (Cummings *et al*., 2006). It was hypothesized that other regulatory systems may have a similar complex mode of action, and the data presented in this study strongly indicate that DegU acts in a similar manner and would therefore allow the subtle integration of distinct physiological responses in a highly controlled manner.

## Experimental procedures

### *Growth conditions and strain construction*

*Escherichia coli* strains were routinely grown in LB medium (10 g NaCl, 5 g yeast extract and 10 g tryptone per litre). *B. subtilis* strains were routinely grown in LB medium and, where appropriate, a MSgg medium [5 mM potassium phosphate and 100 mM MOPS at pH 7.0 supplemented with 2 mM $MgCl_2$, 700 μM $CaCl_2$, 50 μM $MnCl_2$, 50 μM $FeCl_3$, 1 μM $ZnCl_2$, 2 μM thiamine, 0.5% glycerol, 0.5% glutamate and amino acids, as appropriate, at a final concentration of 50 μg $ml^{-1}$ (Branda *et al*., 2001; Chu *et al*., 2006)]. Both *E. coli* and *B. subtilis* strains were grown at 37°C. The antibiotics were used, as required, at the following concentrations: ampicillin 100 μg $ml^{-1}$, chloramphenicol 5 μg $ml^{-1}$, erythromycin 5 μg $ml^{-1}$, and spectinomycin 100 μg $ml^{-1}$. *E. coli* strain MC1061 [*F' lacIQ lacZM15 Tn10 (tet)*] was used for the routine construction and maintenance of plasmids. The *B. subtilis* strains used in this study are listed in Table 2, and for a full strain list, see Table S2. The strains were constructed by transformation of genetically competent cells with chromosomal DNA or plasmids using standard protocols (Harwood and Cutting, 1990). Phage transductions into the *B. subtilis* strain background 3610 were conducted as described previously (Kearns and Losick, 2003).

### *DegU complementation plasmids*

Plasmids pNW11, pNW12 and pNW13 were used to introduce the *degU*, *degU146 (degU-noP)* or *degU32 (degU-hy-P)* alleles of *degU* respectively, under the control of the IPTG-inducible promoter, Pspank-hy, at the non-essential *amyE* locus on the chromosome, and are derivatives of plasmid pDR111 (Britton *et al*., 2002). The appropriate *degU* allele (including the ribosome binding site) was amplified from genomic DNA of *B. subtilis* strains QB4414 (*degU146*) (Dahl *et al*., 1991), QB136 (*degU32*) (Kunst *et al*., 1974) or JH642 (WT), using primers NSW10 (5′-GCTAGAGTATATAAAGCTTGAACAATAATACAAGGAG-3′) and NSW11 (5′-GCCTAAAAAAAGCATGCGACCTGCCTAGTAAAAGG-3′), and was cloned into the HindIII and SphI sites of pDR111 using the restriction sites engineered into the primers (underlined in the primer sequence). The plasmids were sequenced with primers NSW10 and NSW11 to confirm that they each contained the desired sequence of *degU*.

**Table 2.** *Bacillus subtilis* strains used in this study.

| Strain | Relevant genotype[a] | Source/construction[b] |
|---|---|---|
| 3610 | Prototroph | B.G.S.C. |
| QB4414 | *trpC2 degU146* | Dahl *et al.* (1991) |
| QB136 | *leuB8 deg(H)32 trpC2* | Kunst *et al.* (1974) |
| NRS1314 | 3610 *degU*::pBL204 *(cat)* | SPP1 NRS1302 → 3610 |
| NRS1325 | 3610 *amyE::Pspank-hy–degU32–lacI (spc), degU*::pBL204 *(cat)* | SPP1 NRS1302 → NRS1316 |
| NRS1326 | 3610 *amyE::Pspank-hy–degU–lacI (spc), degU*::pBL204 *(cat)* | SPP1 NRS1302 → NRS1317 |
| NRS1327 | 3610 *amyE::Pspank-hy–degU146–lacI (spc), degU*::pBL204 *(cat)* | SPP1 NRS1302 → NRS1318 |
| NRS1358 | 3610 *degS*::pDH64 *(cat)* | SPP1 NRS1136 → 3610 |
| NRS1390 | 3610 *yvcA*::pNW34 *(cat)* | SPP1 NRS1378 → 3610 |
| NRS1415 | 3610 *degU*::pBL204 *(cat) amyE::Pspank-hy–yvcA–lacI (spc)* | SPP1 NRS1719 → NRS1314 |
| NRS1476 | 3610 *amyE::Pspank-hy–gfp–lacI (spc)* | SPP1 NRS1456 → 3610 |
| NRS1582 | 3610 *thrC::PyvcA–lacZ (erm)* | SPP1 NRS1572 → 3610 |
| NRS1583 | 3610 *thrC::PyvcA–lacZ (erm), degU*::pBL204 *(cat)* | SPP1 NRS1572 → NRS1314 |
| NRS1584 | 3610 *thrC::PyvcA–lacZ (erm), amyE::Pspank-hy–degU–lacI (spc), degU*::pBL204 *(cat)* | SPP1 NRS1572 → NRS1326 |
| NRS1585 | 3610 *thrC::PyvcA–lacZ (erm), amyE::Pspank-hy–degU32–lacI (spc), degU*::pBL204 *(cat)* | SPP1 NRS1572 → NRS1325 |
| NRS1586 | 3610 *thrC::PyvcA–lacZ (erm), amyE::Pspank-hy–degU146–lacI (spc), degU*::pBL204 *(cat)* | SPP1 NRS1572 → NRS1327 |
| NRS1561 | 3610 *thrC::PaprE–lacZ (erm)* | SPP1 NRS1534 → 3610 |
| NRS1542 | 3610 *thrC::PaprE–lacZ (erm), degU*::pBL204 *(cat)* | SPP1 NRS1534 → NRS1314 |
| NRS1544 | 3610 *thrC::PaprE–lacZ (erm), amyE::Pspank-hy–degU–lacI (spc), degU*::pBL204 *(cat)* | SPP1 NRS1534 → NRS1326 |
| NRS1543 | 3610 *thrC::PaprE–lacZ (erm), amyE::Pspank-hy–degU32–lacI (spc), degU*::pBL204 *(cat)* | SPP1 NRS1534 → NRS1325 |
| NRS1564 | 3610 *thrC::PaprE–lacZ (erm), amyE::Pspank-hy–degU146–lacI (spc), degU*::pBL204 *(cat)* | SPP1 NRS1534 → NRS1327 |
| NRS1731 | 3610 *yvcA*::pNW34 *(cat) Pspank-hy–yvcA–lacI (spc)* | SPP1 NRS1719 → NRS1390 |
| NRS1777 | 3610 *yvcA*::pNW34 *(cat) PyvcA–yvcA (spc)* | SPP1 NRS1775 → NRS1390 |

**a.** Relevant genotypes are provided. Drug-resistance cassettes are indicated as follows: Spc, spectinomycin resistance; cat, chloramphenicol resistance; and erm, erythromycin resistance.
**b.** The direction of strain construction is indicated with DNA or phage (SPP1) (→) recipient using standard techniques. A full list of the strains used is provided in Table S2.

### *Construction of insertion plasmids*

Plasmid pNW34 was used to disrupt the *yvcA–yvcB–yvzA* locus and was a derivative of pBL132 (Stanley *et al.*, 2003). It contained an internal region of DNA of the *yvcA* coding region and a chloramphenicol-resistance cassette. The internal region of *yvcA* was amplified using primers NSW35 (5′-CGAGGCGAATTCTACCTGCGTTTCAGGAC-3′) and NSW36 (5′-CGAGGCGAATTCCTTGGCAGTGTAAATATC-3′), and was cloned into the EcoRI sites of pBL132 using the restriction sites engineered into the primers (underlined in the primer sequence). Further insertion plasmids were constructed in an identical manner using the primers and plasmids detailed in Table S3.

### *Construction of plasmid pNW69*

Plasmid pNW69 was used to introduce the *yvcA* gene under the control of the IPTG-inducible promoter, Pspank-hy, at the non-essential *amyE* locus and is a derivative of plasmid pDR111 (Britton *et al.*, 2002). The *yvcA* coding region, including ribosome binding site, was amplified from *B. subtilis* strain 3610 using primers NSW73 (5′-CGAGGTCGACCGT GGAGGTTCGTAATGAAAA-3′) and NSW74 (5′-CGAG GCATGCTTATTTCTCCTTTTTATC-3′), and was cloned into the SalI and SphI sites of pDR111 using the restriction sites engineered into the primers (underlined in the primer sequence).

### *Construction of plasmid pNW81*

Plasmid pNW81 was used to introduce the *yvcA* gene under the control of its native promoter at the non-essential *amyE* locus and is a derivative of plasmid pDR111 (Britton *et al.*, 2002). The *yvcA* promoter and coding region was amplified from *B. subtilis* 3610 using primers NSW18 (5′-CGAGGCGAATTCGAACGCCAAGCGGAAAT-3′) and NSW74 (5′-CGAGGCATGCTTATTTCTCCTTTTTATC-3′), and was cloned into the EcoRI and SphI sites of pDR111 using the restriction sites engineered into the primers (underlined in the primer sequence).

### *Construction of P*yvcA–lacZ *and P*aprE–lacZ *reporter fusions*

The *yvcA* and *aprE* promoter regions were amplified using primers NSW18 (5′-CGAGGCGAATTCGAACGCCAAGCGG AAAT-3′) and NSW19 (5′-GAGGCGAATTCGGATCCCCTG TCAGGCAAGT-3′), and NSW61 (5′-GGTAAAGCCTATGA ATTGTGG-3′) and NWS62 (5′-GTCTGAATTCGGATCCGA TCCACAATTTTTTGCT-3′) respectively, from 3610 genomic DNA. The amplified promoter regions were cloned into the EcoRI site located upstream of the *lacZ* gene in pDG1663 (Guerout-Fleury *et al.*, 1996) using the EcoRI sites located in the primers (underlined in the primer sequence). The plasmids were screened to check for those with the correct orientation (pNW204 P*yvcA–lacZ* and pNW51 P*aprE–lacZ*) and subsequently introduced into the chromosome of *B. subtilis* (Table S2).

### *Fluorescence plasmid*

Plasmid pNW101 carrying the *amyE::Pspank-hy–gfp–lacI* construct for integration at the *amyE* locus was generated by ligating the HindIII and SphI *gfp* fragment isolated from

plasmid pMF302 (Fujita *et al.*, 2005) into pDR111 (Britton *et al.*, 2002).

### *Swarm assay*

Swarm assays were performed essentially as described (Kearns and Losick, 2003). Cells were grown to mid-log phase at 37°C in LB. The cultures were concentrated such that 10 μl of cells had an $OD_{600}$ of 10. This was spotted onto the centre of a freshly made 0.7% LB agar plate (5 g NaCl, 5 g yeast extract, 10 g tryptone LB with 7 g agar per litre) that had been allowed to dry in a flow cabinet for 40 min. Plates were incubated at 37°C, and the progression of the bacterial swarm was monitored each hour in mm. For each independently executed experiment ($n = 3$), 2–3 plates were inoculated per bacterial strain. Data were plotted as the mean ± SEM.

### *Protease assay*

Secreted proteases were monitored using LB agar plates supplemented with 1.5% (w/v) skimmed milk. *B. subtilis* cultures to be tested were grown to mid-late exponential phase in LB from a freshly streaked LB plate and subsequently diluted to an $OD_{600}$ of 0.01 in fresh LB medium. In total, 10 μl of the diluted culture was spotted onto a 1.5% milk plate (containing IPTG as indicated) and incubated at 37°C for 18 h. The diameter of the halo surrounding protease-positive strains was measured, and the diameter of the colony was subtracted. The experiment was conducted on at least three independent occasions and plotted as the mean ± SEM.

### *Colony morphology assay*

Analysis of the complex colony architecture was performed essentially as described (Branda *et al.*, 2001). *B. subtilis* cultures to be tested were grown to mid-late exponential phase in LB from a freshly streaked LB plate and subsequently diluted to an $OD_{600}$ of 0.01 in fresh LB medium. In total, 10 μl of the diluted culture was spotted onto an MSgg plate containing 1.5% agar and IPTG as required. The plate was incubated at 37°C for 40 h prior to photography. Images were captured using a Leica MZ16 stereoscope and a Jenoptik Jena digital camera operated with Openlab software (Improvision). When necessary, the colonies were imaged with uniform exposures using fluorescence microscopy with GFP excitation. Photography was performed using a Nikon SMZ1500 stereomicroscope, and the images were captured using a Nikon DXM1200 digital camera with the ACT-1 software package (Nikon). A representative image is presented.

### *β-Galactosidase assays*

A total of 25 ml of biofilm growth medium (10 g NaCl, 5 g yeast extract and 10 g tryptone per litre supplemented with 124 mM potassium phosphate pH 7.0, 15 mM ammonium sulphate, 3.4 mM sodium citrate, 1 mM $MgSO_4$, and 0.1% glucose) was inoculated from an overnight lawn plate to an $OD_{600}$ of 0.01. The cells were grown in 250 ml flasks with shaking at 200 r.p.m., and samples were taken at regular intervals. IPTG was added, when required, at the concentrations indicated after approximately 60 min growth. At each time point, 0.5 ml cell suspension was harvested for analysis and the resulting cell pellet was stored at –20°C. The β-galactosidase assays were developed as described previously (Miller, 1972).

### *Purification of WT DegU–$His_6$*

The C-terminal $His_6$-tag fusion to DegU was constructed as described (Hamoen *et al.*, 2000). Plasmid pNW43 was sequenced to ensure that there were no polymerase chain reaction (PCR)-introduced mutations, and was used to generate DegU–$His_6$ in *E. coli* strain BL21 (DE3). Cells carrying pNW43 were grown to an $OD_{600}$ of 0.5, and DegU–$His_6$ production was induced by addition of 50 μM IPTG and growth overnight at 26°C. The cells were harvested and washed twice in 500 ml of 20 mM Tris-HCl pH 8.0 and 200 mM NaCl. The washed cells were suspended in 3.5 ml lysis buffer per 1 g wet weight cells (20 mM Tris-HCl pH 8.0, 10 mM imadazole, 2 mM benzamidine, 1.0% Triton X-100, 200 mM NaCl, one Roche EDTA minus protease inhibitor cocktail tablet per 7 ml). The suspended cells were incubated in the presence of 1 mg $ml^{-1}$ lysozyme on ice for 30 min prior to sonication (6 bursts of 10 s). After centrifugation, the supernatant was incubated with 2 ml of Ni-NTA beads (Qiagen) at 4°C with rotation for 1 h. The beads were loaded onto a column and washed three times with 2 ml of 20 mM Tris-HCl pH 8.0, 200 mM NaCl and 30 mM imadazole. The protein was eluted with up to 250 mM imadazole, analysed by SDS-PAGE to assess the purity (> 95%), and dialysed against 20 mM Tris-HCl pH 8.0 and 200 mM NaCl. Concentrations were determined using the Bradford assay (Pierce). Aliquots containing 10% glycerol were stocked at –80°C. The eluted protein was used as an antigen for antibody production in a sheep (PTU/BS, Edinburgh, UK).

### *Electrophoretic mobility shift assays*

Protein–DNA gel shift assays were performed using the 550 bp fragment (P*yvcA*) used to make the P*yvcA–lacZ* transcriptional fusion (see above). A control 555 bp fragment internal of the coding sequence of *yvcA* (I*yvcA*) was amplified with primers 5′-GGA GGAT GCA GTAT GAA TGA C-3′ and 5′-CGT ATT CTA CTC CTA GGT TAT CTT CC-3′. Fragments were labelled during amplification by labelling one primer per primer couple beforehand using [γ-$^{32}$P]ATP (Amersham Biosciences) and T4 polynucleotide kinase (New England Biolabs). Binding mixtures, in a total volume of 30 μl, contained: 30 mM Tris-HCl pH 8.0, 1 mM $MgCl_2$, 75 mM NaCl, 4% glycerol, 1 mM dithiothreitol, 0.05% Nonidet P-40, 50 ng $\mu l^{-1}$ bovine serum albumin, 50 ng $\mu l^{-1}$ poly(dI-dC), DegU–$His_6$ as indicated and ~1 ng $^{32}$P-labelled DNA. For the competition experiments, 100-fold excess unlabelled P*yvcA* or IyvcA DNA was included before adding the $^{32}$P-labelled DNA. The assays were initiated by addition of $^{32}$P-labelled DNA, and incubation was at room temperature for 30 min. Samples (15 μl) were loaded onto a 4% polyacrylamide 0.5× TBE gel and run for 75 min at 100 V. Visualization was by autoradiography after exposure overnight to a Fujifilm Phosphoimaging Plate.

*Western blot analysis*

To obtain samples for immunoblot analysis, a single colony from a freshly streaked plate was inoculated into 3 ml of LB and grown to an $OD_{600}$ of 1.0. The culture was subsequently diluted to $OD_{600}$ of 0.05 in fresh LB medium, containing IPTG as required. The cells were grown to an $OD_{600}$ of 2.5, at which point 1 ml of cells was collected by centrifugation. The pellet was suspended in 150 µl SDS-PAGE loading dye and incubated at 95°C for 5 min. The debris was removed by centrifugation, and equal cell volumes were loaded onto a 12% SDS-PAGE and subsequently transferred to nitrocellulose membrane. The membrane was incubated for 2 h at room temperature in 5% dried milk in 1× Tris-buffered saline, then incubated for 1 h at room temperature with the primary antibody at a dilution of 1:5000. The membrane was washed well and incubated with the secondary antibody conjugated with horseradish peroxidase (Rabbit anti-Sheep, Pierce) at a dilution of 1:10 000, washed well again, developed with ECL reagents, and exposed to X-ray film.

**Acknowledgements**

We acknowledge the BBSRC David Phillips Fellowship (Grant Number BB/C520404/1) for funding. T.B.K. was supported in part by an S.G.M. vacation scholarship (VS06/15). We would like to thank Dr R. Britton (Michigan State University) for pDR111, Professor G. Rapoport (Pasteur Institute) for strain QB4414, Dr M. Fujita (University of Houston) for pMF302, Dr A. Moir (Sheffield University) for SPP1 phage, Professor J. Helmann (Cornell University) for plasmid pDG1663, The Sequencing Service (http://www.dnaseq.co.uk) for DNA sequencing, and Professor F. Sargent (University of Dundee), Dr M Hamon (Pasteur Institute), Dr B. Lazazzera (University of California Los Angeles) and Dr D. Kearns (Indiana University) for useful discussions. We would like to thank the anonymous reviewers for very helpful advice and insightful experimental suggestions.

**References**

Amati, G., Bisicchia, P., and Galizzi, A. (2004) DegU-P represses expression of the motility *fla-che* operon in *Bacillus subtilis*. *J Bacteriol* **186:** 6003–6014.

Barraud, N., Hassett, D.J., Hwang, S.H., Rice, S.A., Kjelleberg, S., and Webb, J.S. (2006) Involvement of nitric oxide in biofilm dispersal of *Pseudomonas aeruginosa*. *J Bacteriol* **188:** 7344–7353.

Bassler, B.L., and Losick, R. (2006) Bacterially speaking. *Cell* **125:** 237–246.

Beier, D., and Gross, R. (2006) Regulation of bacterial virulence by two-component systems. *Curr Opin Microbiol* **9:** 143–152.

Boles, B.R., and McCarter, L.L. (2002) *Vibrio parahaemolyticus scrABC*, a novel operon affecting swarming and capsular polysaccharide regulation. *J Bacteriol* **184:** 5946–5954.

Bouche, S., Klauck, E., Fischer, D., Lucassen, M., Jung, K., and Hengge-Aronis, R. (1998) Regulation of RssB-dependent proteolysis in *Escherichia coli*: a role for acetyl phosphate in a response regulator-controlled process. *Mol Microbiol* **27:** 787–795.

Branda, S.S., Gonzalez-Pastor, J.E., Ben-Yehuda, S., Losick, R., and Kolter, R. (2001) Fruiting body formation by *Bacillus subtilis*. *Proc Natl Acad Sci USA* **98:** 11621–11626.

Branda, S.S., Vik, S., Friedman, L., and Kolter, R. (2005) Biofilms: the matrix revisited. *Trends Microbiol* **13:** 20–26.

Branda, S.S., Chu, F., Kearns, D.B., Losick, R., and Kolter, R. (2006) A major protein component of the *Bacillus subtilis* biofilm matrix. *Mol Microbiol* **59:** 1229–1238.

Britton, R.A., Eichenberger, P., Gonzalez-Pastor, J.E., Fawcett, P., Monson, R., Losick, R., and Grossman, A.D. (2002) Genome-wide analysis of the stationary-phase sigma factor (Sigma-H) regulon of *Bacillus subtilis*. *J Bacteriol* **184:** 4881–4890.

Burkholder, P.R., and Giles, N.H. (1947) Induced biochemical mutations in *Bacillus subtilis*. *Am J Bot* **34:** 345.

Caiazza, N.C., Merritt, J.H., Brothers, K.M., and O'Toole, G.A. (2007) Inverse regulation of biofilm formation and swarming motility by *Pseudomonas aeruginosa* PA14. *J Bacteriol* **189:** 3603–3612.

Chu, F., Kearns, D.B., Branda, S.S., Kolter, R., and Losick, R. (2006) Targets of the master regulator of biofilm formation in *Bacillus subtilis*. *Mol Microbiol* **59:** 1216–1228.

Claessen, D., de Jong, W., Dijkhuizen, L., and Wosten, H.A. (2006) Regulation of *Streptomyces* development: reach for the sky!. *Trends Microbiol* **14:** 313–319.

Cummings, C.A., Bootsma, H.J., Relman, D.A., and Miller, J.F. (2006) Species- and strain-specific control of a complex, flexible regulon by Bordetella BvgAS. *J Bacteriol* **188:** 1775–1785.

Dahl, M.K., Msadek, T., Kunst, F., and Rapoport, G. (1991) Mutational analysis of the *Bacillus subtilis* DegU regulator and its phosphorylation by the DegS protein kinase. *J Bacteriol* **173:** 2539–2547.

Dahl, M.K., Msadek, T., Kunst, F., and Rapoport, G. (1992) The phosphorylation state of the DegU response regulator acts as a molecular switch allowing either degradative enzyme synthesis or expression of genetic competence in *Bacillus subtilis*. *J Biol Chem* **267:** 14509–14514.

Dubnau, D., Hahn, J., Roggiani, M., Piazza, F., and Weinrauch, Y. (1994) Two-component regulators and genetic competence in *Bacillus subtilis*. *Res Microbiol* **145:** 403–411.

Fujita, M., Gonzalez-Pastor, J.E., and Losick, R. (2005) High- and low-threshold genes in the Spo0A regulon of *Bacillus subtilis*. *J Bacteriol* **187:** 1357–1368.

Gonzalez-Pastor, J.E., Hobbs, E.C., and Losick, R. (2003) Cannibalism by sporulating bacteria. *Science* **301:** 510–513.

Guerout-Fleury, A.M., Frandsen, N., and Stragier, P. (1996) Plasmids for ectopic integration in *Bacillus subtilis*. *Gene* **180:** 57–61.

Hamoen, L.W., Van Werkhoven, A.F., Venema, G., and Dubnau, D. (2000) The pleiotropic response regulator DegU functions as a priming protein in competence development in *Bacillus subtilis*. *Proc Natl Acad Sci USA* **97:** 9246–9251.

Hamoen, L.W., Venema, G., and Kuipers, O.P. (2003) Controlling competence in *Bacillus subtilis*: shared use of regulators. *Microbiology* **149:** 9–17.

Hamon, M.A., and Lazazzera, B.A. (2001) The sporulation

transcription factor Spo0A is required for biofilm development in *Bacillus subtilis*. *Mol Microbiol* **42:** 1199–1209.
Harwood, C.R., and Cutting, S.M. (1990) *Molecular Biological Methods for Bacillus*. Chichester: John Wiley & Sons.
Henner, D.J., Yang, M., and Ferrari, E. (1988) Localization of *Bacillus subtilis* sacU (Hy) mutations to two linked genes with similarities to the conserved procaryotic family of two-component signalling systems. *J Bacteriol* **170:** 5102–5109.
Hutchings, M.I., Hong, H.J., and Buttner, M.J. (2006) The vancomycin resistance VanRS two-component signal transduction system of *Streptomyces coelicolor*. *Mol Microbiol* **59:** 923–935.
Kaplan, H.B. (2003) Multicellular development and gliding motility in *Myxococcus xanthus*. *Curr Opin Microbiol* **6:** 572–577.
Kearns, D.B., and Losick, R. (2003) Swarming motility in undomesticated *Bacillus subtilis*. *Mol Microbiol* **49:** 581–590.
Kearns, D.B., Chu, F., Branda, S.S., Kolter, R., and Losick, R. (2005) A master regulator for biofilm formation by *Bacillus subtilis*. *Mol Microbiol* **55:** 739–749.
Kunst, F., and Rapoport, G. (1995) Salt stress is an environmental signal affecting degradative enzyme synthesis in *Bacillus subtilis*. *J Bacteriol* **177:** 2403–2407.
Kunst, F., Pascal, M., Lepesant-Kejzlarova, J., Lepesant, J.A., Billault, A., and Dedonder, R. (1974) Pleiotropic mutations affecting sporulation conditions and the syntheses of extracellular enzymes in *Bacillus subtilis* 168. *Biochimie* **56:** 1481–1489.
Kunst, F., Msadek, T., Bignon, J., and Rapoport, G. (1994) The DegS/DegU and ComP/ComA two-component systems are part of a network controlling degradative enzyme synthesis and competence in *Bacillus subtilis*. *Res Microbiol* **145:** 393–402.
Mader, U., Antelmann, H., Buder, T., Dahl, M.K., Hecker, M., and Homuth, G. (2002) *Bacillus subtilis* functional genomics: genome-wide analysis of the DegS-DegU regulon by transcriptomics and proteomics. *Mol Genet Genomics* **268:** 455–467.
Miller, J. (1972) *Experiments in Molecular Genetics*. Cold Spring Harbor, NY: Cold Spring Harbor Laboratory.
Molle, V., Fujita, M., Jensen, S.T., Eichenberger, P., Gonzalez-Pastor, J.E., Liu, J.S., and Losick, R. (2003) The Spo0A regulon of *Bacillus subtilis*. *Mol Microbiol* **50:** 1683–1701.
Morikawa, M., Kagihiro, S., Haruki, M., Takano, K., Branda, S., Kolter, R., and Kanaya, S. (2006) Biofilm formation by a *Bacillus subtilis* strain that produces gamma-polyglutamate. *Microbiology* **152:** 2801–2807.
Msadek, T., Kunst, F., Henner, D., Klier, A., Rapoport, G., and Dedonder, R. (1990) Signal transduction pathway controlling synthesis of a class of degradative enzymes in *Bacillus subtilis*: expression of the regulatory genes and analysis of mutations in degS and degU. *J Bacteriol* **172:** 824–834.
Mukai, K., Kawata, M., and Tanaka, T. (1990) Isolation and phosphorylation of the *Bacillus subtilis* degS and degU gene products. *J Biol Chem* **265:** 20000–20006.
Nakano, M.M., Corbell, N., Besson, J., and Zuber, P. (1992) Isolation and characterization of sfp: a gene that functions in the production of the lipopeptide biosurfactant, surfactin, in *Bacillus subtilis*. *Mol Gen Genet* **232:** 313–321.
Ogura, M., and Tanaka, T. (1996) *Bacillus subtilis* DegU acts as a positive regulator for comK expression. *FEBS Lett* **397:** 173–176.
Ogura, M., Yamaguchi, H., Yoshida, K.-I., Fujita, Y., and Tanaka, T. (2001) DNA microarray analysis of *Bacillus subtilis* DegU, ComA and PhoP regulons: an approach to comprehensive nalysis of *B. subtilis* two-component regulatory systems. *Nucleic Acids Res* **29:** 3804–3813.
Ogura, M., Shimane, K., Asai, K., Ogasawara, N., and Tanaka, T. (2003) Binding of response regulator DegU to the aprE promoter is inhibited by RapG, which is counteracted by extracellular PhrG in *Bacillus subtilis*. *Mol Microbiol* **49:** 1685–1697.
Piggot, P.J., and Hilbert, D.W. (2004) Sporulation of *Bacillus subtilis*. *Curr Opin Microbiol* **7:** 579–586.
Roberts, M.F.C. (1995) Recombination and migration rates in natural populations of *Bacillus subtilis* and *Bacillus mojavensis*. *Evolution* **49:** 1081–1094.
Shimane, K., and Ogura, M. (2004) Mutational analysis of the helix-turn-helix region of *Bacillus subtilis* response regulator DegU, and identification of cis-acting sequences for DegU in the aprE and comK promoters. *J Biochem (Tokyo)* **136:** 387–397.
Stanley, N.R., and Lazazzera, B.A. (2005) Defining the genetic differences between wild and domestic strains of *Bacillus subtilis* that affect poly-gamma-dl-glutamic acid production and biofilm formation. *Mol Microbiol* **57:** 1143–1158.
Stanley, N.R., Britton, R.A., Grossman, A.D., and Lazazzera, B.A. (2003) Identification of catabolite repression as a physiological regulator of biofilm formation by *Bacillus subtilis* by use of DNA microarrays. *J Bacteriol* **185:** 1951–1957.
Steil, L., Hoffmann, T., Budde, I., Volker, U., and Bremer, E. (2003) Genome-wide transcriptional profiling analysis of adaptation of *Bacillus subtilis* to high salinity. *J Bacteriol* **185:** 6358–6370.
Straight, P.D., Willey, J.M., and Kolter, R. (2006) Interactions between *Streptomyces coelicolor* and *Bacillus subtilis*: role of surfactants in raising aerial structures. *J Bacteriol* **188:** 4918–4925.
Tjalsma, H., Kontinen, V.P., Pragai, Z., Wu, H., Meima, R., Venema, G., *et al.* (1999) The role of lipoprotein processing by signal peptidase II in the Gram-positive eubacterium bacillus subtilis. Signal peptidase II is required for the efficient secretion of alpha-amylase, a non-lipoprotein. *J Biol Chem* **274:** 1698–1707.
Webb, J.S., Lau, M., and Kjelleberg, S. (2004) Bacteriophage and phenotypic variation in *Pseudomonas aeruginosa* biofilm development. *J Bacteriol* **186:** 8066–8073.

## Supplementary material

The following supplementary material is available for this article:

**Fig. S1.** Electrophoretic mobility shift assay with DegU and *comK* promoter fragment. The 325 bp *comK* promoter fragment (P*comK*) was prepared by PCR using primers 5′-CCG GAA TTC AGA ATC CCC CCA ATG CC-3′ and 5′-CGG GAT

CCC AGT CTG TTT TCT GAC TCA TAT T-3′ (Hamoen *et al*., 2000; Shimane and Ogura, 2004). As a negative control, a 316 bp fragment internal of the coding sequence of *comK* (I*comK*) was amplified using primers 5′-CGC TGC AAA TTG TCG ACA GA-3′ and 5′-GGT TCT GAG CCA CGC TGT TC-3′. The shifted DegU–*comK* complex is indicated by an arrow. Labelling and assay conditions were as described in the *Experimental procedures*.

**Fig. S2.** DegU~P regulates swarming motility. Swarming motility of: (A) WT (3610), *degS* (NRS1358) and *degU* (NRS1314) strains; (B) the *degU* mutant carrying the $P_{IPTG}$–*degU-noP* allele (NRS1327); (C) the *degU* mutant carrying the $P_{IPTG}$–*degU–WT* allele (NRS1326); and (D) the *degU* mutant carrying the $P_{IPTG}$–*degU-hy-P* allele (NRS1325), in the presence of the indicated IPTG concentrations. Swarming motility was followed as described in the *Experimental procedures*, and plotted is the average radius of the swarm versus time in hours. The bars represent the standard error of the mean.

**Table S1.** Potential DegU-regulated targets.

**Table S2.** *Bacillus subtilis* strains used in this study.

**Table S3.** Primer sequences used to construct insertion mutants.

This material is available as part of the online article from:
http://www.blackwell-synergy.com/doi/abs/10.1111/j.1365-2958.2007.05810.x
(This link will take you to the article abstract).

Please note: Blackwell Publishing is not responsible for the content or functionality of any supplementary materials supplied by the authors. Any queries (other than missing material) should be directed to the corresponding author for the article.

*Microbiology* (2009), **155**, 1–8 **DOI** 10.1099/mic.0.023903-0

Mini-Review

# A pivotal role for the response regulator DegU in controlling multicellular behaviour

Ewan J. Murray, Taryn B. Kiley and Nicola R. Stanley-Wall

Division of Molecular and Environmental Microbiology, College of Life Sciences, MSI/WTB/JBC Complex, University of Dundee, Dundee DD1 5EH, UK

Correspondence
Nicola R. Stanley-Wall
n.r.stanleywall@dundee.ac.uk

Bacteria control multicellular behavioural responses, including biofilm formation and swarming motility, by integrating environmental cues through a complex regulatory network. Heterogeneous gene expression within an otherwise isogenic cell population that allows for differentiation of cell fate is an intriguing phenomenon that adds to the complexity of multicellular behaviour. This review focuses on recent data about how DegU, a pleiotropic response regulator, co-ordinates multicellular behaviour in *Bacillus subtilis*. We review studies that challenge the conventional understanding of the molecular mechanisms underpinning the DegU regulatory system and others that describe novel targets of DegU during activation of biofilm formation by *B. subtilis*. We also discuss a novel role for DegU in regulating multicellular processes in the food-borne pathogen *Listeria monocytogenes*.

## Multicellular behaviour in single-celled prokaryotes

It is easy to forget that when bacteria are grown in the laboratory the conditions used to generate such rapidly dividing free-living cells are very different from those in the natural environment. Most bacteria exist in their natural habitats as sessile multicellular communities called biofilms in which the bacterial population differentiates as part of the development process (Costerton *et al.*, 1995; Vlamakis *et al.*, 2008). That most bacterial species can live and grow within a shared habitat, and co-ordinate complex group behaviour that benefits the whole community, is still a relatively new concept (Shapiro, 1998). Examples of such behaviour leading to the propagation of bacterial spores include fruiting body formation in *Myxococcus xanthus* (Kaplan, 2003), biofilm formation and fruiting-body-like assembly in *Bacillus subtilis* (Branda *et al.*, 2001) and aerial hyphae development in *Streptomyces coelicolor* (Claessen *et al.*, 2006).

## Experimental advances provide insight into multicellular behaviour

*B. subtilis*, like other bacterial species, is capable of manifesting different multicellular processes. Studies have focussed on understanding how this species is able to co-ordinate processes that include sporulation (Piggot & Hilbert, 2004), the uptake of exogenous DNA (genetic competence) (Hamoen *et al.*, 2003), social motility (swarming) (Kearns & Losick, 2003), extracellular protease production (Dahl *et al.*, 1992), and biofilm formation/complex colony development (Branda *et al.*, 2001; Hamon & Lazazzera, 2001). Investigations on multicellular behaviour in *B. subtilis* have advanced through three main approaches. First, investigations using 'wild' isolates led to the discovery that laboratory strains had lost their ability to express some of the multicellular behaviours described above (Branda *et al.*, 2001; Kearns & Losick, 2003; Stanley & Lazazzera, 2005). *B. subtilis* laboratory isolates such as 168 (Spizizen, 1958) were derived from a progenitor strain that was treated with X-rays or chemical mutagens to make the cells more tractable (Srivatsan *et al.*, 2008; Zeigler *et al.*, 2008). The genes in which the mutations were introduced are now recognized as important for social behaviour and their identification helped to elucidate the genetic circuitry underpinning multicellular responses to the environment (Kearns & Losick, 2003, 2005; Kearns *et al.*, 2004; Stanley & Lazazzera, 2005). Second, developments in the use of fluorescent reporter fusions enable gene expression to be monitored readily within the single cell by flow cytometry. Third, advances in microscopy techniques allow the detection of cell differentiation in an otherwise isogeneic bacterial population (Veening *et al.*, 2004, 2005; Vlamakis *et al.*, 2008).

## Co-ordination of multicellular behaviour processes by DegS–DegU

Two-component signal transduction systems are the major family of signalling proteins by which bacteria sense and respond to changes in the environment. They typically consist of a membrane-associated histidine kinase (DegS) and a cytoplasmic response regulator (DegU). The former detects the signal or stress, whereas the latter controls cellular response, predominantly through gene transcription (Mascher *et al.*, 2006). DegU plays a key role in

 

**Smits, W. K., Hoa, T. T., Hamoen, L. W., Kuipers, O. P. & Dubnau, D. (2007).** Antirepression as a second mechanism of transcriptional activation by a minor groove binding protein. *Mol Microbiol* **64**, 368–381.

**Spizizen, J. (1958).** Transformation of biochemically deficient strains of *Bacillus subtilis* by deoxyribonucleate. *Proc Natl Acad Sci U S A* **44**, 1072–1078.

**Srivatsan, A., Han, Y., Peng, J., Tehranchi, A. K., Gibbs, R., Wang, J. D. & Chen, R. (2008).** High-precision, whole-genome sequencing of laboratory strains facilitates genetic studies. *PLoS Genet* **4**, e1000139.

**Stanley, N. R. & Lazazzera, B. A. (2005).** Defining the genetic differences between wild and domestic strains of *Bacillus subtilis* that affect poly-γ-DL-glutamic acid production and biofilm formation. *Mol Microbiol* **57**, 1143–1158.

**Tanaka, T., Kawata, M. & Mukai, K. (1991).** Altered phosphorylation of *Bacillus subtilis* DegU caused by single amino acid changes in DegS. *J Bacteriol* **173**, 5507–5515.

**Tsukahara, K. & Ogura, M. (2008).** Promoter selectivity of the *Bacillus subtilis* response regulator DegU, a positive regulator of the *fla/che* operon and *sacB*. *BMC Microbiol* **8**, 8.

**Veening, J. W., Smits, W. K., Hamoen, L. W., Jongbloed, J. D. & Kuipers, O. P. (2004).** Visualization of differential gene expression by improved cyan fluorescent protein and yellow fluorescent protein production in *Bacillus subtilis*. *Appl Environ Microbiol* **70**, 6809–6815.

**Veening, J. W., Hamoen, L. W. & Kuipers, O. P. (2005).** Phosphatases modulate the bistable sporulation gene expression pattern in *Bacillus subtilis*. *Mol Microbiol* **56**, 1481–1494.

**Veening, J. W., Igoshin, O. A., Eijlander, R. T., Nijland, R., Hamoen, L. W. & Kuipers, O. P. (2008a).** Transient heterogeneity in extracellular protease production by *Bacillus subtilis*. *Mol Syst Biol* **4**, 184.

**Veening, J. W., Smits, W. K. & Kuipers, O. P. (2008b).** Bistability, epigenetics, and bet-hedging in Bacteria. *Annu Rev Microbiol* **62**, 193–210.

**Verhamme, D. T., Kiley, T. B. & Stanley-Wall, N. R. (2007).** DegU co-ordinates multicellular behaviour exhibited by *Bacillus subtilis*. *Mol Microbiol* **65**, 554–568.

**Verhamme, D. T., Murray, E. J. & Stanley-Wall, N. R. (2008).** DegU and Spo0A jointly control transcription of two loci required for complex colony development by *Bacillus subtilis*. *J Bacteriol*, Oct 31 [Epub ahead of print]

**Vlamakis, H., Aguilar, C., Losick, R. & Kolter, R. (2008).** Control of cell fate by the formation of an architecturally complex bacterial community. *Genes Dev* **22**, 945–953.

**Williams, T., Bauer, S., Beier, D. & Kuhn, M. (2005a).** Construction and characterization of *Listeria monocytogenes* mutants with in-frame deletions in the response regulator genes identified in the genome sequence. *Infect Immun* **73**, 3152–3159.

**Williams, T., Joseph, B., Beier, D., Goebel, W. & Kuhn, M. (2005b).** Response regulator DegU of *Listeria monocytogenes* regulates the expression of flagella-specific genes. *FEMS Microbiol Lett* **252**, 287–298.

**Wolfe, A. J. (2005).** The acetate switch. *Microbiol Mol Biol Rev* **69**, 12–50.

**Wolfe, A. J., Chang, D. E., Walker, J. D., Seitz-Partridge, J. E., Vidaurri, M. D., Lange, C. F., Prüss, B. M., Henk, M. C., Larkin, J. C. & Conway, T. (2003).** Evidence that acetyl phosphate functions as a global signal during biofilm development. *Mol Microbiol* **48**, 977–988.

**Wolfe, A. J., Parikh, N., Lima, B. P. & Zemaitaitis, B. (2008).** Signal integration by the two-component signal transduction response regulator CpxR. *J Bacteriol* **190**, 2314–2322.

**Yasumura, A., Abe, S. & Tanaka, T. (2008).** Involvement of nitrogen regulation in *Bacillus subtilis degU* expression. *J Bacteriol* **190**, 5162–5171.

**Zeigler, D. R., Pragai, Z., Rodriguez, S., Chevreux, B., Muffler, A., Albert, T., Bai, R., Wyss, M. & Perkins, J. B. (2008).** The origins of 168, W23, and other *Bacillus subtilis* legacy strains. *J Bacteriol* **190**, 6983–6995.

regulating post-exponential-phase processes in *B. subtilis*, including activation and inhibition of genetic competence (Dubnau *et al.*, 1994; Kunst *et al.*, 1994; Ogura & Tanaka, 1996), activation and inhibition of motility (Amati *et al.*, 2004; Kobayashi, 2007; Verhamme *et al.*, 2007), activation of degradative enzyme production (Dahl *et al.*, 1992; Msadek *et al.*, 1990), activation of poly-$\gamma$-glutamic acid production (Stanley & Lazazzera, 2005) and also the activation and inhibition of biofilm formation (Kobayashi, 2007; Verhamme *et al.*, 2007). DegU has regulatory activity in both its unphosphorylated and phosphorylated states. This initially led to its designation as a 'molecular switch' dependent on DegU phosphorylation by DegS (Dahl *et al.*, 1992). However, recent studies using wild isolates of *B. subtilis* indicate that DegU~P functions as a 'rheostat' that senses and responds to changes in the environment. This, in turn, enables the integration of genetic competence, swarming motility, biofilm formation and exoprotease production along an increasing gradient of DegU phosphorylation (Kobayashi, 2007; Verhamme *et al.*, 2007).

## Mechanism of DegU and DegU~P in response to signalling

In its unphosphorylated state DegU activates genetic competence through the recruitment of ComK (Hamoen *et al.*, 2000). ComK functions as an anti-repressor for the transcriptional repressors Rok and CodY, and thereby allows the expression of its own gene. This permits the establishment of the bistable system pre-required for competence development (Albano *et al.*, 2005; Smits *et al.*, 2007). In contrast, DegU~P recruits RNA polymerase at promoter regions of genes such as *yvcA* and *aprE* to activate biofilm formation and exoprotease production respectively (Ogura *et al.*, 2003; Verhamme *et al.*, 2007). Recent genome-wide transcription and proteomic studies have identified over 170 genes (~4 % of the *B. subtilis* genome) that are regulated by DegU~P under various growth conditions (Kobayashi, 2007; Mader *et al.*, 2002; Ogura *et al.*, 2001). Therefore the mechanism by which DegU~P coordinates multicellular behaviour processes in response to signal perception is challenging. One simple model supported by *in vitro* data indicates that DegU~P has specific affinities for different promoter regions. For example, the *flgB* promoter has a higher affinity for DegU~P than the *sacB* promoter. This provides the molecular basis by which swarming motility could be activated prior to other multicellular processes (Kobayashi, 2007; Tsukahara & Ogura, 2008). Variations in promoter binding affinities by transcription factors may represent a common mechanism mediating control over multicellular behaviour responses. High- and low-affinity binding sites in *B. subtilis* are used within the promoter regions of genes controlled by Spo0A. At low levels of Spo0A phosphorylation, biofilm formation and cannibalism are regulated. In contrast, the activation of sporulation occurs at high levels of Spo0A phosphorylation (Fujita *et al.*, 2005). However, the question arises: Why does a process that is activated at lower levels of signal perception not occur in the presence of a high level of the signal? The first possibility is that when low-affinity promoters are triggered, a negative feedback loop blocks the process that is controlled by the high-affinity promoters. Second, the promoter regions contain multiple binding sites, with specific affinities, that result in the activation of transcription at low levels of signal perception but inhibition of transcription at high levels of signal. Third, multiple environmental conditions need to be sensed and integrated by the cell to activate a physiological response.

## A three-tiered regulatory system controls DegS–DegU activity

Given the central role that DegS and DegU have in coordinating multicellular responses in *B. subtilis* it is not surprising that the DegS–DegU regulatory system is finely controlled at the following three stages within the cell: *degU* transcription, DegU phosphorylation and DegU~P activity.

### *degU* transcription

The *degSU* operon contains three promoters (Veening *et al.*, 2008a; Yasumura *et al.*, 2008). The first is upstream of *degS* and drives the expression of *degS* and *degU*. The second is located within the coding region of *degS* and increases the level of *degU* under nitrogen-limiting conditions. The third is located in the *degS–degU* intergenic region and increases the level of *degU* in response to DegU~P. In laboratory isolates, the positive auto-regulation of *degU* transcription (Fig. 1) by DegU~P leads to the heterogeneous expression of *degU* within the population (Veening *et al.*, 2008a, b).

### DegU phosphorylation

DegS is a cytoplasmic bifunctional protein that exhibits kinase and phosphatase activities (Tanaka *et al.*, 1991). DegS interacts with the SMC–ScpA–ScpB complex, which controls DNA condensation and repair. The interaction of DegS with ScpA inhibits its kinase activity and results in a decrease in the pool of DegU~P within the cell. As the level of SMC–ScpA–ScpB complex decreases during stationary phase there is an increase in the level of DegU~P in that growth phase (Dervyn *et al.*, 2004). Transfer of the phosphate moiety from DegS to DegU (Fig. 1) is enhanced in the presence of DegQ, a small protein of 46 amino acids (Kobayashi, 2007). Some laboratory isolates of *B. subtilis* contain a point mutation within the promoter of *degQ* that reduces the level of DegQ synthesized (Stanley & Lazazzera, 2005); this in turn, reduces the level of DegU~P in the cell (Kobayashi, 2007; Stanley & Lazazzera, 2005; Verhamme *et al.*, 2007). This single point mutation highlights one of the key genomic differences between wild and laboratory isolates of *B. subtilis* that influences multicellular behaviour (Kearns *et al.*, 2004; Kobayashi, 2008; Stanley & Lazazzera, 2005). Transcription of *degQ* is regulated by the quorum-sensing-responsive transcription factor ComA (Msadek *et al.*, 1991). This ensures that DegU~P in the cell increases alongside an increase in cell density and is maximal at

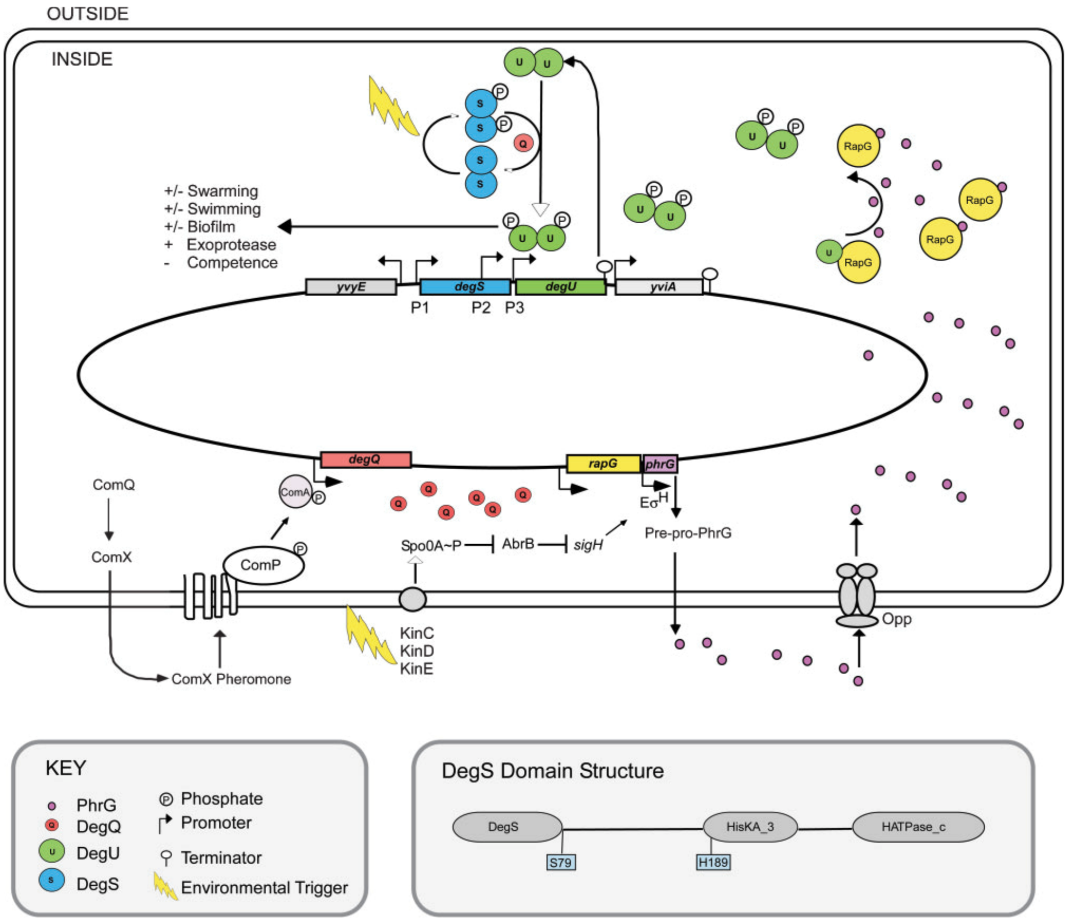


**Fig. 1.** The DegS–DegU regulatory system of *B. subtilis*. The names of the genes are indicated. Open arrowheads indicate a change in the phosphorylation state. The lower left-hand insert provides a symbol key and the lower right-hand insert depicts the domain structure of DegS, with the HisKA_3 and HATPase_c domains identified by Pfam shown in grey. S79 represents serine amino acid number 79; H189 represents the site of autophosphorylation on histidine 189. '+' represents activation and '–' represents inhibition.

stationary phase. DegQ does not affect the stability of DegS~P or block the intrinsic phosphatase action of DegS (Kobayashi, 2007); therefore the mechanism by which DegS controls the balance of phosphatase and kinase activity remains unknown.

### DegU~P activity

The **r**esponse regulator **a**spartyl **p**hosphatase (Rap) RapG binds to DegU, without affecting the latter's phosphorylation status. This suggests that RapG inhibits the ability of DegU to bind to target promoter DNA (Ogura *et al.*, 2003). RapG is encoded in an operon with PhrG, a **ph**osphatase **r**egulator (Phr). Although *rapG* and *phrG* share a common promoter upstream of *rapG*, the transcription of *phrG* is also activated by a $\sigma^H$-dependent promoter on entry to stationary phase (Britton *et al.*, 2002). At high levels of PhrG production, PhrG interacts with RapG, lessening RapG inhibition of DegU activity. As the RapG–PhrG system functions as a quorum-sensing system (Fig. 1), DegU~P activity increases in parallel with an increase in cell density (Lazazzera *et al.*, 1999; Ogura *et al.*, 2003).

## New roles for DegU activity in *B. subtilis* during biofilm formation

DegU was first identified as a positive regulator of biofilm formation in a study using *B. subtilis* isolate RO-FF1

(Stanley & Lazazzera, 2005). Currently, three targets that are activated by DegU~P are known. The first is poly-γ-glutamic acid, an extracellular polymer that can form part of the extracellular matrix of some isolates of *B. subtilis*, though not in NCIB 3610 (Branda *et al.*, 2006; Morikawa *et al.*, 2006; Stanley & Lazazzera, 2005). This suggests that the specific requirements to form a multicellular community differ in a strain-dependent manner and highlights the value of scrutinizing different natural isolates. The other two targets for DegU are the proteins, YuaB and YvcA. YuaB is a small secreted protein required for pellicle formation and complex colony development in ATCC 6051 and NCIB 3610 (Kobayashi, 2007; Verhamme *et al.*, 2008). YvcA is a putative membrane-bound lipoprotein required for complex colony development in NCIB 3610 but not for pellicle formation in ATCC 6051 (Kobayashi, 2007; Verhamme *et al.*, 2007). A complex genetic circuit that is dependent on activation of DegU and Spo0A ensuring *yvcA* and *yuaB* transcription during complex colony development in *B. subtilis* NCIB 3610 has recently been described (Verhamme *et al.*, 2008).

## Heterogeneous *degU* expression and exoprotease production

During biofilm formation by *B. subtilis*, cells differentiate into specific subpopulations that become responsible for matrix production or sporulation (Chai *et al.*, 2008; Vlamakis *et al.*, 2008). This finding suggests that biofilm matrix production altruistically benefits the entire population/community, not just the producer cells. During heterogeneous gene expression, threshold levels of a key regulator controlling cell state need to be attained. This can be mediated by a positive feedback loop at the transcription stage (Losick & Desplan, 2008). Intriguingly it was recently reported that while *degU* transcription is auto-activated it is not sufficient to generate heterogeneous expression in wild-type laboratory isolates. However, when genetic manipulations are used to increase the level of DegU~P, a distinct bistable population was observed (Veening *et al.*, 2008a). In the same study it also was demonstrated that a small population of cells in which *aprE*, the gene encoding the major exoprotease of *B. subtilis*, is copiously transcribed can be established (Veening *et al.*, 2008a). Two criteria must be met for this to happen in the small subset of cells. First, Spo0A~P levels must increase to a threshold that stimulates derepression of *aprE* transcription (but not to such a level that the cells sporulate). Second, the levels of DegU~P in the cell must be high. This dual requirement of DegU and Spo0A activation as part of a genetic logic-AND network might represent a common mechanism for co-ordinating entry into the different multicellular behavioural processes of *B. subtilis* (Veening *et al.*, 2008a, b; Verhamme *et al.*, 2008). It remains to be seen whether intracellular fluctuations of phosphorylated DegU and Spo0A combined with intrinsic differences in promoter binding affinities co-ordinate the different multicellular behavioural processes manifested by *B. subtilis*.

## Motility and biofilm formation regulation by DegU in *L. monocytogenes*

The role of DegU in co-ordinating multicellular behaviour is not restricted to *B. subtilis*. *Listeria monocytogenes* is a Gram-positive facultative intracellular pathogen that causes listeriosis. DegU (encoded by *lmo2515*) regulates motility, biofilm formation and virulence in *Listeria* species (Gueriri *et al.*, 2008b; Knudsen *et al.*, 2004; Williams *et al.*, 2005a, b). The genome sequences of the pathogenic strain *L. monocytogenes* EGD-e and non-pathogenic strain *L. innocua* are remarkably similar to that of *B. subtilis* (Glaser *et al.*, 2001). However, in the region surrounding *degU*, the *degS* homologue is conspicuously absent despite other major genome features being maintained (Gueriri *et al.*, 2008b; Knudsen *et al.*, 2004). The absence of *degS* appears to be specific to the *Listeria* species (Fig. 2), although further evolutionary analyses are needed to establish whether *degS* has been lost from *Listeria* or gained by *Bacillus* (Gueriri *et al.*, 2008b).

Biofilm formation by *L. monocytogenes* is dependent on flagellar motility to propel the cells towards a surface prior to attachment (Lemon *et al.*, 2007). DegU was recently identified as a positive activator of flagellum biosynthesis (Knudsen *et al.*, 2004; Williams *et al.*, 2005a, b). When grown at $\leqslant 30$ °C *L. monocytogenes* has four to six simple peritrichous glycosylated flagella. The flagellum is glycosylated at multiple sites on the flagellin protein FlaA, with up to six glycosylation moieties per monomer. The glycosylation moiety is transferred to FlaA post-translationally by the bifunctional *O*-GlcNAc transferase GmaR (Shen *et al.*, 2006). The physiological significance of the glycosylation is not yet fully understood but it is proposed that it may be an important factor for environmental adaptation outside the host. At temperatures $\geqslant 37$ °C *L. monocytogenes* is typically non-motile. Inhibition of motility at high temperatures occurs through the tightly controlled repression of *flaA* transcription by the protein MogR, which binds to the *flaA* upstream promoter region (Shen & Higgins, 2006). It was initially proposed that DegU served as a direct activator of *flaA* transcription at low temperature, although later work showed that this role is indirect (Shen & Higgins, 2006). At low temperatures DegU activates transcription of *gmaR*, which encodes GmaR, the transcriptional activator of *flaA*. How DegU activates *gmaR* transcription at low temperatures but not at high temperatures remains unknown. GmaR is a bifunctional protein that first binds to MogR, removes it from the *flaA* promoter, and then glycosylates the FlaA protein. DegU also controls flagellin levels post-transcription, as transcription of *flaA* in a *mogR degU* strain background per se is not sufficient to restore motility (Shen & Higgins, 2006). This unique regulatory mechanism ensures that flagella of *L. monocytogenes* are only synthesized at low temperatures and that the flagella are fully glycosylated.

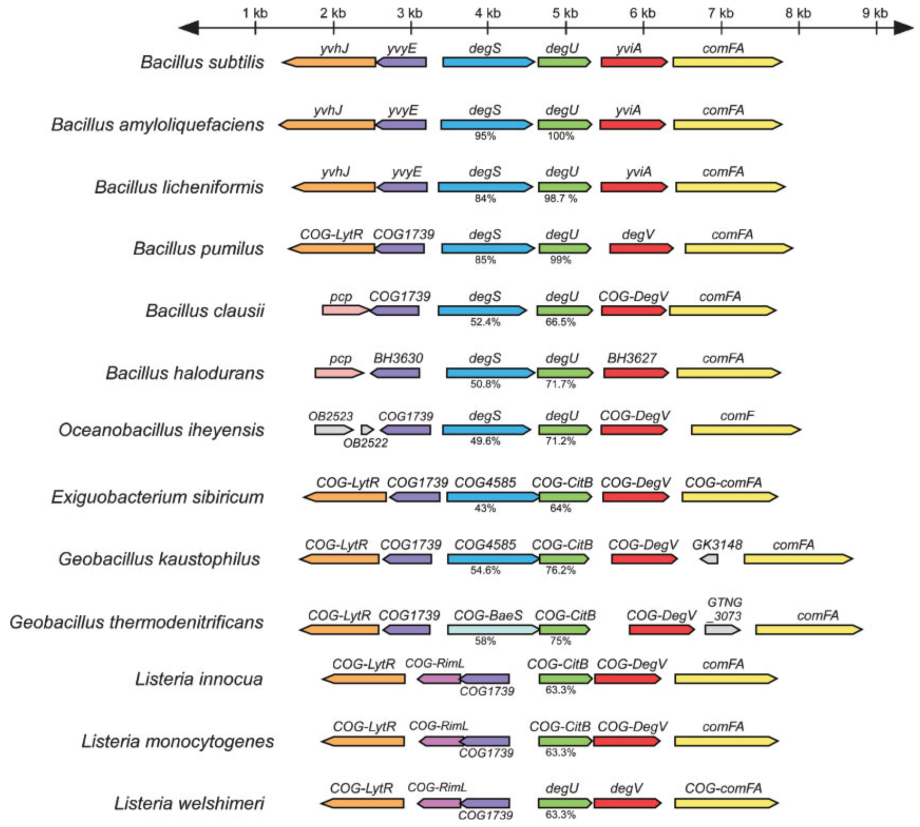


**Fig. 2.** Genome context of *degU* on the chromosome of *B. subtilis* with respect to other Gram-positive bacteria. The percentage identity at the protein level is indicated for *degU* and *degS* homologues under the gene. The gene size, position and direction are drawn to the scale indicated at the top of the diagram.

### DegU regulates virulence in *L. monocytogenes*

Although the mechanism for DegU-dependent motility is relatively well known, how DegU affects virulence is not yet understood. DegU mutant strains are still able to enter host cells with an efficiency that is comparable to, or even better than, that of wild-type cells (Williams *et al.*, 2005a). However, the bacterial load maintained within the spleen and other organs of the host is lower (Knudsen *et al.*, 2004). DegU-dependent control of virulence is not due to the non-motile phenotype because flagella-minus strains of *L. monocytogenes* remain virulent (Shen & Higgins, 2006). It will be exciting to understand how DegU contributes to virulence and how this is co-ordinated with its other roles in controlling motility and activation of biofilm formation (Gueriri *et al.*, 2008b).

### DegU is an orphan response regulator in *L. monocytogenes*

The absence of *degS* in *L. monocytogenes* raises questions about whether DegU can be phosphorylated, and if so, whether DegU~P is required to activate flagella-based motility and/or virulence. Although DegU is an orphan response regulator in *L. monocytogenes,* importantly there are no orphan sensor kinases encoded in its genome (Williams *et al.*, 2005a). It is possible that in the absence of a cognate or orphan sensor kinase, DegU could be phosphorylated by a non-cognate sensor kinase. However, this is very unlikely due to the inbuilt specificity mechanisms in a two-component regulatory system (Laub & Goulian, 2007). Alternatively, phosphorylation of DegU could be mediated via a small molecular phosphate donor such as acetyl phosphate. This is becoming increasingly

recognized as a global regulator of gene transcription (Wolfe *et al.*, 2003, 2008). The presence of an 'orphan' response regulator, or sensor kinase that also has phosphatase activity, suggests that acetyl phosphate may play a role in the signal transduction system (Wolfe, 2005). A study on motility and ethanol resistance by *L. monocytogenes* investigated whether DegU is required to be phosphorylated in order to carry out its regulatory function (Mauder *et al.*, 2008). These authors constructed a strain of *L. monocytogenes* carrying a variant of *degU* with a point mutation in the proposed phosphorylation site. They demonstrated a partial restoration of swimming motility in comparison with the *degU* mutant, though motility was less than that observed in the wild-type. These findings indicate that DegU retains some functionality in its unphosphorylated state, but do not rule out the possibility that DegU~P has some physiological role. Consistent with this suggestion, DegU of *L. monocytogenes* can be phosphorylated by acetyl phosphate *in vitro* and alterations in the level of acetyl phosphate *in vivo* control motility and biofilm formation (Gueriri *et al.*, 2008a). As the level of acetyl phosphate varies with both growth condition and growth phase (Klein *et al.*, 2007; Wolfe, 2005) it is possible that DegU functions as a read-out of the metabolic status of *L. monocytogenes*.

## Future studies

Since the advent of single-cell analyses and the observation of multicellular behaviour, the full potential of DegU as a central regulator in both *L. monocytogenes* and *B. subtilis* is becoming apparent. There remain many unanswered questions about how DegU functions in both *Bacillus* and *Listeria* species. A recent phosphoproteome screening of *B. subtilis* found that DegS can be phosphorylated on amino acid serine 79. This is outside the HisKA_3 domain containing histidine 189, which is the site (Fig. 1) of autophosphorylation (Macek *et al.*, 2007). This raises questions about whether phosphorylation on serine 79 has any physiological role in *B. subtilis*. For example, is the phosphorylation of serine 79 and histidine 189 responsible for controlling separate multicellular behaviour processes that are dependent on DegU~P in the face of different environmental stimuli? Additionally, growing evidence indicates that the function of DegU in laboratory isolates differs from that of wild isolates of *B. subtilis* (Kobayashi, 2007; Stanley & Lazazzera, 2005; Veening *et al.*, 2008a; Verhamme *et al.*, 2007). Therefore it remains to be established whether heterogeneous expression of *degU* occurs in wild isolates (e.g. NCIB 3160) of *B. subtilis*. If heterogeneous expression is observed, what influence does this have over the capacity to integrate multicellular behaviour responses? For *L. monocytogenes*, which lacks *degS*, it is important to establish whether a heterogeneous population dependent on DegU can be formed. If so, does the differentiation of tasks within the cell population confer any survival advantage to the bacterium both within and outside the host?

## Concluding remarks

It is likely that the DegS–DegU regulatory system will continue to provide an excellent model of a 'systems biology' approach. Thus objectives will be to understand how bacteria co-ordinate the decision-making processes that occur within the cell to ensure that the desired physiological response occurs in the face of different environmental conditions. Our ability to study multicellular behaviour in *B. subtilis*, and other closely related species, will be enhanced upon completion of genome sequences of natural isolates collected from a variety of geographical locations (http://www.bacillusgenomics.org/bsubtilis/index.html) (Earl *et al.*, 2007, 2008; Srivatsan *et al.*, 2008). Such data could be used to determine the impacts of genome polymorphisms on behaviour and adaptation.

## Acknowledgements

This work was supported by the Biotechnology and Biological Sciences Research Council (grant number BB/C520404/1, BB/E001572/1). We thank Professor Frank Sargent for helpful discussions and Professor Geoff Gadd for a critical assessment of the manuscript. We are grateful to the two anonymous reviewers and Dr Alisdair McLean for their expert comments, which significantly helped to improve the manuscript.

## References

**Albano, M., Smits, W. K., Ho, L. T., Kraigher, B., Mandic-Mulec, I., Kuipers, O. P. & Dubnau, D. (2005).** The Rok protein of *Bacillus subtilis* represses genes for cell surface and extracellular functions. *J Bacteriol* **187**, 2010–2019.

**Amati, G., Bisicchia, P. & Galizzi, A. (2004).** DegU-P represses expression of the motility *fla-che* operon in *Bacillus subtilis*. *J Bacteriol* **186**, 6003–6014.

**Branda, S. S., Gonzalez-Pastor, J. E., Ben-Yehuda, S., Losick, R. & Kolter, R. (2001a).** Fruiting body formation by *Bacillus subtilis*. *Proc Natl Acad Sci U S A* **98**, 11621–11626.

**Branda, S. S., Chu, F., Kearns, D. B., Losick, R. & Kolter, R. (2006).** A major protein component of the *Bacillus subtilis* biofilm matrix. *Mol Microbiol* **59**, 1229–1238.

**Britton, R. A., Eichenberger, P., Gonzalez-Pastor, J. E., Fawcett, P., Monson, R., Losick, R. & Grossman, A. D. (2002).** Genome-wide analysis of the stationary-phase sigma factor (Sigma-H) regulon of *Bacillus subtilis*. *J Bacteriol* **184**, 4881–4890.

**Chai, Y., Chu, F., Kolter, R. & Losick, R. (2008).** Bistability and biofilm formation in *Bacillus subtilis*. *Mol Microbiol* **67**, 254–263.

**Claessen, D., de Jong, W., Dijkhuizen, L. & Wosten, H. A. (2006).** Regulation of *Streptomyces* development: reach for the sky! *Trends Microbiol* **14**, 313–319.

**Costerton, J. W., Lewandowski, Z., Caldwell, D. E., Korber, D. R. & Lappin-Scott, H. M. (1995).** Microbial biofilms. *Annu Rev Microbiol* **49**, 711–745.

**Dahl, M. K., Msadek, T., Kunst, F. & Rapoport, G. (1992).** The phosphorylation state of the DegU response regulator acts as a molecular switch allowing either degradative enzyme synthesis or expression of genetic competence in *Bacillus subtilis*. *J Biol Chem* **267**, 14509–14514.

**Dervyn, E., Noirot-Gros, M. F., Mervelet, P., McGovern, S., Ehrlich, S. D., Polard, P. & Noirot, P. (2004).** The bacterial condensin/cohesin-like protein complex acts in DNA repair and regulation of gene expression. *Mol Microbiol* **51**, 1629–1640.

**Dubnau, D., Hahn, J., Roggiani, M., Piazza, F. & Weinrauch, Y. (1994).** Two-component regulators and genetic competence in *Bacillus subtilis*. *Res Microbiol* **145**, 403–411.

**Earl, A. M., Losick, R. & Kolter, R. (2007).** *Bacillus subtilis* genome diversity. *J Bacteriol* **189**, 1163–1170.

**Earl, A. M., Losick, R. & Kolter, R. (2008).** Ecology and genomics of *Bacillus subtilis*. *Trends Microbiol* **16**, 269–275.

**Fujita, M., Gonzalez-Pastor, J. E. & Losick, R. (2005).** High- and low-threshold genes in the Spo0A regulon of *Bacillus subtilis*. *J Bacteriol* **187**, 1357–1368.

**Glaser, P., Frangeul, L., Buchrieser, C., Rusniok, C., Amend, A., Baquero, F., Berche, P., Bloecker, H., Brandt, P. & other authors (2001).** Comparative genomics of *Listeria* species. *Science* **294**, 849–852.

**Gueriri, I., Bay, S., Dubrac, S., Cyncynatus, C. & Msadek, T. (2008a).** The Pta-AckA pathway controlling acetyl phosphate levels and the phosphorylation state of the DegU orphan response regulator both play a role in regulating *Listeria monocytogenes* motility and chemotaxis. *Mol Microbiol*, doi:10.1111/j.1365-2958.2008.06496.x.

**Gueriri, I., Cyncynatus, C., Dubrac, S., Arana, A. T., Dussurget, O. & Msadek, T. (2008b).** The DegU orphan response regulator of *Listeria monocytogenes* autorepresses its own synthesis and is required for bacterial motility, virulence and biofilm formation. *Microbiology* **154**, 2251–2264.

**Hamoen, L. W., Van Werkhoven, A. F., Venema, G. & Dubnau, D. (2000).** The pleiotropic response regulator DegU functions as a priming protein in competence development in *Bacillus subtilis*. *Proc Natl Acad Sci U S A* **97**, 9246–9251.

**Hamoen, L. W., Venema, G. & Kuipers, O. P. (2003).** Controlling competence in *Bacillus subtilis*: shared use of regulators. *Microbiology* **149**, 9–17.

**Hamon, M. A. & Lazazzera, B. A. (2001).** The sporulation transcription factor Spo0A is required for biofilm development in *Bacillus subtilis*. *Mol Microbiol* **42**, 1199–1209.

**Kaplan, H. B. (2003).** Multicellular development and gliding motility in *Myxococcus xanthus*. *Curr Opin Microbiol* **6**, 572–577.

**Kearns, D. B. & Losick, R. (2003).** Swarming motility in undomesticated *Bacillus subtilis*. *Mol Microbiol* **49**, 581–590.

**Kearns, D. B. & Losick, R. (2005).** Cell population heterogeneity during growth of *Bacillus subtilis*. *Genes Dev* **19**, 3083–3094.

**Kearns, D. B., Chu, F., Rudner, R. & Losick, R. (2004).** Genes governing swarming in *Bacillus subtilis* and evidence for a phase variation mechanism controlling surface motility. *Mol Microbiol* **52**, 357–369.

**Klein, A. H., Shulla, A., Reimann, S. A., Keating, D. H. & Wolfe, A. J. (2007).** The intracellular concentration of acetyl phosphate in *Escherichia coli* is sufficient for direct phosphorylation of two-component response regulators. *J Bacteriol* **189**, 5574–5581.

**Knudsen, G. M., Olsen, J. E. & Dons, L. (2004).** Characterization of DegU, a response regulator in *Listeria monocytogenes*, involved in regulation of motility and contributes to virulence. *FEMS Microbiol Lett* **240**, 171–179.

**Kobayashi, K. (2007).** Gradual activation of the response regulator DegU controls serial expression of genes for flagellum formation and biofilm formation in *Bacillus subtilis*. *Mol Microbiol* **66**, 395–409.

**Kobayashi, K. (2008).** SlrR/SlrA control the initiation of biofilm formation in *Bacillus subtilis*. *Mol Microbiol* **69**, 1399–1410.

**Kunst, F., Msadek, T., Bignon, J. & Rapoport, G. (1994).** The DegS/DegU and ComP/ComA two-component systems are part of a network controlling degradative enzyme synthesis and competence in *Bacillus subtilis*. *Res Microbiol* **145**, 393–402.

**Laub, M. T. & Goulian, M. (2007).** Specificity in two-component signal transduction pathways. *Annu Rev Genet* **41**, 121–145.

**Lazazzera, B. A., Palmer, T., Quisel, J. D. & Grossman, A. D. (1999).** Cell density control of gene expression and development in *Bacillus subtilis*. In *Cell–Cell Signaling in Bacteria*, pp. 27–46. Edited by G. M. Dunny & S. C. Winas. Washington, DC: American Society for Microbiology.

**Lemon, K. P., Higgins, D. E. & Kolter, R. (2007).** Flagellar motility is critical for *Listeria monocytogenes* biofilm formation. *J Bacteriol* **189**, 4418–4424.

**Losick, R. & Desplan, C. (2008).** Stochasticity and cell fate. *Science* **320**, 65–68.

**Macek, B., Mijakovic, I., Olsen, J. V., Gnad, F., Kumar, C., Jensen, P. R. & Mann, M. (2007).** The serine/threonine/tyrosine phosphoproteome of the model bacterium *Bacillus subtilis*. *Mol Cell Proteomics* **6**, 697–707.

**Mader, U., Antelmann, H., Buder, T., Dahl, M. K., Hecker, M. & Homuth, G. (2002).** *Bacillus subtilis* functional genomics: genome-wide analysis of the DegS–DegU regulon by transcriptomics and proteomics. *Mol Genet Genomics* **268**, 455–467.

**Mascher, T., Helmann, J. D. & Unden, G. (2006).** Stimulus perception in bacterial signal-transducing histidine kinases. *Microbiol Mol Biol Rev* **70**, 910–938.

**Mauder, N., Williams, T., Fritsch, F., Kuhn, M. & Beier, D. (2008).** Response regulator DegU of *Listeria monocytogenes* controls temperature-responsive flagellar gene expression in its unphosphorylated state. *J Bacteriol* **190**, 4777–4781.

**Morikawa, M., Kagihiro, S., Haruki, M., Takano, K., Branda, S., Kolter, R. & Kanaya, S. (2006).** Biofilm formation by a *Bacillus subtilis* strain that produces γ-polyglutamate. *Microbiology* **152**, 2801–2807.

**Msadek, T., Kunst, F., Henner, D., Klier, A., Rapoport, G. & Dedonder, R. (1990).** Signal transduction pathway controlling synthesis of a class of degradative enzymes in *Bacillus subtilis*: expression of the regulatory genes and analysis of mutations in *degS* and *degU*. *J Bacteriol* **172**, 824–834.

**Msadek, T., Kunst, F., Klier, A. & Rapoport, G. (1991).** DegS–DegU and ComP–ComA modulator–effector pairs control expression of the *Bacillus subtilis* pleiotropic regulatory gene *degQ*. *J Bacteriol* **173**, 2366–2377.

**Ogura, M. & Tanaka, T. (1996).** *Bacillus subtilis* DegU acts as a positive regulator for *comK* expression. *FEBS Lett* **397**, 173–176.

**Ogura, M., Yamaguchi, H., Yoshida, K., Fujita, Y. & Tanaka, T. (2001).** DNA microarray analysis of *Bacillus subtilis* DegU, ComA and PhoP regulons: an approach to comprehensive analysis of *B. subtilis* two-component regulatory systems. *Nucleic Acids Res* **29**, 3804–3813.

**Ogura, M., Shimane, K., Asai, K., Ogasawara, N. & Tanaka, T. (2003).** Binding of response regulator DegU to the *aprE* promoter is inhibited by RapG, which is counteracted by extracellular PhrG in *Bacillus subtilis*. *Mol Microbiol* **49**, 1685–1697.

**Piggot, P. J. & Hilbert, D. W. (2004).** Sporulation of *Bacillus subtilis*. *Curr Opin Microbiol* **7**, 579–586.

**Shapiro, J. A. (1998).** Thinking about bacterial populations as multicellular organisms. *Annu Rev Microbiol* **52**, 81–104.

**Shen, A. & Higgins, D. E. (2006).** The MogR transcriptional repressor regulates nonhierarchal expression of flagellar motility genes and virulence in *Listeria monocytogenes*. *PLoS Pathog* **2**, e30.

**Shen, A., Kamp, H. D., Grundling, A. & Higgins, D. E. (2006).** A bifunctional *O*-GlcNAc transferase governs flagellar motility through anti-repression. *Genes Dev* **20**, 3283–3295.

comprehensive analysis of *B. subtilis* two-component regulatory systems. *Nucleic Acids Res* **29:** 3804–3813.
Olivares-Illana, V., Meyer, P., Bechet, E., Gueguen-Chaignon, V., Soulat, D., Lazereg-Riquier, S., *et al.* (2008) Structural basis for the regulation mechanism of the tyrosine kinase CapB from *Staphylococcus aureus*. *PLoS Biol* **6:** e143.
Petranovic, D., Michelsen, O., Zahradka, K., Silva, C., Petranovic, M., Jensen, P.R., and Mijakovic, I. (2007) *Bacillus subtilis* strain deficient for the protein-tyrosine kinase PtkA exhibits impaired DNA replication. *Mol Microbiol* **63:** 1797–1805.
Petranovic, D., Grangeasse, C., Macek, B., Abdillatef, M., Gueguen-Chaignon, V., Nessler, S., *et al.* (2009) Activation of *Bacillus subtilis* Ugd by the BY-kinase PtkA proceeds via phosphorylation of its residue tyrosine 70. *J Mol Microbiol Biotechnol* **17:** 83–89.
Piggot, P.J., and Hilbert, D.W. (2004) Sporulation of *Bacillus subtilis*. *Curr Opin Microbiol* **7:** 579–586.
Shimane, K., and Ogura, M. (2004) Mutational analysis of the helix-turn-helix region of *Bacillus subtilis* response regulator DegU, and identification of cis-acting sequences for DegU in the aprE and comK promoters. *J Biochem (Tokyo)* **136:** 387–397.
Soldo, B., Lazarevic, V., Pagni, M., and Karamata, D. (1999) Teichuronic acid operon of *Bacillus subtilis* 168. *Mol Microbiol* **31:** 795–805.
Soulat, D., Grangeasse, C., Vaganay, E., Cozzone, A.J., and Duclos, B. (2007) UDP-acetyl-mannosamine dehydrogenase is an endogenous protein substrate of *Staphylococcus aureus* protein-tyrosine kinase activity. *J Mol Microbiol Biotechnol* **13:** 45–54.
Srivatsan, A., Han, Y., Peng, J., Tehranchi, A.K., Gibbs, R., Wang, J.D., and Chen, R. (2008) High-precision, whole-genome sequencing of laboratory strains facilitates genetic studies. *PLoS Genet* **4:** e1000139.
Stanley, N.R., and Lazazzera, B.A. (2005) Defining the genetic differences between wild and domestic strains of *Bacillus subtilis* that affect poly-gamma-dl-glutamic acid production and biofilm formation. *Mol Microbiol* **57:** 1143–1158.
Steil, L., Hoffmann, T., Budde, I., Volker, U., and Bremer, E. (2003) Genome-wide transcriptional profiling analysis of adaptation of *Bacillus subtilis* to high salinity. *J Bacteriol* **185:** 6358–6370.
Talaat, A.M., Howard, S.T., Hale, W., IV, Lyons, R., Garner, H., and Johnston, S.A. (2002) Genomic DNA standards for gene expression profiling in *Mycobacterium tuberculosis*. *Nucleic Acids Res* **30:** e104.
Tsukahara, K., and Ogura, M. (2008) Promoter selectivity of the *Bacillus subtilis* response regulator DegU, a positive regulator of the fla/che operon and sacB. *BMC Microbiol* **8:** 8.
Veening, J.W., Igoshin, O.A., Eijlander, R.T., Nijland, R., Hamoen, L.W., and Kuipers, O.P. (2008) Transient heterogeneity in extracellular protease production by *Bacillus subtilis*. *Mol Syst Biol* **4:** 184.
Verhamme, D.T., Kiley, T.B., and Stanley-Wall, N.R. (2007) DegU co-ordinates multicellular behaviour exhibited by *Bacillus subtilis*. *Mol Microbiol* **65:** 554–568.
Verhamme, D.T., Murray, E.J., and Stanley-Wall, N.R. (2009) DegU and Spo0A jointly control transcription of two loci required for complex colony development by *Bacillus subtilis*. *J Bacteriol* **191:** 100–108.
Vlamakis, H., Aguilar, C., Losick, R., and Kolter, R. (2008) Control of cell fate by the formation of an architecturally complex bacterial community. *Genes Dev* **22:** 945–953.
Wang, J.Y., and Koshland, D.E., Jr (1978) Evidence for protein kinase activities in the prokaryote *Salmonella typhimurium*. *J Biol Chem* **253:** 7605–7608.
Wu, J., Ohta, N., Zhao, J.L., and Newton, A. (1999) A novel bacterial tyrosine kinase essential for cell division and differentiation. *Proc Natl Acad Sci USA* **96:** 13068–13073.

## Supporting information

Additional supporting information may be found in the online version of this article.

Please note: Wiley-Blackwell are not responsible for the content or functionality of any supporting materials supplied by the authors. Any queries (other than missing material) should be directed to the corresponding author for the article.

Molecular Microbiology (2010) ■ doi:10.1111/j.1365-2958.2010.07382.x

# Post-translational control of *Bacillus subtilis* biofilm formation mediated by tyrosine phosphorylation

**Taryn B. Kiley and Nicola R. Stanley-Wall***
*Division of Molecular Microbiology, College of Life Sciences, University of Dundee, Dundee DD1 5EH, UK.*

## Summary

**A biofilm is a complex community of cells enveloped in a self-produced polymeric matrix. Entry into a biofilm is exquisitely controlled at the level of transcription and in the Gram-positive organism *Bacillus subtilis* it requires the concerted efforts of three major transcription factors. Here, we demonstrate that in addition to transcriptional control, *B. subtilis* utilizes post-translational modifications to control biofilm formation; specifically through phosphorylation of tyrosine residues. Through our work we have assigned novel roles during biofilm formation to two proteins; the protein tyrosine kinase PtkA and the protein tyrosine phosphatase PtpZ. Furthermore by introducing amino acid point mutations within the catalytic domains of PtkA and PtpZ we have identified that the kinase and phosphatase activities, respectively, are essential for function. PtkA contains a conserved C-terminal tyrosine cluster that is the site of autophosphorylation; however, our *in vivo* analysis demonstrates that this domain is not required during biofilm formation. With the aim of identifying the target(s) of PtkA controlled during biofilm formation we used a systematic mutagenesis approach but, despite extensive efforts, it remained elusive. Our findings highlight the complexity of biofilm development by revealing an additional level of regulation in the form of protein tyrosine phosphorylation.**

## Introduction

Bacteria are capable of 'multicellular' behaviours that benefit the bacterial community as a whole. These processes are diverse in both nature and utility. This can be seen using *Bacillus subtilis* as an example where the processes encompass the production of exoproteases (Veening *et al.*, 2008), swarming motility (Kearns and Losick, 2003), genetic competence (Dubnau, 1991; Bai *et al.*, 1993; Hamoen *et al.*, 2000), sporulation (Piggot and Hilbert, 2004) and biofilm formation (Branda *et al.*, 2001; Hamon and Lazazzera, 2001). A biofilm is a complex population of cells, which adhere to a solid surface or interface that are encased in a protective self-secreted polymeric matrix (Branda *et al.*, 2005). In the natural environment bacteria exist predominantly in biofilms, and in such communities, contribute towards the majority of chronic infections (Costerton *et al.*, 1995). As well as being important in clinical and industrial settings, biofilm formation presents an ideal system for investigating the complex network of transcription events used by bacteria while co-ordinating cell fate decisions (Lopez and Kolter, 2010).

Biofilm formation by *B. subtilis* can be manifested in the laboratory as the formation of a structured pellicle at the air–liquid interface or as a colony with complex architecture on nutrient agar (Branda *et al.*, 2001). The initiation of biofilm formation is dependent on three key transcription factors, namely ComA (Lopez *et al.*, 2009a), Spo0A (Branda *et al.*, 2001; Hamon and Lazazzera, 2001) and DegU (Stanley and Lazazzera, 2005). ComA is activated by phosphorylation at high cell density and triggers the production of the lipopeptide surfactin (Nakano and Zuber, 1991). The release of surfactin into the environment triggers the activation of Spo0A by phosphorylation (Lopez *et al.*, 2009b). Phosphorylation of Spo0A is mediated by a phosphorelay system that is, in addition, stimulated by starvation (Piggot and Hilbert, 2004). Spo0A~P regulates the expression of approximately 120 genes according to the specific affinity of the promoter element for Spo0A~P (Fawcett *et al.*, 2000; Molle *et al.*, 2003; Fujita *et al.*, 2005). This allows the activation of different subgroups of genes at different levels of Spo0A~P (Fujita *et al.*, 2005). The main role of Spo0A~P during the activation of biofilm formation is to facilitate the activation of transcription from the *epsA–O* and *yqxM–sipW–tasA* operons that are required for the biosynthesis of the extracellular matrix (Lopez *et al.*, 2009c). Spo0A~P achieves this by removing the directly mediated inhibition of transcription exerted by two repressor proteins called SinR and AbrB (Kearns *et al.*, 2005; Chu *et al.*, 2006; 2008; Murray *et al.*, 2009a).

Accepted 27 August, 2010. *For correspondence. E-mail n.r.stanleywall@dundee.ac.uk; Tel. (+44) (0) 1382 386335; Fax (+44) (0) 1382 388216.

DegU is a response regulator that is activated by phosphorylation through DegS, its cognate histidine sensor kinase, in response to various environmental signals (Mukai *et al.*, 1990; Steil *et al.*, 2003; Murray *et al.*, 2009b). Changes to the phosphorylation state of DegU alter its ability to bind to different promoter regions and thus it can regulate incompatible processes such as protease production and motility (Kobayashi, 2007; Verhamme *et al.*, 2007; Tsukahara and Ogura, 2008). DegU~P activates the transcription of *yuaB* and *yvcA* that encode two proteins that are needed for biofilm formation (Kobayashi, 2007; Verhamme *et al.*, 2007; 2009).

In addition to controlling biofilm formation, SinR and DegU are involved in the regulation of other multicellular behaviours in *B. subtilis* (Gaur *et al.*, 1986; 1991; Kodgire *et al.*, 2006) (Mukai *et al.*, 1990; Amati *et al.*, 2004; Shimane and Ogura, 2004). This knowledge suggested to us that there may be an intimate link between the two regulators. As a consequence of initial experiments designed to investigate this, we have identified that biofilm formation by *B. subtilis* is controlled at the post-translational level by protein tyrosine phosphorylation. Modulation of protein activity using phosphorylation of serine/threonine/tyrosine (Ser/Thr/Tyr) residues was initially believed to be confined to eukaryotes (Deutscher and Saier, 2005). Prokaryotes were thought to be limited to phosphorylation of histidine and aspartic acid residues; a key signalling feature of two-component signal transduction systems (Hoch, 2000). However, this paradigm was revoked in the late 1970's by the identification of Ser/Thr phosphorylation in bacteria (Wang and Koshland, 1978; Manai and Cozzone, 1979) and again when tyrosine phosphorylation was detected in the mid 1990's (Duclos *et al.*, 1996). Serine, threonine and tyrosine phosphorylation has subsequently emerged as an important mechanism for mediating the dynamic control of diverse cellular processes in bacteria, including polysaccharide biosynthesis (Morona *et al.*, 2000; Grangeasse *et al.*, 2003; Soulat *et al.*, 2007), DNA metabolism (Petranovic *et al.*, 2007), cell division (Wu *et al.*, 1999) and resistance to antimicrobial compounds (Lacour *et al.*, 2008).

Bacterial tyrosine kinases are structurally different from their eukaryotic counterparts and thus have been proposed as novel targets for antimicrobial compounds (Lee *et al.*, 2008; Olivares-Illana *et al.*, 2008; Grangeasse *et al.*, 2009). Therefore, understanding the mechanism(s) and role(s) of modification of tyrosine residues by phosphorylation in bacteria is important. Like eukaryotic tyrosine kinases, bacterial tyrosine kinases (hereafter BY-kinases) are ATP-dependent; but the active site of ATP binding and hydrolysis is not conserved between the eukaryotic and prokaryotic proteins (Lee and Jia, 2009). Furthermore, BY-kinases possess unique conserved motifs that are needed for catalytic activity, which are absent from the eukaryotic tyrosine kinases and, as such, could represent potential targets for small molecule inhibitors (Grangeasse *et al.*, 2009; Lee and Jia, 2009). In Gram-negative bacteria BY-kinases are a single polypeptide where the kinase catalytic activity and modulator domains are fused (Mijakovic *et al.*, 2005a). In contrast, in Gram-positive bacteria the BY-kinase is split into two proteins where the genes encoding the modulator and kinase domains are colocated on the chromosome and cotranscribed (Grangeasse *et al.*, 2007). In Gram-positive bacteria the C-terminal domain of the membrane bound modulator protein interacts with the N-terminal region of the cytoplasmic kinase to allow activation (Mijakovic *et al.*, 2003; Grangeasse *et al.*, 2009).

*Bacillus subtilis* contains one confirmed and one predicted BY-kinases known as PtkA and EpsB respectively. EpsB (also known as PtkB) is a predicted BY-kinase and is encoded in the 15 gene operon *epsA–O* that is required for the production of a secreted exopolysaccharide (EPS) needed for biofilm formation (Branda *et al.*, 2001; Mijakovic *et al.*, 2003). PtkA is a confirmed and promiscuous BY-kinase (Mijakovic *et al.*, 2003; Jers *et al.*, 2010). *B. subtilis* also possesses three bacterial protein tyrosine phosphatases. First, there is PtpZ that belongs to the polymerase and histidinol phosphatase family and functions to dephosphorylate the targets of PtkA (Mijakovic *et al.*, 2003; 2005b). Second, *B. subtilis* possesses two tyrosine phosphatases belonging to the low molecular weight protein tyrosine phosphatase family, YwlE and YfkJ, that modulate a distinct set of targets from PtpZ (Mijakovic *et al.*, 2005a). Our study began with an investigation into the link between SinR and DegU and the impact that simultaneous deletion of these regulators had on biofilm formation. These experiments led to the discovery of a novel role for tyrosine phosphorylation mediated by PtkA during biofilm formation by *B. subtilis*. We go on to demonstrate that the known and/or predicted substrates of PtkA are not targeted during post-translational regulation of biofilm formation.

## Results and discussion

### *DegU and SinR function in parallel to control biofilm formation*

Recently we hypothesized that DegU and SinR were part of two separate but converging pathways that are required for biofilm formation by *B. subtilis* (Verhamme *et al.*, 2009). Epistasis analysis presented here supports this conclusion. Mutations in *sinR* and *degSU* were introduced separately, and in combination, into the *B. subtilis* isolate NCIB3610. Colony architecture and pellicle formation were used as two independent measures of the capability to form a biofilm (Branda *et al.*, 2001). The

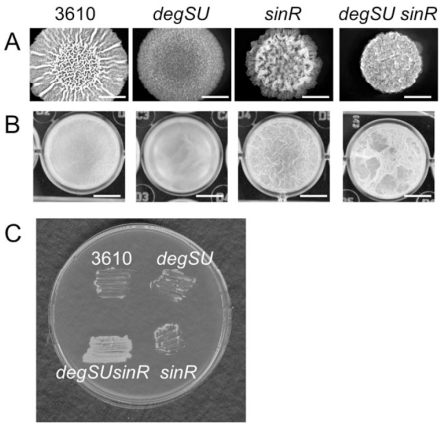


**Fig. 1.** Complex colony architecture assay of *B. subtilis*.
A. Strains 3610, *degSU* (NRS1499), *sinR* (NRS1859) and *degSUsinR* (NRS1860) were grown on MSgg agar plates for 40 h at 37°C prior to photographing. Scale bar represents 5 mm.
B. Pellicles were allowed to grow in MSgg media overnight at 37°C prior to photography.
C. Strains as detailed above were patched onto an LB agar plate and grown for 16 h at 37°C prior to scraping and photography.

phenotype exhibited by the following strains was assessed with respect to the wild-type parental strain (NCIB3610); *degSU* (NRS1499), *sinR* (NRS1859) and *degSU sinR* (NRS1860). The *degSU sinR* (NRS1860) double mutant exhibited a morphology that was distinct from the wild-type strain and was dissimilar from either of the previously characterized single mutant strains, *degSU* (NRS1499) and *sinR* (NRS1859) (Fig. 1A). Consistent with previous findings, the *degSU* mutant strain was unable to form a robust stable pellicle (Stanley and Lazazzera, 2005; Kobayashi, 2007; Verhamme *et al.*, 2007) and the *sinR* mutant formed a very robust rugose pellicle (Fig. 1B) (Kearns *et al.*, 2005). The *degSU sinR* double mutant formed a pellicle that was distinct from either single mutant strain or wild-type strain (Fig. 1B).

### *DNA microarray analysis identifies subset of genes co-regulated by DegU and SinR*

It was noted that by comparison with both the wild-type and single mutant strains, the double *degSU sinR* mutant (NRS1860) tightly adhered to the surface of an agar plate (Fig. 1C). This led to the hypothesis that a novel set of DegU and SinR co-regulated genes existed and that one (or more) was responsible for the enhanced adhesion phenotype. It also provided a possible mechanism to identify novel loci involved in the control of biofilm formation. To identify these potential gene(s), DNA microarray analysis was used. As the number of genes controlled by DegU is significantly greater than those controlled by SinR, the expression profile of the *degSU* strain was compared with that of the *degSU sinR* strain (see *Experimental procedures*) (Dartois *et al.*, 1998; Ogura *et al.*, 2001; Tsukahara and Ogura, 2008) (Kearns *et al.*, 2005; Chu *et al.*, 2006; Kodgire *et al.*, 2006). By identifying loci that were upregulated more than twofold in the *degSUsinR* strain compared with the *degSU* strain, a combination of putative DegU and SinR co-regulated genes, and known SinR-regulated genes, was generated (Table S1). A finalized list of 11 DegU and SinR co-regulated genes was compiled by removing known SinR-repressed genes (Table S1). For a subset of the genes (*ptpZ, yomI, ywbC* and *yvfO*) semi-quantitative reverse transcription polymerase chain reaction (RT-PCR) was used to verify the DNA microarray results. An increase in transcription that was at least threefold higher in the *degSU sinR* mutant versus the wild-type strain ($P < 0.05$) was observed confirming that transcription was elevated in the absence of DegU and SinR (Fig. S1).

### *Screening of genes for a role in biofilm formation*

We next tested if one of the genes identified through the DNA microarray analysis was responsible for the enhanced surface adhesion exhibited by the *degSU sinR* strain. To do this, a mutation in each gene was constructed and introduced into the wild-type and *degSU sinR* mutant strains (Table S3). None of the mutations screened were successful in relieving the enhanced cell-surface adhesion phenotype (data not shown). It is likely that a combination of mutations would be required to relieve this phenotype but this was not tested. In parallel, taking into account the role that DegU and SinR have in controlling biofilm formation (Kearns *et al.*, 2005; Kobayashi, 2007; Verhamme *et al.*, 2007) the impact of deleting each gene on biofilm formation was assessed. The biofilm morphology after 24 and 48 h incubation was monitored. Mutation of 10 of the 11 genes identified by DNA microarray analysis did not affect biofilm formation but deletion of *ptpZ* (NRS1827) altered the architecture of the biofilm by comparison with the wild-type strain (Fig. S2). For the remainder of this study, focus was devoted to the characterization of the *tkmA* operon and its members to which *ptpZ* was shown to belong (Fig. 2).

### *Organization of the* tkmA *locus*

The gene encoding PtpZ is found within a region of the chromosome including *tkmA, ptkA* and *ugd.* Initially we wanted to establish if these four genes formed an operon.

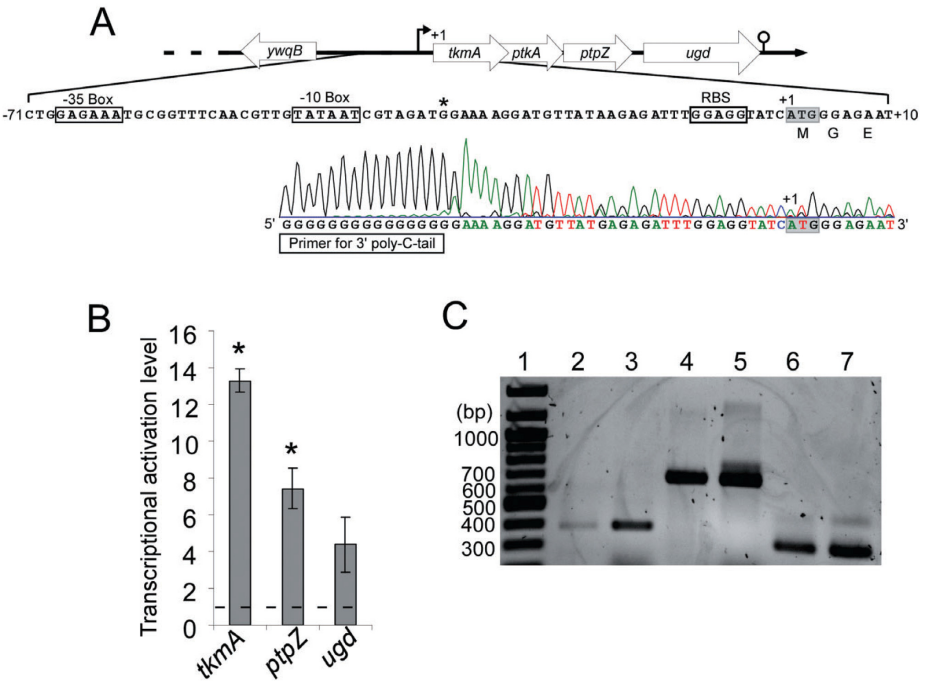


**Fig. 2.** Transcriptional analysis of the *tkmA* operon.
A. 5′RACE analysis was used to identify the transcriptional start site of the *tkmA* operon. Genes are represented by hollow arrows containing the gene name in italics. A black, stalked arrow schematically indicates the start position of transcription. A stalked, hollow circle indicates the translational stop site. A section of the *tkmA* promoter sequence can be found directly below the operon structure schematic. Positive and negative numbers refer to the position of the nucleotide with reference to the translational start site, designated as +1. The translational start codon ATG is highlighted by a grey box. Conserved sequences, including the ribosome binding site (RBS), −10 TATAA box and −35 box, are outlined in black. The proposed transcriptional start site (−33 bp downstream of the translational start site) is highlighted by an asterisk. The capital letters M, G, E indicate the translated sequence ot TkmA. A DNA sequencing readout showing the predicted transcriptional start site preceded by an engineered poly-G tail can be seen directly below the DNA sequence of *tkmA*.
B. RT-PCR analysis of the *tkmA* operon using cDNA synthesized from *degSUsinR* (NRS1860) RNA. The level of transcription shown was obtained by comparison with wild-type levels of transcription and normalized to the transcription of the control gene *veg*. The dashed line represents the transcriptional level of 1 in the wild-type strain, 3610. The asterisks indicate genes whose transcription is significantly different from wild-type transcription levels ($P$-value $< 0.05$) where $n \geq 3$. The error bars represent standard error of the mean.
C. Amplification of regions of DNA internal to *tkmA*, *ptpZ* and *ugd* was amplified from cDNA generated using an *ugd*-specific reverse primer. Lane 1 contains 100 bp ladder (NEB Biolabs™). Lanes 2 and 3 contain *tkmA*; lanes 4 and 5 contain *ptpZ*; and lanes 6 and 7 contain *ugd* PCR product. Lanes 2, 4 and 6 show PCR products amplified from cDNA template, while lanes 3, 5 and 7 show PCR products amplified from gDNA template. Primer combinations used for amplification of *tkmA*, *ptpZ* and *ugd* can be found in Table S4.

This was necessary to establish as: (i) the DNA microarray analysis only identified *ptpZ* as differentially expressed, (ii) *ugd* is not colocated in the same region of the genome in other Gram-positive bacteria (data not shown) and (iii) there is a 198 bp gap between the stop codon of *ptpZ* and the start codon of *ugd* that could contain a promoter element (Fig. 2A). We tested whether, as seen for *ptpZ* (Fig. S2), transcription of *tkmA* and *ugd* was upregulated in the absence of DegU and SinR. We used RT-PCR analysis with cDNA synthesized from RNA isolated from the wild-type (NCIB3610) and the *degSUsinR* mutant strain (see *Experimental procedures*). For *tkmA*, *ptpZ* and *ugd*, respectively, a 10-fold, sevenfold and threefold increase in transcription was observed in the absence of SinR and DegU by comparison with the wild-type strain (Fig. 2B). These findings are consistent with the genes being co-regulated and suggest that the DNA microarray analysis was the limiting factor in the identifi-

cation of *tkmA*, *ptkA* and *ugd* as differentially expressed in the absence of *degU* and *sinR*.

### tkmA, ptkA, ptpZ *and* ugd *are cotranscribed*

To determine whether *tkmA, ptkA, ptpZ* and *ugd* were encoded on a single transcript, mRNA was isolated from wild-type *B. subtilis* and cDNA was synthesized using a reverse *ugd* gene-specific primer (Fig. 2C). The cDNA generated corresponded to the *ugd* transcript and was used as a template for PCR with three primer pairs that were specific to the internal coding regions of *tkmA*, *ptpZ* and *ugd*. As a negative control, a sample that had been subjected to the same treatment but which lacked the reverse transcriptase was used to ensure that the PCR products were not the result of any contaminating genomic DNA (data not shown). As a positive control, genomic DNA was used to ensure the product amplified was the correct size (Fig. 2C). All three gene-specific PCR products were amplified from the cDNA indicating that *tkmA, ptkA, ptpZ and ugd* are cotranscribed (Fig. 2C).

### *Location of the transcription start site*

To determine the transcription start site of the *tkmA* operon 5′RACE was used and the start site was localized to either –33 or –32 bp upstream of the *tkmA* coding sequence initiation codon (Fig. 2A). It was not possible to distinguish this more specifically as the anchor primer that is needed for the 5′RACE (NSW367) contains a series of guanine residues, which cannot be distinguished from guanine residues in the amplified promoter region (Fig. 2A). We, however, favour the guanine located at –33 bp upstream from the initiation codon of *tkmA* for the transcriptional start site. Our reasoning being that there is a perfect –10 binding site (TATAAT) for the housekeeping RNA polymerase Sigma-A centred 10 bp upstream from this nucleotide (Fig. 2A). Additionally a sequence with a four out of six base pair match (TGGAGA) to the canonical –35 binding site (TTGACA) for the housekeeping RNA polymerase Sigma-A is centred at 35 bp upstream from the nucleotide (Fig. 2A) (Moran *et al.*, 1982). When 5′RACE was applied to the region upstream from the *ugd* translation start site, no transcription initiation site could be identified (data not shown). Taken together the simplest explanation is that the *tkmA–ptkA–ptpZ–ugd* operon is a single transcript that is upregulated in the absence of DegU and SinR and driven from a single transcriptional start site at 33 bp upstream from the translation initiation codon of *tkmA* (Fig. 2A).

### *Electrophoretic mobility shift analysis*

We wanted to establish whether DegU and/or SinR directly regulated transcription from the *tkmA* promoter. To test this we used *in vitro* electrophoretic mobility shift assays with purified and phosphorylated DegU-$_{His6}$ and purified SinR-$_{His6}$. Prior to EMSA analysis we confirmed that purified DegS-$_{His6}$ was capable of phosphorylating DegU-$_{His6}$ *in vitro* using [$\gamma$-$^{32}$P]-ATP (data not shown). A 542 bp region of DNA upstream from the translation start site of *tkmA* was amplified by PCR. The results showed that the mobility of the promoter region of *tkmA* was impeded by the addition of 1 μM DegU~P during gel electrophoresis (Fig. 3A). Greater retention was seen with increasing amounts of DegU~P (3 μM). Unlabelled DNA corresponding to the *tkmA* promoter was able to outcompete access to the binding domain of DegU~P on the radiolabelled DNA indicating that the interaction was specific (Fig. 3A). Consistent with this a region of DNA corresponding to the internal coding region of *tkmA* was not able to compete for the binding domain of DegU~P (Fig. 3A). As transcription from the *tkmA* promoter is upregulated in the absence of *degU* (Fig. S1) we conclude that DegU~P functions as an inhibitor, and not an activator, of transcription. It is important to note that while DegU activates biofilm formation (Stanley and Lazazzera, 2005; Kobayashi, 2007; Verhamme *et al.*, 2007) DegU also functions to inhibit biofilm formation (Verhamme *et al.*, 2007). These findings add to the loci regulated by DegU~P during the formation of a biofilm (Kobayashi, 2007; Verhamme *et al.*, 2007; 2009).

In contrast, SinR-$_{His6}$ did not interact with the *tkmA* promoter DNA (Fig. 3B). The activity of purified SinR-$_{His6}$

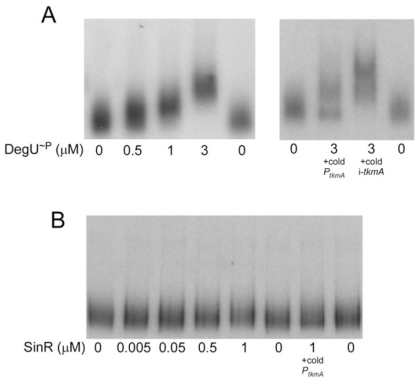


**Fig. 3.** Electrophoretic mobility shift analysis of the *tkmA* operon promoter region. DNA binding reactions were conducted with $\gamma$-$^{32}$P labelled DNA corresponding to the region –500 to +42 bp. Labelled DNA (1 ng) was loaded into each lane, with or without purified (A) DegU~P-$_{His6}$ or (B) SinR-$_{His6}$. Further binding reactions include the addition of 100 ng of unlabelled *tkmA* promoter region PCR product ($P_{tkmA}$) (–500 to +42 bp fragment) or unlabelled internal *tkmA* (i-*tkmA*) (+3 to +379 bp) to the EMSA reaction.

protein was established by the presence of a positive interaction between the known SinR-regulated promoter, $P_{yqxM}$ and the purified SinR-$_{His6}$ (Chu *et al.*, 2006) (data not shown). These results were as anticipated as *in silico* analysis of the *tkmA* promoter region did not identify any DNA sequences corresponding to the SinR consensus binding (Chu *et al.*, 2006). The inhibitory action exerted by SinR on transcription from the *tkmA* promoter is therefore unlikely to be directly mediated (Figs S1 and 3B). However, we cannot exclude the possibility that the increase in transcription may in fact be due to pleiotropic effects on gene expression that occur when *sinR* and *degU* are deleted in combination. In addition, we cannot rule out the possibility that SinR may require an additional transcriptional regulator in order to exert its regulatory effect on the transcription of the *tkmA* operon. Such a situation exists for the *lytABC* operon where SlrR and SinR are required for a protein–DNA interaction to be established (Chai *et al.*, 2010). It is also interesting to note that transcription of the *tkmA* operon is also directly regulated by Spo0A~P (Fawcett *et al.*, 2000; Molle *et al.*, 2003). This provides the second example of a locus involved in biofilm formation where the Spo0A and DegU regulatory cascades converge; the first being the promoter element of *yuaB* (Verhamme *et al.*, 2009).

### *Construction and analysis of in frame deletion strains*

Having defined the structure of the *tkmA* operon we wanted to establish the role of tyrosine phosphorylation during the formation of a biofilm. The initial *ptpZ* mutant that was constructed as part of the screening process was generated using single cross-over disruption (Fig. S2). As *tkmA–ptkA–ptpZ–ugd* form an operon (Fig. 2), in frame deletions in *ptkA* and *ptpZ* were made to circumvent downstream effects on transcription and/or the stoichiometry of the remaining proteins (see *Experimental procedures*). It has been reported that PtkA and PtpZ play a role in controlling DNA replication (Petranovic *et al.*, 2007) and that a *ptpZ* mutant exhibits a severe growth defect (Petranovic *et al.*, 2007). A growth defect would render interpretation of biofilm formation ambiguous; therefore, we tested whether either the Δ*ptkA* strain or the Δ*ptpZ* strain had a reduced growth rate. In both Luria–Bertani (LB) (data not shown) and MSgg liquid medium the Δ*ptkA* and Δ*ptpZ* mutants had a doubling time equal to that of the parental strain (Fig. 4A). Absence of PtkA has been shown to have deleterious effects on cell length and nucleoid positioning (Petranovic *et al.*, 2007). Therefore, we analysed cell size and nucleoid distribution at the single cell level using microscopy. Deletion of neither *ptkA* nor *ptpZ* influenced cell size or nucleoid positioning (Fig. 4B and C). *In toto*, in NCIB3610, deletion of either *ptkA* or *ptpZ* does not result in a gross growth or DNA

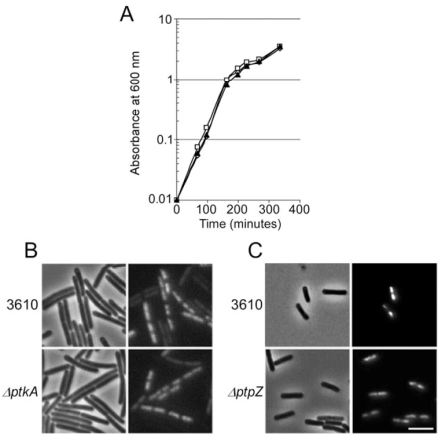


**Fig. 4.** Growth and nucleoid localization of Δ*ptkA* and Δ*ptpZ* mutants compared with 3610. (A) Growth of 3610, Δ*ptkA* (NRS2544) and Δ*ptpZ* (NRS2222) in MSgg media. Results are representative of > 3 independent rounds. Phase-contrast and fluorescent images of NCIB3610, Δ*ptkA* (B) and Δ*ptpZ* (C) collected using Zeiss Axio Imager M1. Scale bars represent 5 μm.

replication defect. It is possible that differences in either the method of strain construction or the genetic background may explain this discrepancy.

### *Tyrosine phosphorylation mediated by PtkA is required for biofilm maturation*

Having established that the Δ*ptkA* and Δ*ptpZ* mutants did not exhibit a growth defect, the impact of deleting *ptkA* and *ptpZ* on biofilm formation was tested. Three independent indicators of biofilm formation were assessed; namely complex colony architecture, pellicle formation and the ability to form environmentally resistant spores (Branda *et al.*, 2001; Vlamakis *et al.*, 2008). All of these processes have been linked with the biosynthesis and assembly of the extracellular matrix. Starting with the Δ*ptkA* strain (NRS2544); we determined that it was unable to develop the complex radial structures typical of the mature *B. subtilis* biofilm on semi-solid agar (Fig. 5B). In contrast to the reduction in colony architecture complexity (Fig. 5B), the pellicle formed by the Δ*ptkA* strain showed extensive three dimensional structural complexity but it entirely lacked the 'fruiting body structures' that are present on the wild-type pellicle (compare Fig. 5E with F). The altered colony morphology and lack of 'fruiting body' formation on the pellicle correlated with the decreased ability of the Δ*ptkA* strain to sporulate. After 24 h incubation under biofilm formation conditions 13 ± 2.5% of the

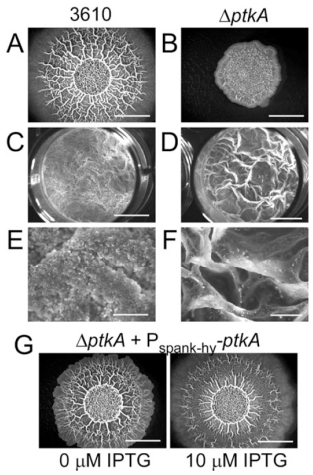


**Fig. 5.** Complex colony architecture and pellicles of Δ*ptkA*. Strains 3610 (A) and Δ*ptkA* (B) (NRS2544) were assessed as described in Fig. 1. Scale bar represents 5 mm (A–D) and 1 mm (E and F). (G) Δ*ptkA* + *amyE*–$P_{spank\text{-}hy}$–*ptkA*–*lacI* (NRS2804) was grown on MSgg agar with and without the addition of 10 μM IPTG. The scale bar represents 5 mm.

Δ*ptkA* mutant population had sporulated by comparison with the wild type that exhibited 25 ± 4% sporulation ($n = 3$; $P < 0.06$ Student's two-way *t*-test). After 72 h the difference in the sporulation efficiency widened such that only 37 ± 10% of the Δ*ptkA* cells in the colony had sporulated by comparison with 103 ± 9% of the wild-type strain ($n = 3$; $P < 0.01$ Student's two-way *t*-test). In contrast after 72 h planktonic growth there was no difference between the sporulation levels of the wild-type strain and that of Δ*ptkA* mutant indicating that the decrease in sporulation did not reflect a reduction in the sporulation efficiency *per se* (data not shown) (Vlamakis *et al.*, 2008). To confirm that the biofilm morphology of the Δ*ptkA* mutant was specific to the absence of PtkA, a wild-type copy of *ptkA* was introduced into the *amyE* locus under the control of a heterologous promoter; $P_{spank\text{-}hy}$–*ptkA*–*lacI* (NRS2804). The biofilm architecture was fully restored compared with that shown by the wild-type strain both in the absence of IPTG and in the presence of 10 μM IPTG (compare Fig. 5B with G). These findings confirm that the altered biofilm phenotype was specific to the disruption of *ptkA*.

### *The kinase activity of PtkA is required for biofilm formation*

Bacterial tyrosine kinases (BY-kinase) share sequence conservation and recent structural analysis of a PtkA homologue showed that the Walker A, Walker B and 'DxD' motifs are required to co-ordinate and stabilize four water molecules and an $Mg^{2+}$ ion into the active site (Fig. 6A) (Olivares-Illana *et al.*, 2008). Therefore, the activity of PtkA is dependent on binding and hydrolysis of ATP coupled to the transfer of the released phosphate moiety onto a target substrate protein(s) (Mijakovic *et al.*, 2003). We aimed to confirm whether or not the catalytic kinase activity of PtkA was needed during biofilm formation. To achieve this, two strains were made that resulted in substitutions on the chromosome leading to alterations in the PtkA amino acid sequence: (i) an amino acid point mutation in the second of the aspartic acid residues in the conserved 'DxD' motif required for ATP hydrolysis catalysis; (PtkA $D^{83}A$; NRS2795) and (ii) a dual 'DxD' aspartic acid to alanine substitution; (PtkA $D^{81}A$ and $D^{83}A$; NRS2796). The nucleotide substitutions were introduced into the chromosome using pMAD (Arnaud *et al.*, 2004) and in each case an isolate that had been subjected to the mutagenesis but had retained the wild-type sequence was retained as a control (see *Experimental procedures*). Each of the negative control strains exhibited wild-type morphology (data not shown). Consistent with the 'DxD' motif being required for the activity of PtkA, mutation to 'AxA' resulted in a biofilm morphology that was indistinguishable from the complete in frame Δ*ptkA* strain (NRS2544) (compare Figs 5B with 6D). Additionally con-

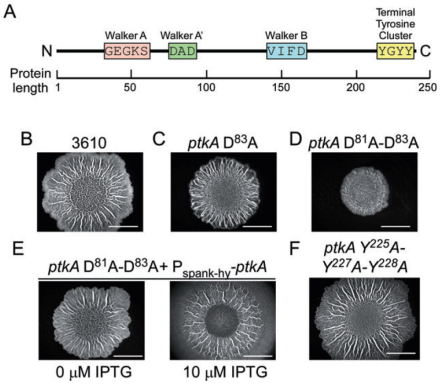


**Fig. 6.** Complex colony architecture of Δ*ptkA* point mutation strains. (A) Schematic representation of PtkA protein sequence. Conserved motifs are highlighted by coloured boxes containing the specific motif residues. Amino and carboxyl termini are indicated by N and C respectively. Strains (B) 3610, (C) *ptkA* $D^{83}A$ (NRS2795), (D) *ptkA* $D^{81}A$–$D^{83}A$ (NRS2796), (E) *ptkA* $D^{81}A$–$D^{83}A$ + $P_{spank\text{-}hy}$–*ptkA* (NRS2807) and (F) Δ*ptkA* $Y^{225}A$–$Y^{227}A$–$Y^{228}A$ (NRS2799) were grown on MSgg agar plates with and without the addition of 10 μM IPTG as required for 40 h at 37°C prior to photographing. Scale bar represents 5 mm.

**Table 1.** Strains used in this study.

| Strain | Relevant genotype[a] | Source/construction[b] |
|---|---|---|
| NCIB3610 | Prototroph | BGSC |
| NRS1499 | 3610 Δ*degSU (spc)* | SPP1 NRS1183 → NCIB3610 |
| NRS1859 | 3610 Δ*sinR (kan)* | SPP1 NRS1858 → NCIB3610 |
| NRS1860 | 3610 Δ*sinR (kan)* Δ*degSU (spc)* | SPP1 NRS1858 → NRS1499 |
| NRS3541 | 3610 Δ*tkmA* | pNW395 → NCIB3610 |
| NRS2544 | 3610 Δ*ptkA* | pNW341 → NCIB3610 |
| NRS3528 | 3610 Δ*tkmA*Δ*ptkA* | pNW387 → NCIB3610 |
| NRS2222 | 3610 Δ*ptpZ* | pNW330 → NCIB3610 |
| NRS2471 | 3610 Δ*ugd* | pNW331 → NCIB3610 |
| NRS3232 | 3610 *tuaD*::pNW377 *(cml)* | SPP1 NRS3227→ 3610 |
| NRS2227 | 3610 Δ*ytcA (kan)* | SPP1 NRS2059 → 3610 |
| NRS3231 | 3610 Δ*ugd* + Δ*ytcA (kan)* + *tuaD*::pNW377 *(cml)* | SPP1 NRS3227 › NRS2821 |
| NRS2795 | 3610 *ptkA* $D^{83}A$ | pNW348 → NCIB3610 |
| NRS2796 | 3610 *ptkA* $D^{81}A$–$D^{83}A$ | pNW348 → NCIB3610 |
| NRS2799 | 3610 *ptkA* $Y^{225}A$–$Y^{227}A$–$Y^{228}A$ | pNW349 → NCIB3610 |
| NRS3544 | 3610 Δ*tkmA* + *amyE*::$P_{spank\text{-}hy}$–*tkmA–lacI (spc)* | SPP1 NRS3255 → NRS3541 |
| NRS3536 | 3610 Δ*tkmA*Δ*ptkA* + *amyE*::$P_{spank\text{-}hy}$–*tkmA ptkA–lacI (spc)* | SPP1 NRS3265 → NRS3528 |
| NRS3535 | 3610 Δ*tkmA*Δ*ptkA* + *amyE*::$P_{spank\text{-}hy}$–*tkmA–lacI (spc)* | SPP1 NRS3255 → NRS3528 |
| NRS3537 | 3610 Δ*tkmA*Δ*ptkA* + *amyE*::$P_{spank\text{-}hy}$–*ptkA–lacI (spc)* | SPP1 NRS3255 → NRS2801 |
| NRS2804 | 3610 Δ*ptkA* + *amyE*::$P_{spank\text{-}hy}$–*ptkA–lacI (spc)* | SPP1 NRS2801 → NRS2544 |
| NRS2807 | 3610 *ptkA* $D^{81}A$–$D^{83}A$ + *amyE*::$P_{spank\text{-}hy}$–*ptkA–lacI (spc)* | SPP1 NRS2801 → NRS2796 |
| NRS2467 | 3610 Δ*ptpZ* + *amyE*::$P_{spank\text{-}hy}$–*ptpZ–lacI (spc)* | SPP1 NRS2173 → NRS2222 |
| NRS2468 | 3610 Δ*ptpZ* + *amyE*::$P_{spank\text{-}hy}$–*ptpZ* ($H^{196}A$)–*lacI (spc)* | SPP1 NRS2193 → NRS2222 |

**a.** Antibiotic resistance cassettes are indicated as follows: *spc*, spectinomycin resistance; *kan*, kanamycin resistance.
**b.** Arrow indicates direction of strain construction. Plasmids (DNA) and SPP1 (phage) were used to transform or transduce recipient strain noted above. Full plasmid and primer lists can be found in Tables S4 and S3 respectively. BSGC represents the Bacillus genetic stock centre.

sistent with the altered colony morphology 32 ± 9% of the mutant cell population sporulated after 72 h incubation by comparison with 103 ± 9% of the wild-type cells after 72 h incubation ($n = 3$; $P < 0.006$ Student's two-way *t*-test). The specificity of the 'DxD' point mutations could be demonstrated as wild-type morphology was restored upon introduction of the $P_{spank\text{-}hy}$–*ptkA–lacI* allele at the *amyE* locus (NRS2807) (compare Fig. 6D with E). A strain carrying the single 'DxD' alanine substitution had a phenotype that was intermediate between the parental strain and the Δ*ptkA* (compare Fig. 6C and D with Fig. 5B), thus underscoring the importance of both aspartic acid residues in the BY-kinase (Mijakovic *et al.*, 2003).

It has been previously noted that in addition to its role as a bacterial tyrosine kinase, PtkA also exhibits ATPase activity (Mijakovic *et al.*, 2003). To (indirectly) distinguish whether the ATPase or kinase activity of PtkA was responsible for its role in biofilm formation, an in frame deletion of *tkmA* was constructed (NRS3541) (Table 1). TkmA is the cognate BY-kinase modulator that interacts with PtkA allowing it to phosphorylate its target proteins (Mijakovic *et al.*, 2003; Jers *et al.*, 2010). Thus in the absence of TkmA, PtkA is unable to exhibit kinase activity and can no longer phosphorylate substrate proteins but its ATPase activity remains intact (Mijakovic *et al.*, 2003). Upon deletion of *tkmA* we observed a reduction in colony complexity and a loss of complex aerial structures and fruiting bodies (Fig. 7C); consistent with TkmA (and thus PtkA) being

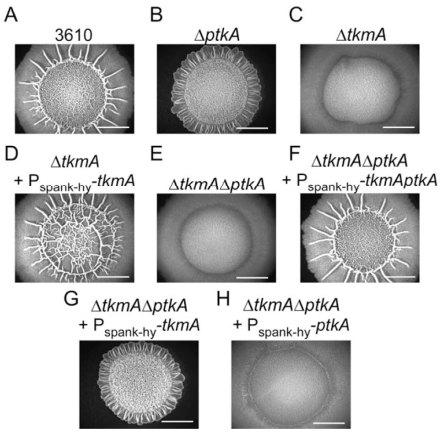


**Fig. 7.** Complex colony architecture of Δ*tkmA* and Δ*tkmA*Δ*ptkA* deletion strains. Strains (A) 3610, (B) Δ*ptkA* (NRS2544), (C) Δ*tkmA* (NRS3541), (D) Δ*tkmA* + $P_{spank\text{-}hy}$–*tkmA* (NRS3544), (E) Δ*tkmA*Δ*ptkA* (NRS3528), (F) Δ*tkmA*Δ*ptkA* + $P_{spank\text{-}hy}$–*tkmA–ptkA* (NRS3536), (G) Δ*tkmA*Δ*ptkA* + $P_{spank\text{-}hy}$–*tkmA* (NRS3535) and (H) Δ*tkmA*Δ*ptkA* + $P_{spank\text{-}hy}$–*ptkA* (NRS3537) were grown on MSgg agar plates without the addition IPTG for 40 h at 30°C prior to photographing. Scale bar represents 5 mm.

required for biofilm formation. The heterologous expression of *tkmA* under the control of the $P_{spank\text{-}hy}$ promoter was able to complement the *tkmA* mutation (in the absence of IPTG) (Fig. 7D). Taken together this demonstrates that TkmA is required for biofilm formation and supports the hypothesis that the kinase activity of PtkA is essential for its role during biofilm formation.

Interestingly, deletion of *tkmA* did not phenocopy the Δ*ptkA* strain (NRS2544) (compare Fig. 7B with C). Therefore, we hypothesized that TkmA retained activity in the absence of PtkA and that TkmA was capable of interacting with other proteins. To test this we constructed a strain lacking both *tkmA* and *ptkA* (NRS3528) (Table 1). We predicted that if our hypothesis was correct restoration of *tkmA* expression in the strain mutant for both *tkmA* and *ptkA* would return the colony phenotype to that of a *ptkA* mutant. When grown on MSgg media Δ*tkmA*Δ*ptkA* (NRS3528) displayed a complex colony architecture that was indistinguishable to the Δ*tkmA* mutant (NRS3541) (compare Fig. 7C with E). We confirmed that addition of both the *tkmA* and *ptkA* coding regions (NRS3536) under the control of an inducible promoter was necessary and sufficient to return the mutant phenotype back to that of wild-type *B. subtilis* (Fig. 7F). From this we conclude that both TkmA and PtkA are required for biofilm formation and that TkmA is epistatic to PtkA. Next, only the *tkmA* coding region was introduced into the Δ*tkmA*Δ*ptkA* mutant strain (NRS3535). The complex colony architecture of this strain was indistinguishable from the Δ*ptkA* mutant (NRS2544) (compare Fig. 7G with B). As a change to colony architecture was observed upon expression of *tkmA*, this indicated that, as hypothesized above, TkmA can function (at least in part) in the absence of PtkA. In contrast, expression of only the *ptkA* coding region in the Δ*tkmA*Δ*ptkA* mutant strain (NRS3537) had no impact on complex colony architecture (Fig. 7H). This further supports the conclusion that substrate phosphorylation by PtkA during biofilm formation relies on activation of its kinase activity through interaction with TkmA. When taken together we conclude that the kinase activity of PtkA is required for its role during biofilm formation, whereas the ATPase activity of PtkA is not.

### *The terminal tyrosine residues of PtkA are not required for biofilm formation*

The conserved C-terminal tyrosine domain serves as the site of autophosphorylation on PtkA (Fig. 6A); a process that is dependent on the catalytic activity of PtkA. *In vitro* assays indicate that the C-terminal tyrosine residues are not needed for phosphorylation of substrate proteins (Mijakovic *et al*., 2003) but structural analysis of a PtkA homologue demonstrates that the C-terminal tyrosine domain interacts with the neighbouring kinase active site (Olivares-Illana *et al*., 2008). Taken together, these findings render the role of the conserved tyrosine residues ambiguous. The influence that PtkA has on colony morphology presents a robust and simple route to clarify if the terminal tyrosine residues play a role *in vivo* during biofilm formation. To investigate the role of the terminal tyrosine cluster of PtkA during biofilm formation we constructed a strain in which the three terminal tyrosine residues were mutated to alanine (PtkA $Y^{225}A$; $Y^{227}A$; $Y^{228}A$; NRS2799) (Fig. 6A).

In sharp contrast to mutating the 'DxD' motif of PtkA, mutation of the terminal tyrosine residues to alanine (NRS2799) did not alter the morphology the colony formed (Fig. 6F). These findings clearly demonstrate that the C-terminal tyrosine residues are not required *in vivo* by PtkA during biofilm formation. While the C-terminal tyrosine cluster is a conserved feature of BY-kinases' (Mijakovic *et al*., 2005a), the effects of phosphorylation of these residues are not conserved. For example, phosphorylation of the terminal tyrosine cluster of CpsD from *Streptococcus pneumonia* activates polysaccharide production (Bender *et al*., 2003; Morona *et al*., 2003); whereas in *Acinetobacter lwoffii* dephosphorylation is thought to activate the kinase Wzc (Nakar and Gutnick, 2003). It is unusual to conserve features of a protein, which serve no obvious purpose; therefore, further investigation into the role of the terminal tyrosine cluster is required as it remains to be identified if it is required for other processes controlled by PtkA, for example, protein localization (Jers *et al*., 2010).

### *Tyrosine dephosphorylation controlled by PtpZ influences early stages of biofilm formation*

An approach similar to that used for PtkA was taken to assess the impact of deleting *ptpZ* on biofilm formation. As determined for the Δ*ptkA* mutant, the Δ*ptpZ* mutant was unable to develop the complex radial structures typical of the maturing *B. subtilis* biofilm at 24 h. Once more, in contrast to the reduction in colony architecture complexity (Fig. 8A), the pellicle formed by the Δ*ptpZ* strain showed extensive three dimensional structural complexity but entirely lacked the 'fruiting bodies' that are present on the wild-type pellicle (compare Figs. 5E with 8B). These alterations in colony morphology and pellicle morphology were accompanied by a reduction in the level of sporulation from ~25 ± 4% in the wild-type strain to ~8.0 ± 3.6% in the Δ*ptpZ* mutant ($n = 3$; $P < 0.05$ two-way Student's *t*-test). The decrease in sporulation was found to be specific to cells growing in the biofilm colony as after 24 h growth in liquid medium the wild-type strain and the Δ*ptpZ* mutant had sporulated at a frequency of ~33 ± 1.5% and ~40 ± 9% respectively. However, in contrast to the Δ*ptkA* mutant, the impact of deleting Δ*ptpZ*

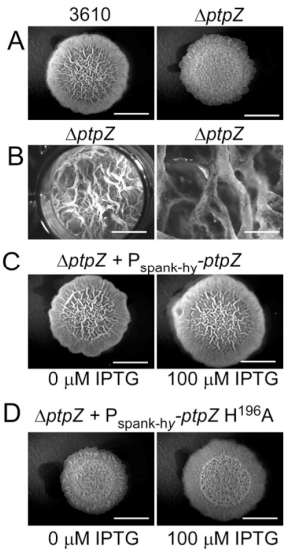


**Fig. 8.** Complex colony architecture of Δ*ptpZ* point mutation strains.
A. Strains 3610, Δ*ptpZ* (NRS2222) were assessed in the 3610 background as described in Fig. 1. Scale bar represents 5 mm.
B. Pellicles of Δ*ptpZ* (NRS2222) were assessed in the 3610 background as described in Fig. 1. Scale bar represents 5 mm (left) and 1 mm (right).
C and D. Strains (C) Δ*ptpZ* + $P_{spank-hy}$–*ptpZ* (NRS2467) and (D) Δ*ptpZ* + $P_{spank-hy}$–*ptpZ* ($H^{196}$A) (NRS2468) were grown on MSgg media with or without the addition of 100 μM IPTG.

became less apparent over time; such that by 48 h the lack of PtpZ had only a minor impact on the ability to form a biofilm (data not shown). The sporulation analysis confirmed this conclusion. After 72 h incubation ~65 ± 3% of the *ptpZ* mutant population had sporulated, a value that was not significantly different from the wild-type strain ($n = 3$; $P = 0.09$ two-way Student's *t*-test). As dephosphorylation is less energetically demanding by comparison with the energy required to phosphorylate a tyrosine residue; perhaps this may explain the decrease in impact of the Δ*ptpZ* mutation over time?

To ensure that the Δ*ptpZ* mutant phenotype was specific to the absence of PtpZ, a wild-type copy of *ptpZ* was introduced to the *amyE* locus in the Δ*ptpZ* mutant under the control of a heterologous promoter; $P_{spank-hy}$–*ptpZ*–*lacI* (NRS2467). In the presence of 100 μM IPTG biofilm architecture was comparable to that of the wild-type strain (Fig. 8C). These findings confirm that the altered biofilm phenotype was specific to the disruption of *ptpZ*. The phosphatase activity of PtpZ has been shown to be reduced by ~95% when histidine at position 196 is mutated to alanine (Mijakovic *et al.*, 2005b). Therefore, to establish whether the phosphatase activity of PtpZ was required to control biofilm formation a mutant allele of *ptpZ* (PtpZ–$H^{196}$A) was introduced into the *amyE* locus under the control of a heterologous promoter; $P_{spankhy}$–*ptpZ*–$H^{196}$A–*lacI* (NRS2468). In contrast to the wild-type allele of PtpZ, the mutant PtpZ–$H^{196}$A protein was not capable of restoring wild-type colony morphology (Fig. 8D). These findings support the conclusion that the phosphatase activity of PtpZ is required.

It is interesting to note that deletion of both *ptkA* and *ptpZ* results in a loss of colony complexity and a reduction of sporulation because of the lack of formation of fruiting body like structures. The a *priori* is that kinase and phosphatase pairs act to counteract the effects of one another in order to finely tune the activity of their target protein and therefore, the mutant strains would have opposite phenotypes. Our results contradict this assumption. However, consistent with our findings a decrease in polysaccharide production and biofilm formation was observed in *Burkolderia cepacia* upon mutation of both the tyrosine autokinase BceF and its low molecular tyrosine phosphatase partner, BceD (Ferreira *et al.*, 2007). We therefore favour the hypothesis that a cycle of phosphorylation and dephosphorylation facilitated by TkmA/PtkA and PtpZ, respectively, is required to form a mature *B. subtilis* biofilm.

### *Biofilm formation is independent of the activity of Ugd*

We wanted to identify the downstream target(s) of PtkA that is phosphorylated during biofilm formation. *In vitro* analysis currently indicates that PtkA has 13 confirmed substrates (Mijakovic *et al.*, 2003; 2006; Jers *et al.*, 2010). Additionally, using phosphoproteome analysis a further eight proteins have been identified as tyrosine phosphorylated (Levine *et al.*, 2006; Eymann *et al.*, 2007; Macek *et al.*, 2007) (Table S2). One obvious potential target of PtkA during biofilm formation was Ugd. Ugd is regulated by both PtkA and PtpZ (Mijakovic *et al.*, 2003; 2005b) and is cotranscribed with *ptkA* and *ptpZ* (Fig. 2). Ugd is a uridine-5′-diphophoglucose (UDP-glucose) dehydrogenase (Mijakovic *et al.*, 2003). When phosphorylated on tyrosine-70 by PtkA, Ugd is activated and can catalyse the oxidation of UDP-glucose to UDP-glucuronate (Petranovic *et al.*, 2009). UDP-glucuronate is subsequently used as a precursor for the production of teichuronic acid, which is a component of the cell wall (Soldo *et al.*, 1999). It has been postulated that Ugd may be required for biofilm formation (Mijakovic *et al.*, 2005a; Hung *et al.*, 2007). To test whether Ugd was required for biofilm formation we constructed an in frame deletion in *ugd* (NRS2471). The Δ*ugd* mutant exhibited a colony mor-

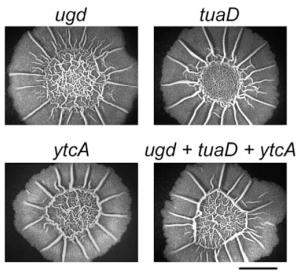


**Fig. 9.** Complex colony architecture of Δ*ugd, tuaD*::pNW377 and Δ*ytcA*, as single mutants and in combination. Strains Δ*ugd* (NRS2471), *tuaD*::pNW377 (NRS3232), Δ*ytcA* (NRS2227) and Δ*ugd* + *tuaD*::pNW377 + Δ*ytcA* (NRS3231) were assessed in the 3610 background as described in Fig. 1. Scale bar represents 5 mm.

phology that was indistinguishable from the parental strain biofilm (Fig. 9), indicating that Ugd is not needed. However, there is one additional proven and one putative, UDP-glucose dehydrogenase encoded on the *B. subtilis* chromosome by *tuaD* and *ytcA* respectively (Mijakovic *et al.*, 2003; 2005a). Functional redundancy between these proteins is a possibility; therefore, a series of single, double and a triple deletion mutant strains were constructed and the ability to form a mature and robust colony was tested. None of the strains tested had an influence on colony architecture (Figs 9 and S3). Taken together these findings indicate that Ugd, YtcA and TuaD are not the downstream substrates of PtpZ and PtkA regulated during post-translational control of biofilm formation by *B. subtilis*.

### *Biofilm formation is independent of any of the known tyrosine phosphorylated proteins*

Having eliminated Ugd, TuaD and YtcA as targets of PtkA during biofilm formation, we widened our search. Global phosphoproteome analyses have broadened our understanding of the processes that are regulated by tyrosine phosphorylation in bacteria (Levine *et al.*, 2006; Eymann *et al.*, 2007; Macek *et al.*, 2007). We therefore chose to take a systematic mutagenesis approach to try and identify the target of PtkA during biofilm formation. After removing Ugd and TuaD (Fig. 9), 19 proteins have been identified as tyrosine phosphorylated and therefore potential targets of PtkA (Table S2). Seven genes are known to encode essential proteins (*asd, aspS, yaaD, yurY, infA, ssbA* and *eno*) and thus were excluded from our analysis. The gene *ssbB* was also excluded from the analysis as SsbB shares 63% identity and 81% similarity to SsbA, an essential protein. This left 11 proteins (AhpF, CitC, Ldh, OppA, RocA, YjoA, YvyG, YnfE, SdhA, YxxG and YorK) of which mutations could be constructed in nine of the corresponding genes (*ahpF, citC, ldh, oppA, rocA, yjoA, yvyG, ynfE* and *yorK*). Mutations of both *sdhA* and *yxxG* were found to result in a severe growth defect (data not shown). After construction and verification of the mutant strains the impact on colony morphology was tested. None was found to influence colony formation (Fig. S4). Therefore, despite extensive efforts to identify the substrate phosphorylated by PtkA it remained elusive. It is of course possible that one or more of the essential protein is (are) the target of PtkA; however, it is important to remember that *B. subtilis* strain NCIB3610 is the progenitor of the *B. subtilis* 168 strain that was used in the phosphoproteome analyses and they contain several single nucleotide polymorphisms (Srivatsan *et al.*, 2008) (Levine *et al.*, 2006; Eymann *et al.*, 2007; Macek *et al.*, 2007). Some of these genome level differences alter the ability of the two strains to form a biofilm (Branda *et al.*, 2001; Kobayashi, 2008). The NCIB3610 strain also contains a plasmid of ~85 kbp, which could conceivably encode proteins that are tyrosine phosphorylated and required for biofilm formation (Earl *et al.*, 2007). Therefore, it will be necessary to conduct global proteome analyses using NCIB3610 to identify further possible targets of PtkA that are modulated during biofilm formation.

### *Concluding remarks*

The principal finding of this work is that *B. subtilis* uses tyrosine phosphorylation as a mechanism of influencing biofilm formation. To achieve this it uses TkmA, a BY-kinase modulator; PtkA, a BY-kinase and PtpZ, a protein tyrosine phosphatase. In addition, we have shown for the first time that TkmA, the BY-kinase modulator is capable of interacting with an additional target(s) in the absence of PtkA. It will be interesting to investigate whether or not TkmA is able to interact with the predicted tyrosine kinase EpsB as has previously been speculated (Mijakovic *et al.*, 2005a) or if it has an entirely unrelated function. EPS biosynthesis is essential for biofilm formation and in a wide range of bacterial species tyrosine phosphorylation is an important mechanism that regulates EPS biosynthesis. For example, in *Escherichia coli*, a tyrosine kinase (Wzc) and phosphatase (Wzb) pair regulate the biosynthesis and export of colonic acid (Lacour *et al.*, 2008), a thick mucoid polymer that is required for biofilm structure and depth (Danese *et al.*, 2000). Additionally, in *Streptococcus thermophilus*, a tyrosine kinase (EpsD) and phosphatase (EpsB) pair control the biosynthesis of EPS by regulating the phosphogalactosyltransferase activity of EpsE (Minic *et al.*, 2007). It would seem reasonable to suggest that EpsB plays this more tradi-

tional role in EPS biosynthesis in *B. subtilis* given its location on the chromosome and the requirement for the *epsA–O* operon for biofilm formation (Branda *et al.*, 2001; Mijakovic *et al.*, 2005a). In contrast with these examples, PtkA and PtpZ are not located within an operon involved in the biosynthesis of an EPS that is required for biofilm formation as deletion of *ugd* did not impact biofilm formation (Fig. 9). Thus the mechanism by which PtkA and PtpZ influence biofilm formation using tyrosine phosphorylation is novel and warrants further investigation.

## Experimental procedures

### *Growth conditions and strain construction*

*Escherichia coli* and *B. subtilis* strains were routinely grown in LB medium (10 g NaCl, 5 g yeast extract and 10 g tryptone per litre) at 37°C unless otherwise stated. *E. coli* strain MC1061 [*F′ lacIQ lacZM15 Tn10* (*tet*)] was used for the routine construction and maintenance of plasmids. Where appropriate MSgg medium (5 mM potassium phosphate and 100 mM MOPS at pH 7.0 supplemented with 2 mM $MgCl_2$, 700 μM $CaCl_2$, 50 μM $MnCl_2$, 50 μM $FeCl_3$, 1 μM $ZnCl_2$, 2 μM thiamine, 0.5% glycerol, 0.5% glutamate) (Branda *et al.*, 2001) was used for analysis of biofilm formation. *B. subtilis* strains used in this study are listed in Tables 1 and S3. Strains were constructed using standard protocols (Harwood and Cutting, 1990). Phage transductions were conducted as described previously (Kearns and Losick, 2003). When required, antibiotics were used at the following concentrations: ampicillin 100 μg $ml^{-1}$, chloramphenicol 5 μg $ml^{-1}$, erythromycin 1 μg $ml^{-1}$, lincomycin 25 μg $ml^{-1}$, kanamycin 25 μg $ml^{-1}$and spectinomycin 100 μg $ml^{-1}$. When required, IPTG was added to the medium at the concentrations specified.

### *Surface adhesion assay*

Cell-surface adhesion of strains constructed from the NCIB3610 parent strain was assessed by patching each strain on a 1.5% LB agar plate. Strains were grown for 16 h at 37°C prior to the cells being scraped from the surface of the agar plate using a disposable pipette tip ensuring equal pressure was applied to each patch.

### *Construction of plasmid pNW312*

Plasmid pNW312 used to introduce the *ptpZ* gene under the control of the IPTG inducible promoter, $P_{spankhy}$ at the non-essential *amyE* locus is a derivative of plasmid pDR111 (Britton *et al.*, 2002). The *ptpZ* coding region, including ribosome binding site, was amplified from genomic DNA isolated for NCIB 3610 using primers NSW172 (5′-GGATGTCGAC CATCGTGCCCGTTATTTATTT-3′) and NSW173 (5′-GGAT GCATGCGAATCGGCTGTTAAAAAAAACC-3′). The PCR was cloned into the SalI and SphI sites of pDR111 using the restriction sites engineered into the primers (underlined in the primer sequence). The insert was sequenced to ensure that PCR-generated mistakes were not introduced into *ptpZ*. Additional plasmids were constructed in an identical manner for *tkmA* and *ptkA*, separately and in combination, using the primers and plasmids detailed in Tables S4 and S5.

### *Construction of plasmid pNW316*

Plasmid pNW316 was used to introduce the *ptpZ* gene containing a point mutation encoding for a substitution of histidine at position 196 to an alanine, under the control of the IPTG inducible promoter, $P_{spankhy}$ at the non-essential *amyE* locus and is a derivative of plasmid pNW312. The point mutation was introduced using primers NSW205 (5′-GTAGCCTCAGATGCCGCTAATGTGAAAACGAGA-3′) and NSW206 (5′-TCTCGTTTTCACATTAGCGGCATCTGAGGC TAC-3′). Following PCR of methylated template DNA the reaction was digested using DpnI (NEB). The remaining DNA was transformed into *E. coli*. Plasmids containing the insert were sequenced. Additional point mutations were inserted in an identical manner for *ptkA* using the primers and plasmids detailed in Tables S4 and S5.

### *Construction of in frame deletion strains*

Plasmid pNW330 used for the construction of an in frame, markerless deletion of *ptpZ* was constructed as follows. Primers NSW225 (5′-GCATGGATCCGGAGTGGACATTTT GGCGCT-3′) and NSW218 (5′-GCATGTCGACATCGATCA TGTCCTAGCCCCC-3′) were used to amplify the region located upstream from the coding sequence of *ptpZ*. The PCR product was cloned into pMAD (Arnaud *et al.*, 2004) using the restriction sites engineered into the primers (underlined in the primer sequence) resulting in pNW328. Primers NSW219 (5′-GCATGTCGACGGTTTTTTTTAACAGCCGATT CTC-3′) and NSW220 (5′-GCATCCCGGGCACTGTGCTTT TCGTTACCAC-3′) were used to amplify the region located downstream from the coding sequence of *ptpZ*, which was cloned into pNW328 using the restriction sites engineered into the primers (underlined in the primer sequence) resulting in pNW330. To introduce the mutation into NCIB3610, pNW330 was transformed into 168. Phage was harvested and was used to transduce NCIB3610. NRS2222 was constructed by integration and curing of pNW330 in NCIB3610. Further plasmids were constructed for in frame mutations in an identical manner for *tkmA*, *ptkA*, *ugd* and for *tkmA* and *ptkA* simultaneously using the primers and plasmids detailed in Tables S4 and S5.

### *Construction of chromosomal directed substitutions*

Plasmid pNW348 was used for the construction of an in frame, markerless point mutation of *ptkA* at the 'DxD' motif. Primers NSW246 (5′-GGGCGATATCGGATCCGCATACT TTTGATTATGATTGTAACCGCG-3′) and NSW249 (5′-CCGGGAGCTCGAATTCTTTCTCTAGAACATAAAGAGCCT CTTGA-3′) were used to amplify *ptkA*, which was cloned into pUC19 using the restriction sites engineered into the primers (underlined in the primer sequence). Primers NSW250 (5′-AAAGTGCTCCTGATTGCTGCTGCTTTGCG AAAACCAACA-3′) and NSW251 (5′-TGTTGGTTTTCGCA

AAGCAGCAGCAATCAGGAGCACTTT-3′) were used to introduce point mutations as previously described. The resulting product was sequenced to ensure that the desired mutations were introduced. The region of DNA carrying *ptkA* ($D^{51}A–D^{53}A$) was cloned into pMAD using the restriction sites engineered into the primers. The point mutations were introduced into NCIB3610 as described above for the in frame deletions. Further plasmids were constructed for in frame mutations in an identical manner for *ptkA* ($Y^{225}A–Y^{227}A–Y^{228}A$) using the primers and plasmids detailed in Tables S4 and S5.

### *Biofilm analysis*

Analysis of biofilm formation was performed as described (Branda *et al.*, 2001; Verhamme *et al.*, 2007). *B. subtilis* strains were inoculated from a fresh LB plate and grown to mid-late exponential phase in LB. The undiluted culture (10 μl) was spotted onto an MSgg plate containing 1.5% agar (containing IPTG as required) and incubated at 37°C for the time period indicated. For pellicle formation the culture was diluted 1000-fold into 1.5 ml MSgg media in a 24-well plate and was incubated for 16 h at 37°C. Images of the pellicles and bacterial colonies were captured using a Leica MZ16 FA stereoscope using LAS software version 2.7.1.

### *Sporulation analysis*

Sporulation analysis was conducted as described previously (Vlamakis *et al.*, 2008). Colonies were grown on solid MSgg media for 24 or 72 h at 37°C prior to cell collection. Liquid cultures were prepared by growing cells in 10 ml MSgg media inoculated with cells from an OD600 of 0.01. Cultures were grown for 24 or 72 h with shaking at 37°C.

### *Single cell image analysis*

Strains for analysis were grown in LB at 37°C with shaking to an OD600 of 0.3. Cells were collected by centrifugation and were concentrated fivefold by resuspension in wash buffer [15 mM $(NH^4)_2SO^4$, 80 mM $K_2HPO^4$, 44 mM $KH_2PO^4$, 3.4 mM sodium citrate, 1 mM $Mg^2SO^4$]. The concentrated cell suspensions were stained using Hoechst 33342 (10 ng $ml^{-1}$) (Invitrogen™) for 5 min and were washed twice in wash buffer. Stained cell suspension (2 μl) was spotted onto thin agarose slides and viewed using an Axio Imager M1 microscope (Zeiss). Images were analysed using AxioVision Rel. version 4.6 image capture software (Zeiss).

### *RNA isolation*

Cells for RNA isolation were inoculated into 25 ml of LB at an OD600 of 0.01 from an overnight lawn plate and grown at 37°C with shaking at 200 r.p.m. in 250 ml flasks. When an OD600 of 1 was reached, 3 ml of cells were harvested by centrifugation at 13 000 *g* for 1 min and immediately processed for RNA extraction using the RiboPure™-Bacteria RNA extraction kit (Ambion®) according to the manufacturer's instructions. RNA was checked for quality by running on an agarose gel and quantified using a Nanodrop™.



### *DNA microarray analysis*

*Bacillus subtilis* microarrays consisting of 4105 gene-specific oligonucleotides (Compugen) were printed at the Research Technology Support Facility at Michigan State University. Five oligonucleotides that have no significant similarity to the *B. subtilis* genome were used as negative controls. To identify the genes that were upregulated in the absence of both SinR and DegU, RNA was extracted from a *degSU* (NRS1499) and a *degSUsinR* (NRS1686) mutant strain. For the DNA array analysis two independent RNA samples were used for each strain and two technical DNA array replicates were conducted. cDNA was synthesized using either 3 or 6 μg of total RNA by reverse transcribed with Superscript III (Invitrogen) for 2 h at 50°C in the presence of amino-allyl-dUTP (Sigma). RNA was degraded by hydrolysis using 15 μl of 0.1 M NaOH and incubation at 70°C for 10 min. The sample was neutralized by the addition of 15 μl of 0.1 M HCl and the cDNA purified using a MinElute PCR purification kit (Qiagen) and eluted in 10 μl $H_2O$. To fluorescently label the cDNA, 0.5 μl of fresh 1 M $NaHCO_3$ was added to the cDNA and was used to hydrate an aliquot of either GE Healthcare Fluorolink Cy3 dye (*degSU* cDNA) or GE Healthcare Fluorolink Cy5 dye (*degSUsinR* cDNA). After 1 h incubation at room temperature unincorporated dye was removed using the MinElute PCR purification kit. Both labelled cDNA populations were applied onto a microarray and hybridized overnight at 42°C for 16–18 h. After washing, hybridized microarray slides were analysed using a GenePix™ 4100A array scanner (Axon Instruments). Images were processed using the GenePix Pro 5.0 software, which generates red-green fluorescent intensity values for each spot. The fluorescent signal intensities were imported into Microsoft Excel (available from http://www.lifesci.dundee.ac.uk/groups/nicola_stanley-wall/). The microarray datasets were filtered to remove those genes that were expressed at levels less than two standard deviations above the average background values in both channels. The intensity values were normalized relative to the ratio generated by dividing the total value of Cy3 fluorescence with that of the total value of Cy5 fluorescence measure per array. The average value from the four spots per gene was calculated and those genes with an expression level of greater than 2.0 after normalization were selected. At this point the genes that had previously been identified as directly repressed by SinR were eliminated (Chu *et al.*, 2006), for example, genes in the *epsA–O* operon and the *yqxM–sipW–tasA* operon (Table S1). This resulted in a group of 11 genes that had an average expression value of $> 2.0$ and that had previously not been demonstrated to be SinR repressed.

### *Semi-quantitative RT-PCR*

RNA was isolated from cultures of 3610, *degSU*, *sinR* and *degSUsinR* as described above. The harvested RNA was DNase treated and cDNA was synthesized as previously published (Stanley and Lazazzera, 2005). To ensure the RNA samples were free from contaminant DNA, samples of RNA lacking Superscript III (Invitrogen) were treated in parallel with samples intended for cDNA synthesis. Synthesized cDNA (1 μl) was used in a standard 20 μl PCR reaction using Qiagen Taq DNA polymerase with the addition of 3.5 mM

$MgCl_2$ and 8.3 nl $ml^{-1}$ SyberGreen (Sigma). PCR samples were held at 95°C for 10 min prior to a 25-cycle PCR reaction involving a melting step at 95°C, followed by an annealing step at 50°C and then an elongation step at 72°C. Each PCR step was held for the duration of 25 s. The genes *ptpZ, yomI, ywbC* and *yvfO* were amplified using gene-specific primers detailed in Table S4. To determine the melting temperatures of the PCR products the set point temperature was increased in 40 cycles (10 s each) by 1°C per cycle, starting from 50°C. Expression of *ptpZ, yomI, ywbC* and *yvfO,* was calculated as fold changes relative to the wild-type strain using the formula: Fold change = $2^{-\Delta\Delta Ct}$; with $-\Delta\Delta Ct = [Ct_{(gene\ x)} - Ct_{(constitutive\ gene)}]_{condition\ I} - [Ct_{(gene\ x)} - Ct_{(constitutive\ gene)}]_{condition\ II}$ (Talaat *et al.*, 2002). The level of transcription of each gene was measured using Corbett qPCR reader, run using Rotorgene 8 software (Corbett) with expression of *veg* monitored as a reference gene (Hamon *et al.*, 2004).

### tkmA *operon analysis*

RNA was isolated from NCIB3610 grown in LB to an OD600 of 0.01, as described above. cDNA was synthesized using the reverse *ugd*-specific primer NSW220 and the resulting mixture was treated with RNase H (Invitrogen) for 20 min at 37°C. The following primer pairs were used for amplification of an internal region of *ptkA* (NSW225 and NSW254), *ptpZ* (NSW195 and NSW249) or *ugd* (NSW165 and NSW220). See Table S4 for primer sequences.

### *5′ RACE*

The transcription start site of *tkmA* was determined using 5′RACE conducted using DNase treated RNA harvested from NCIB3610 as described previously. To synthesize cDNA corresponding to the promoter region of the *tkmA* gene, 5 μg of DNase treated RNA was incubated with 2.5 pmol NSW227 (5′-GGGCTCTTAATGATGACA-3′) at 70°C for 10 min. The reaction mixture was made up to a total volume of 25 μl with the addition of 1× first strand buffer, 11.2 μM DTT and 0.4 mM dNTPs. The mixture was incubated at 42°C for 1 min prior to the addition of 200 U of Superscript II (Invitrogen™) and then incubated for a further 50 min. The reverse transcriptase was heat inactivated by incubation at 70°C for 15 min. To remove any remaining RNA template, RNase H. 500 ng of synthesized cDNA was 5′ dC-tailed using 20 units of terminal transferase (Tdt) (New England Biolabs™), supplemented with 1× Terminal Transferase Reaction Buffer (20 mM Tris-acetate, 50 mM potassium acetate and 10 mM Magnesium Acetate), 0.25 mM $CoCl_2$ and 200 μM dCTP. The reaction was incubated at 37°C for 10 min and then 10 min at 65°C for to heat inactivate the Tdt. Touchdown PCR was used to amplify the *tkmA* promoter region using primers NSW367 (5′-GGCCACGCGTCGACTAGTACGGGUUGGGUUGGGUUG-3′) and NSW228 (5′-GGGTGTAAGTGCGAAGAAA-3′). The standard PCR reaction mixture included 1.5 mM $MgCl^2$, 5 μl of dC-tailed cDNA, 0.4 mM each primer, 1 HotStart Taq bead and 1× PCR buffer (Promega). Annealing temperature was gradually reduced from 58°C to 48°C in 0.5 increments, with a final 20 cycles at 48°C. The resulting PCR product was visualized by gel electrophoresis and staining prior to recombination into the TOPO-TA vector pCR2.1 (Invitrogen™). The inserts cloned were sequenced and the transcription start site identified.

### *Purification of DegU, DegS and SinR*

$DegU\text{-}_{His6}$ was purified as described previously (Verhamme *et al.*, 2007) with the following alteration. Following IMAC purification $DegU\text{-}_{His6}$ was purified from contaminating DNA by application to a DEAE-FF column (GE Healthcare™). Purified $DegU\text{-}_{His6}$ was dialysed before use [20 mM Tris-HCl (pH 8.0) 50 mM NaCl]. $SinR\text{-}_{His6}$ was purified as previously described (Verhamme *et al.*, 2009). The histidine tag used for purification was removed using Novagen's thrombin cleavage capture kit. For the overproduction of $DegS\text{-}_{His6}$, plasmid pET28b–$degS\text{-}_{His6}$ (Kobayashi, 2007), was induced by the addition of 500 μM IPTG at OD600 0.4. Growth was continued for 3 h prior to collection by centrifugation at 4°C. Cells were washed with ice cold 10 mM Tris-HCl (pH 7.6). $DegS\text{-}_{His6}$ was purified from inclusion bodies according to the BugBuster protocol (Novagen). $DegS\text{-}_{His6}$ was incubated on ice for 2 h in denaturing buffer [50 mM Tris-HCl (pH 7.6), 150 mM NaCl, 8 M urea and 10 mM imidazole] before the protein solution was applied to a HisTrap FF column (GE healthcare). $DegS\text{-}_{His6}$ was slowly renatured by gradual removal of the urea over the course of 90 min at room temperature. $DegS\text{-}_{His6}$ was eluted from the column by the addition of 500 mM imidazole and was dialysed in 50 mM Tris-HCl (pH 7.6), 200 mM KCl, 10 mM $MgCl_2$, 0.1 mM EDTA, 1 mM dithiothreitol (DTT) and 50% glycerol.

### *Electrophoretic mobility shift assay*

A PCR product corresponding to the promoter region of *tkmA* ($P_{tkmA}$) was amplified using primers NSW146 and NSW147 and purified by gel extraction. The promoter DNA was labelled using 50 μCi [$\gamma$-$^{32}$P]-ATP (Perkin-Elmer) and T4 polynucleotide kinase (New England Biolabs). Unincorporated ATP was removed from the labelled DNA using an Illustra Microspin G-25 column (GE healthcare). Phosphorylated purified DegU was produced essentially as described previously (Gueriri *et al.*, 2008), with the exception that a final concentration of 10 μM purified DegU and 0.78 μM purified DegS was added to the phosphorylation reaction. The reaction was incubated for 30 min at 25°C. EMSA binding mixtures were prepared containing 15 mM Tris-HCl (pH 7.6), 0.2% Tween-20, 1 mM $MgCl_2$, 60 mM NaCl, 4% glycerol, 15 mM DTT, 0.5 mg $ml^{-1}$ bovine serum albumin, 1 μg poly (dI-dC) and a range of concentrations of DegU–P, made up to a total volume of 30 μl. The reactions were initiated by the addition of 2 ng of $^{32}$P-labelled DNA probe. The reaction mixtures (15 μl) were loaded onto a 5% polyacrylamide (AccuFLOWGel; Acrylamide : Bis-Acrylamide solution 29:1) Tris Glycine gel (50 mM Tris-HCl, 400 mM glycine, 1.75 mM EDTA), which was run at 100 V for ~1–2 h. Dried gels were exposed to X-ray film overnight at –70°C prior to development.

## Acknowledgements

This work was funded by a BBSRC David Phillips Fellowship grant [BB/C520404/1]. T.B.K. is a recipient of a BBSRC doc-

toral training grant [BB/D526161/1]. We would like to thank the following people: the Sequencing Service (College of Life Sciences, University of Dundee, Scotland, http://www.dnaseq.co.uk) for DNA sequencing, Professor Lazazzera, Professor Burkholder, Professor Britton and Professor Kroos for access to the *B. subtilis* oligonucleotides used to synthesis the DNA microarray slides, and Professor Norman Pratt and Dr Katie Robertson (Ninewells Hospital, University of Dundee) for use of the GenePix™ 4100A array scanner. We thank Dr Kazou Kobayashi for kindly providing plasmid pETdegS.

## References

Amati, G., Bisicchia, P., and Galizzi, A. (2004) DegU-P represses expression of the motility fla-che operon in *Bacillus subtilis*. *J Bacteriol* **186:** 6003–6014.

Arnaud, M., Chastanet, A., and Debarbouille, M. (2004) New vector for efficient allelic replacement in naturally nontransformable, low-GC-content, gram-positive bacteria. *Appl Environ Microbiol* **70:** 6887–6891.

Bai, U., Mandic-Mulec, I., and Smith, I. (1993) SinI modulates the activity of SinR, a developmental switch protein of *Bacillus subtilis*, by protein-protein interaction. *Genes Dev* **7:** 139–148.

Bender, M.H., Cartee, R.T., and Yother, J. (2003) Positive correlation between tyrosine phosphorylation of CpsD and capsular polysaccharide production in *Streptococcus pneumoniae*. *J Bacteriol* **185:** 6057–6066.

Branda, S.S., Gonzalez-Pastor, J.E., Ben-Yehuda, S., Losick, R., and Kolter, R. (2001) Fruiting body formation by *Bacillus subtilis*. *Proc Natl Acad Sci USA* **98:** 11621–11626.

Branda, S.S., Vik, S., Friedman, L., and Kolter, R. (2005) Biofilms: the matrix revisited. *Trends Microbiol* **13:** 20–26.

Britton, R.A., Eichenberger, P., Gonzalez-Pastor, J.E., Fawcett, P., Monson, R., Losick, R., and Grossman, A.D. (2002) Genome-wide analysis of the stationary-phase sigma factor (Sigma-H) regulon of *Bacillus subtilis*. *J Bacteriol* **184:** 4881–4890.

Chai, Y., Norman, T., Kolter, R., and Losick, R. (2010) An epigenetic switch governing daughter cell separation in *Bacillus subtilis*. *Genes Dev* **24:** 754–765.

Chu, F., Kearns, D.B., Branda, S.S., Kolter, R., and Losick, R. (2006) Targets of the master regulator of biofilm formation in *Bacillus subtilis*. *Mol Microbiol* **59:** 1216–1228.

Chu, F., Kearns, D.B., McLoon, A., Chai, Y., Kolter, R., and Losick, R. (2008) A novel regulatory protein governing biofilm formation in *Bacillus subtilis*. *Mol Microbiol* **68:** 1117–1127.

Costerton, J.W., Lewandowski, Z., Caldwell, D.E., Korber, D.R., and Lappin-Scott, H.M. (1995) Microbial biofilms. *Annu Rev Microbiol* **49:** 711–745.

Danese, P.N., Pratt, L.A., and Kolter, R. (2000) Exopolysaccharide production is required for development of *Escherichia coli* K-12 biofilm architecture. *J Bacteriol* **182:** 3593–3596.

Dartois, V., Debarbouille, M., Kunst, F., and Rapoport, G. (1998) Characterization of a novel member of the DegS-DegU regulon affected by salt stress in *Bacillus subtilis*. *J Bacteriol* **180:** 1855–1861.

Deutscher, J., and Saier, M.H., Jr (2005) Ser/Thr/Tyr protein phosphorylation in bacteria – for long time neglected, now well established. *J Mol Microbiol Biotechnol* **9:** 125–131.

Dubnau, D. (1991) Genetic competence in *Bacillus subtilis*. *Microbiol Rev* **55:** 395–424.

Duclos, B., Grangeasse, C., Vaganay, E., Riberty, M., and Cozzone, A.J. (1996) Autophosphorylation of a bacterial protein at tyrosine. *J Mol Biol* **259:** 891–895.

Earl, A.M., Losick, R., and Kolter, R. (2007) *Bacillus subtilis* genome diversity. *J Bacteriol* **189:** 1163–1170.

Eymann, C., Becher, D., Bernhardt, J., Gronau, K., Klutzny, A., and Hecker, M. (2007) Dynamics of protein phosphorylation on Ser/Thr/Tyr in *Bacillus subtilis*. *Proteomics* **7:** 3509–3526.

Fawcett, P., Eichenberger, P., Losick, R., and Youngman, P. (2000) The transcriptional profile of early to middle sporulation in *Bacillus subtilis*. *Proc Natl Acad Sciences USA* **97:** 8063–8068.

Ferreira, A.S., Leitao, J.H., Sousa, S.A., Cosme, A.M., Sa-Correia, I., and Moreira, L.M. (2007) Functional analysis of *Burkholderia cepacia* genes bceD and bceF, encoding a phosphotyrosine phosphatase and a tyrosine autokinase, respectively: role in exopolysaccharide biosynthesis and biofilm formation. *Appl Environ Microbiol* **73:** 524–534.

Fujita, M., Gonzalez-Pastor, J.E., and Losick, R. (2005) High- and low-threshold genes in the Spo0A regulon of *Bacillus subtilis*. *J Bacteriol* **187:** 1357–1368.

Gaur, N.K., Dubnau, E., and Smith, I. (1986) Characterization of a cloned *Bacillus subtilis* gene that inhibits sporulation in multiple copies. *J Bacteriol* **168:** 860–869.

Gaur, N.K., Oppenheim, J., and Smith, I. (1991) The *Bacillus subtilis* sin gene, a regulator of alternate developmental processes, codes for a DNA-binding protein. *J Bacteriol* **173:** 678–686.

Grangeasse, C., Obadia, B., Mijakovic, I., Deutscher, J., Cozzone, A.J., and Doublet, P. (2003) Autophosphorylation of the *Escherichia coli* protein kinase Wzc regulates tyrosine phosphorylation of Ugd, a UDP-glucose dehydrogenase. *J Biol Chem* **278:** 39323–39329.

Grangeasse, C., Cozzone, A.J., Deutscher, J., and Mijakovic, I. (2007) Tyrosine phosphorylation: an emerging regulatory device of bacterial physiology. *Trends Biochem Sci* **32:** 86–94.

Grangeasse, C., Terreux, R., and Nessler, S. (2009) Bacterial tyrosine-kinases: structure-function analysis and therapeutic potential. *Biochim Biophys Acta* **1804:** 628–634.

Gueriri, I., Bay, S., Dubrac, S., Cyncynatus, C., and Msadek, T. (2008) The Pta-AckA pathway controlling acetyl phosphate levels and the phosphorylation state of the DegU orphan response regulator both play a role in regulating *Listeria monocytogenes* motility and chemotaxis. *Mol Microbiol* **70:** 1342–1357.

Hamoen, L.W., Werkhoven, A.F.V., Venema, G., and Dubnau, D. (2000) The pleiotropic response regulator DegU functions as a priming protein in competence development in *Bacillus subtilis*. *Proc Natl Acad Sci USA* **97:** 9246–9251.

Hamon, M.A., and Lazazzera, B.A. (2001) The sporulation transcription factor Spo0A is required for biofilm development in *Bacillus subtilis*. *Mol Microbiol* **42:** 1199–1209.

Hamon, M.A., Stanley, N.R., Britton, R.A., Grossman, A.D., and Lazazzera, B.A. (2004) Identification of AbrB-regulated

genes involved in biofilm formation by *Bacillus subtilis*. *Mol Microbiol* **52:** 847–860.
Harwood, C.R., and Cutting, S.M. (1990) *Molecular Biological Methods for* Bacillus. Chichester, England: John Wiley &Sons Ltd.
Hoch, J.A. (2000) Two-component and phosphorelay signal transduction. *Curr Opin Microbiol* **3:** 165–170.
Hung, R.J., Chien, H.S., Lin, R.Z., Lin, C.T., Vatsyayan, J., Peng, H.L., and Chang, H.Y. (2007) Comparative analysis of two UDP-glucose dehydrogenases in *Pseudomonas aeruginosa* PAO1. *J Biol Chem* **282:** 17738–17748.
Jers, C., Pedersen, M.M., Paspaliari, D.K., Schutz, W., Johnsson, C., Soufi, B., *et al.* (2010) *Bacillus subtilis* BY-kinase PtkA controls enzyme activity and localization of its protein substrates. *Mol Microbiol* **77:** 287–299.
Kearns, D.B., and Losick, R. (2003) Swarming motility in undomesticated *Bacillus subtilis*. *Mol Microbiol* **49:** 581–590.
Kearns, D.B., Chu, F., Branda, S.S., Kolter, R., and Losick, R. (2005) A master regulator for biofilm formation by *Bacillus subtilis*. *Mol Microbiol* **55:** 739–749.
Kobayashi, K. (2007) Gradual activation of the response regulator DegU controls serial expression of genes for flagellum formation and biofilm formation in *Bacillus subtilis*. *Mol Microbiol* **66:** 395–409.
Kobayashi, K. (2008) SlrR/SlrA controls the initiation of biofilm formation in *Bacillus subtilis*. *Mol Microbiol* **69:** 1399–1410.
Kodgire, P., Dixit, M., and Rao, K.K. (2006) ScoC and SinR negatively regulate epr by corepression in *Bacillus subtilis*. *J Bacteriol* **188:** 6425–6428.
Lacour, S., Bechet, E., Cozzone, A.J., Mijakovic, I., and Grangeasse, C. (2008) Tyrosine phosphorylation of the UDP-glucose dehydrogenase of *Escherichia coli* is at the crossroads of colanic acid synthesis and polymyxin resistance. *PLoS ONE* **3:** e3053.
Lee, D.C., and Jia, Z. (2009) Emerging structural insights into bacterial tyrosine kinases. *Trends Biochem Sci* **34:** 351–357.
Lee, D.C., Zheng, J., She, Y.M., and Jia, Z. (2008) Structure of *Escherichia coli* tyrosine kinase Etk reveals a novel activation mechanism. *EMBO J* **27:** 1758–1766.
Levine, A., Vannier, F., Absalon, C., Kuhn, L., Jackson, P., Scrivener, E., *et al.* (2006) Analysis of the dynamic *Bacillus subtilis* Ser/Thr/Tyr phosphoproteome implicated in a wide variety of cellular processes. *Proteomics* **6:** 2157–2173.
Lopez, D., and Kolter, R. (2010) Extracellular signals that define distinct and coexisting cell fates in *Bacillus subtilis*. *FEMS Microbiol Rev* **34:** 134–149.
Lopez, D., Vlamakis, H., Losick, R., and Kolter, R. (2009a) Paracrine signaling in a bacterium. *Genes Dev* **23:** 1631–1638.
Lopez, D., Fischbach, M.A., Chu, F., Losick, R., and Kolter, R. (2009b) Structurally diverse natural products that cause potassium leakage trigger multicellularity in *Bacillus subtilis*. *Proc Natl Acad Sci USA* **106:** 280–285.
Lopez, D., Vlamakis, H., and Kolter, R. (2009c) Generation of multiple cell types in *Bacillus subtilis*. *FEMS Microbiol Rev* **33:** 152–163.
Macek, B., Mijakovic, I., Olsen, J.V., Gnad, F., Kumar, C., Jensen, P.R., and Mann, M. (2007) The serine/threonine/tyrosine phosphoproteome of the model bacterium *Bacillus subtilis*. *Mol Cell Proteomics* **6:** 697–707.
Manai, M., and Cozzone, A.J. (1979) Analysis of the protein-kinase activity of *Escherichia coli* cells. *Biochem Biophys Res Commun* **91:** 819–826.
Mijakovic, I., Poncet, S., Boel, G., Maze, A., Gillet, S., Jamet, E., *et al.* (2003) Transmembrane modulator-dependent bacterial tyrosine kinase activates UDP-glucose dehydrogenases. *EMBO J* **22:** 4709–4718.
Mijakovic, I., Petranovic, D., Bottini, N., Deutscher, J., and Jensen, P.R. (2005a) Protein-tyrosine phosphorylation in *Bacillus subtilis*. *J Mol Microbiol Biotechnol* **9:** 189–197.
Mijakovic, I., Musumeci, L., Tautz, L., Petranovic, D., Edwards, R.A., Jensen, P.R., *et al.* (2005b) In vitro characterization of the *Bacillus subtilis* protein tyrosine phosphatase YwqE. *J Bacteriol* **187:** 3384–3390.
Mijakovic, I., Petranovic, D., Macek, B., Cepo, T., Mann, M., Davies, J., *et al.* (2006) Bacterial single-stranded DNA-binding proteins are phosphorylated on tyrosine. *Nucleic Acids Res* **34:** 1588–1596.
Minic, Z., Marie, C., Delorme, C., Faurie, J.M., Mercier, G., Ehrlich, D., and Renault, P. (2007) Control of EpsE, the phosphoglycosyltransferase initiating exopolysaccharide synthesis in *Streptococcus thermophilus*, by EpsD tyrosine kinase. *J Bacteriol* **189:** 1351–1357.
Molle, V., Fujita, M., Jensen, S.T., Eichenberger, P., Gonzalez-Pastor, J.E., Liu, J.S., and Losick, R. (2003) The Spo0A regulon of *Bacillus subtilis*. *Mol Microbiol* **50:** 1683–1701.
Moran, C.P., Jr, Johnson, W.C., and Losick, R. (1982) Close contacts between sigma 37-RNA polymerase and a *Bacillus subtilis* chromosomal promoter. *J Mol Biol* **162:** 709–713.
Morona, J.K., Paton, J.C., Miller, D.C., and Morona, R. (2000) Tyrosine phosphorylation of CpsD negatively regulates capsular polysaccharide biosynthesis in *Streptococcus pneumoniae*. *Mol Microbiol* **35:** 1431–1442.
Morona, J.K., Morona, R., Miller, D.C., and Paton, J.C. (2003) Mutational analysis of the carboxy-terminal (YGX)4 repeat domain of CpsD, an autophosphorylating tyrosine kinase required for capsule biosynthesis in *Streptococcus pneumoniae*. *J Bacteriol* **185:** 3009–3019.
Mukai, K., Kawata, M., and Tanaka, T. (1990) Isolation and phosphorylation of the *Bacillus subtilis* degS and degU gene products. *J Biol Chem* **265:** 20000–20006.
Murray, E.J., Strauch, M.A., and Stanley-Wall, N.R. (2009a) σX is involved in controlling *Bacillus subtilis* biofilm architecture through the AbrB homologue Abh. *J Bacteriol* **191:** 6822–6832.
Murray, E.J., Kiley, T.B., and Stanley-Wall, N.R. (2009b) A pivotal role for the response regulator DegU in controlling multicellular behaviour. *Microbiology* **155:** 1–8.
Nakano, M.M., and Zuber, P. (1991) The primary role of comA in establishment of the competent state in *Bacillus subtilis* is to activate expression of srfA. *J Bacteriol* **173:** 7269–7274.
Nakar, D., and Gutnick, D.L. (2003) Involvement of a protein tyrosine kinase in production of the polymeric bioemulsifier emulsan from the oil-degrading strain *Acinetobacter lwoffii* RAG-1. *J Bacteriol* **185:** 1001–1009.
Ogura, M., Yamaguchi, H., Yoshida, K., Fujita, Y., and Tanaka, T. (2001) DNA microarray analysis of *Bacillus subtilis* DegU, ComA and PhoP regulons: an approach to